Development of Silk based Bio-polymeric Porous Matrices for Tissue Engineering Applications

A THESIS SUBMITTED

FOR THE AWARD OF THE DEGREE

OF

DOCTOR OF PHILOSOPHY

IN

BIOTECHNOLOGY AND MEDICAL ENGINEERING

BY

MAHESH KUMAR SAH

(ROLL NO. 507BM002)

NATIONAL INSTITUTE OF TECHNOLOGY
ROURKELA - 769008, INDIA

2013

National Institute of Technology, Rourkela

CERTIFICATE

This to certify that the thesis entitled "**Development and Characterization of Silk based Bio-polymeric Porous Matrices for Tissue Engineering Applications**" being submitted by **Mr. Mahesh Kumar Sah** for the award of the degree of Doctor of Philosophy in Biotechnology & Medical Engineering of NIT Rourkela, is a record of bonafide research work carried out by him under my supervision and guidance. Mr. Mahesh Kumar Sah has worked for more than five years on the above problem in the Department of Biotechnology & Medical Engineering, National Institute of Technology Rourkela and his work has reached the standard for fulfilling the requirements and the regulation relating to the degree. The contents of this thesis, in full or part, have not been submitted to any other University or Institution for the award of any degree or diploma.

(Dr. Krishna Pramanik)

Professor& Head
Deptt. of Biotechnology & Medical Engineering,
NIT Rourkela

Place: Rourkela

Date:

Dedicated To

God & My Parents

ACKNOWLEDGEMENTS

At this moment of accomplishment, first of all I pay homage to my guide, Dr. (Mrs.) K. Pramanik. This work would not have been possible without her guidance, support and unflinching encouragement from the very early stage of this research. Under her guidance, I successfully overcame many difficulties and learned a lot. I can't forget her hard times to review my thesis progress, providing valuable suggestions and necessary corrections. Her unflinching courage and conviction will always inspire me, and I hope to continue to work with her noble thoughts. I can only say a proper thanks to her through my future work. I am indebted to her more than she knows.

I gratefully thank Doctoral Research Committee (DSC) members, Prof. Amit Biswas, Prof. Mukesh Gupta, Prof. Subhankar Paul and Prof. Kunal Pal of the department and Prof. Surojit Das from the department of Life Sciences for their constructive comments to improve the quality of this thesis. I am thankful that in the midst of all their activity, they accepted to be members of the committee.

Collective and individual acknowledgments are also owed to research group members, I belong to, Bhism Narayan Singh, Chinmaya Mohapatra, Akalabya Bissoyi, Sadanand Jinna,Rajdeep Kaur, Partha Sarthi Majhi, Nadeem Sidiqui, Varshini Viswanath, Rukmini Roy, Manalee Survey and Supriya Patil whose presence somehow perpetually refreshed, helpful, and memorable. Many thanks go in particular to Prof. Sirsendu Ray, Prof. Indranil Banerjee, Prof. Amitesh Kumar and Prof. B. P. Nayak, for giving me such a pleasant time since I knew them in NIT Rourkela. I forward my special gratitude for Prof. Arvind Kumar from Department of Chemical Engineering who has helped me a lot while my stay in NIT Rourkela

Words fail me to express my appreciation to my special friends whose dedication, love and persistent confidence in me, has taken the load off my shoulder.

Finally, I would like to thank everybody who was important to the successful realization of thesis, as well as expressing my apology that I could not mention personally one by one. This thesis has been kept on track and been seen through to completion with the supportand

encouragement of numerous people including my well wishers, my friends, colleagues andvarious institutions. At the end of my thesis I would like to thank all those people who made thisthesis possible and an unforgettable experience for me. At the end of my thesis, it is a pleasant taskto express my thanks to all those who contributed in many ways to the success of this study andmade it an unforgettable experience for me.

Mahesh Kumar Sah

ABSTRACT

Development and Characterization of Silk based Bio-polymeric Porous Matrices for Tissue Engineering Applications

Tissue engineering has emerged as a promising approach for the development of artificial body organs, repair, recover or improve tissue structures and functionality. 3D porous scaffolds possessing biomimicking properties are needed to support the neogenesis of tissues and mass transport of cells, nutrients and metabolic waste. Keeping this in view, the present dissertation work was undertaken for the development of SF based scaffolds with improved surface, mechanical and biological properties that can be used as artificial extracellular matrices for tissue regeneration. The silk fibroin was extracted from *B. mori* silk cocoon and the process was optimized by Response surface methodology using Box-Behnken Design. Porous SF and SF/PVA) blend scaffolds were prepared by salt leaching process and characterized for morphological (SEM), structural (XRD and FTIR), thermal (DSC and TGA) and mechanical (compressive strength) behaviour. The SF scaffolds were further modified with soluble eggshell membrane protein (SEP) with the aim of improving cell affinity for tissue regeneration. The pore size of the prepared SEP-SF and SEP-(SF/PVA) scaffold were in the range of 250-350μm and porosity of 90-93%. The measured compressive strength of SF and SF/PVA (50:50) scaffold were 279.8 ± 36.2 KPa and 235 ± 67.1 KPa respectively. The existence of soluble eggshell membrane protein on the scaffold surface, structural and thermal stability was confirmed by EDX, XRD, FTIR, DSC and TGA analysis. An increase in compressive strength of the prepared SF scaffolds was achieved by modification with SEP (321.5 ± 42.2 KPa for SEP-SF and247.5 ± 23.7 KPa for SEP-(SF/PVA) scaffolds). The cell culture study has indicated the significant improvement in cell adhesion and proliferation observed with hMSCs cultured on SF and SF/PVA scaffolds modified with SEP. The cyto-compatibility of the SEP conjugated SF scaffolds was confirmed by *in-vivo* animal model testing. This study has demonstrated that the biomimic property of SF scaffold can be enhanced by surface modification with SEP. Finally, it is concluded that the SEP conjugated SF/PVA (50:50) has the potential for use as artificial extra cellular matrix particularly for soft and other non-load bearing tissue engineering applications.

Key Words: *Biopolymer, Silk Fibroin, Tissue Engineering, Eggshell Membrane Protein, Surface Modification, PVA, Biocompatibility*

Table of Contents

ACKNOWLEDGEMENT……..*i-ii*
ABSTRACT……..*iii*
TABLE OF CONTENTS……*iv-vi*
LIST OF FIGURES ……..……*vii-ix*
LIST OF TABLES……..…..……*x*
LIST OF ABBREVIATIONS……..…..*x-xii*

CHAPTER 1: GENERAL INTRODUCTION……..……**1-18**

1.1. Background……..…..…..2

1.2. General strategies for tissue regeneration……..……...…..3

1.3. Overview of potential Tissue Engineering applications…….....4

1.4. Tissue Engineering challenges & future prospects………...…..…..5

1.4.1. TE Research & Development……..…..…..5
1.4.2. TE Clinical Barriers……...…..5
1.4.3. Industrial challenges……..…..…..6
1.4.4. Future Prospective of Tissue Engineering……...…..…6

1.5. Silk as ideal biopolymer for Tissue Engineering……..…..…7

1.5.1. Structure and composition……..…..8
1.5.2. Bio-relevant Properties……...……..10
1.5.3. Control of morphology of silk biomaterials…….....15

1.6. Scope and Objective…….....…17

1.7. Thesis Outline……...…..18

CHAPTER 2: LITERATURE REVIEW…….…….....**19-40**

2.1. Biomaterials for scaffold development…….……...…….....20

2.1.1. Natural polymers……...……...……...…..…..20
2.1.2. Synthetic Polymers…….....….22
2.1.3. Ceramics…….....22
2.1.4. Polymer/Polymer blend or Polymer/Ceramic Composite……...…..…..23

2.2. Scaffold Fabrication Methods…….....…..23

2.3. Silk biomaterial as TE matrices……...…..…..30

2.4. Surface modification and Composite development……...…..…31

2.5. PVA as traditional biomaterials for SF based scaffolds development……..…,…33

2.6. Utility of SF based matrices in Tissue Regeneration……..…….34

2.7. Conclusions……..…….....39

CHAPTER 3: MATERIALS AND METHODS……...……..…..**41-55**

3.1. Materials……..…..…..42

3.2. Preparation and Characterization of Polymer(s) solutions……..…..…..42

3.2.1. Preparation of regenerated silk fibroin aqueous solution……..…...42
3.2.2. Process optimization for SF extraction……....43
3.2.3. Characterization of RSF solution…….....45
3.2.4. Preparation of Soluble Egg Shell Membrane Protein (SEP)……..……...…...46
3.2.5. Preparation of SF/PVA blend solution……..……..…....46

3.3. Preparation and Characterization of SF and SF based matrices…….....46

3.3.1. Preparation of Silk Fibroin Hydrogels and Sponges……..…….....46
3.3.2. Fabrication of silk fibroin porous scaffold……..…….....47
3.3.3. Preparation of SEP-SF Scaffolds ……..…….....47
3.3.4. Preparation of SF/PVA Scaffold……..…….....47
3.3.5. Preparation of SEP-(SF/PVA) scaffolds…….....47
3.3.6. Physico-chemical and Thermal characterization……..…….....47
3.3.7. Mechanical Property……..……...…...49
3.3.8. Swelling assay & Biodegradability…..…..……..…….....49
3.3.9. Contact angle measurement……..…….....50
3.3.10. *In vitro* Cell Study……..…….....50
3.3.11. *In vivo* biocompatibility test in animal model…….....54
3.3.12. Statistical analysis…….....…....55

CHAPTER 4: RESULTS & DISCUSSION…….....56-138

***Part I:* Extraction of Silk Fibroin from *B. mori* Silk Cocoon & Its Characterization.…… …….....57-75**

4.1.1. Degumming of *B. mori* silk cocoon…….……....58
4.1.2. Preparation of regenerated aqueous SF solution…….……..….....63
4.1.3. Characterization of regenerated aqueous SF solution…….....…..67
4.1.4. Optimization of process conditions by RSM…….…….....68
4.1.5. Validation of the model…….....…75
5

***Part II:* Preparation, Characterization & *In vitro* Biocompatibility Study of Silk Fibroin Hydrogel…….....76-90**

4.2.1. Morphological Study …….....77
4.2.2. Swelling property ……..……...…...79
4.2.3. Thermo-rheological Behavior…….……..…….....81
4.2.4. Structural Analysis…….……..…….....82
4.2.5. Thermal Analysis…….……..…….....85
4.2.6. *In vitro* Biocompatibility Study ……..…….....87

***Part III*: Development of Porous SF Scaffolds with and without SEP conjugation ……..……...…….....91-112**

4.3.1. Morphological Study…….……..…….....92
4.3.2. Pore size and Porosity…….……..…….93
4.3.3. SEP conjugated SF scaffold……..……..…95
4.3.4. Elemental Analysis…….……..…….....97
4.3.5. Structural Analysis ....…….....…97
4.3.6. Thermal Properties…….……..…….....99
4.3.7. Compressive Strength…….……..…….102
4.3.8. Swelling behavior…….……..…….....102

4.3.9. Biodegradability……..…..103
4.3.10. Hydrophilicity…….....104
4.3.11. Characterization of MSCs…..…….....104
4.3.12. Cell Morphology in Scaffolds…….....107
4.3.13. Cell Adhesion and Proliferation…….....108
4.3.14. ALP Activity Assay…….....109
4.3.15. *In vivo* Biocompatibility Study…….....110

PART IV: **Development of Porous SF/PVA Scaffolds with and without SEP conjugation.....113-137**

4.4.1. Miscibility SF/PVA Blend……..….115
4.4.2. Morphological Study……...117
4.4.3. Structural Characterization.....…….....121
4.4.4. Thermal Analysis……..…….....123
4.4.5. Mechanical Property……....124
4.4.6. Swelling Behavior……...…….....126
4.4.7. *In vitro* Biodegradation……..….127
4.4.8. Hydrophilicity…….....128
4.4.9. *In vitro* Cell Culture Study…….....129
4.4.10. ALP Activity of Scaffolds…….....132
4.4.11. *In vivo* Evaluation of Scaffolds ……....……....133
Comparison of the results……...……...137

CHAPTER 5: SUMMARY AND CONCLUSION ……...…138-142

BIBLIOGRAPHY**……..143-170**
APPENDIX: A**…….....….171**
PUBLICATIONS**…….....172**
BIOGRAPHY**……...173**

List of Figures

Figure 1.1	SEM image showing (A) cross section of *B. mori* silk fiber, (B) structure of silk fibre and (C, D) schematic structure of *B. mori* SF protein…….....	**12**
Figure 2.1	Silk for different tissue engineering application……...	**30**
Figure 3.1	Scematic diagram for extraction of fibroin protein from *B. mori* silk cocoon…..	**43**
Figure 3.2	Stepwise representation of cell based bone regeneration……..…	**53**
Figure 4.1.1	Effect of Na_2CO_3 salt concentration on degumming of silk cocoon……...	**60**
Figure 4.1.2	Effect of degumming time……	**61**
Figure 4.1.3	Effect of degumming temperature……..	**62**
Figure 4.1.4	SEM micrographs of degummed silk fibre……...	**64**
Figure 4.1.5	Effect of temperature on solubility of SF protein…….	**65**
Figure 4.1.6	Effect of concentration of LiBr on the solubility of protein…….	**66**
Figure 4.1.7	Effect of exposure time on dissolution of silk fibroin……...	**66**
Figure 4.1.8	(a) SDS-PAGE and (b) Particle size distribution of silk fibroin…….	**68**
Figure 4.1.9	Normal % probability versus residual error in RSM……	**72**
Figure 4.1.10	Predicted versus actual response for SF extraction……...	**73**
Figure 4.1.11	RSM plots representing the effect of Na_2CO_3 concentration and temperature & their reciprocal interaction on SF yield…….	**74**
Figure 4.1.12	RSM plots representing the effect of LiBr concentration and temperature & their reciprocal interaction on SF yield…….	**74**
Figure 4.2.1	(a) Simple vertical view and (b, c, d) microscopic images of SF hydrogel…….....	**78**
Figure 4.2.2	SEM micrographs showing (a) porous leaf-like lyophilized & (b) hydrogel sponge……	**78**
Figure 4.2.3	Pictorial view of (a) Dehydrated and (b) Swollen hydrogel……	**80**
Figure 4.2.4	Thermo-rheological behaviour of SF hydrogel…….	**81**
Figure 4.2.5	X-ray diffraction of (a) degummed silk fiber and (b) lyophilized SF hydrogel…	**83**
Figure 4.2.6	Sol-gel transition of silk fibroin……	**83**

Figure 4.2.7	FT-IR spectra of (a) degummed silk fibers and (b) lyophilized SF hydrogel…..	**84**
Figure 4.2.8	TGA curves of (a) degummed silk fibers and (b) Lyophilized SF hydrogel……	**85**
Figure 4.2.9	DSC curves of (a) degummed silk fibre and (b) lyophilized SF hydrogel……..	**86**
Figure 4.2.10	Microscopic imaging of hMNCs cultured in SF hydrogels……..……	**88**
Figure 4.2.11	Phase contrast micrographs of hMNCs adhered on hydrogel surface……..	**89**
Figure 4.2.12	SEM morphology of cell encapsulated SF hydrogel……	**90**
Figure 4.2.13	Micrograph of hMNCs seeded fibroin hydrogel cultured over 2 weeks……...	**90**
Figure 4.3.1	Microscope images of (a,b) SF hydrogel and (c,d) ESM ……	**93**
Figure 4.3.2	SEM of SF scaffold prepared by salt leaching method using NaCl as porogen...	**94**
Figure 4.3.3	Mechanism of SEP conjugated with SF scaffold……..	**96**
Figure 4.3.4	SEM of SEP conjugated SF scaffold……	**96**
Figure 4.3.5	XRD pattern of (a) SF scaffold, (b) SEP-SF scaffold & (c) SEP…….	**98**
Figure 4.3.6	FT-IR spectra of (a) SF scaffold, (b) SEP-SF scaffold & (c) SEP…….	**99**
Figure 4.3.7	TGA curves (a) SF scaffold, (b) SEP-SF scaffold & (c) SEP……...	**100**
Figure 4.3.8	DSC curves (a) SF scaffold, (b) SEP-SF scaffold & (c)SEP……	**101**
Figure 4.3.9	Stress-Strain Curve of (a) SF & (b) SEP-SF scaffolds……	**102**
Figure 4.3.10	Swelling behavior of SF & SEP-SF scaffolds……...	**103**
Figure 4.3.11	Biodegradability of SF & SEP-SF scaffolds……	**104**
Figure 4.3.12	Morphology of cultured cells observed under phase contrast microscope at different magnification…….	**105**
Figure 4.3.13	Flow cytometry analysis for CD34, CD45, CD90 and CD105 expressions for hMSCs……...	**106**
Figure 4.3.14	SEM images of cell-scaffold construct on day 3(a, b), 7(c, d) & 14(e, f) days of culture……	**107**
Figure 4.3.15	Comparison of optical density of MTT formazan on SF and SEP-SF Scaffolds…….	**109**
Figure 4.3.16	ALP assay of hMSCs grown on SF and SEP-SF scaffolds……..	**110**
Figure 4.3.17	*In vivo* biocompatibility study with SEP-SF scaffolds using ICR mice model (a) Implantation of scaffold in male (b) Surgical recovery after one month in female……	**111**

Figure 4.3.18	Histological section of subcutaneous skin of mice at the site of implanted SEP-SF scaffolds……	**112**
Figure 4.4.1	SEM images of SF/PVA blends under varying process condition……...	**116**
Figure 4.4.2	SEM images of porous SF/PVA (0:100) scaffold…….	**118**
Figure 4.4.3	SEM images of SF/PVA scaffolds at blending ratio: 25/75(a, d, g), 50/50(b, e, h), 75/25 (c, f, i)……	**119**
Figure 4.4.4	SEM images of SEP conjugated SF/PVA scaffolds ……	**120**
Figure 4.4.5	XRD pattern of SF/PVA scaffolds with different blend ratios (100:0, a; 75:25, b; 50:50, c; 25:75; e 0:100, f) & SEP-(SF/PVA) (50:50, d) scaffolds……..	**122**
Figure 4.4.6	FTIR spectra of SF/PVA scaffolds with different blend ratios (100:0, a; 75:25, b; 50:50, c; 25:75; e 0:100, f) & SEP-(SF/PVA) (50:50, d) scaffolds……..	**122**
Figure 4.4.7	DSC thermograms of SF/PVA scaffold with different blend ratios (PVA:SF; 100:0, a; 75:25, b; 50:50, c; 25:75, e; 0:100, f) & SEP-(SF/PVA) (50:50, d) scaffolds……	**124**
Figure 4.4.8	Stress–strain graphs of SF/PVA scaffolds with different blend ratios (100:0, a; 75:25, b; 50:50, c; 25:75, e; 0:100, f) & SEP-(SF/PVA) (50:50, d) scaffolds…..	**125**
Figure 4.4.9	Swelling Index of SF, PVA, SF/PVA (50:50) & SEP-(SF/PVA) scaffolds…….	**127**
Figure 4.4.10	%Weight loss of SF, PVA, SF/PVA (50:50) & SEP-(SF/PVA) scaffolds……...	**128**
Figure 4.4.11	MTT Assay of hMSCs in SF (control), PVA, SF/PVA (50:50) & SEP-(SF/PVA) scaffolds for different culture period……...	**130**
Figure 4.4.12	SEM images of cell-scaffold constructs developed from SF/PVA (a,c,e,g) & SEP-(SF/PVA) (b,d,f,h) scaffolds……	**131**
Figure 4.4.13	H&E stained cross-section of the constructs developed from SF/PVA (a&b) and SEP-(SF/PVA) (c&d) scaffolds……..	**132**
Figure 4.4.14	ALP activity of hMSCs grown on developed scaffolds for 1 day, 7 days and 14 days……..……	**133**
Figure 4.4.15	Implantation of (a) SF/PVA (50:50) & (b) SEP-SF/PVA scaffold for *in vivo* biocompatibility study……...	**134**
Figure 4.4.16	Histological section of subcutaneous skin of ICR mice at the site of implanted SF/PVA (50:50) scaffolds after (a) 7 days & (b) 4 weeks……	**135**
Figure 4.4.17	Histological section of subcutaneous skin of ICR mice at the site of implanted SEP-(SF/PVA) scaffolds after (a) 7 days & (b) 4 weeks …….	**136**

List of Tables

Table 1.1	Amino acid content of *B. mori* silk fibroin…….	**9**
Table 1.2	Comparison of mechanical property of B. mori silk with other biomaterial fibers & tissues……	**13**
Table 2.1	Silk as a biomaterial for TE scaffold development……	**31**
Table 3.1	Experimental range and levels of independent variables for extraction…….	**44**
Table 4.1.1	Selection of a satisfactory model for protein extraction…….	**69**
Table 4.1.2	Box–Behnken design matrix of three variables in coded units along with the experimental and predicted values of protein yield……	**70**
Table 4.1.3	Analysis of variance for fitted quadratic polynomial model of protein yield….	**71**
Table 4.1.4	Regression coefficients & their significance of the quadratic model of protein yield……....	**71**
Table 4.2.1	Water uptake capacity of dehydrated hydrogel…….	**80**
Table 4.3.1	Pore size & porosity of SF and SEP-SF scaffolds……..	**95**
Table 4.3.2	Elemental composition of SEP, SF &SEP-SF scaffolds…….....	**97**
Table 4.4.1	Pore size & porosity of SF/PVA scaffolds prepared from SF & PVA blends….	**117**
Table 4.4.2	Water contact angles measured on various SF scaffolds……..	**128**
Table 4.4.3	Comparison of different SF based matrices……..	**137**

List of Abbreviations

3D	Three Dimensional
ALP	Alkaline Phosphatase
ANOVA	Analysis of Variance
BBRD	Box-Behnken Rotatable Design
BMP-2	Bone Morphogenic Protein-2
CD	Cluster of Differentiation
CAD	Computer Aided Design
DMEM	Dulbecco's modified Eagle's medium

DSC	Differential Scanning Calorimetry
ECM	Extracellular Matrix
EDC	1-ethyl-3-(3-[dimethylamino]propyl) carbodiimide)
EDTA	Ethylene diamine tetraacetate
ESM	Eggshell Membrane
FACS	Fluorescence Assisted Cell Shorting
FBS	Foetal Bovine Serum
FDA	Food and Drug Administration
FITC	Fluorescein Isothiocyanate
FTIR	Fourier Transformation-Infra Red
GMP	Good Manufacturing Practices
H&E	Hematoxylin & Eosin
HFIP	Hexa-Fluoro Isopropanol
hMNCs	Human Mononuclear Cells
hMSCs	Human Mesenchymal Stem Cells
hFOB	Human Fetal Osteoblastic
HA	Hydroxyapatite
ICR	Imprinting Control Region (Mice strain)
LIPS	Liquid Induced Phase Separation
MPC	2- methacryloyloxyethyl phosphoryl choline
MTT	3-[4,5-dimethyltriazol-2-y1]-2,5-diphenyl tretrazolium
MW	Molecular Weight
MWD	Molecular Weight Distribution
MWCO	Molecular weight cut-off
NHS	N-hydroxysuccinimide
OD	Optical density
PBS	Phosphate Buffer Saline
PE	Phycoerythrin
PEO	Poly(ethylene oxide)
PEG	Poly(ethylene glycol)
PHAs	Polyhydroxyalkanoates
PLA	Poly Lactic Acid
PLLA	Poly-l-lactic acid
PGA	Polyglycolic acid

PVA	Poly-(vinyl alcohol)
R&D	Research & Development
RGD	Arg-Gly-Asp (Cell adherence sequence from fibronectin)
RSF	Regenerated Silk Fibroin
RSM	Response Surface Methodology
RP	Rapid Prototyping
RT	Room temperature
SDS-PAGE	Sodium Dodecyl Sulfate Polyacrylamide Gel Electrophoresis
SEM	Scanning Electron Microscopy
SEP	Soluble Eggshell Membrane Protein
SF	Silk Fibroin
TCP	Tri-calcium phosphate
TE	Tissue Engineering
TIPS	Thermally Induced Phase Separation
TGA	Thermal Gravimetric Analysis
TGF-β	Transforming Growth Factor beta
UCB	Umbilical Cord Blood
UTS	Ultimate Tensile Strength
v/v	volume over volume
w/w	weight over weight
XRD	X-ray Diffraction

CHAPTER 1

General Introduction

GENERAL INTRODUCTION

1.1. Background

Millions of patients worldwide suffer from tissue or organ failures because of the consequencse of trauma, injury, systemic disorders, infection or other conditions that include transplantation, surgical repair and chemotherapy in few cases [Langer and Vacanti, 1993; Vacanti, 2006]. Tissue and organ failure accounts for approximately fifty percentage of total annual expenditure in health care in US [Lanza et al., 1993] and much lesser in India despite of the great need of expenditure that ultimately results in more number of patients death [Deolalikar et al., 2008]. Moreover, the current clinical treatment methods such as autologous or allogenic grafting suffer from several drawbacks including immune-rejection, disease transmission and lack of sufficient donor organs [Fuchs et al., 2001; Lanza et al., 2000; Saltzman et al., 2004]. As a result, none of these techniques can fully recover the structure and function of damaged and/or diseased tissue [Asnaghi et al., 2009]. In recent years, tissue engineering is considered as most promising approach to overcome these limitations through the development of an artificial functional tissue construct. It has been reported that tissue engineering transplant having autologous cells can effectively surmount the limitations of direct transplantation including the graft rejection and disease transmission. Most importantly such approach reduces the requirement of donors [Minas et al., 1999; Dorfman et al., 1998]**.** However, the main challeneges lie in engineering a suitable polymeric matrix, cell with their regenerative potential and delivery of signalling molecules. In this context, the design and fabrication of three dimensional scaffolds from biocompatible and biodegradable materials with tailor properties is an essential component to regulate vital cellular function such as morphogensis, differntiation, proliferation, adhesion and migration. The material properties of the scaffods and its structural charatcteristics are time factors that can affect cellular behaviour and ultimately determine the performance of a tissue engineered construct [Sundelacruz et al., 2009]. It is further evident that a single biomaterial may not possess all the desired properties and hence the development of a suitable polymer blend or composite material with appropriate composition [Cai et al., 2002] is prime requirement.

1.2. General strategies for tissue regeneration

Tissue engineering (TE) applies the principles and methods of interdisciplinary engineering and life sciences to fundamentally understand the tissue structure/function and their replacement. This medical approach offers remedy to existing problems through delivery of stem cells and bioactive molecules onto three dimensional (3D) artificial extracellular matrix [Langer and Vacanti, 1993]. During past two decades, most of the development in guided TE techniques has been based on either cells or matrices only. However, present trend in TE deals with a combination of both in addition to active macromolecules to achieve the target tissue. Thus, TE approaches can be classified on the basis of these three phenomena, either studied individually or in combination [Langer and Vacanti, 1993; Fuchs et al., 2001]:

1.2.1. *Cell and cell based therapies:* Isolated cells are directly injected intravenous or into specific host organ in cell based TE approach. Injected cells in such approach utilize blood stream as source of nutrients and bioactive molecules while the host tissue matrix as cell support system for adherence, recognition and proliferation [Matas et al., 1976]. Pros of injection approach includes the cell specificity that is needed to be supplied, and avoids any kind of surgery complications. This approach has find application in restoring lost organ metabolic function. However, the application in replacement of organ structure/function is limited. The cell based *in vivo* repair can be enhanced by *in vitro* production of specific tissues.

1.2.2. *Inducing tissue regeneration by soluble bioactive factors:* Bioactive signaling molecules such as low-molecular-weight (LMW) drugs, oligonucleotides and proteins (cytokines, chemokines, hormones, growth factors) that are capable of regulating specific cellular metabolism inside host. Such specific cellular response includes cell survival, growth, migration and differentiation of a specific subset of cells by triggering specific activation reaction in metabolic pathway [Chen et al., 2009]. Based on their cellular response, these signaling molecules can find place in overlapping classes of mitogens (stimulating cell division), growth factors (proliferation-inducing) and morphogens (controlling cell differentiation). Precise regulation of bioactivity of such signaling molecules at the damaged site may effectively control regeneration process. ECM (natural/synthetic) contains a wide range of adhesive molecules on interfacial surface to bind and modulate the bioactivity of signaling molecules [Discher et al., 2005; Ramirez et al., 2003].

1.2.3. *Employing artificial support system (scaffold)*: In this approach, cellular or acellular scaffold system consisting of natural or synthetic biomaterial is implanted into the host. In cell culture study it has been found that detached adult cells tend to reform their original structures in different set of micro-environmental conditions [Folkman et al., 1980]. Isolated donor cells also have the potential for morphogenesis but limited when injected as a suspension into the host. This is primarily due to of absence of 3D support system immerged in a pool of bioactive molecules that provide *in vivo* microenvironment. In addition, implantation of larger tissue volume faces limited interaction with host environment for nutrients uptake, gas exchange and waste elimination. Such findings have lead to developing artificial tissue construct by attaching cells on scaffold templates.

1.3. Overview of potential Tissue Engineering applications

Tissue engineering aims at regenerating the diseased tissues (and organs as a future perspective) *in vitro* or through a combination of *in vitro* and *in vivo* processes and implanting the product at the diseased site to achieve full functionality. Improved healing processes and a higher quality of life are expected results, probably leading to lower costs of treatment in the long term. It offers the potential of a paradigm shift in medicine: new forms of therapy can be envisioned which allow the repair or regeneration of cells, tissues and organs which have lost their function due to disease, injury or congenital defects. Potential applications of tissue engineering are envisioned in the following fields:

i. Skin,
ii. Cartilage,
iii. Bone,
iv. Cardiovascular diseases,
v. Organs,
vi. Central nervous system,
vii. Miscellaneous e.g. ligaments, tendon, skeletal muscle etc.

Although tissue engineering research is being carried out in all these fields, only a very few products have already entered the market, and the present state of the art in science and technology does not allow a precise assessment which of these developments will finally yield new therapeutic options and commercially viable products. Therefore, a broad variety of information sources and methods has to be used for potential tissue engineering.

1.4. Tissue Engineering challenges and future prospects

1.4.1. TE Research & Development

The field challenge concerns acquiring a **fundamental understanding of tissue differentiation mechanisms** that might be harnessed for the development of tissue-engineered products. One product that the tissue engineering industry is pursuing is "bone-on-demand," to be used in cases where new bone formation is needed. One component is the availability of **biomaterials that act as scaffolds** for tissue repair and reconstruction, or for the deposition of engineered tissues and cells preceding implantation. Recent research is directed towards addressing these scaffolds with the goal of creating materials that have the desired functional properties for tissue engineering applications. For example, so-called blended-polymer scaffolds have an extended lifetime in the body that is more suitable for orthopedic applications than non-blended scaffolds [Spain et al., 1998]. Development of new materials of this type that enable different applications of tissue engineering is likely to be the focus of considerable future research. For the biological component of tissue engineering, rapid advances are being made in **identifying new cell types** for use in tissue regeneration. For example, undifferentiated stem cells are attracting intense interest because of their capacity to be transformed into almost any cell type that may be needed.

1.4.2. TE Clinical Barriers

The ultimate goal of tissue engineering is to produce tissues that will function successfully for the lifetime of the recipient. According to Griffith and Naughton [Griffith et al., 2003] specific methods are needed to assess quantitatively the long-term outcome of engineered connective tissues, such as cartilage, tendon and blood vessels. Failure of these engineered tissues may be fetal. To date, tissue engineering has been successful in producing simple vascular tissues, such as skin and cartilage which are sufficiently thin to receive oxygen and other nutrients by passive diffusion [Malda et al., 2003]. Molecular diffusion is only relevant at very small length-scales, and thus found inadequate to support mass transfer in a thick tissues. A major obstacle in tissue engineering is the inability to maintain large masses of living cells upon transfer from ~~the~~ in vitro culture conditions into the host in vivo [Mooney et al., 1999]. In order to achieve complex-engineered tissues and organs, vascularization of the regenerating tissue is essential. Vasculature and in particular capillaries, are required to supply essential nutrients to the cells, supplying oxygen, removing waste and providing a biochemical communication "highway" [Koet al.,

2007; Cassell et al., 2002; Eiselt et al., 1998; Nerem et al., 1998; Nguyen et al., 2001a; Nguyen et al., 2001b]. All tissues and organs (with the exception of a minority of tissues such as cartilage) need to be vascularized to be able to survive.

1.4.3. Industrial Challenges

Quality control of the materials used in various surgical applications is a key challenge for the tissue engineering industry. For example, living human cells are being used in scaffolds to repair structural tissue damage. These materials need to be produced and cultured under good manufacturing practice (GMP) conditions to meet FDA standards especially the cells that are grown *ex vivo*. As a result, the tissue engineering industry is striving to create appropriate quality control standards and evaluate them.

1.4.4. Future Prospective of Tissue Engineering

With the advancement of the concept of "regenerative medicine" and in particular the field of tissue engineering a completely new form of medical treatment can be envisaged with the potential to change medical practice profoundly. Tissue engineering is emerging as a vibrant industry with a huge potential market. The biomaterials, scaffolds, artificial organs, and differentiating cells that are combined to create a tissue engineering product address significant medical needs, such as major tissue and organ damage or failure. The industry still faces numerous technical challenges including the establishment of a consensus quality control program that ensure the functionality and safety of tissue engineering products. Efforts to address these issues are underway, and if past success is any indication, this technology is certainly one that will have major impact in future health care practice.

Tissue engineering has significant market potential and financial investment continues apace. The positive results regarding specific products and processes in clinical settings will support the R&D scenario of field. Technical advances in the various components of the industry will contribute to market growth. In future, efforts will likely increasingly focus on the development of tissue-engineered products under consensus safety and efficacy standards, including potential source of cells and tissues, characterization and testing of materials, quality assurance and control, preclinical and clinical evaluation [Omstead et al., 1998]. The FDA has already provided some regulatory guidance concerning specific materials, such as certain marketed artificial skin products; in the next few years, these guidelines will likely be increasingly formalized and

structured, ensuring that tissue engineering products not only work but are also safe. Significant future developments will include the continued development of artificial organs that use cells embedded into appropriate support structures. The range of human tissue that can be engineered will also increase dramatically in the future, so in addition to the traditional targets, such as skin and liver, other tissues and organs will see their day. A great deal of excitement in clinical circles is that of developing artificial human thyroid tissues which are capable of producing T cells, and this will be a major area for continued R&D [Martin et al.,2000]. Finally, stem cells and their manipulation for therapeutic purposes will continue to be a major area of development, because of the pluripotency of these cells.

1.5. Silk as Ideal Biopolymer for Tissue Engineering

In general, silks are defined as protein polymers that are produced by *Lepidoptera* larvae undergoing complete metamorphosis or adult forms eg. silkworms, spiders, scorpions, mites and flies [Altman et al., 2003] which differ at the molecular level. Silk has been of interest since its discovery in china in around 5000 years back and is being manufactured through sericulture across Asia and Europe. India is the second largest producer and largest consumer in the world [Giridhar et al., 2010]. The commercial interest of silk is not only for its textile properties such as texture, tenacity and dyeing butalso for its application in cosmetic products andpharmaceuticals [Brooks et al., 1989]. The wide application of silk as biomedical sutures over decades have shown path to their utilization as bio-polymeric scaffolds in tissue engineering. Besides the biocompatibility with host tissue, the mechanical strength of a biomaterial plays important role in scaffold designing [Li et al., 2002; Ko et al., 1998; Ko et al., 1999]. The viscoelastic nature of biological tissues confines the application of synthetic polymers since it has been observed that increase in strength compromises with toughness of synthetic polymers. Silk finds the ideal candidature for biomedical applications because of combined strength and toughness, primarily due to its antiparallel β pleated molecular structure. Among varieties of silk sources, those from silkworm silk (*Bombyx mori*) and spider silk (*Nephila clavipes*) are most extensively used for various applications. While the availability of *Bombyx mori* silk is abundant due to farming, the practice is almost impossible with *Nephila clavipes* because of their predatory nature. The progress in biotechnology have made possible to produce recombinant type spidroinin a variety of host organisms.This chapter deals with the silk protein from most common silkworm species, *Bombyx mori* and its application in bio-scaffold development for tissue regeneration.

1.5.1. Structure and composition

Silkworm silk is commonly produced from the cocoons of domestic moths, *Bombyx mori*. Silk fibers are 10-25 μm in diameter. Each fiber consists of core protein covered by a coating of hydrophilic proteins called sericins (20–310 kDa) that glues core fibers together [Sinohara et al., 1979; Kaplan et al., 1998; Zhou et al., 2000; Inoue et al., 2000]. The fibers are not circular in cross section but appear triangular as shown in Figure 1.1. Twenty-five to thirty percent of the silk cocoon mass is sericin, which is removed during the de-gumming process. The core protein consists of three chains: heavy chain (~390 kDa), light chain (~26 kDa) and a glycoprotein, P25 (25 kDa) [Inoue et al., 2000]. The disulfide linkage between the Cys-c20 (twentieth residue from the carboxyl terminus) of the heavy chain and Cys-172 of the light chain holds the fibroin together and a 25 kDa glycoprotein, named P25, is non-covalently linked to these proteins [Tanaka et al.,1999]. Light chain is necessary for the secretion of protein from the silk glands. P25 is connected to both heavy and light chains by noncovalent interactions. P25 is necessary for the assembly of heavy and light chains [Inoue et al., 2000]. Heavy chain is fiber forming protein and its structure determines properties of silk fiber. Heavy chain is commonly referred as fibroin protein. Electrophoretic analyses of silk cocoons have revealed the presence of several minor proteins of unknown function. These low molecular weight proteins are classified as non-structural silk proteins [Kodrik et al., 1992].

- The gene for the fibroin protein (*H-fib* gene) is located on 25th chromosome of *Bombyx mori* silkworm and consists of two exons and one intron [Zhou et al., 2000, Zhou et al., 2001]. A number of silk polymorphs have been reported, including the glandular state prior to crystallization (silk I), the spun silk state which consists of the β-sheet secondary structure (silk II), and an air/water assembled interfacial silk (silk III, with a helical structure) [Kaplan et al., 1998; Jin et al., 2003; Motta et al., 2002]. The silk I structure is the water-soluble state and upon exposure to heat or physical spinning easily converts to a silk II structure. The silk fibroin obtained from silkworm cocoon exists in silk II structure consisting of 5263 residues with molecular weight of 39.1kDa. The primary structure of heavy chain consists of 12 repetitive regionscalled crystalline regions and 11 non-repetitive interspaced regions called amorphous regions [Zhou et al., 2001].

- The crystalline regions make up 94% of the sequence and each repetitive region in an average 413 residues in length and consist of Gly-X repeats (X=Ala/ Ser/Thr/Val) [Zhou et al., 2001] forming hexapeptides sub-domain including: GAGAGS, GAGAGY, GAGAGA and GAGYGA as shown in table 1.1. These sub domains end with tetrapeptides such as GAAS or GAGS [Zhou et al., 2000; Zhou et al., 2001; Gage et al., 1980]. The repeat GAGAGS is the most frequently (70%) occurring hexapeptide repeat sequence. The crystalline repetitive region is responsible for the secondary structure (antiparallel β-pleated sheets) of the protein. Each crystal is on an average made up of 4 individual β strands each 11 amino acids long. The β strands are connected to one another by β turn made up of GAAS amino acids. The full form of abbreviations used for amino acids is given in **appendix A.**

- The β-sheet structures are asymmetrical with one side occupied with hydrogen side chains from glycine and the other occupied with the methyl side chains from the alanines that populate the hydrophobic domains. The β-sheets are arranged in such a way that the methyl groups and hydrogen groups of opposing sheets interact to form the inter-sheet stacking in the crystals. Strong hydrogen bonds and van der Waals forces generate a structure that is thermodynamically stable [Kaplan et al., 1998]. The inter and intra-chain hydrogen bonds form between amino acids perpendicular to the axis of the chains and the fiber [Kaplan et al., 1998].

Table 1.1: Amino acid content of *B. mori* silk fibroin [Kaplan et al., 1998; Gandhi M.R., 2007]

AAs content		**Hexapeptide repeats content**	
Gly	45.9%	GAGAGS	70%
Ala	30.3%	GAGAGY	20%
Ser	12.1%	GAGYGA	6%
Tyr	5.3%	GAGAGA	4%
Val	1.8%		
Other AAs	4.7%		

- The amorphous regions consist of 42-43 residues and are linkers between repetitive domains [Zhou et al., 2001]. The less crystalline forming regions of the fibroin heavy chain, also known as linkers, are between 42–44 amino acid residues in length. All the linkers have an

identical 25 amino acid residue (non-repetitive sequence) which is composed of charged amino acids not found in the crystalline regions [Zhou et al., 2001]. The primary sequence results in a hydrophobic protein with a natural co-block polymer design.

1.5.2. Bio-relevant Properties

1.5.2.1. Physical properties

- Silk fibres from the *Bombyx mori* silkworm have a triangular cross section with rounded corners, 5-10 μm wide. The fibroin-heavy chain is composed mostly of beta-sheets, due to a 59 aminoacid repeat sequence with some variations [Lewin et al., 2006]. The flat surfaces of the fibrils reflect light at many angles, giving silk a natural shine. Silkworm fibres are naturally extruded from two silkworm glands as a pair of primary filaments (brin), which are stuck together, with sericin proteins that act like glue, to form a bave (Fig 1.1A. SEM photographs).
- Silk has a smooth, soft texture that is not slippery, unlike many synthetic fibers.
- Silk is one of the strongest natural fibres but loses up to 20% of its strength when wet. It has a good moisture regain of 11%. Its elasticity is moderate to poor if elongated even a small amount, it remains stretched.
- Silk is a poor conductor of electricity and thus susceptible to static cling.
- Natural and synthetic silk is known to manifest piezoelectric properties in proteins, probably due to its molecular structure [Fukada et al., 1983].
- An important feature of silk as a biomaterial, compared with other fibrous proteins such as collagen, is the versatility of options for **sterilization** [Sugihara et al., 2000]. Sterilization of silk fibroin scaffolds by autoclaving does not change morphology [Meinel et al., 2004a] or β-sheet structure when heated to 120°C [Furuzono et al., 2004]. Comparatively, collagen denatures at these temperatures [McClain et al., 1972]. Silk fibroin scaffolds can also be sterilized using ethylene oxide [Altman et al., 2003], γ-radiation, or 70% ethanol [Karageorgiou et al., 2004; Li et al., 2006].

1.5.2.2. Chemical properties

- The high proportion (50%) of glycine, which is a small amino acid, allows tight packing and the fibers are strong and resistant to breaking. The tensile strength is due to the existence of

many inter seeded hydrogen bonds that works when fibres are stretched, resisting breakage due to the applied force.

- Silk is resistant to most mineral acids, except sulfuric acid. Silk becomes yellow in colour by perspiration.
- The silk I structure is observed in vitro in aqueous conditions and converts to a β-sheet structure when exposed to methanol or potassium chloride [Huemmerich et al., 2006].
- The silk II structure excludes water and is insoluble in several solvents including mild acid and alkaline conditions, and several chaotropes. Silk is insoluble in most solvents, including water, dilute acid or dilute alkaline solutions.

1.5.2.3. Mechanical Properties

The properties of silk are due to the extensive hydrogen bonding, hydrophobic nature of protein, and significant crystallinity. The elastic modulus of *Bombyx mori* silk is 15-17 GPa and has a tensile strength of 610-690 MPa [Altman et al., 2003]. While spider silk has strength as high as 1.75 GPa with a breaking elongation of over 26%. The geometry and mechanical properties are important design criteria for Tissue engineering scaffolds. The study conducted by Altman G.H. et al [Altman et al., 2003] is summarized in table 1.2. It indicates that the tensile strength of silk is much higher than polylactic acid (PLA) which is most commonly used biomaterial. PLA has the tensile strength of 28-50 MPa. In tissue engineering, scaffolds provide initial framework for the cells to grow and attach. The strength should be high enough to withstand initial loading conditions. Tendon and bone has the tensile strength of 150 and 160 MPa respectively. PLA with the low tensile strength is not able to provide strong support for the tendon or bone cells to proliferate. Cross linked collagen with the tensile strength of 47-72 MPa is also not strong enough. Silk which is much stronger than PLA and cross linked collagen, will provide enough support.

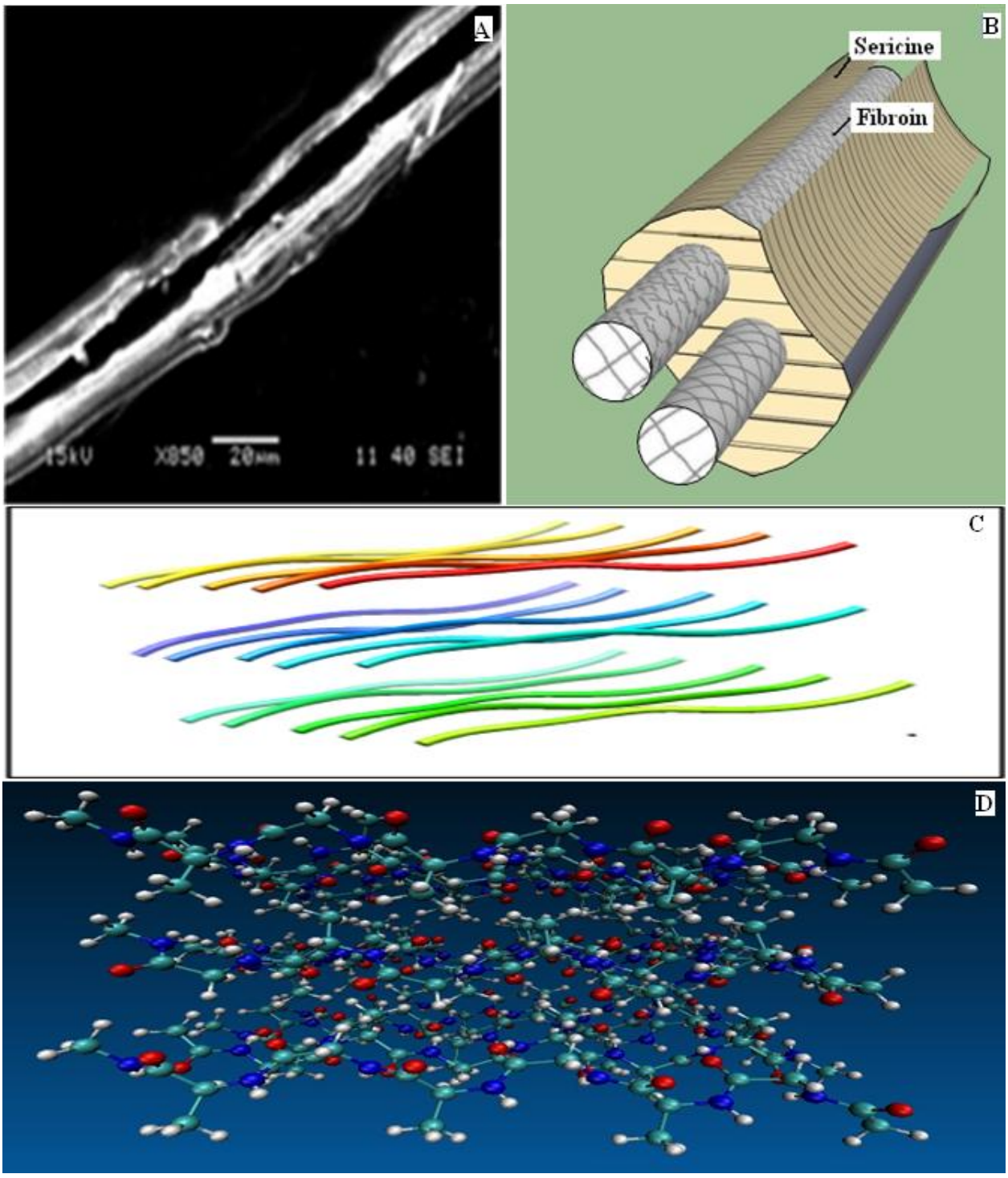

Figure 1.1: (A) SEM image showing cross section of *Bombyx mori* silk fiber (B) structure of silk fibre and (C, D) the schematic of structure of *Bombyx mori* silk fibroin protein. The primary structure consists of 12 repetitive regions interspaced by 11 non-repetitive regions. The repetitive region is responsible for the formation of β-sheets crystals while the non-repetitive region forms the amorphous part of the protein.

Table 1.2: Comparison of mechanical property of *B. mori* silk fiber with other biomaterial fibers and tissues [Gosline et al., 1999; Cunniff et al., 1994]

Fibre	UTS (MPa)	Elastic Modulus(GPa)	% Strain at break
B. mori silk	740	10	20
Spider silk	875-972	11-13	17-18
Tendon (comprised of mainly collagen)	150	1.5	12
Bone	160	20	3
Kevlar 49 fiber	3600	130	2.7
Synthetic Rubber	50	0.001	850

1.5.2.4. Biological Properties

Apart from the geometry and mechanical properties; biocompatibility and biodegradation are important considerations for the fabrication of scaffolds. Silk materials are of considerable interest due to their structural properties and superior biocompatibility.

1.5.2.4.1. Biocompatibility

There were several concerns regarding the biocompatibility of silk from *Bombyx mori*. Sutures made from virgin silk compared with sutures from de-gummed silk showed differences in hypersensitivity [Altman et al., 2003]. The inflammatory response of de-gummed silk fibroin *in vitro* compared with polystyrene and poly(2-hydroxyethyl methacrylate) showed less adhesion of immuno-competent cells [Santin et al., 1999]. Virgin silk (fibroin containing sericin gum) is potential allergen but degummed silk in which sericin is removed is biocompatible. Sericin, a glue-like protein that holds the fibroin fibres together, has been identified as the source of immunogenic reactions [Soong et al., 1984, Panilaitis et al., 2003]. Numerous in vitro studies have demonstrated that once sericin is extracted, fibroin supports cell attachment and proliferation for a variety of cell types [Gupta et al., 2007; Roh et al., 2006; Servoli et al., 2005; Minoura et al., 1995; Jin et al., 2004; Inouye et al., 1998]. *In vitro* evaluation of degummed fibroin demonstrates that the interactions of fibroin with the humoral components of the inflammatory system are comparable with those of polystyrene and poly (2-hydroxyethyl methacrylate), the two materials used extensively for biomedical applications [Santin et al., 1999]. Silk films implanted *in vivo* induced a lower inflammatory response than collagen films and PLA films [Meinel et al., 2005]. Silk fibroin non-woven mats implanted subcutaneously in

rats induced a weak foreign body response and no occurrence of fibrosis. There was little upregulation of inflammatory pathways at the implantation site and no invasion by lymphocytes after six months *in vivo* [Dal et al., 2005].

1.5.2.4.2. Biodegradation

The degradation of biomaterials is important in terms of restoring whole tissue structure and function *in vivo*. Control over the rate of degradation is an important feature of functional tissue design, such that the rate of scaffold degradation matches the rate of tissue growth [Lanza et al., 2000]. Silk fibroin fibers retain more than 50% of their mechanical properties after two months of implantation *in vivo*; thus, they are defined as a non-degradable biomaterial by the United States Pharmacopeia [Horan et al., 2005]. Natural polymers like collagen and silks degrade via the action of proteases. The rate of silk fibroin degradation depends upon the structure, morphology, mechanical and biological conditions at the location of implantation. Degradation studies involving the systematic exposure of silkworm silk to enzymes have found that silk will degrade as a result of proteolysis [Taddei et al., 2006], with protease being reported to have the greatest effect [Arai et al., 2004; Horan et al.,2005; Li et al., 2003]. A correlation between *in vitro* and *in vivo* rates of degradation of silk fibroin fibers has also been established [Horan et al., unpublished]. Arai *et al*. [Arai et al., 2004] compared degradation of silk fibers with silk films when exposed to different amounts and types of enzymes. Silk fibroin porous sponges from regenerated *B. mori* fibers degraded differently with different processing conditions [Kim et al., 2005c]. Silk fibroin degradation could be regulated by changing crystallinity [Minoura et al., 1990a], pore size, porosity, and molecular weight distribution (MWD) of the silk fibroin. A change in MWD can be achieved by treating silk fibroin under alkaline conditions and heat. A decrease in MWD may disrupt ordered structures and reduce cross-links, potentially resulting in faster degradation. It will be useful to understand the mechanism and correlation of silk fibroin degradation with mechanical properties. The degradation of silk fibroin material also depends on the processing method for biomaterial development. The degumming process may cause unwanted degradation of fibroin [Jiang et al., 2006] while methanol treatment may significantly reduce the rate of degradation [Minoura et al., 1990b; Uebersax et al., 2006]. Fibroin films are reported to experience more significant degradation than fibres [Arai et al., 2004] and aqueous-derived silk fibroin scaffolds degrade more rapidly than hexa-fluoro isopropanol (HFIP) derived scaffolds [Kim et al., 2005c], possibly due to increased surface area. The potential to

manipulate the rate of degradation is important for tissue engineering applications, and control over the physical form and post-treatment of a silk biomaterial may allow tailoring of the degradation. In the case of bone, for example, the ability of a scaffold to maintain structural integrity over an extended period of time is crucial as it allows mass transport of nutrients and waste products while bone ingrowth, matrix deposition and remodelling occurs and a vascular network is formed. In other situations, such as wound healing, more rapid degradation may be desirable. Silkworm silks have similar structural characteristics to amyloid [Li et al., 2001] and dissolved fibroin has been reported to accelerate amyloid accumulation in mice [Lundmark et al., 2005]. The presence of amyloids in the body has been linked with neuro-degenerative diseases including Alzheimer's and Parkinson's.

1.5.3. Control of morphology of silk biomaterials

Several different material morphologies can be formed from aqueous or solvent formulations of the natural fiber form of silk for utilization as biomaterials in biomedical applications. The fibers must first be dissolved in aqueous systems, followed by reprocessing into desired material formats. The processibility of silk into a number of forms provides flexibility in their application for different kinds of tissue engineering. The commonly applied forms of native silk may be classified as below:

1.5.3.1. Silk fibers—Silk fibers can be obtained by reeling from silkworm cocoons [Kaplan et al., 1998]. Sutures braided from silk fibers have been used for centuries in gummed (virgin) and de-gummed (black braided silk) forms as sutures for surgical options [Altmanet al., 2003]. A thorough review of the utilization of virgin and black braided silk (coated with silicone or wax to prevent fraying) and associated immune responses has been previously described [Altman et al., 2003]. Silk sutures have been used for tendon tissue engineering [Kardestuncer et al., 2006]. Sutures modified with immobilized Arg-Gly-Asp (RGD) peptide to increase cell attachment, were cultured with human tenocytes and supported increased adhesion after 3 days when compared with unmodified silk fiber and tissue cultured plastic [Kardestuncer et al., 2006]. An increase in collagen type I and decorin transcript levels was observed on the RGD-modified sutures compared with unmodified silk and tissue culture plastic at six weeks [Kardestuncer et al., 2006].

1.5.3.2. Non-woven silk fibroin mats—Non-woven mats are of interest due to the increased surface area and rougher topography for cell attachment. Silk fibroin has been used to generate non-woven silk mats from reprocessed native silk fibers or by electrospinning. Electrospun fibers can be produced in a wide range of diameters, ranging from a few nanometers to a few microns depending on the mode of processing [Reneker et al., 1996]. Electrospinning of aqueous silk fibroin solution mixed with poly(ethylene oxide) (PEO) was established and fiber morphology based on scanning electron microscopy (SEM) analysis showed uniform fibers less than 0.8 μm in diameter [Jin et al., 2002]. hMSCs cultured on these mats showed attachment and spreading [Jin et al., 2004]. Silk fibroin mats prepared from formic acid with fiber diameters averaging 100 nm showed a Young's modulus of 515 MPa, ultimate tensile strength (UTS) of 7.25 MPa and strain of 3% [Ayutsede et al., 2005]. Electrospun non-woven meshes can be prepared as predominately random coil structure from which β-sheet structures can be formed via methanol treatment [Min et al., 2004].

1.5.3.3. Silk fibroin films—Silk fibroin films have been cast from aqueous or organic solvent systems, as well as after blending with other polymers. Silk films prepared from aqueous silk fibroin solution had oxygen and water vapor permeability dependent on the content of silk I and silk II structures [Minoura et al., 1990a, 1990b]. Alteration of silk structure was induced by treatment with 50% methanol for varying times. Changes in silk structure resulted in differing mechanical and degradability properties of the films [Minoura et al., 1990b]. Nanoscale silk fibroin films can also be formed from aqueous solution using a layer-by-layer technique [Wang et al., 2005]. These ultrathin films were stable due to hydrophobic interactions and predictable film thickness could be obtained based on control of solution conditions.

1.5.3.4. Silk fibroin hydrogels—Hydrogels are three-dimensional polymer networks which are physically durable to swelling in aqueous solutions but do not dissolve in these solutions. Hydrogel biomaterials provide important options for the delivery of cells and cytokines. Silk fibroin hydrogels have been prepared from aqueous silk fibroin solution and are formed from β-sheet structures [Kim et al., 2004; Ayub et al., 1993]. An increase in silk fibroin concentration, increase in temperature, decrease in pH, and an increase in Ca^{++} concentration decreased the time of silk fibroin gelation. Hydrogel pore size was controllable based on silk fibroin concentration and temperature [Kim et al., 2004].

1.5.3.5. Silk fibroin porous sponges—Porous sponge scaffolds are important for tissue engineering applications for cell attachment, proliferation, and migration, as well as for nutrient and waste transport. Regenerated silk fibroin solutions, both aqueous and solvent, have been utilized in the preparation of porous sponges. Sponges have been formed using porogens, gas foaming, and lyophilization [Nazarov et al., 2004]. Solvent-based sponges were prepared using salt or sugar as porogen. Solvents like 1,1,1,3,3,3-hexafluroisopropanol (HFIP) do not solubilize salt or sugar; so pores sizes in the sponges reflect the size of the porogen used in the process [Nazarov et al., 2004].

1.6. Scope and Objective

It is fact that there is urgent need of alternative treatment for tissue diseases, tissue injuries and organ failure because of having several limitations associated with the current clinical methods including insufficient tissue regeneration because of poor cell retention and survival, immuno-rejection, significant donor site morbidity leading to loss of functional tissue. In this situation, recently, tissue engineering has been emerged as an attractive alternative technique for the clinical treatment of damaged and/or diseased tissue through the generation of functional tissue. In this context, the design and fabrication of a suitable three dimensional (3D) artificial extra cellular matrix from biocompatible and biodegradable materials with tailor properties is the main challenge. Among the various polymeric biomaterials, silk fibroin obtained from silk cocoon has been reported to be a potential candidate for the tissue engineering application. It is ultimately demonstrated that a combination of different polymers and/or their composites with other bioactive substances are essential to meet the desired properties of the scaffold for clinical tissue engineering application. In this strategy, in the present work 3-D matrices with desired surface, structural and biological properties will be fabricated from silk fibroin protein and PVA polymers by applying salt leaching method.

The objectives of the thesis work are:

i. Optimization of process conditions for extraction of silk fibroin from *B. mori* silk cocoon
ii. To prepare silk fibroin based porous scaffold by salt leaching method
iii. To modify the surface properties of scaffold for enhanced cell adhesion and proliferation
iv. To characterize the prepared scaffolds
v. To study the biocompatibility of scaffolds by *in vitro* cell culture and *in vivo* animal model

1.7. Thesis Outline

The whole thesis work has been organized in 5 chapters as follows: **Chapter 1-** includes the introduction and significance of the research work**, Chapter 2-** presents the literature review including concepts and fundamental understanding of recent advancement in silk based tissue engineering and possible improvement in potency of current implantable silk fibroin biopolymers in tissue repair. It has also been discussed, the need and possible ways to improve their bio-relevant properties of SF scaffold to make it more effective to be used as tissue engineering scaffold materials, **Chapter 3-**presents the materials and methods employed for the preparation of silk fibroin matrices and heir physical, chemical and biological characterisation, **Chapter 4-** deals with the results and discussion of experimental work which is subdivided into the following parts: ***Part I*** reports the optimization of process conditions to rgenerate native silk into silk fibroin solution and its characterization. The objective of ***Part II*** is to examine the processability of concentrated aqueous silk fibroin solutions into highly porous gel spongesand study of their various properties for possible tissue engineering applications. ***Part III*** deals with the development and characterization of salt leached silk fibroin scaffolds and their comparative study after cross-linking with eggshell membrane (ESM) protein. ***Part IV*** demonstrates the green process for the fabrication of SF/PVA scaffolds of various pore sizes and their modification with SEP with an aim to study their bio-relevant properties, **Chapter 5-** includes a brief summary and conclusion of the thesis work along with suggested future study.

CHAPTER 2

Literature Review

LITERATURE REVIEW

2.1. Biomaterials for scaffold development

According to the European Society for Biomaterials (ESB), the definition of 'Biomaterial' is material intended to interface with biological systems to evaluate, treat, augment or replace any tissue, organ or function of the body [Williams et al., 1999]. In general, a biomaterial is a non-living substance used as a medical device that is designed to regulate the cellular behavior in biological microenvironment [Davis et al., 2005]. Biomaterial-based 3D porous systems present an ideal substrate for cell–cell and cell–material communications both in culture and inside the body, and their properties can be modified to induce differentiation of cells into specific lineages [Sundelacruz et al., 2009]. In recent years, wide range of natural and synthetic biomaterials have been developed and designed for this purpose. Typically, three main classes of biomaterials, such as ceramics, synthetic polymers and natural polymers, are used for scaffolds fabrication in tissue engineering.

2.1.1. Natural polymers

The use of natural polymers as scaffold materials is most promising for tissue engineering and other biomedical applications because of their excellent biocompatibility and biodegradability. In the last decade natural materials, such as collagen, silk fibroin, various proteoglycans, alginate based substrates and chitosan, have drawn much attention in the field of tissue engineering [Pati et al., 2013; Bhat et.al. 2013; Liu et al., 2010; Gomathi et al., 2003]. The scaffolds made up of natural polymers are biologically active and promote cell proliferation and adhesion. In addition, they are biodegradable and replaced by biological ECM over time. However, such scaffolds face challenges being homogenous, reproducibility of structure and load bearing strength for orthopedic applications.Therefore, it is reported that these polymers must be further modified with improved form [Das et al., 2012] and property that is desirable for tissue engineering applications [Jayasinghe et al., 2010]. Polymers from natural sources such as proteins, polysaccharides and polyesters are considered to be potential candidates for scaffold preparation.

2.1.1.1. Protein-derived polymers

The most important protein derived polymers used for scaffold preparation are collagen and silk fibroin proteins. Type I Collagen is the most abundant and widely investigated for tissue

engineering applications [Hayashi, 1994]. Heat treatments and/or chemical glycation procedures are used to fabricate matrices with adequate mechanical properties. Collagen microsponges into synthetic polymeric scaffolds increase their mechanical performance [Chen et al., 2004]. Collagen-based scaffolds, combined with active agents like growth factors have more therapeutic influence on tissue engineering approaches [Wallace and Rosenblatt, 2003]. Another important polymer is silk protein that has robust mechanical properties due to presence of highly repetitive primary sequence of simple amino acids leading to formation of β-sheets. Research have shown the utilisation of silk fibroin in tissue engineering applications, particularly where high mechanical strength and slow biodegradation is required [Altman et al., 2003]. Experimental studies of MSCs seeded highly porous silk scaffolds for in vitro cartilage [Wang et al., 2005] and bone [Kim et al., 2005] regeneration have shown promising results.

2.1.1.2. Polysaccharides

Polysaccharides have wide applications in tissue engineering particularly for the enhancement of desired mechanical properties. These biopolymers can broadly be divided into four major groups according to the sources from which these are obtained. The polysaccharides are subdivided, based on their chemical structure. Starch and cellulose are the most important plant saccharides having tissue engineering application particularly for bone regeneration [Wan et al., 2006; Salgado et al., 2002]. The cohesive and hydrogen-bonded structure of cellulose fibres makes it exceptionally water insoluble with great strength exhibiting poor degradation in vivo. Alginate, an algal polysaccharide has potential to combine with calcium [Percival and McDowell, 1990] and this property is reported to have mineralisation effect in orthopaedic tissue engineering. Chitin and its derivative chitosan obtained from animal exoskeleton have been studied for bone regeneration and have been found with excellent biodegradability and cell-adhesive property [Venkatesan and Kim, 2010]. Hyaluronic acid, an important GAG component has been used for finishing the scaffold surface for improving its biocompatibility [Mao et al., 2003]. Non-toxicity of Pullulan and unique rheological properties of xantan gum from microbial culture also finds application in vivo. Bacterial cellulose (BC) has high water- holding capacity, crystallinity, biocompatibility and shows high tensile strength in wet state [Mano et al., 2007].

2.1.1.3. Naturally derived polyesters

Polyhydroxyalkanoates (PHAs) obtained from micro-organisms are thermoplastic polyesters with good biodegradability and biocompatibility. Among various PHAs, PH (Butyrate) and PH (Butyrate- co-Valerate) are commonly used for tissue engineering applications. More flexible, less crystalline and easy to process scaffold materials can be produced by copolymerization of pure PHB. These materials can be used as support material for tissue engineering application [Masaeli et al., 2013].

2.1.2. Synthetic Polymers

Various synthetic polymers have been employed for scaffolds development including poly-l-lactic acid (PLLA), polyglycolic acid (PGA) and their copolymer poly-dl-lactic-co-glycolic acid (PLGA). These materials have been much successful towards cartilage, bone, skin, bladder, and liver TE since their architecture and degradation can be well controlled by varying individual polymer composition [Lu et al., 2000; Oh et al., 2003; Rowlands et al., 2007]. However, limitations of these polymers include the risk of implant rejection due to less bioactivity and the degradation byproduct (CO_2 gas) that lowers the local pH finally responsible for cell and tissue necrosis [Liu et al., 2006].

2.1.3. Ceramics

Ceramic scaffolds, such as hydroxyapatite (HA) and tri-calcium phosphate (TCP) can be used for bone regeneration and generally not used for soft tissue regeneration. Such scaffolds are characterized by high mechanical strength, low elasticity, and a hard brittle surface. In bone tissue engineering, they exhibit chemical and structural similarity to the mineral phase of native bone and enhance osteoblast differentiation and proliferation [Hench et al., 1998; Ambrosio et al., 2001]. The application of ceramics is common in dental and orthopedic surgery for filling and coating implant surface of host bone. However, due to their brittleness and difficulty in remodeling check their clinical application of scaffold based bone regeneration [Wang et al., 2003]. In addition, with ceramic scaffolds, difficulty has been reported to control their biodegradation rate [Tancred et al., 1998].

2.1.4. Polymer/Polymer blend and Polymer/Ceramic Composite

Each of the individual biomaterial groups mentioned above has some pros and cons, so the development of composite scaffolds comprising a number of phases is becoming increasingly important. For example, different research groups have attempted to integrate ceramics into polymeric scaffolds [Kim et al., 2006; Huang et al., 2008] while many others have combined natural polymers with other natural [Cai et al., 2002] or synthetic polymers [Wu et al., 2007] in order to improve their biological activity. Composite or blend materials, combining natural and synthetic polymers, have been developed to combine the desired characteristics of both polymer to overcome the drawbacks of organic material classes. Such scaffolds show some promise towards successful implantation, at least one phase cause problem associated with biocompatibility, biodegradability or both. Most of the biomaterials in scaffolds can be improved by modifying their surfaces chemically or physically, and a variety of such surface modified scaffolds have been used for investigating cells behaviour [Mano et al., 2007]. Modification of biomaterials and understanding of cell behavior have made it clinically possible to replace or reconstruct damaged host cells and tissues [Beckstead et al., 2006]. Development of cell-material microarrays has allowed rapid testing of biomaterial interactions with cells [Peters et al., 2009]. Considerable research work has been done to develop, design and demonstrate the increasing advantages of polymer based cell system in tissue regeneration [Chen et al., 2004; Chen et al. 2002]. As far as there is advancement in biomaterial research, new biomaterials and novelty in their usage will continue to emerge.

2.2. Scaffold Fabrication Methods

A variety of well-known fabrication techniques are used in scaffold design for TE applications. A well-designed three-dimensional scaffold is one of the fundamental requirements that guide tissue formation *in vitro* and *in vivo.* Frontiers areas in medicine is changing rapidly from utilizing synthetic implants and tissue grafts to a tissue engineering approach that uses degradable porous scaffolds integrated with biological cells or molecules to regenerate tissues [Hollister et al., 2005]. Therefore, the selection of scaffold is important to enable the cells to behave in the desired manner to generate tissues and organs of the desired shape and size. In the body, cells and tissue are organized into three-dimensional architecture. To engineer these functional tissue and organs, scaffolds have to be fabricated by different methodology to

facilitate the cell distribution and guide their growth into three-dimensional space. The main techniques for scaffolds fabrication are summarized below:

2.2.1. Solvent casting

Solvent casting is a very simple, easy and inexpensive method for scaffold fabrication. It does not require any large equipment; it is totally based upon the evaporation of some solvent in order to form scaffolds by one of the two routes. One method is to dip the mold into polymeric solution and allow sufficient time to draw off the solution; as a result a layer of polymeric membrane is created. Other method is to add the polymeric solution into a mold and provide the sufficient time to evaporate the solvent that create a layer of polymeric membrane, which adhere to the mold [Mikos et al., 2004]. One of the main drawbacks of this technique is the use of toxic solvent that denatures the protein and may affect other solvents. There is a possibility that the scaffolds designed by these techniques may also retain some of the toxicity. To overcome these problems scaffolds are fully dried by vacuum process to remove toxic solvent. However, this is very time consuming technique and to overcome these problems some researchers have combined it with particulate leaching techniques [Mikos et al., 1993a; 1993b; 1996] for the fabrication of scaffolds.

2.2.2. Particulate-leaching techniques

Particulate leaching is one of the most common methods that are widely used for preparation of scaffolds with controlled porosity [Ma & Langer, 1999; Lu et al, 2000]. Salt, wax or sugars as porogens are used to create the pores or channels. In this method, salt is grounded into small particles and those particles that have desired size are poured into a mold and filled with the porogen. A polymer solution is then cast into the salt-filled mold. After the evaporation of the solvent, the salt crystals are leached away using water to form the pores of the scaffold. The process is easy to carry out. The pore size can be controlled by controlling the amount, size and shape of the porogen [Plikk et al., 2009]. The particulate leached scaffold with porosity up to 93 % and pore diameter up to 500 micrometers can be prepared [Mikos et al., 1993a; 1993b]. Main advantage of this technique is its simplicity, versatility and easy to control the pore size and geometry. Pore geometry is controlled by the selection of the shape for specific porogen agent, where as pore size is controlled by sieving the porogen particle to the specific dimensional range [Mano et al., 2007]. However, certain critical variables such as pore shape and inter-pore

openings are not controlled [Moore et al., 2004]. To overcome these drawbacks advanced fabrication technologieshave been developed as described below.

2.2.3. Gas foaming

Many of the fabrication techniques require use of organic solvents and high temperature. The residues that remains after completion of process can damage cells and nearby tissues. This may also denature the biologically active molecules incorporated within the scaffolds. The gas foaming technique does not require the use of organic solvents and high temperature. This technique uses high pressure soluble inert gas, e.g. CO_2 or N_2, in the supercritical region as blowing agent for the fabrication of highly porous scaffolds [Harris et al., 1998; Singh et al., 2004; Wang et al., 2006]. The porosity and porous structure of the scaffolds depend upon the amount of gas dissolved in the polymer. Instead of using a single polymer, this method is also applicable for composites of polymer and (bio) ceramic to employ in hard TE constructs [Kim et al., 2006]. The advantage is the elimination of solvent, thus avoid the risk of remaining solvent residue, and the low processing temperatures preventing degradation of the polymer during processing. The scaffolds often have a closed surface (skin) and mainly non-percolated pores which can be a serious problem as these characteristics limit nutrient transport through the scaffold. The porosity of the scaffolds is controlled by combining the method with particulate leaching [Ikada et al., 2006]. The mix polymer and porogen are exposed to high pressure until they have completed its saturation with carbon dioxide, followed by the removal of porogen by foaming process and thereby a highly interconnected pore structure is formed [Huang & Mooney, 2005].

2.2.4. Freeze drying

Freeze drying technique is used for the fabrication of porous scaffolds [Whang et al., 1995; Schoof et al., 2001]. This technique is based upon the principle of sublimation. Polymer is first dissolved in a solvent to form a solution of desired concentration. The solution is frozen and solvent is removed by lyophilization under high vacuum that fabricate the scaffold with high porosity and inter connectivity [Mandal & Kundu, 2009 a, b]. This techniques were applied to a number of different polymers including silk proteins [Vepari & Kaplan, 2007, Altman et al., 2003], PGA, PLLA, PLGA, PLGA/PPF blends. The pore size can be controlled by the freezing rate and pH, however a fast freezing rate produces smaller pores. Controlled solidification in a

single direction has been used to create a homogenous 3D-pore structure [Schoof et al., 2001]. The main advantage of this technique is that, it neither requires high temperature nor separate leaching step. The main drawback of this technique is smaller pore size and long processing time [Boland et al., 2004].

In **emulsion freeze-drying**, homogenization of a polymer–solvent system and water leads to formation of an emulsion [Ho et al., 2004; Whang et al., 1995]. An emulsion exists of two phases, a continuous phase and a dispersed phase. The continuous phase consists of the polymer-rich phase, whereas water is the dispersed phase. The emulsion is cooled quickly to freeze the solvent and water, resulting in solidification of the polymer directly from the liquid state and the creation of a porous polymer structure. Subsequently, the frozen solvent and water are removed by freeze-drying. Emulsion freeze-drying is attractive for creation of relatively thick scaffolds with large pores. Additionally, incorporation of proteins is enabled during the fabrication of the scaffold. The obtained morphology is mainly non-percolated (solid-wall like pores), which is the major drawback of freeze drying as this often limits cell in-growth and nutrient transport through the scaffold.

2.2.5. Phase separation

Phase separation technique for scaffolds designing requires temperature change that separates the polymeric solution in two phases, one having low polymer concentration (polymer lean phase) and other having the high polymer concentration (polymer rich phase). Methods often used for phase separation are e.g. liquid induced phase separation (LIPS, immersion precipitation) [Kim et al., 2004; Liu et al., 2004; Zoppi et al., 1999] and thermally induced phase separation (TIPS) [Guan et al., 2005; Hua et al., 2002; Li et al., 2004; Nam et al., 1999]. Polymer is dissolved in phenol or naphthalene, followed by dispersion of biologically active molecule in these solutions. By lowering the temperature liquid-liquid phase is separated and quenched to form a two phase solid and the solvent is removed by extraction, evaporation and sublimation [Mikos et al., 2004] to give porous scaffolds with bioactive molecules integrated in to the structure [Sachlos & Czernuszka, 2003; Hua et al., 2002]. An appropriate liquid-liquid phase separation is critical for the preparation of nanofibers and does not occur in all solvents which involves the selection of solvent. Furthermore, the phase separation temperature is crucial for the formation of nanofibers. Advantage of the phase separation technique is that, it can easily combine with other fabrication technology (Particulate leaching) to design three dimensional structures with controlled pore

morphology. It can also be combined with rapid prototyping to create nano fibrous scaffolds for tissue engineering applications [Smith et al., 2006]. These methods allow processing of pure polymers as well as composites of polymer–(bio) ceramic for application in hard TE [Causa et al., 2006].

2.2.6. Electrospinning

Electrospinning (ESP) technique for the scaffolds designing is based upon the charging of a polymer solution utilizes the electrostatic force and subsequent ejection of polymer solution through a capillary tip or needle for the production of polymeric fiber ranging from nanoscale to microscale [Bhattarai et al., 2006; Riboldi et al., 2005]. This process is controlled by high intensity electric field between two electrodes having electric charges of opposite polarity. To obtain continuous fibers, the method requires solutions containing relatively high polymer concentrations usually in the range of 10-15 wt%. Varying the process parameters, e.g. distance between needle and collector, strength of the electric field and polymer concentration allows tuning of the fiber diameter [Moroni et al., 2006; Boudriot et al., 2006]. More than 200 polymers are used for electrospinning like silk fibroin [Zarkoob et al., 2004; Sukigara et al., 2003; Jin et al., 2004], collagen [Matthews et al., 2002], chitosan [Ohkawa et al., 2004], gelatin [Ma et al., 2005] etc. The process is very versatile in terms of use of polymers, non-invasive and does not require the use of coagulation chemistry or high temperature for fiber generation. One of the main advantages of this technique is the high flexibility and fiber resolution of the obtained scaffold suitable for growth of the cell and subsequent tissue organization [Li & Tuan, 2009; Liang et al., 2007; Leong et al., 2008]. Additionally, alignment of the electrospun fibers is enabled to induce cell and tissue alignment [Buttafoco et al., 2006] favorable for better cellular growth for *in vitro* and *invivo*. A drawback of electrospinning is the risk of breaking fibers during fabrication, which might lead to inferior quality of the scaffold.

2.2.7. Fiber mesh

Fiber mesh technique for scaffold fabrication consists of individual fiber either woven or interweave into three dimensional pattern of variable pore size [Martins et al., 2009]. The method is developed by Mikos and his coworkers [Mikos et al., 1993a]. PGA is the first biocompatible and biodegradable polymer to spun into the fiber and used as a synthetic suture thread. It is prepared by the deposition of polymer solution over a nonwoven mesh of another

polymer PLLA [Chen et al., 2002] or collagen [Eberli et al., 2009] matrix followed by subsequent evaporation [Ikada et al., 2006]. At a temperature above the melting temperature of PGA, fiber bonding occurs and subsequently, the PLLA matrix of the composite is removed by dissolving in methylene chloride agent [Sachlos and Czernuszka, 2003] utilizing the fact that PGA is insoluble in this solvent. This process yields the scaffolds of PGA fiber that is bonded together by heat treatment. PGA mesh provides the high porosity and surface area to polymer mass ratio [Mooney et al., 1996]. This provides the mechanical stability and allows the tissue ingrowths. Main advantage of this technique is to provide the large surface area for cell attachment and rapid diffusion of nutrient that is favorable for cell survival and growth [Chen et al., 2002].

2.2.8. Self assembly

Self assembly is the spontaneous organization of the molecule into well defines acheiving an ordered structure required for specific function [Zhang et al., 2003]. Self assembly of natural or synthetic molecule produced nanoscale fibers known as nanofibers. Amphiphilic peptide sequence is a common method for the fabrication of 3D nanofibrous structure for tissue engineering. In aqueous solution, the hydrophobic and hydrophilic domains within these peptides interact together with the help of weak non covalent bonds [Joshi et al., 2009; Zhang et al., 2006] such as hydrogen bond, Van der Waals interactions, ionic bond and hydrophobic interaction. This produces distinct fast recovering hydrogel, with the hydrophobic interactions as the molecules come together. The di- and tri-block peptide ampholites (PAs) are designed that are self-assembled into a rod-like architecture. So a new technique for the self-assembly of PAs into nanofibers by controlling pH and by engineering the peptide head group of the PAs is developed [Hartgerink et al., 2002]. The fabricated nanofibers have amino acid residues that may be chemically modified by the addition of bioactive moieties. Other advantage of this technique is to avoid the use of organic solvent and reduce the cytotoxicity because it is carried out in aqueous salt solution or physiological media [Ma et al., 2005]. Main disadvantage of this technique is its complicated and elaborated process.

2.2.9. Melt molding/ Sintering

Melt molding generally referred to the processing of polymeric powders at high temperature while the term “sintering” is for ceramics, metals, glasses and their composites to make the

particles adhere to each other. Melt molding process involves the filling of teflon mould with PLGA powder and gelatin microspheres of specific diameter followed by heating the mould above the glass transition temperature of PLGA while applying pressure to the mixture [Thompson et al., 1995a, 1995b]. This action causes the PLGA particle to attach together. Once the mould is removed, gelatin microspheres are dissolved by immersing the mixture into water and scaffolds are then dried. Scaffolds produced by this technique assume the shape of the mould. Melt molding process can be modified to incorporate short fiber of hydroxyapatite (HA). Uniform distribution of HA fiber throughout the PLGA scaffolds could only be achieved by using the solvent casting technique to prepare the composite material of HA fiber, PLGA matrix and gelatin or salt porogen, which are used in melt molding process [Hou et al., 2003]. Scaffolds fabricated by sintering are mainly for hard TE constructs. The possibility of creating controlled and graded porosity is the main advantage of sintering. The major disadvantage is the possible risk of low interconnectivity of the pores and the brittleness of the fabricated scaffold in case of using certain biomaterials.

2.2.10. Rapid prototyping (RP)

RP is also called as solid free-form technique. This technique is more advanced technique for scaffold fabrication It can rapidly produce 3D object by using layer by layer manufacturing method. RP technique generally comprises the design of scaffold model by using the computer aided design (CAD) software, which is then expressed as a series of cross section [Lin et al., 2008, Woodfield et al., 2009]. Corresponding to each cross section RP machine lays down a layer of material starting from the bottom and moving up a layer at a time to create the scaffolds. In typical example, image of bone defect in a patient can be taken and develop 3D CAD model. The computer then can reduce the model to slice or layers. The 3D objects are constructed layer by layer by using RP techniques such as fused deposition modeling (FDM), selective laser sintering (SLS), 3D printing (3D-P) or stereolithography. Now-a-days, RP is an efficient way for generating the scaffolds of desired property.Other advantage of this technique is to produce the parts with highly reproducible architecture (size, shape, inter connectivity, branching, geometry and orientation) and compositional variations yielding biomimetic structure, that varying in design and material composition. The method is able to control the mechanical property, biological effects and degradation kinetics of scaffolds [Kai et al., 2009; Hutmacher et al., 2000;

2001]. One of the main drawbacks of this technique is achieved low resolution by current systems and types of polymeric materials that are used for this technique.

2.2.11. Membrane lamination

Membrane lamination is another SFF-like technique used for constructing three-dimensional biodegradable polymeric foam scaffolds with precise anatomical shapes. Membrane lamination is prepared by solvent casting and particle leaching and introducing peptide and proteins layer by layer during the fabrication process. The membranes with appropriate shape are soaked with solvent, and then stacked up in three-dimensional assemblies with continuous pore structure and morphology [Maquet & Jerome, 1997]. The bulk properties of the final 3D scaffolds are identical to those of the individual membrane. This method generates the porous 3D polymer foams with defined anatomical shape, since it is possible to use the computer assisted modeling to design the template with desired implant shape. The disadvantage of this technique is that layering of porous sheets, result in lesser pore interconnectivity [Hutmacher et al., 2000; 2001] and that it is a time consuming process.

2.3. Silk biomaterial as TE matrices

Silk from *B. mori* has been utilized as universal biomaterial with a wide range of processability and applications as demonstrated through figure 2.1 and table 2.1.

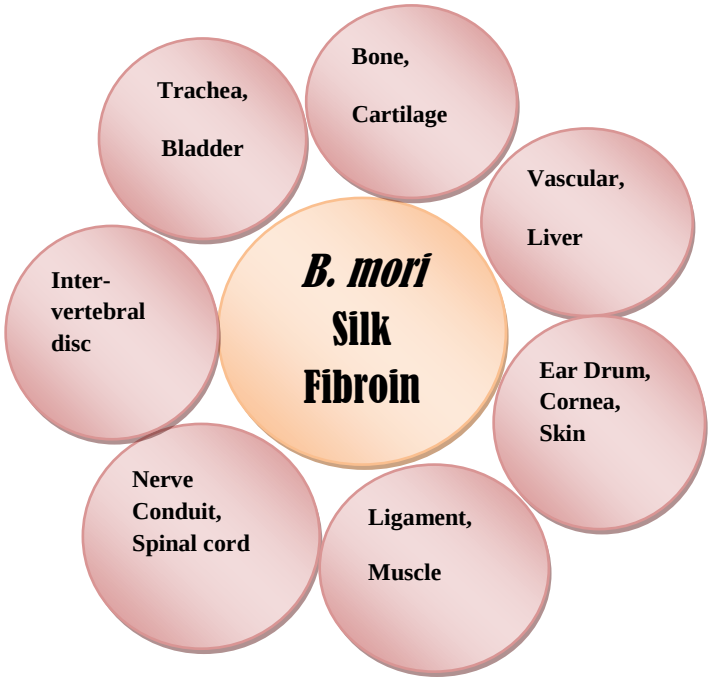

Figure 2.1: Silk for different tissue engineering application [Kasoju and Bora, 2012]

Table 2.1: Silk as a biomaterial for TE scaffold development

***B. mori* Silk Fibroin form**	**Fabrication method**	**TE application**	**References**
Fibers		Tendon tissue engineering Ligament tissue engineering	Kardestuncer et al., 2006; Chen et al., 2003 Altman et al., 2002; Moreau et al., 2005
Films	Casting Layer-by-Layer Deposition	Wound dressings Bone tissue engineering Hepatic tissue engineering Anti-thrombogenesis	Hu et al. , 2006; Sugihara et al., 2000; Yeo et al.,2000 Karageorgiou et al., 2004; Sofia et al., 2001; Cai et al. , 2002 Kino et al., 2006 Lee et al., 1998
Non woven Mats	Electrospinning Fiber deposition	Connective tissue Endothelial and blood Vessel Guided bone repair Wound dressing/skin repair	Dal et al.,2005 Fuchs et al.,2006; Unger et al.,2004 Kim et al.,2005b Min et al.,2004a; 2004b
Hydrogel	Sol–gel transition in the presence of acid, ions, and other additives	Cartilage and Bone tissue engineering	Aoku et al., 2003; Fini et al.2005
Sponge (3D porous sponge)	Salt leaching Gas foaming Lyophilization	Wound dressings Bone tissue engineering Cartilage tissue engineering	Karageorgiou et al., 2006; Sakabe et al., 1989 Meinel et al.,2004b;2005; 2006a,2006b; Marolt et al., 2006 Wang et al., 2005; 2006; Meinel et al.,2004a; Marolt et al., 2006

2.4. Surface modification and Composite/blend development

The brittleness of pure SF scaffold restricts their application and thus their physical properties are enhanced by mixing with other synthetic or natural polymers and other biomaterials [Gobin et al., 2005; Kweon et al., 2003; Du et al., 2006]. The cross-linking of such blended system may results into different degradation under physiological conditions [Ma et al., 2003] in addition to improved mechanical strength [Sabato et al., 2001]. The interaction of such composite scaffolds towards host cells have not been explored much. The improvement in tissue engineering biopolymers can be achieved by utilizing polymers of natural or synthetic origin, separately or in

blended form, with grafted or cross-linked networks. Mixing of glycerin (a commonly used plasticizer) has been reported to improve the mechanical properties of silk film [Lu et al., 2010] and also to reduce phase separation between silk and PVA in the blend [Dai et al., 1999]. After mixing with silk, glycerin molecules interact with silk chains via intermolecular hydrogen bond formation between -OH groups of glycerin and -NH groups of silk [Dai et al., 1999]. Chen et al. successfully fabricated electrospun silk fibroin [SF]/chitosan [CS] composite nanofibers [NFs] that could both support the proliferation (SF component) and osteogenic differentiation (CS component) of human fetal osteoblastic [hFOB] cells [Chen et al., 2012a]. Silk-CNT composite scaffolds developed by Chen et al. showed improved neuron differentiation efficiency from hESCs [Chen et al., 2012b].

Surface modification via physical adsorption or chemical immobilization of a protein or ligand improves biomaterial properties towards cellular behaviour [Jayasinghe et al., 2010; Chrzanowski et al., 2012]. Silk surfaces are hydrophobic, and can be functionalized using the AA side chain chemistry. The surface of silk fibroin biomaterials is modified using carbodiimide chemistry, which uses amine or carboxyl groups on silk. For example, arginine residues of silk fibroin were modified by 1,2-cyclohexanedione resulted into improved cell attachment and proliferation [Gotoh et al., 1998]. SF surface coupled with poly(ethylene glycol) (PEG) showed decreased attachment of fibroblasts [Gotoh et al., 1997] and also showed protein adsorption and hMSC attachment related to the amount of PEG on the surface [Vepari et al., 2010].Surface properties of SF biomaterials for improved cell adhesion and proliferation can be modulated by conjugation with integrin recognition RGD sequence via carbodiimide coupling [Ruoslahti et al., 1987]. The RGD peptide plays vital role in cellular adhesion by engaging integrins present over surface of many cell types [Hersel et al., 2003]. The remarkable improvement in cellular attachment and differentiation promotes ligament, [Chenet al., 2003] bone, [Meinel et al., 2004b] and dental [Petrini et al., 2013; Karageorgiou et al., 2004] tissue engineering [Xu et al., 2008]. It's fascinating to know that some wild type of silkworms like *Antheraea pernyi* have RGD in their silk fibroin sequence [Minouraet al., 1995]. Sofia et al. reported the covalent attachment of RGD to silk fibroin films resulting in increased number of mineral modules formed by Saos-2 cells in osteogenic media [Sofia et al., 2001]. T.Damrongrungruang fabricated RGD-modified electrospun Thai silk fibroin nanofibers to compare adhesion of human fibroblast cell line between RGD- and non-RGD modified electrospun nanofibers and observed a

significantly higher cell number in RGD modified silk fibre compared to conventional ones [Damrongrungruang, 2010].

Cell differentiation occurs in response of gradients of morphogens during embryogenesis and is repeated during adult tissue regeneration [Teixeira and Urist, 1998]. These signaling cues required for tissue development would be useful in biomaterial designing. Protein-based growth factors covalently attached to SF scaffolds has also been promising to promote cell differentiation cultured within scaffolds. One of the most common growth factor for bone tissue engineering is bone morphogenic protein (BMP-2) that can be directly immobilized on SF films, [Karageorgiou et al., 2004], scaffolds [Karageorgiou et al., 2006; Kirker et al., 2007] and electrospun mats [Li et al., 2006] via carbodiimide coupling. Gradients of BMP-2 were covalently immobilized and adsorbed over three-dimensional silk fibroin sponges and studied with hMSCs results into significantly higher expression of osteogenic markers [Vepari et al., 2010].

Several chemical modification methods to improve SF blood compatibility have been reported. Many of them have been modeled after the structure of commonly used anticoagulant, heparin the highly sulfated polysaccharide. Strategies have been employed to incorporate sulfate groups into SF in order to mimic the heparin structure. SF derivatives produced through the reaction with chlorosulfonic acid [Tamada et al., 2004] and sulfonated silk blends [Ma et al., 2006] or grafting of 2-methacryloyloxyethyl phosphorylcholine (MPC) onto silk fabric [Furuzono et al., 2000] were shown to be effective approaches in SF modification for applications where these materials will be in blood contact. Sulfated SF derivatives have also shown Anti-HIV activity [Gotoh et al., 2000]. Similarly, incorporation of phosphorylcholine (PC) into silk reduces inflammatory reactions to these materials *in vivo* by significantly reducing platelet adhesion [Furuzono et al., 2000]. Liu et al. reported the improved mechanical properties and lower inflammatory response of modified silk fibre with gelatin in place of sericin using NDGA as a cross-linking agent for ligament tissue engineering applications [Liu et al., 2007].

2.5. PVA as traditional biomaterial for SF scaffold development

PVA, a synthetic polymer has excellent hydrophilicity, biocompatibility, biodegradability and processability with ability to form high strength fibres suitable for medical applications [Mansur

and Costa, 2008; Mansur et al., 2004]. In addition, the published literature has indicated that no significant difference is found in quantitative or qualitative cytotoxicity evaluation of PVA. It is also shown that the amount of PVA accumulated in organs is too small to affect the biological fate, which suggested that PVA is excreted to the same extent as for example PEG, supporting the cytocompatibility of PVA [Yamaoka et al., 1995]. Furthermore, due to its solubility at room (25°C) or body temperature (37°C), it doesn't easily leach out into water or cell culture medium. A wide range of natural/synthetic polymers blended with PVA have been investigated for tissue engineering applications [Choi et al., 2013]. Development of scaffolds from PVA and PVA blends with other biopolymers, involves the crosslinking of PVA either chemically (with difunctional gluteraldehyde in presence of sulfuric acid, acetic acid or methanol) [Dai et al., 1999; Kim et al., 1993] or physically (with electron beam or gamma irradiation [Mathew et al., 2013; Wang et al., 1998], heat-treatment). Recently PVA gels have been prepared without crosslinking agents as a cell adhesive surface [Gupta et al., 2011]. Furthermore, a number of natural/synthetic polymer blended with PVA [Choi et al., 2013] and Poly(vinylidene fluoride) [Dikshit and Nandi, 2001] have been investigated for TE applications.Incorporation of PVA solution in chitosan has shown improvement in biocompatibility of the blend system [Huang et al., 2005]. Silk fibroin and PVA have been separately investigated as materials for tissue engineered constructs [Meinel et al., 2004a; Hofmann et al., 2007] and many research groups have studied the preparation method and properties of SF/PVA blends for improved stiffness of SF [Li et al., 2002; Dai et al., 2002; Li et al., 2001; Tanaka et al., 1998; Tanaka et al., 1997; Tsukada et al., 1994]. However, silk fibroin/PVA scaffolds have not yet been explored much for cytocompatibility and potential bone tissue engineering application.

2.6. Utility of SF based matrices in Tissue Regeneration

An ideal scaffold for tissue engineering application must have the property of biocompatibility with host tissue, biodegradability and non immunogenic in nature. Therefore much of the research is being done on natural polymer which fulfills these criteria. Silk, which is a naturally derived polymer, has been in use for medical application such as suture material due to its high mechanical and compressive strength. It proves to be an ideal polymer for tissue engineering application owning to its better bioactive properties as compared to synthetic polymers which is an important prerequisite for a polymer for the development of construct. They can be easily

modified in combination with other materials to acheive required mechanical and surface properties of scaffold. Therefore silk is considered as a promising biomaterial for tissue engineering application.

2.6.1. Skin wound healing

Research groups [Chiarini et al., 2003; Dal et al., 2003] have reported the in-vitro dermal fibroblasts spreading and proliferation on fibroin substrate without secretion of pro-inflammatory interleukins accountable for host response against foreign body. In vitro study of oral keratinocytes on woven fibroin meshes have shown promising proliferation [Min et al., 2004]. In another study, fibroin-alginate sponges [Roh et al., 2006] and fibroin-chitosan blend [Gobin et al., 2006] have been found to enhance skin wound healing compared to currently used clinical materials. The effects of the transparent fibroin film (silk film) and dressing were compared with an objective to regenerate the epidermis and dermis of the wound and reported the superiority of silk films with additional advantages of cost effectiveness, ease of availability, sterilizability, and easy observation of tissue recovery due to transparent nature [Sugihara et al., 2000]. Naksupan et al. studied the healing effect and toxicity of silk fibroin gel in skin wound ofanimal model and observed the accelerated epidermal (keratinocytes) cell proliferation, migration to wound and remodeling of wound site without any trace of cytotoxicity anatomical change. This study indicates the potential use of silk fibroin gel for wound dressing application in clinical trial [Naksupan et al., 2012].

2.6.2. Skeletal tissues

2.6.2.1. Cartilage

Major research on the application of silk fibroin based 3D scaffolds for cartilage tissue engineering were reported by D. L. Kaplan group, most often fabricated by salt-leaching [Wang et al., 2006; Marolt et al., 2006; Meinel et al., 2004a; Hofmann et al., 2007]. In vitro human articular chondrocytes [Wang et al., 2006] and mesenchymal stem cells (MSCs) [Marolt et al., 2006; Meinel et al., 2004a; Hofmann et al., 2006] cultured on these scaffolds have demonstrated chondrogenesis as elevated amount of collagen type II and GAG both in static [Meinel et al., 2004a, 2004c] and dynamic [Marolt et al., 2006] cultures. Hofmann et al. studied the effect of serum in culture media in terms of support to chondrogenesis on silk and collagen scaffolds and reported that cartilage synthesis on silk scaffolds in serum-free conditions is highly significant.

In the absence of serum, the GAG level was significantly higher on the fibroin scaffolds as compared to collagen controls but lower in presence of serum, indicating the promotion of chondrogenesis due to surface properties of the silk scaffolds and its potential clinical applications where the use of serum is avoided [Hofmann et al., 2006]. However, the engineered cartilage tissue had inferior mechanical properties to those of native cartilage [Hofmann et al., 2006; Marolt et al., 2006] and lower GAG content produced by differentiated MSCs than by chondrocytes [Marolt et al., 2006], indicating further need to optimize the culture conditions with respect to scaffold properties, cell differentiation and mechanical stimulation. Silk fibroin sponges developed by thermally induced phase separation (TIPS) method showed support to chondrocyte proliferation for up to 28 days [Morita et al., 2002] with inferior mechanical properties as of native tissue due to the inferior expression of synthesized extracellular matrix. Alteration in cell culture protocol using the same scaffolds resulted in higher expression of type II collagen, GAG and extracellular matrix throughout the culture period of 28 days, signifying the application in hyaline cartilage tissue engineering [Aoki et al., 2003].

2.6.2.2. Bone

Tissue engineering approach for the repair of bones with different morphologies using silk fibroin scaffolds in various forms have been reported [Fini et al., 2005; Kim et al., 2005a; Kirker-Head et al., 2007; Hofmann et al., 2007;Marolt et al., 2006; Meinel et al., 2004b; Kim et al., 2005b; Meinel et al., 2005]. Initial efforts deal with silk fibroin hydrogels [Fini et al., 2005] and membranes/nets [Kim et al., 2005b] without pre-seeded cells for guided bone regeneration. While in this decade, techniques have been developed to use 3D porous silk fibroin scaffolds seeded with MSCs for the repair of bone defects with complex dimension mostly done by D. L. Kaplan group [Meinel et al., 2006a; Kim et al., 2005a; Meinel et al., 2005; Kim et al., 2005b]. In their study, regenerated silk fibroin solution (RSF) was processed into films [Sofia et al., 2001, Wang et al., 2005], electrospun to form scaffolds [Li et al., 2006] or a 3-D porous scaffold by salt-leaching [Kirker-Head et al., 2007; Hofmann et al., 2007;Marolt et al., 2006; Meinel et al., 2006a; Kim et al., 2005c; Meinel et al., 2005]. The addition of RGD functionality [Meinel et al., 2005; Meinel et al., 2004b] or growth factors [Kirker-Head et al., 2007; Karageorgiou et al., 2006; Li et al., 2006] was reported to enhance surface properties for cellular activities. Fibroin films coupled with RGD peptides incubated with osteoblast-like cells were found to produce mineralized matrix [Sofia et al., 2001]. Silk fibroin films and scaffolds immobilized with bone

morphogenic protein-2 (BMP-2) have been demonstrated to induce osteogenesis in vitro [Meinel et al., 2006b; Karageorgiou et al., 2004] and bone formation when implanted with or without seeded pre-differentiated and undifferentiated MSCs in non-load bearing [Karageorgiou et al., 2006] and load-bearing [Meinel et al., 2006a] bone defect sites *in vivo*. Bone formation at the site of implantation with fibroin scaffolds seeded with undifferentiated cells *in vitro* induces early osteogenesis than scaffolds withoutpreseeded cells. SF scaffolds cultured with cells before implantation also has shown better mechanical properties [Meinel et al., 2006a]. SF based hyodrogels have been reported to outperform *in vivo* bone ingrowth than commercially available synthetic polymers [Fini et al., 2005]. For the bone regeneration at bone defect site with complex dimension meant that several smaller scaffolds have to be stacked together instead of using a larger one. Larger scaffolds though can support bone formation with better mechanical properties but problem of mass transport limits their use [Meinel et al., 2006b]. Most reports demonstrate the culture medium supplementation when BMP-2 is involved; however, Meinel et al. successfully differentiated MSCs along osteogenic lineages with BMP-2 applied via viral transfection [Meinel et al., 2006b]. Reports demonstrate the successful differentiation of MSCs into osteogenic lineages grown over Fibroin–nano-hydroxyapatite composite films [Tanaka et al., 2007] and have been observed to promote osteogenesis at both non-load bearing [Kim et al., 2005b; Meinel et al., 2005] and load-bearing [Meinel et al., 2006a] sites implanted in rodent models.

2.6.2.3. Ligament/tendon

The adaptability of silk biomaterial into controllable physical and mechanical properties makes it promising for ligament and tendon tissue engineering. The natural twisted and wire-rope geometrical configuration of silk fibers provide better mechanical properties and larger surface area for cell attachment and ECM deposition in a pattern similar to collagen fibers present in ligaments and tendons. Silk fibroin fibers devoid of sericin, has been investigated for proliferation and differentiation of MSCs towards ligament tissue, expression of ligament-specific markers (collagen type I, collagen type III, tenascine-C) and cellular response for mechanical stimulus [Altman et al., 2002]. Gelatin coated fibroin fibers have been demonstrated to restore the mechanical properties that are reduced by sericin removal without influencing *in vitro* cytotoxic effects and *in vivo* inflammatory response for ligament tissue engineering [Liu et al., 2007; Takezawa et al., 2007]. RGD coated silk fibroin matrix showed enhanced ECM

production by both MSCs and anterior cruciate ligament (ACL) fibroblasts [Chen et al., 2003] and increased expression of Collagen type I (the main constituent of ligaments) as compared to unmodified silk fibroin controls. Investigations also reported the mechanical stimulation of MSCs seeded in RGD-coated matrices. MSCs remained attached and aligned in the direction of the stimulus and shown further improvement by addition of growth factors for ligament tissue engineering [Moreau et al., 2005]. Ligament tissue engineering has been better supported by silk-based scaffolds and sponges as demonstrated by better proliferation of ACL fibroblasts seeded with MSCs [Liu et al., 2008; Seo et al., 2007]. Research report have demonstrated the maximum load of 2337 ± 72 N, an elastic modulus of 354 ± 26 N/mm and a strain at failure of 38.6 ± 2.4% the silk fibroin matrices, which are similar to ACL [Laurencin et al., 2005]. In a similar study silk fibroin scaffolds showed support for adherence, spreading, proliferation and differentiation of adult human MSCs towards ligament neogenesis [Altman et al., 2002]. The mechanical strength of scaffold was retained during three weeks of culture with expression of ligament-related transcripts (tenascin-C, collagen type III (Col-III) and Col-I) from second week. The expression of bone or cartilage related transcripts were not significantly affected suggesting the silk fibroin scaffolds promoted the ligament-specific hMSCs differentiation [Altman et al., 2002]. Studies on cabled yarns have shown that they are suitable for load-bearing applications, whereas braided and textured yarns were found suitable for non-load-bearing tissues with enhanced cell seeding and tissue ingrowth but with limitation of mass transport and mechanical fixation observed *in vivo* [Altman et al., 2002]. The group led by Vunjak-Navakovik designed a 6-cord silk fiber matrix with decreased scaffold stiffness and more void space (>90%) while maintaining the tensile strength which contribute to an enhanced tissue support and infiltration for neotissue formation [Vunjak-Novakovic et al., 2004]. Type-I collagen and mRNA levels for decorin (the most abundant proteoglycan in tendon tissue) were found to be highest on silk-RGD followed by silk films than on the control [Kardestuncer et al., 2006].

2.6.2.4. Vascular tissues

Silk fibroin scaffolds are a possible alternative for vascular grafts due to combination of their unique mechanical properties to withstand vascular pulsating pressureand biocompatibility towards endothelial cells and smooth muscle cells [Zhang et al., 2008; Soffer et al., 2008]. Soffer et al. fabricated electrospun nanofibrous tubular structures from silk fibroin with an objective to bioengineer small diameter vascular grafts. Human endothelial cells and smooth muscle cells

were successfully proliferated on substratum indicating their potential use as scaffolds for vascular grafts [Soffer et al., 2008]. Scaffold porosity of 80% and above is reported ideal for endothelialization of vascular grafts [Zhou et al., 2009]. Tubular silk scaffolds electrospun out of formic acid can resist up to 575 mmHg, which is much higher than physiological pressure of 120 mmHg [Marelli et al., 2010]. Drawback of using organic solvents, such as formic acid and HFIP, is that traced remained after processing may affect cyto-compatibility. Sulphonated and heparinized silk fibroin films have shown suitable mechanical properties for use as artificial blood vessels in addition to anticoagulant activity and support to endothelial cell culture [Ma et al., 2005]. Reports demonstrates that the blood compatibility of silk fibroin is enhanced by the grafting of hydrophilic polymers such as 2- methacryloyloxyethyl phosphoryl choline (MPC) [Furuzono et al., 2000], or blending with S-carboxymethyl kerateine [Lee et al., 1998], or coating with fibronectin or collagen [Unger et al., 2004; Fuchs et al., 2006]. Couet et al. have developed collagen-silk filament composites for vascular tissue engineering [Couet et al., 2007]. For the successful engineering of bone and other tissues, it is mandatory for silk fibroin to promote vascularization process in the regenerating tissue [Mooney and Mikos, 1999].

2.6.2.5. Other tissues

Studies have shown that collagen-fibroin blends [Hu et al., 2006; Cirillo et al., 2004] and lactose-silk fibroin conjugates [Gotoh et al., 2004] support the attachment and proliferation of hepatocytes. It is also been reported that cells cultured on SF-containing films are able to eliminate ammonia and synthesize urea [Cirillo et al., 2004], suggesting potential applications for liver tissue engineering. Silk fibroin has also been demonstrated to support the growth and proliferation of rat dorsal root ganglia (DRG) and Schwann cells on the substrate made up of purified silk fibroin fibers [Yang et al., 2007] and has, therefore, been proposed as a potential candidate for nerve tissue engineering.

2.7. Conclusions

In recent years, a wide range of biomaterials have been developed and designed by the scientists for tissue engineering includes various types of sysnthetic and natural polymers and their composites. The main limitation of using synthetic polymers is the risk of implant rejection due to lowering of local pH by their degradation byproduct (CO_2 gas) and thus lead to cell and tissue necrosis. Whereas, the matrices of natural polymers are biodegradable, biologically active and

these promote cellular ingrowth for ECM formation. Gelation of naturally derived polymers is reported to be less controllable, although the hydrogels formed are more compatible for hosting cell and bioactive molecules.The properties of biopolymer can, further, be modified to induce differentiation of cells into specific lineages. The improvement in tissue engineering biopolymers can be achieved by utilizing polymers of natural or synthetic origin, separately or in blend form, and grafted or cross-linked networks. Surface modification via physical adsorption or chemical immobilization of a protein or ligand improves the material properties towards cellular behavior. The addition of RGD functionality or growth factors is reported to enhance surface properties of the scaffold.

Among the biopolymers, silk fibroin is reported to be the most attractive candidate for developing matrices for tissue regeneration and cell based therapy. *In vivo* and *ex vivo* experiments have demonstrated that silk based biomaterials show a wide range of advantages related to physical, chemical, mechanical, thermal and biological properties that help in regaining function at cell-adhesion sites. However, many problems still to be solved to use them for actual clinical application. There is a need to study and develop different silk based hybrid scaffolds that could efficiently replace the organ structure and function. The detailed study of cell attachment, cell infiltration and vascularization can help in efficient integration of the implants into the patient's body, avoiding the generation of fibrosis around the implants. Moreover, silk fibroin based hybrid scaffolds should be analyzed for their biodegradation properties. Finally, before using silk fibroin based tissue engineering products in medicine, the biocompatibility and the possible generation of heterologous amyloid must be tested *in vivo*, with the purpose of assuring their biosafety.

CHAPTER 3

Materials & Methods

3.1. Materials

Bombyx mori silk cocoons were obtained from silkworms reared in controlled conditions at the mulberry *farms* in Chittoor district, Hyderabad (Andhra Pradesh, India). Analytical grade Na_2CO_3 (S. D. Fine chemicals, India) and LiBr (>99% purity, Sigma Aldrich, Germany) and chemicals for Bradford Assay were used as such without further purification. Poly (vinyl alcohol) (Himedia, RM 6170) were used as blend polymeric materials for scaffold preparation and NaCl (Himedia, RM 583) as porogen. Freshly broken double membrane bound eggshells were collected from the canteen of National Institute of Technology, Rourkela, India for the preparation of soluble eggshell membrane protein (SEP). Standard stainless steel sieves (Fisher Scientific) (100 µm, 200 µm, 300 µm, 500 µm) were used for sorting NaCl particles into various particle size ranges. Clinical grade of laboratory chemicals and Milli-Q water were utilized in processing of scaffold fabrication and cell culture studies.

3.2. Preparation and Characterization of Polymer(s) solutions

3.2.1. Preparation of regenerated silk fibroin aqueous solution

Dried *B. mori* silk cocoon shells were cut into small pieces and treated with boiling aqueous solution of sodium carbonate of varying concentration for 20 min with stirring. The whole mass was washed with Milli-Q water repeatedly to remove the glue-like sericin protein and then dried in hot air oven. Before further use, the silk was dried in vacuum drying oven at 80°C for 6h. The degummed silks were completely dissolved in 9.3M LiBr aqueous solution at 70°C for 2½ h with stirring. The fibroin solution was dialyzed in a cellulose membrane based dialysis cassette (molecular cutoff 12,400) against deionized water for 3 days with changing of water every 6 h in order to remove LiBr. The dialysed regenerated silk fibroin (RSF) solution was centrifuged at 5-10˚C and 9000 rpm for 20 min and stored at 4°C for further study. The concentration of silk fibroin aqueous solution was calculated by measuring the volume of solution and weighing the remaining solid after drying. The concentration of SF solution was calculated using the formula:

$$V_2 = V_1 \times \frac{C_1}{C_2}$$

Where, V_1 and V_2 are the volume of fibroin solution before and after evaporation, C_1 is the concentration of the fibroin solution before evaporation and C_2 is the concentration that is required in the experiment.

The concentration of SF solution was measured as 12% (w/v). Finally, the SF solution with concentration 4-6% (w/v) was prepared by dilution. The sequential experimental procedure for protein extraction from *B. mori* silk cocoon has been shown in Figure 3.1.

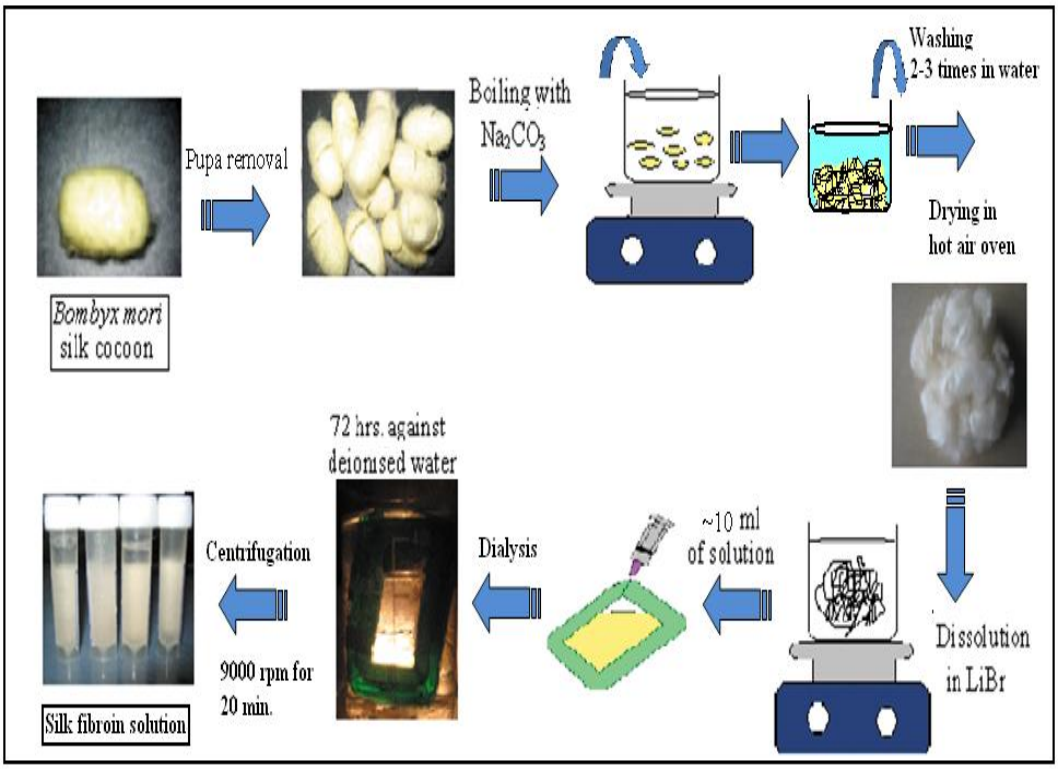

Figure 3.1. Schematic diagramme for extraction of fibroin protein from *Bombyx mori* silk cocoon

3.2.2. Process optimization of SF extraction

3.2.2.1. Measurement of protein concentration

The concentration of fibroin protein was measured by the Bradford protein assay method [Bradford, 1976]. The fibroin solution was added to the Bradford reagent and incubated at 30°C for 5 min. The absorbance of resultant solution was measured at 595nm. The Bradford assay relies on the binding of the dye Coomassie Blue G-250 to protein. Thus, the quantity of protein is estimated by determining the amount of dye in the blue ionic form, usually achieved by measuring the absorbance of solution at 595 nm. Bovine serum albumin was used as a standard protein.

3.2.2.2. Degumming loss

Degumming loss, a quantitative evaluation of the degumming efficiency, is represented by the weight loss of the fabric (expressed as a percentage of the initial weight) after degumming. Before the measurement of weight loss, the samples were kept at 37°C in hot air oven for 24 h. The degumming loss was calculated as,

$$D(\%) = (W_i - W / W_i) X 100$$

Where, D is Degumming loss, W_i is initial wt. of silk cocoon and W is wt. of silk fibroin recovered after degumming.

3.2.2.3. Experimental design for response surface methodology

Box-Behnken rotatable design (BBRD) for three independent variables each at three levels was adopted in this study. A total of 17 experiments were necessary for the estimation of the various coefficients of the model. The quadratic response surface model was fitted to the following equation [Evans et al., 2003; Guaracho et al., 2009]:

$$Y = \beta_0 + \sum_{i=1}^{k} \beta_i X_i + \sum_{i=1}^{k} \beta_{ii} X_i^2 + \sum_{j=1}^{k} \beta_{ij} X_i X_{ij} + \varepsilon \quad (1)$$

Where, $X_1, X_2, \ldots\ldots, ..X_k$ are the input variables, which influence on the response Y; $\beta_i (i = 1,2,\ldots., k)$, $\beta_{ij} (i = 1,2,\ldots., k; j = 1,2,\ldots\ldots., k)$ the unknown parameters and ε is a random error [Guvenc et al., 2007]. Actual values of independent variables in Box-Behnken design for the protein extraction using silk cocoon is shown in Table 3.1.

Table 3.1: Experimental range and levels of independent variables for extraction

X_i	**Range and levels**		
	-1	0	+1
X_1 **: Na_2CO_3 concentration (mg/l)**	0.01	0.02	0.03
X_2 **: LiBr concentration (mg/l)**	9.10	9.30	9.50
X_3 **: Temperature (^oC)**	55	70	85

It is important to include the second order model to provide good prediction throughout the region of interest. The second order response surface design is rotatable; this means that the variance of the predicted response is the same at all points. Rotatability is a reasonable basis for the selection of response surface design. Because the purpose of response surface methodology (*RSM*) is optimization and as the location of the optimum is unknown prior to running the experiment, it makes sense to use design that provides equal precisions of estimation in all directions [Kumar et al., 2008]. For Model Fitting and Statistical Analysis, a three-dimensional response surface and contour plots of the independent variables and their interactions were generated using the statistical software, Design Expert software version 6.0.6 (STAT-EASE Inc., Minneapolis, US). The main aim of the optimization of protein extraction process was to establish the maxima levels within the independent variables such as Na_2CO_3 concentration (X_1), $LiBr$ concentration (X_2) and temperature (X_3).

3.2.3. Characterization of RSF solution

3.2.3.1. Rheological properties

The rheological property of the prepared silk fibroin solution was assessed by measuring the viscosity by a cone and plate viscometer (BOHLIN VISCO-88, Malvern, U.K.). The cone angle is 5.4^o and diameter 30mm. A gap of 0.15mm was maintained between the cone and plate for all the measurements. The temperature was maintained using an external water circulator as 30°C, 35°C, 40°C, 45°C, 50°C ±1°C. The experiment was done in triplicate (n=3).

3.2.3.2. Measurement of molecular weight

The molecular weight of the regenerated silk fibroin was determined by sodium dodecyl sulfate polyacrylamide gel electrophoresis (SDS-PAGE) according to the method described in published literature [Laemmli, 1970]. The running gel was prepared using 12% acrylamide gel and 5% condensing gel. The gel was stained with the Easy Stain Commassie Blue Kit (Invitrogen, Carlsbad, CA).

3.2.3.3. Particle size analysis

The average particle size of the prepared regenerated SF solution was determined by Zetasizer Nano ZS (Malvern, U.K) particle analyzer based on laser beam scattering technique. The measurement was done at 30°C after discarding the precipitated impurities of the solution centrifuged at 9000 rpm for 10 min at 10°C. The optic unit contained a 4 mW He–Ne (633 nm) laser.

3.2.4. Preparation of Soluble Egg Shell Membrane Protein (SEP)

Freshly broken double membrane bound eggshells, collected from our institute canteen were immediately stored in chilled water. The raw eggshell was washed properly and then peeled off manually from the membrane. The sample was kept in aqueous acetic acid (70%) for two days to dissolve residual eggshell followed by rinsing with Milli-Q water repeatedly to remove acidity and then dried in hot air oven (50ºC) for two days [Tsai et al., 2006]. Finally, the SEP was obtained by reductive cleavage of disulfide bonds present in ESM with aqueous 3-mercaptopropionic acid (3-MPA) at 90ºC in presence of 10% acetic acid, following the method published earlier [Yi et al, 2003; Yi et al., 2004]. The average particle size of the prepared SEP solution was determined by same method as mentioned above for the RSF solution.

3.2.5. Preparation of SF/PVA blend solution

Aqueous PVA solution (10% w/v) was prepared by dissolving PVA powder under continuous magnetic stirring at 80°C for 4 h. The hot polymeric solution was cooled to ambient temperature and stored for further study. The aqueous SF (12% w/v) and PVA (10% w/v) solutions were blended with varying ratios of SF to PVA in the range 75/25 to 25/75, under magnetic stirring at 40°C for 48 h. Glycerin (4% (w/v), Himedia, RM 018) was added to the SF/PVA blend solution for minimizing phase difference. SF/PVA solution was cooled to room temperature and the pH of the blend was adjusted to 2.00 with 0.1 N HCl (Merck, India).

3.3. Preparation and Characterization of SF and SF based matrices

3.3.1. Preparation of Silk Fibroin Hydrogels and Sponges

The prepared regenerated silk fibroin was kept at 20ºC for 3 days under humid environment to form translucent silk fibroin hydrogels (thermgels).The hydrogels were then kept at -20ºC for 24 h and lyophilized for 24 h to prepare fibroin sponges.

3.3.2. Fabrication of silk fibroin porous scaffold

Porous scaffolds were prepared from silk fibroin solution by salt leaching method using NaCl as porogen. The silk fibroin was diluted to 8% (w/v) with Milli-Q water and poured into a circular mould (15mm dia.) either before or after NaCl was added as a porogen. Samples were then left covered in the mould for 24 h and placed in methanol for 30 min followed by the transfer into deionized water for salt leaching for 48 h. The salt leached samples were kept in vacuum dryer for 24 h at 40°C and stored in a dessicator [Kim et al., 2005c].

3.3.3. Preparation of SEP-SF Scaffolds

The SF scaffolds were steam sterilized and dried in ethanol ambiance. The scaffolds were then soaked in SEP solution 2% (w/v) and incubated in hot air oven at 37 ºC for 24 h for drying. The dried samples were cross-linked by pouring onto it a few drops of 1-ethyl-3-(3-[dimethylamino]propyl) carbodiimide (EDC) solution (10 mg/ml) mixed with N-hydroxysuccinimide (NHS) solution (10 mg/ml) (50:50), and then incubated at 37ºC for 12 h [Hafemann et al., 2001]. The cross-linked samples were desalted with 70% ethanol and dehydrated with 99.5% ethanol, before drying under an air stream at 37ºC for 24 h. The cross-linked SF-SEP scaffolds were kept in desiccator for further study.

3.3.4. Preparation of SF/PVA Scaffold

A series of scaffold samples with varying SF/PVA blend ratio were prepared in triplicate using porogen of different particle size (100-200, 200-300 and 300-500 µm). 4g of granular NaCl (air-dried) was kept in autoclavable teflon moulds and 2ml of different blend solutions were poured into it. Sample container was covered and kept at 40-50ºC in hot air oven for 24 h. Few drops of methanol were added into the samples and kept for 30min for the conformational transition to occur and then dried in vacuum drying oven. The dried samples were kept in deionized water for 48 h for leaching of NaCl from the samples. These final product samples are dried in vacuum drying oven for 48 h and stored in desiccator for further study.

3.3.5. Preparation of SEP-(SF/PVA) scaffolds

The prepared SF-PVA scaffold was steam sterilized and dried in ethanol ambiance The scaffolds were then soaked in 2% (w/v) SEP solution and dried in hot air oven at 37 ºC for 24 h. The dried scaffolds were cross-linked by pouring onto it few drops of 1-ethyl-3-(3-[dimethylamino]propyl) carbodiimide (EDC) solution (10 mg/ml) mixed with N-hydroxysuccinimide (NHS) solution (10 mg/ml) (50:50), and incubated at 37 ºC for 12 h in 4-morpholinoethanesulfonic acid (MES) reaction buffer [Hafemann et al., 2001; Hermanson et al., 1996]. The cross-linked sample was desalted (with 70% ethanol) and dehydrated (with 99.5% ethanol), before being dried under an air stream at 37 ºC for 24 h. The cross-linked SEP–(SF/PVA) scaffolds were kept in desiccator for further study.

3.3.6. Physico-chemical and Thermal characterization

3.3.6.1. Porosity and Pore size distribution

The porosity of the scaffolds were measured by liquid displacement methodfollowing the procedure discussed in published literature [Kim et al., 2005] using hexane as the displacement liquid since it is a

nonsolvent for silk and is able to permeate easily through the scaffold without causing swelling or shrinkage. In brief, a sample of weight *W* was immersed in a known volume (*V*1) of hexane in a graduated cylinder. The sample was left covered in hexane for 5 min. During this time, the contents in the cylinder underwent an evacuation- repressurization cycle to force the hexane to pass through the pores. The total volume of the hexane and the hexane impregnated scaffold was *V*2. The volume difference (*V*2 - *V*1) is the volume of the polymer scaffold. The hexane impregnated scaffold is then removed from the cylinder and the residual hexane volume is recorded as *V*3. The quantity (*V*1 - *V*3), volume of hexane within the scaffold, was determined as the void volume of the scaffold. All measurements were carried out in duplicate.

The total volume (V) of the scaffold was,

$$V = (V_2 - V_1) + (V_1 - V_3)$$

and the porosity of the scaffold (π) was obtained by,

$$\pi = \frac{(V_1 - V_3)}{(V_2 - V_3)}$$

Mercury intrusion porosimetry was used to measure pore size distribution of scaffolds.

3.3.6.2. Phase Contrast and Scanning Electron Microscopy

The morphology of raw and regenerated samples was observed under phase contrast microscope (Carl Zeiss, Axiovert 40 C) equipped with a cannon 3 CCD color video camera. The surface morphology of degummed silk fibre, raw ESM,SF scaffolds and SEP conjugated SF scaffolds were examined by SEM (JEOL JSM -6480LV SEM) observation at different magnification. Scaffold samples were air-dried while ESM was kept in 2.8% gluteraldehyde solution overnight before SEM analysis. The samples were affixed via carbon tape to the SEM sample holders and vacuum-coated with a 20-nm layer of platinum. SEM was performed at a voltage of 15 kV and room temperature. To measure the aperture of the porous structure, the SEM analysis was done using image analysis software (JEOL SMileView) and the average pore size was calculated. The elemental composition of soluble egg shell membrane protein was also determined by EDX analysis.

3.3.6.3. X-ray diffraction

The diffraction pattern of samples was recorded by an X-ray diffractometer (Phillips PW-1830) with Ni-filterd Cu-Kα radiation operating at 35 kV and 30mA. The samples were scanned from 20° (2θ) to 70° (2θ) at a scanning rate of 3.0/min. Crystallinity was determined by integration using KaleidaGraph (Synergy Software).

3.3.6.4. Fourier transform infrared (FTIR) spectroscopy

The FTIR analysis was performed using a FTIR spectrometer (model system IRPrestige-21, Shimadzu) interfaced with IR microscope operated in absorbance mode. The spectrum was measured and recorded solid samples in KBr pellets in the 500–4000 cm^{-1} region with a resolution of 4.0 cm^{-1}. The spectra were smoothened with constant smooth factor for comparison.

3.3.6.5. Differential scanning calorimetry

The thermal behavior of scaffolds was determined by differential scanning calorimetry (DSC) (Mettler Toledo DSC822e). 10-15 mg of each sample was scanned between the range of 30-300°C at a rate of 20°C / min under nitrogen atmosphere.

3.3.6.6. Thermal gravimetric Analysis

The thermal stability of scaffolds samples were investigated by TGA using a DTG-6H (Simadzu). The amount of samples for each measurement were about 1 mg, and all the measurements were carried out with a heating rate of 10°C min^{-1} in flowing N_2 heated up to 500 °C.

3.3.7. Mechanical Property

Compressive tests were performed to determine compressive modulus of the scaffolds (dry state) by using a Universal Testing Machine (H10 KS TINIUS OLSEN) with a 1 kN load cell at room temperature. The size of the tested specimens was measured with a micrometer. The lengths and diameters of the tested specimens for SF scaffolds were 11.94 ± 0.22 mm and 5.64 ± 0.26 mm, respectively. The cross-head speed was set at 2 mm min^{-1} and compressive moduli of scaffolds (n = 4) were calculated from the slopes of compressive stress–strain curves.

3.3.8. Swelling assay and Biodegradability

3.3.8.1. Swelling property of silk hydrogel

The swelling properties of the hydrogels were studied using conventional gravimetric method [Vazquez et al., 1997]. The swelling behavior of dried (60°C for 24 h) and pre-weighed hydrogels (disc-shaped) was determined by immersing in double-distilled water at 37°C. Swollen gels were weighed by an electronic balance at pre-determined time intervals after wiping excess surface liquid by filter paper [Gupta and Shivakumar, 2010]. The swelling index (SI) was calculated from the following equation:

$$SI = \frac{M_t - M_o}{M_o} \times 100$$

Where M_t is the mass of the swollen gel at time t, and M_0 is the mass of the dry gel at time 0.

3.3.8.2. Swelling property and biodegradability of scaffolds

The preliminary cytocompatibility of the scaffold was investigated using a protein-free acellular simulated body fluid medium (SBF or Kokubo solution) of pH 7.40 and ionic composition- Na^+ 142.0, K^+ 5.0, Ca^{2+} 2.5, Mg^{2+} 1.5, Cl^- 147.8, HCO^{3-} 4.2, HPO_4^{2-} 1.0, SO_4^{2-} 0.5 mM [Kim et al., 1999]. The SF based scaffold were cut into 5.0mm×5.0 mm square pieces with initial weight measured as W_0 and soaked in SBF at 37°C and pH 7.4. The samples were soaked in SBF for different time period (30 min., 2 h, 4 h, 24 h, 96 h and 192 h). After soaking, the remaining solution were carefully removed from the medium, excess water on the surface was removed using lint-free tissue paper and weights (W1) were determined. Samples were then dried at 40°C in an oven for 24 h and theweights of dried samples were measured as W_2. The initial change in weight refers to fluid-uptake measurements (swelling) while the final weight difference after sample drying indicates the biodegradability of samples in SBF. Each experiment was performed in triplicate. Swelling index (S) is calculated as,

$$S = \frac{W_1 - W_0}{W_0} \times 100$$

Whereas the biodegradation (B) in SBF is calculated as,

$$B = \frac{W_2 - W_0}{W_0} \times 100$$

3.3.9. Contact angle measurement

The hydrophilicity of developed scaffolds was evaluated in terms of contact angle measurement using a sessile drop technique with a Digital Contact Angle Measurement System fitted with a CCD camera (KGV-5000) [Kim et al., 2003]. First of all, scaffolds were attached smoothly to the silicon wafer surface by gradual evaporation of small water droplets placed along each edge of scaffold (2×2 cm^2). A 5 µl droplet of pure water (Milli-Q-water) was pipetted onto the scaffold surface and temporal images were automatically taken. Using the computer simulation software, the contact angles were calculated from these images. The experiment was performed at 25°C and about 60% humidity. The measured contact angle value reflects the hydrophilicity of scaffold with respect to the pure water (Milli-Q-water) as lower the contact angle more is the hydrophilicity of scaffold.

3.3.10. *In vitro* Cell Study

3.3.10.1. Preparation of matrices for cell study

The scaffolds were soaked in 10% NH_4OH to neutralize any acidity, and rinsed 3 times with sterilized distilled water. The samples were then sterilized by exposure to saturated steam and then immersed in

70% ethanol for 24 h for sterilization followed by rinsing with sterile PBS 3–4 times. After drying, samples were kept in UV radiation for 6 h on each side. Sterilized samples were then soaked in PBS overnight on a shaker (25 rpm) and immersed in the culture medium for 4–10 h to result in a more hydrophilic surface for optimal cell adhesion.

3.3.10.2. Isolation and culture of hMNCs on silk hydrogels

Mononuclear cells (MNCs) were isolated from fresh peripheral blood of healthy, middle aged human using Ficoll-paque separation technique as described previously [Neagu et al., 2005]. The work was approved by Institutional Ethical Committee. The hMNCs culture was expanded in growth media containing 90% DMEM-F12, 10% foetal bovine serum (FBS), 100 U/mL penicillin, 1000 U/mL streptomycin and 0.2% fungizone antimycotic. After passaging of culture 3 times, the cells were cultured to obtain a cell density of $3x10^7$ cells/ml. Autoclaved 15 ml of sterilized SF solution (12% w/v) were supplemented with powder DMEM-F12 and $NaHCO_3$. For the induction of gelation, solutions were sonicated for 20 min in a laminar hood. After sonication, solution was cooled to room temperature. A volume of 50 µL cell suspension was added and well mixed with SF solution to make the final concentration of $1X10^5$ cells/ml. The solution was put into 5 culture petridishes (Tarson, 32 mm) and incubated at 37°C and 5% CO_2. At the end of day 3 & 7, small plugs were punched out of the gels, washed 2-3 times with PBS, cut into two halves and incubated in Trypan blue for 15 min at 37°C.

3.3.10.3. Isolation and culture of hMSCs

Human umbilical cord blood (UCB) was collected from nearby Ispat General Hospital, Rourkela, India from 37year old delivery patient with informed consent and due approval from the Institutional Ethics Committee. Mononuclear cells (MNCs) were isolated from UCB by Ficoll gradient centrifugation technique and cultured in Dulbecco's modified Eagle's medium (DMEM), supplemented with 10% fetal calf serum (FCS), 1% non essential amino acids, L-ascorbic acid (0.150 g/l), 1% of 200 mM L-glutamine, 2% of 1 M HEPES, penicillin (100 U/ml) and streptomycin (0.1 mg/ml) at 37°C, under 5% CO_2 and 80% RH environment with the medium being replaced every 2–3 days. hMSCs were selected due to their property of short-term adherence to tissue culture flasks when incubated under standard conditions (37 °C, 5% CO_2 and 80% RH). After 24 h, non-adherent cells were discarded and adherent cells were further cultured, with the medium being replaced every 2–3 days.When culture flasks became semiconfluent after about 7 days, the cells were detached and serially subcultured [Kamihira et al., 2007]. hMSCs harvested at third to four cycles of passaging at viable cells/ml were used for seeding into scaffolds.

3.3.10.4. Phenotypic characterization of hMSCs by Flowcytometry

Phenotypic analysis of cultured hMSCs was performed by flow cytometry study. The fourth passage of cultured hMSCs were detached and properly washed with PBS followed by incubation for 20 min in 5% FBS (Foetal bovine serum) in PBS. The cells (1×10^5 cells per antibody) were resuspended in 100 µl PBS after washing with PBS. 1 µl of phycoerythrin (PE) or fluorescein isothiocyanate (FITC) conjugated mouse monoclonal antibodies against human CD34, CD45, CD90 (BD Biosciences, San Jose, CA) and CD105 (Invitrogen, Carlsbad, CA, USA) were added and incubated for 60 min in the dark at 4°C. After thorough washing cells three times with PBS, cells were resuspended in 400 µl PBS and analysed by BD LSR Fortessa and FACS Diva software (Becton Dickinson, San Jose, USA).

3.3.10.5. Cell seeding and culture

The sterilized scaffolds were placed in a 6 well plate. MSCs were seeded with $1x10^5$ cells/ml into the scaffoldby static methodand cultured in CO_2 incubator at 37°C, 5% CO_2 and 80% RH. The cultural medium was replaced every 2-3 days. The MSCs-seeded scaffolds were grown *in vitro*. MSCs seeded-scaffold was then assessed for cell attachment, proliferation and viability at various time points over the 14 days period of culture.

3.3.10.6. Cell Morphology

The photomicrographs of cells were observed under phase contrast microscope (Carl Zeiss, Axiovert 40 C) equipped with CCD camera. The surface morphology of MSCs on the scaffolds was examined by SEM (JEOL JSM -6480LV SEM) observation at different magnification. Adhered hMSCs in culture plate and cell seeded scaffolds were kept in 2.8% gluteraldehyde solution overnight before SEM analysis. The samples were affixed via carbon tape to the SEM sample holders and vacuum-coated with a 20-nm layer of platinum. SEM was performed at a voltage of 15 kV and room temperature.

3.3.10.7. *Cell seeding efficiency and cell proliferation assay*

For the study of cytocompatibility of salt leached SF scaffolds, (3-[4,5-dimethyltriazol-2-y1]-2,5-diphenyl tretrazolium) (Sigma, St Louis, MO, USA) assay was performend as reported in the published literature [Cory et al., 1991; Wilson et al., 2000]. This colorimetric assay is based on the ability of live cells to reduce yellow MTT reagent to a purple formazan product [Mosmann ey al., 1983]. In brief, 5×10^4 cells were seeded on scaffolds in a 96-well plate. The cells were incubated at 37°C in humidified atmosphere containing 5% CO_2. After 24 h incubation, supernatant of each well was replaced with MTT

diluted in serum free medium and the plates incubated at 37°C for 4 h. After that, 10%SDS/ 0.04 N HCl solution was added to supernatant and plates were re-incubated for 24 h, 200µl was transferred to a clean 96-well plate and absorbance was measured at 595 nm using ASYS EXPERT PLUS spectrometric microplate reader. For analysis, all data were expressed as average ± standard deviation for number of 3 replicates (n=3).

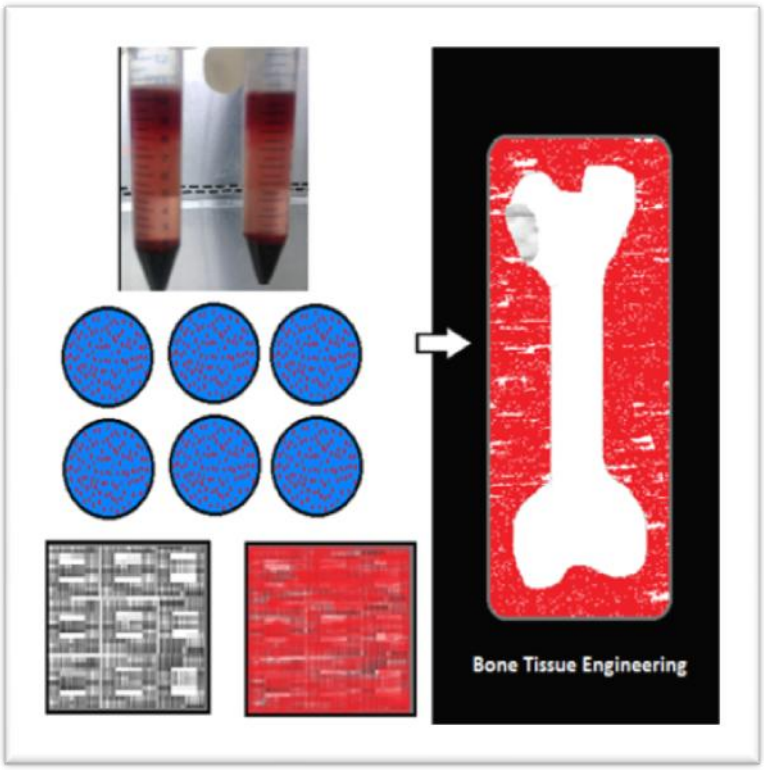

Figure 3.2: Stepwise representation of cell based bone regeneration. MSCs isolated and characterized from adult tissues, incorporated into scaffold, cultured, proliferated and differentiated, finally implanted into defective site.

3.3.10.8.Alkaline phosphatase (ALP) Assay

ALP assay is based on measuring the change in colorimetric absorbance of colourless para-nitrophenol phosphate (pNPP) cleaved to yellowish (paranitrophenol + phosphate) by membrane bound alkaline phosphatise enzyme. The alkaline phosphatase (ALP) activity of hMSCs grown on the scaffold was estimated to investigate the osteogenic differentiation following the method described in literarture [Mauney et al., 2005]. In brief, the hMSCs seeded scaffolds were cultured in osteogenic differentiation medium for 1, 7 and 14 days.At each time interval, the scaffold were thoroughly washed with PBS to remove the residual serum and then 1 ml of 0.02% Triton® X-100 was added to dissolve the cells. The

solutions were centrifuged at 14,000 rpm at 4°C for 15 min. 100 µl 1 mol/l Tris-HCl, 20 µl 5 mmol/l $MgCl_2$ and 20 µl 5 mmol/l p-nitrophenylphosphate were added to the supernatant and incubated for 30 min at 37°C. The reaction was stopped with 50 µl of 1N NaOH and the absorbance was measured at 410 nm using a UV-VIS spectrophotometer (Systronis-117). The standard curve was prepared using p-Nitrophenol of known concentrations [Sun et al., 2008]. All solutions were components of the Alkaline Phosphatase Assay Kit (Abcam, Cambridge, MA, ab83369-500).

3.3.10.9. Histology

Samples were fixed in 10% neutral buffered formalin (4% formaldehyde in phosphate buffered saline), embedded in paraffin, sectioned (5 µm thick) and observed histologically by hematoxylin and eosin (H&E). The cross-sections of the grafts were analyzed after 3, 7 and 14 days of *in vitro* culture. A general assessment of histology was performed using light microscopy.

3.3.11. *In vivo* biocompatibility test in animal model

The developed scaffolds were transplanted under the skin of 4- to 6-week-old ICR recipient mice as per procedure described previously [Jung et al., 2008] with a slight modification. In brief, Intra-peritoneal injection of avertin (Tri-bromoethanol, 0.25 mg/g of body weight; 2-methyl-2-butanol, 0.16 ml/g) was performed to anesthetize the mice and the skin was sterilized with 70% (v/v) ethanol. Approximately ~1 cm linear incision was made on the dorsolateral side of the skin and a small pouch was created in the subcutaneous layer. Scaffolds of dimension 5 x $5mm^2$ were transplanted into the surgically-created subcutaneous pouch and the incision was closed using nylon suture. The mice were monitored routinely for the skin and systemic diseases, if any. After one month, they were sacrificed by cervical dislocation and the scaffolds were explanted. Histological analysis was done with the skin around the site of transplantation. The skin samples were fixed in 10% (v/v) neutral buffered formalin and dehydrated in ascending grades of 40%, 60%, 80%, 95% and 100% ethanol and embedded in the paraffin wax. 5µm thick slices of specimens were made by microtome sectioning and were examined histologically after hematoxylin and eosin staining. All testing were performed under the aseptic conditions in compliance with the Guide for the Care and Use of Animals in Research and Teaching, published by the Federation of Animal Science Societies (3rd Edition, 2000) in Bio-Organ Research Centre, Konkun University, South Korea, and were approved by the Institutional Biosafety and Ethical Committee. Efforts have been given to ameliorate the suffering of animals.

3.3.12. Statistical analysis

Statistical significance was determined for all groups of scaffold samples for a number of 3 replicates and P values were generated by ANOVA using the Dunnett Test for multiple comparisons to one control (p 0.05, n≥3 assays). This method relies on assumptions of normality and homogeneity of the variances of the distributions.

CHAPTER 4

Result & Discussion

PART I

Extraction ofsilk fibroin protein extraction from *B. mori* silk cocoon and its characterization

Silk fibroin (SF), a natural macromolecule derived from domestic silkworm (*Bombyx mori*), has attracted the interest of scientists of various disciplines for a long time. It has a long history of use in medicine, for example, as sutures and artificial ligaments. Recently it has been considered asa promising biomaterial that offers a wide range of biomedical applications because of its excellent mechanical properties, environmental stability, biocompatibility and biodegradability [Ning et al. 1999; Altman et al., 2003]. These properties make SF as most attractive and promising biomaterial for bone, cartilage and ligament tissue engineering [Altman et al., 2003]. Silk consists of two different proteins: sericin and fibroin [Perez-Rigueiro et al., 1998]. Silk must be regenerated into a desirable form to meet a specific biomedical application. Removal of sericin from silk fibre traditionally known as degumming requires a thermo-chemical treatment [Perez-Rigueiro et al., 2002]. The detail procedure and reason for degumming of the silk has been reported earlier [Kadhar et al., 2008]. The weakening of non-covalent bonds with fibroin and involvement of hydrophilic bond with ionic solution leads to removal of sericine. The fibroin has highly oriented crystalline domain and it is insoluble. The fibroin content of naturally spun silk fibers can be separated from sericin *in vitro*[Rui et al., 1998]. Degummed silk fibers is soluble in certain high ionic-strength aqueous solutions of chaotropic salts namely $CaCl_2$, LiBr and so on, which destabilize proteins in solution and increase their solubility [Kweon et al., 2001a], leading to a transparent solution [Ayub et al., 1993; Sashina et al., 2006]. To date many researchers have attempted to find suitable solvents for preparing SF solutions, which may be subsequently spun into fibers. However, very few published reports are available that can provide complete processing of silk, optimization of process conditions and the characterization of silk solution. In this chapter, effort has been given to study the effect of various key process parameters to maximize the yield of SF from silkworm cocoon.The study uses Box–Behnken design for the optimization purpose using RSM to understand the effect of important process variables and their interactions on SF extraction process.

4.1.1. Degumming of *B. mori* silk cocoon

Degumming is a method of removing sericine from silk cocoon. The mechanism of sericin removal in chemical degumming is a combination of various effects such as: dispersion/solubilization and hydrolysis of different sericin polypeptides [Freddi et al., 1996]. Hydrolysis prevails when strong alkaline compounds are added to the degumming bath. Therefore, it was investigated the effects of key process parameters, such as temperature, time, and salt concentration on sericin removal

without triggering the hydrolytic degradation of fibres, that is easily induced by the presence of harsh chemicals in the treatment bath.

4.1.1.1. Effect of Na_2CO_3 salt concentration

To study the effect of salt concentration on the extent of sericin removal, the chopped silk cocoons were treated with varying concentration of aq. Na_2CO_3 in the range 0.01 to 0.04M. The degumming temperature and treatment time were kept constant at 70°C and 60 min. The effect of salt concentration on the formation of degummed silk fibers is shown in Figure 4.1.1. It is observed that the amount of silk fiber sharply decreased with increase in salt concentration from 0.01M to 0.02M which may be due to the loss of most of sericine from the silk fibre into the solution. The degumming loss was found to be increased from 19.9 % to 24.4 % with increase in concentration from 0.01 to 0.02M Na_2CO_3 solution and no significant increase in degumming loss with further increase in concentration of Na_2CO_3 is observed. However, the maximum degumming loss of 25.4 % was achieved at the concentration of 0.04M (Fig. 4.1.1). Therefore 0.02M Na_2CO_3 has been established as the most favourable salt concentration for degumming achieving maximum sericine removal. The minimum salt concentration also offers the silk fibre to be intact as high concentration of harse chemical may cause hydrolytic degradation of silk fibroin. Furthermore, at 0.02M, the silk surface was found smoother as compared to higher concentration as revealed by SEM (Fig. 4.1.4).

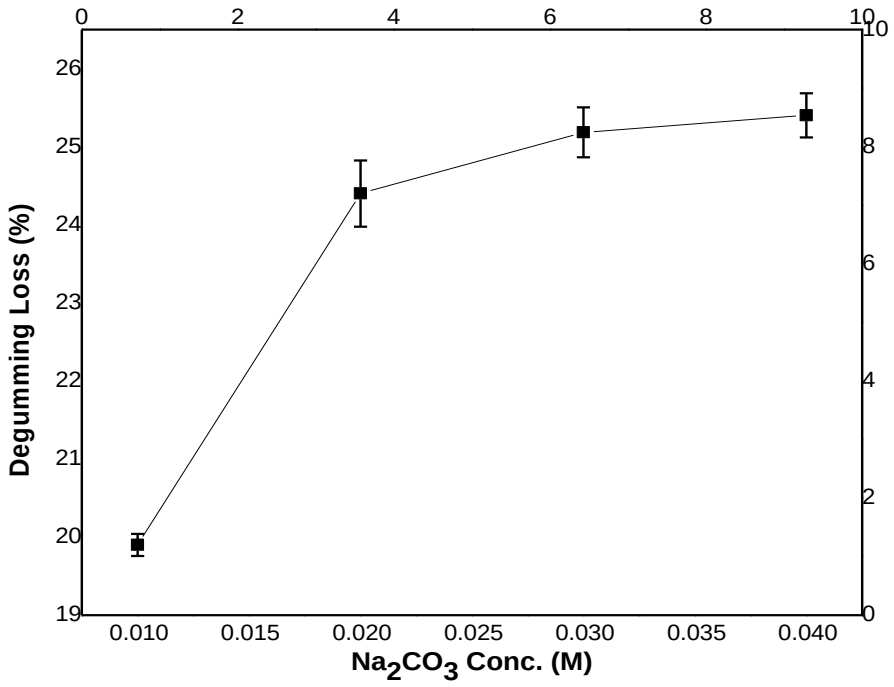

Figure 4.1.1: Effect of aq. Na_2CO_3 concentration on degumming of silk at 70°C and 60 min, The degumming loss is increasing with increase in Na_2CO_3 concentration. However most of the degumming loss representing maximum sericine removal is acheived with 0.02M Na_2CO_3.

4.1.1.2. Effect of degumming time

The treatment time has a significant influence on the degumming of silk [Kadhar et al., 2008]. To study the effect of the treatment time on the extent of sericin removal, the silk cocoon were treated with 0.02M aq. $NaCO_3$ solution at 70°C at a varying time period in the range 20-80 min. At 20 min., degumming loss was calculated as only 11% recovery of 8.9 g of silk fibre as shown in Fig. 4.1.2. At 40 min the loss increases to 18.8 % and the amount of silk recovered was 8.12 g. A loss of degumming 25.1 % was achieved after 60 min. Though a slightly increase in degumming loss (25.6 %) was observed with 80 min treatment time, the recovery of silk fibroin was found to be less (Fig. 4.1.2). This reduction in recovery of silk fibre with longer treatment time may be due to increased hydrolysis of interlinking bond between sericine and fibroin and more solubility of sericin into the solution. Moreover, the increase in treatment time probably exposes sericin to the action of hydrolysis by salt. Therefore, it has been established that 60 min is the most favourable degumming time.

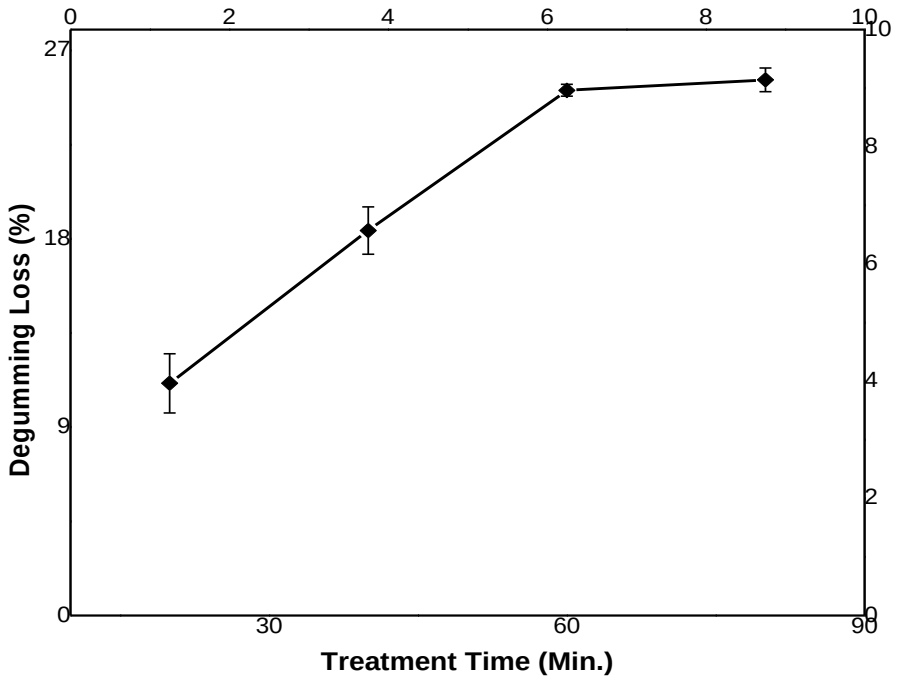

Figure 4.1.2: Effect of treatment time on degumming process performed at 0.02M $NaCO_3$ and 70°C. Degumming loss is increased steadily with increase in treatment time and reached maximum at 60 min.

4.1.1.3. Effect of degumming temperature

It is evident that sericincan be removed using water alone, but high temperature is required to attain complete degumming (110–120ºC, under pressure) [Freddi et al., 1996]. The effect of degumming temperature on the sericin removal was studied by conducting degumming experiment at varying temperature range 60-90ºC. Below 60ºC no significant degumming is achieved as reported earlier [Sukigara et al., 2003]. The concentration of Na_2CO_3 and treatment time were kept constant at 0.02M and 60 min respectively. The degumming temperature of 60ºC probably contributed to enhance the solubility of partially hydrolyzed sericin fractions adhering to the fibrous core of the silk as depicted in Fig. 4.1.3. The rise in temperature from 60 to 70ºC resulted in the loss of most of the sericin acheiving 24.4% degumming loss. A slight increase in degumming loss was observed at 80ºC and 90ºC. The corresponding degumming loss is 25.1% and 25.5% (Fig. 4.1.3). Thus, degumming temperature of 70ºC is established as optimum temperature. The rise in temperature not

only provides the activation energy for the breakdown of interlinking bonds but also increases the solubility of sericin into solution [Kadhar et al., 2008].

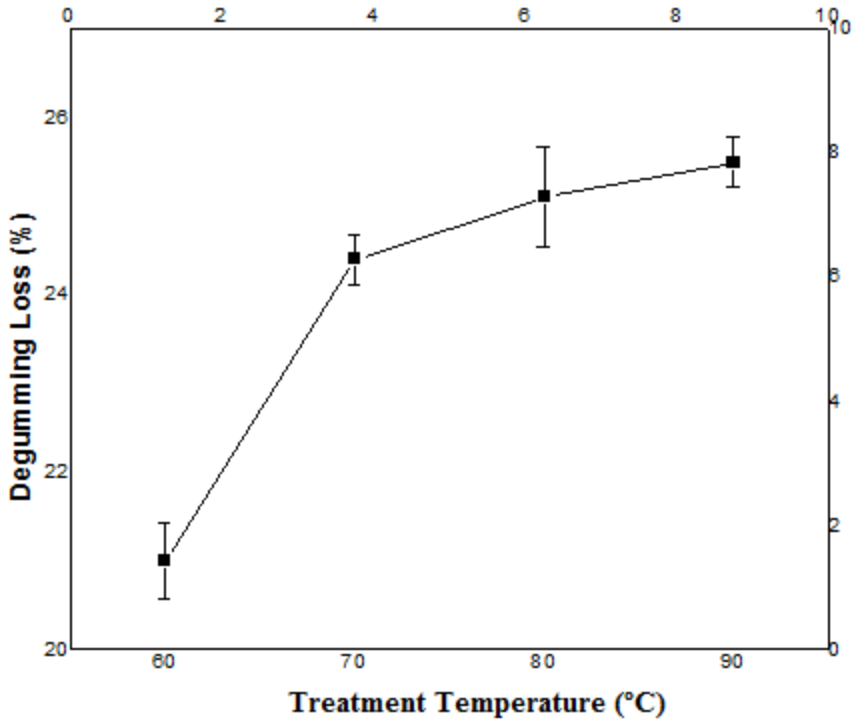

Figure 4.1.3: Effect of temperature on degumming process. The graph showing an increase in degumming loss with temperature and most of the degumming is achieved between 60-70°C.

4.1.1.4. SEM study with degummed silk fiber

The SEM observation of silk fibers obtained by the treatment with different concentration of Na_2CO_3 salt is shown in Fig.4.1.4. It is observed that the removal of sericin resulted in the separation of the individual silk filaments, which were glued together by sericin and sizing agents in the raw silk. This conferred on the fabric the denser texture and rough surface typical of light weight silk fibres. The dull appearance and stiff handle of the raw silk fibre disappeared, and the degummed silk became shiny, soft, and scroopy. Fig. 4.1.4(a) clearly confirms the presence of sericin stick as white spots to the surface of silk fiber. The presence of sericin in silk fiber is more when treated with 0.01M salt concentration showing non-uniform removal of gum from interlacing regions of fibers compared to the use of 0.03M salt concentration. So it is concluded that increase in concentration of Na_2CO_3 decreases the sericin content of silk fiber. The closer observation of SEM images of the silk fibroin fibre showed that the individual silk filaments split off and their surface

was clean and free of sericin. On the other hand, the presence of sercicin on the fibre was observed when silk degummed with lower salt concentration. Furthermore, it is interesting to note that the deposits were mainly located at the cross over points between silk fibers making it stick together. The diameter of silk fibre was analysed and measured as 10-12 µm using SEM JEOL software.

4.1.2. Preparation of regenerated aqueous SF solution

The solubility of silk fibroin in ionic liquids depends on the identity of both the cation and anion, with the anion having a much larger effect. It is reported that more the cation and anion are able to participate in hydrogen bonding, the greater the solubility of the silk fibroin [Phillips et al., 1989]. Presumably, the ionic liquid disrupts hydrogen bonding present in the β-sheets. The solubility depends on various factors like temperature, salt concentration and exposure time. Therefore, the effect of these parameters on solubilisation of degummed silk fibre was investigated in this study.

4.1.2.1. Effect of temperature on solubilization

The effect of temperature on solubility of protein is shown in figure 4.1.5. It is observed that the solubility is steadily increased with increases in temperature from 50 to 70°C and then becomes almost constant with further increase in temperature. However, the complete dissolution of silk fibre occurs at 70°C and higher temperature. Furthermore, though a reasonable solubilisation was obtained at 60°C, it was very difficult to separate SF solution. Thus, it is established that 70°C is the optimal temperature for dissolving degummed silk fibre.

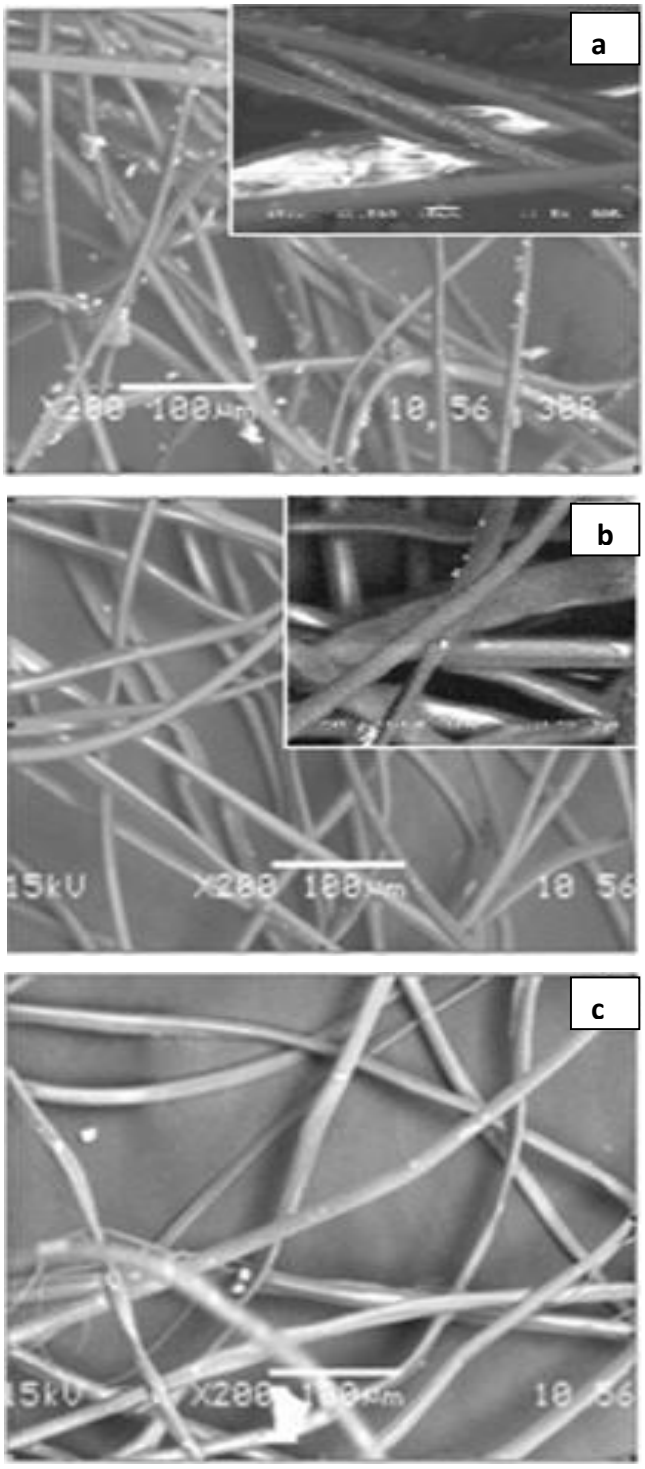

Figure 4.1.4: SEM micrographs illustrating morphology of degummed silk fibre with (a) 0.01M Na_2CO_3, shows comparatively incomplete removal of sericin. (b) 0.02M Na_2CO_3, shows relatively smooth and individual longitudinal strands and (c) 0.03M Na_2CO_3, shows individual longitudinal strands.

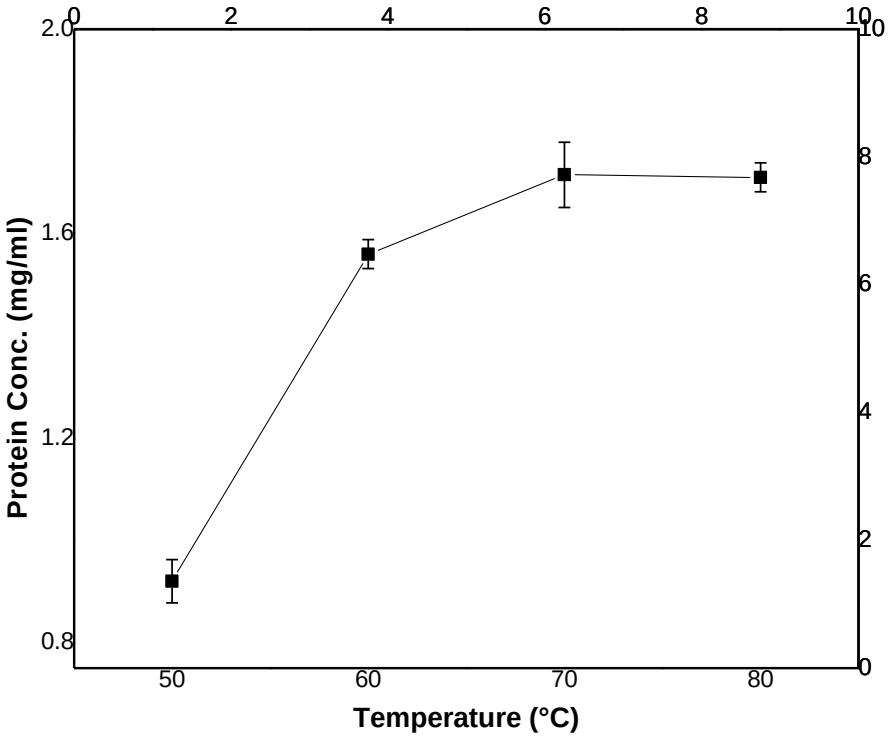

Figure 4.1.5: Effect of temperature on solubility of SF protein. A steady increase in solubility of silk fibroin is observed with temperature upto 70 °C

4.1.2.2. Effect of LiBr concentration on solubilization

The effect of LiBr concentration on solubility of protein is shown in Fig.4.1.6. LiBr is selected among other chaotropic reagents viz. $CaCl_2$ and NaSCN due to its higher dissolving ability as reported earlier [Addis and Raina, 2013]. The amount of protein present is more at 9.3M than obtained with other salt concentrations. So as the concentration of LiBr increases, the solubility of protein also increases. At concentration of 9.1M, protein concentration is 1.4 mg/ml that increases to 1.7 mg/ml at 9.3M concentration. There is no further increase in protein concentration beyond 9.3M. An increase in solubility is obserbed upto 9.3M that may be due to enhanced breaking of disulfide bonds between the heavy and light chains of silk fibroin [Kweon et al., 2001]. A comparable protein concentration is also obtained with LiBr concentration of 9.4M and 9.5M. However, the maximum protein concentration is obtained with 9.3M LiBr concentration. The slight decrease in protein concentration may be due to increased partial molar concentarion of salt in solution.

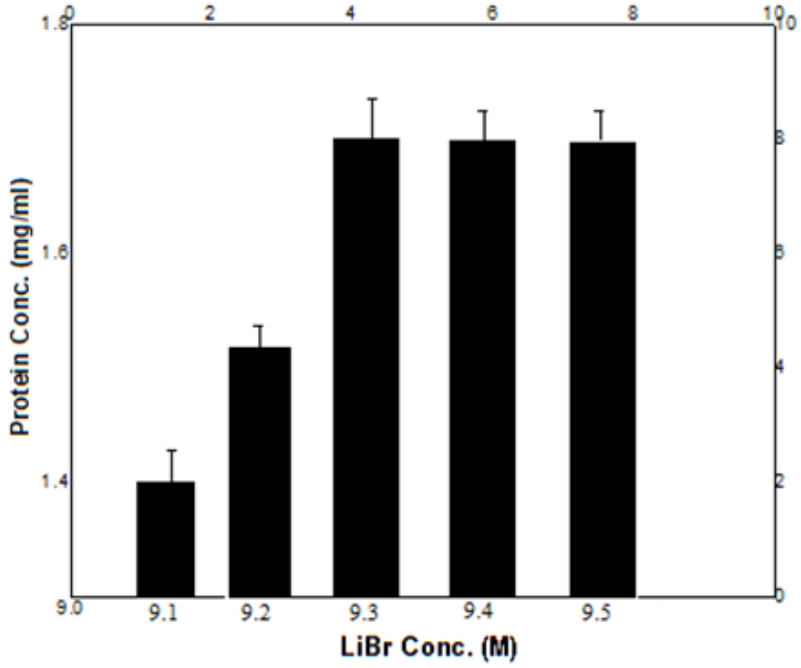

Figure 4.1.6: Effect of LiBr concentration on the solubility of protein. Protein concentration increases with increase in concentration of LiBr upto 9.3M and then a decline in trend is observed.

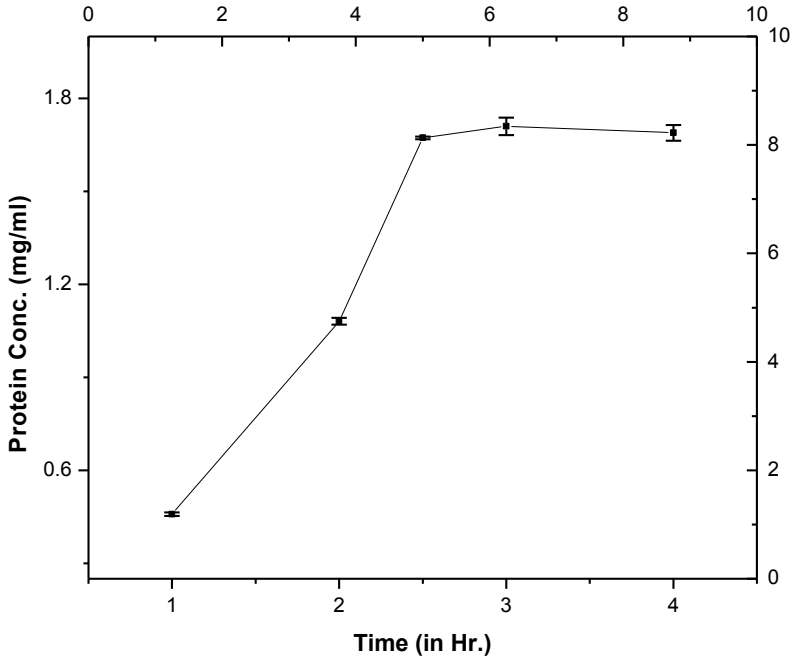

Figure 4.1.7: Effect of exposure time on dissolution of silk fibroin. Figure shows a steady increase in dissolution of SF with treatment time 1-3 h achieving maximum dissolution and no signicant change is observed beyond 3h.

4.1.2.3. Effect of exposure time on solubilization

The exposure time facilitates the solute with thermal energy to break bonds that binds molecules together. More is the exposure time, more of the heat energy accumulates to break inter and intra-chain covalent bonds in silk fibroin. Therefore, the effect of exposure time on solubilization of degummed silk fiber was studied with 9.3M LiBr solution at 70 °C. As it is indicated in Fig. 4.1.7, the SF concentration found to increase with increase in exposure time from 1-3 h. There is no further increase in SF concentration observed beyond 3 h of exposure.

4.1.3. Characterization of regenerated aqueous SF solution

During dissolution of degummed silk fiber in LiBr, the amide bonds of fibroin molecular chain is reported to cleave to a different extent resulting in easy solubilization in water. This regenerated silk fibroin is easily denatured and gelled by various factors [Zhang et al., 2005]. Besides temperature and pH, the stability of silk fibroin solution largely depends on its molecular weight [Zhang et al., 2005]. The particle size measurement of polymeric materials confirms the structural stability in solution and provides a high degree of control over processed material performance [Horiba Scientific Inc., 2012]. The prepared SF aqueous solutions were kept at 4°C and characterized by SDS-PAGE and particle size analysis within a month. Fig. 4.1.8a (SDS-PAGE) shows a smear band of silk fibroin corresponding to molecular marker ranging between 200 kDa to 30 kDa. As the result indicates that the regenerated protein solution are composed of a mixture of polypeptides with different molecular weights. A broad dull band at 200 to 35 kDa and dense band at 25 kDa are observed in Fig. 4.1.8a. The former band may be attributed to the degradation products of heavy chain (350 kDa) formed by the cleavage of amide bonds of raw silk protein, while the band at 25 kDa corresponds to light chain of raw silk protein. The result is further confirmed by particle size analysis of silk fibroin solution as shown in Fig. 4.1.8b. The particle size distribution profile is observed to be binodal, with peaks at around 100nm and 5µm. Since particle size of the starting SF solution is disintegrated due to extraction process with salts, the result shows the presence of light chain (25 kDa) with disintegrated heavy chain(350 kDa) [Horan et al., 2005].

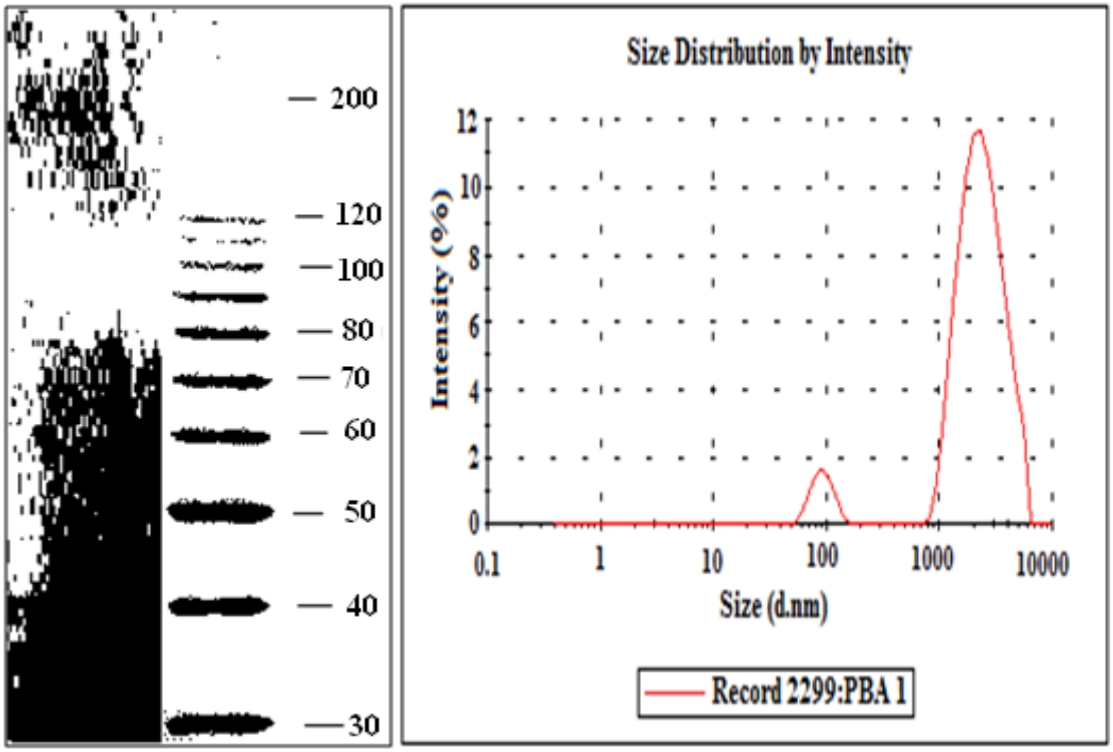

Figure 4.1.8: (a) SDS-PAGE (12% gel) of silk fibroin protein. Marker and fibroin lanes mean the standard protein ladder from 10 to 200 kDa (Gibco Co., USA) and molecular mass range of silk fibroin, respectively and (b) Particle size distribution of silk fibroin.

4.1.4. Optimization of SF extraction by RSM

The optimization of any process using response surface methodology (RSM) is more advantageous than the traditional single parameter optimization in terms of saving time, working space and raw material. Therefore, an attempt has been made in the present study to establish the optimum conditions of key variables for maximum SF protein extraction. The process variables used are the Na_2CO_3 concentration (X_1), LiBr concentration (X_2) and temperature for dissolution (X_3). All the experiments were conducted for optimizing the three individual parameters using Box–Behnken design (Table 4.1.1). The results were analyzed by multiple regression analysis. Table 4.1.2 shows the experimental conditions and results of extracted SF yield based on the factorial design. Maximum yield of protein (2.10 mg/ml) was recorded under the experimental conditions of Na_2CO_3 concentration 0.01 M, LiBr concentration 9.10 M, and temperature $70\,^{o}C$.

Table 4.1.1: Selection of a satisfactory model for protein extraction

Sequential Model Sum of Squares						
Source	Sum of Squares	df	Mean Square	F	p	Remark
Mean	49.20	1	49.20	-	-	-
Linear	0.36	3	0.12	11.56	0.0006	-
2FI	0.019	3	6.217E-003	0.53	0.6735	-
Quadratic	0. 11	3	0.035	20.60	0.0008	suggested
Cubic	3.875E-003	3	1.292E-003	0.64	0.6299	Aliased
Residual	8.120E-003	4	2.030E-003	-	-	-
Total	49.70	17	2.92	-	-	-
Lack of Fit Tests						
Source	Sum of Squares	df	Mean Square	F	p	Remark
Linear	0.13	9	0.014	7.03	0.0380	-
2FI	0.11	6	0.018	9.01	0.0259	-
Quadratic	3.875E-003	3	1.292E-003	0.64	0.6299	suggested
Cubic	0.000	0	-	-	-	Aliased
Pure error	8.120E-003	4	2.030E-003	-	-	-
Model Summary Statistics						
Source	Std. Dev.	R^2	Adj. R^2	Pre. R^2	PRESS	Remark
Linear	0.10	0.7274	0.6645	0.4501	0.28	-
2FI	0.11	0.7647	0.6235	-0.1233	0.56	-
Quadratic	0.041	0.9761	0.9453	0.8509	0.075	suggested
Cubic	0.045	0.9838	0.9352	-	-	Aliased

To decide about the adequacy of the model for SF yield, three different tests such as Sequential Model Sum of Squares, Lack of Fit Tests and Model Summary Statistics were carried out and *p* values for all the regressions were found to be lower than 0.01 (see Tab. 4.1.2). This means that at least one of the terms in the regression equation had a significant correlation with the response variable. The model summary statistic showed the highest regression coefficient as $R^2 = 0.9761$ for the quadratic model with minimum standard deviation of 0.041. ANOVA analysis confirmed that

the form of the model chosen to explain the relationship between the factors and response is validated [Tarangini et al., 2009].

Table 4.1.2:.Box–Behnken design matrix of the three variables in coded units along with the experimental and predicted values of protein yield

Trial no	X_1	X_2	X_3	**Protein yield (mg/ml)**	
				Experimental	Predicted
1	0.01	9.10	70	1.89	1.92
2	0.01	9.50	70	1.84	1.85
3	0.03	9.10	70	1.71	1.70
4	0.03	9.50	70	1.65	1.62
5	0.02	9.10	55	1.45	1.45
6	0.02	9.50	55	1.30	1.32
7	0.02	9.10	85	1.76	1.74
8	0.02	9.50	85	1.74	1.74
9	0.01	9.30	55	1.64	1.61
10	0.03	9.30	55	1.50	1.51
11	0.01	9.30	85	2.1	2.09
12	0.03	9.30	85	1.72	1.75
13	0.02	9.30	70	1.70	1.72
14	0.02	9.30	70	1.69	1.72
15	0.02	9.30	70	1.73	1.72
16	0.02	9.30	70	1.80	1.72
17	0.02	9.30	70	1.70	1.72

In order to determine the significance of quadratic model, ANOVA analysis was done. The *p*-values were used as a tool to verify the significance of each coefficient, which also indicates the interaction strength of each parameter. The smaller the *p*-values are, the bigger is the significance of the corresponding coefficient [Zhao et al., 2009]. Here, the *p*-value of the model is found to be smaller than 0.0001, which indicates that the model is suitable for use in this experiment. The P-value of ‘‘lack of fit” is 0.64 (p> 0.01), which indicates that ‘‘lack of fit” is not significant relative to the pure error. The coefficient of determination (R^2) and adjust coefficient of determination

($Adj.R^2$) are shown in Table 4.1.3. The values indicate that the accuracy and general availability of the polynomial model are adequate [Tarangini et al., 2009]. The regression coefficients and the corresponding *p*-values are presented in Table 4.1.4. From the *p*-values of each model term, it is concluded that three linear coefficients (X_1, X_2, X_3), three quadratic coefficients (X_1^2, X_2^2, X_3^2), and three cross-product coefficients (X_1X_3) are significant. Using the designed experimental data (Table 4.1.1), the polynomial model for the protein extraction was regressed as follows (in terms of actual factors):

$$Y = -132.13 - 16.70X_1 + 29.08X_2 - 0.02X_3 + 1130X_1^2 - 1.62X_2^2 - 4.32E - 004X_3^2 + 0.01X_1X_3 \quad (3)$$

Table 4.1.3: Analysis of variance for the fitted quadratic polynomial model for protein yield

R^2=0.9761; Adj R^2=0.9453

Source	Sum of squares	df	Mean square	F-value	Probability (*p*)>F
Model	0.49	9	0.054	31.71	<0.0001
Lack of fit	0.0039	3	0.0013	0.64	0.6299
Pure error	0.0082	4	0.002		
Correlation total	0.50	16	-	-	-

Table 4.1.4: Regression coefficients and their significance of the quadratic model for protein yield

Model term	Coefficient estimate	Df	Standard error	Probability (*p*)>F
Intercept	1.72	1	0.019	-
X_1	-0.11	1	0.015	0.0001
X_2	-0.35	1	0.015	0.0481
X_3	0.18	1	0.015	<0.0001
X_1^2	0.11	1	0.020	0.0008
X_2^2	-0.065	1	0.020	0.0151
X_3^2	-0.097	1	0.020	0.0019
X_1X_3	-0.060	1	0.021	0.0230

A normal probability and a dot plot of residuals are shown in Fig. 4.1.9. The data points on this plot lie reasonably close to a straight line, indicating that X_1, X_2, X_3, X_1^2, X_2^2, X_3^2, and X_1X_3 are the only significant effects and that the underlying assumptions of the analysis are satisfied. Fig. 4.1.10 shows the relationship between the actual and predicted values of *Y* for protein extraction from *Bombyx mori* silk cocoon. It is observed from Fig. 4.1.9 that the developed models are adequate as indicated by the residuals for the prediction of each response are minimum.

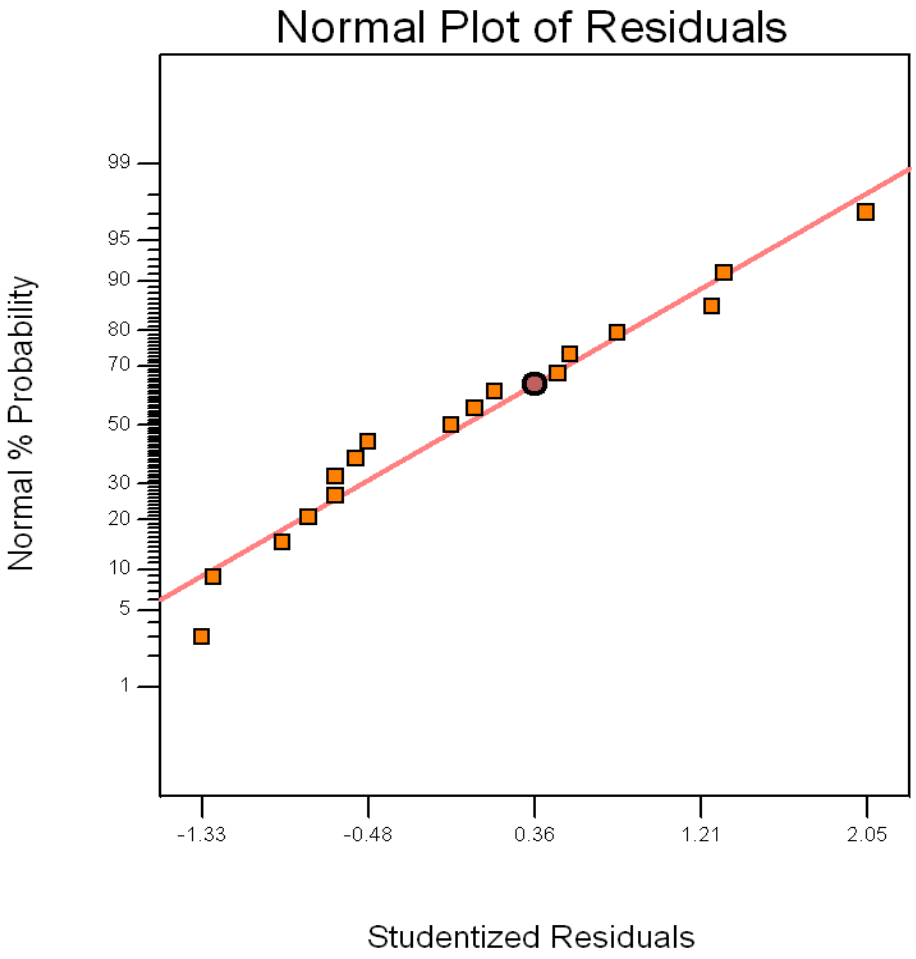

Figure 4.1.9: Normal % probability versus residual error

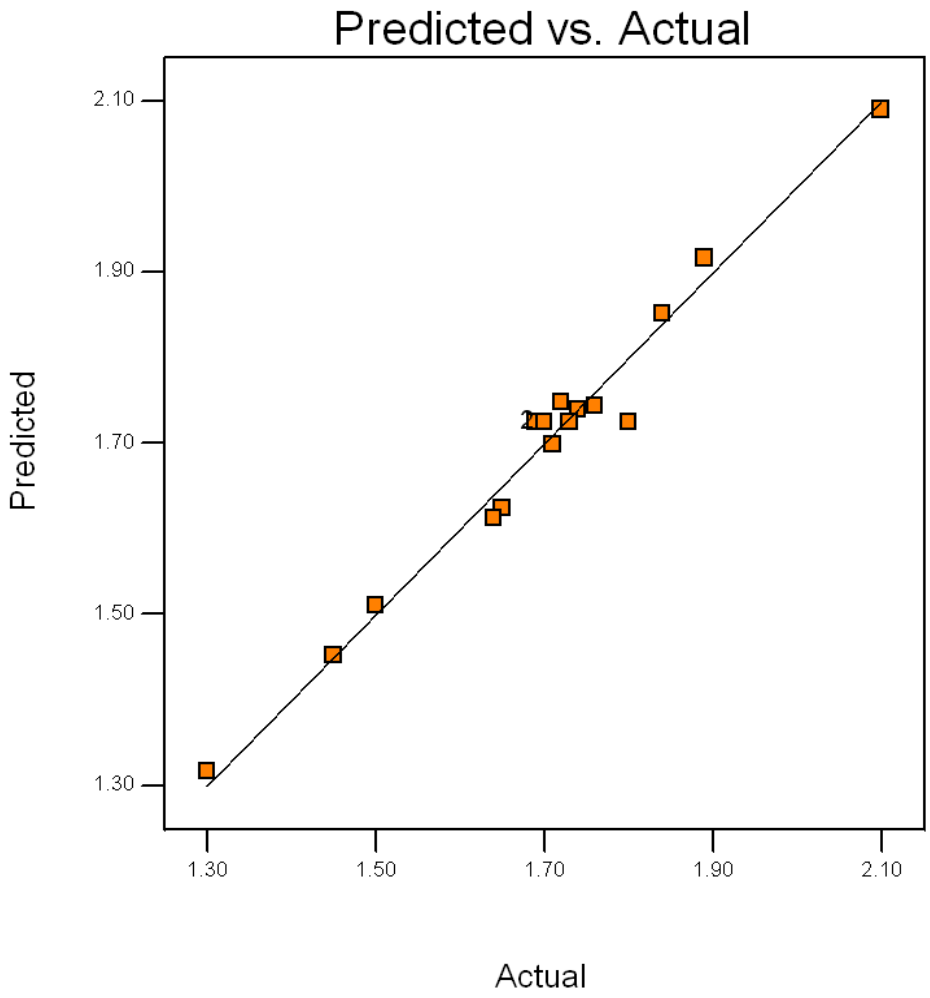

Figure 4.1.10: Scatter diagram of predicted versus actual response for silk fibroin extraction

Many parameters can influence the extraxtion of protein. Eq. (3) shows that the yield of SF protein has a complex relationship with independent variables that encompass both first and second-order polynomials and may have more than one maximum point. Fig. 4.1.11 represents the effects of Na_2CO_3 concentration, temperature and their reciprocal interactions on protein yield. The degumming SF yield is shown to increase with increase in temperature at constant Na_2CO_3 concentration. However, the maximal SF protein yield is obtained at of $85\,^oC$. Fig. 4.1.12 shows the effects of $LiBr$ concentration, temperature and their reciprocal interactions on protein yield. At a high temperature, the SF yield is increased with increase in temperature.

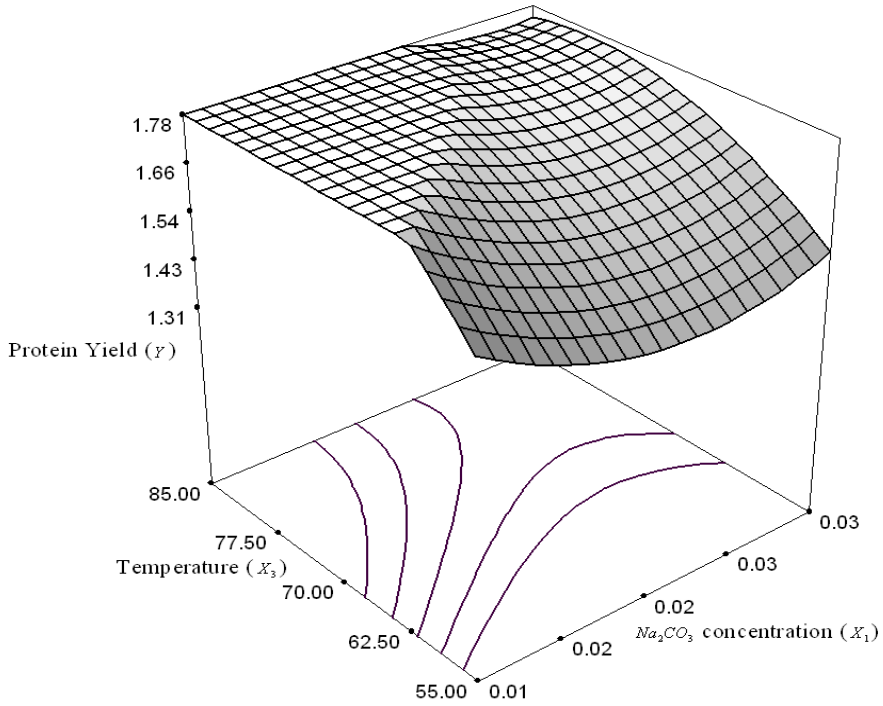

Figure 4.1.11: Response surface plots representing the effect of Na_2CO_3 concentration and temperature and their reciprocal interaction on SF yield

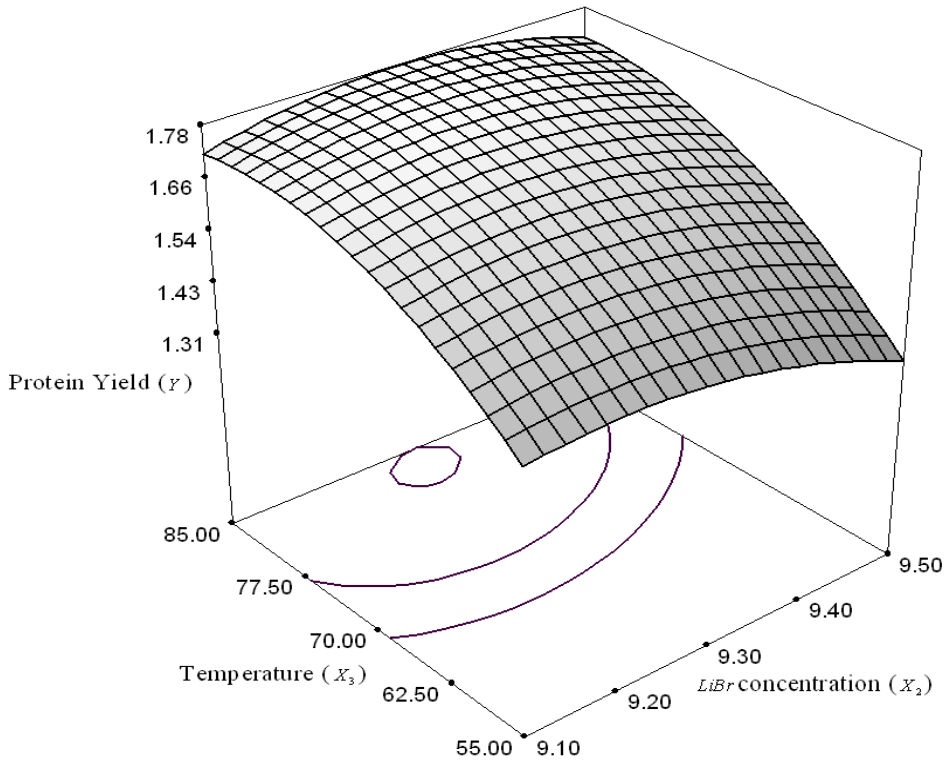

Figure 4.1.12: Response surface plots representing the effect of LiBr concentration, temperature and their reciprocal interaction on SF yield

4.1.5. Validation of the model

The optimal values of the selected variables were dtermined by solving the regression equation (Eq. 3) using Design-Expert 6 software. The optimal conditions for SF protein yield estimated by the model equation are as follows: Na_2CO_3 concentration, X_1= 0.01 M, *LiBr* concentration, X_2= 9.23 M and temperature, X_3= 85^oC. The theoretical protein yield (*Y*) predicted under the above conditions is 2.09 mg/ml. In order to verify the prediction of the model, the optimal reaction conditions were applied to three independent replicates for protein yield. The average protein yield is measured as 2.1±0.01 mg/ml which is quite matching with the estimated value using model equation. This demonstrated the validation of *RSM* model. The good correlation between these results confirmed that the response model is adequate for reflecting the expected optimization. The results also suggest that the models of Eq. (3) are satisfactory and accurate.

PART II

Preparation, characterization and *in vitro* biocompatibility study of silk fibroin hydrogel

Hydrogels are three-dimensional polymeric networks that are prepared by physical or chemical crosslinking and resist swelling in aqueous solution without dissolving in it [Vepari et al., 2007; Lee et al., 2001]. Since hydrogels are highly hydrated hydrophilic polymer networks that contain pores and void spaces between the polymer chains, it can be implanted for tissue restoration or local release of therapeutic factors. Such hydrogels are biocompatible and provide many advantages over the conventional solid scaffold materials, including an enhanced supply of nutrients and oxygen for the cells and space to cells for proliferation and expansion. Due to their high water content, hydrogels have similarities to some tissues and extracellular matrices (ECM) [Park et al., 1992]. Because of this property, hydrogel has been considered as an attractive biomaterial and widespread research is under way on using hydrogels as scaffold materials for possible application in tissue engineering. Hydrogels prepared from a variety of polymers such as alginates, chitosan, and collagen have been studied for use as scaffold material [Lee et al., 2001; Drury et al., 2003]. Hydrogels made from synthetic polymers offer the benefit of gelation and gel properties that are controllable and reproducible through the use of specific molecular weights, block structures, and modes of crosslinking. However, the less biocompatibility and use of toxic reagents for their preparation limit their applications. Generally, gelation of naturally derived polymers is reported to be less controllable, although their hydrogel forms are reported to be more compatible for hosting cell and bioactive molecules [Lee et al., 2001; Smidsrod et al., 1990]. Injectable biomaterials for tissue engineering are defined as cell seeded engineered scaffolds that directly injected at the site of defect. Such fluidly material takes the complex shape of site, fixes it and exchanged with body fluid while the seeded cells proliferate and differentiate to form tissues. Such approach in tissue engineering has been reported to reduce surgical operations [Balakrishnanet al., 2005; Kretlow et al., 2007]. Therefore, in this part of thesis work, efforts have been given to examine the processability of concentrated aqueous silk fibroin solutions into highly porous gel sponges and study their properties for possible tissue engineering applications.

4.2.1. Morphological Study

Morphologically, the hydrogels shows a sponge-like cross-linked structure formed by physical entanglement as well as chemical hydrogen and covalent bindings. Water-stable hydrogels were formed from SF aqueous solutions after 24 h of incubation that leads to the formation of porous matrices. The formation of porous matrices is due to the induction of a sol-gel transition in concentrated solution sample [Garg et al., 2012].

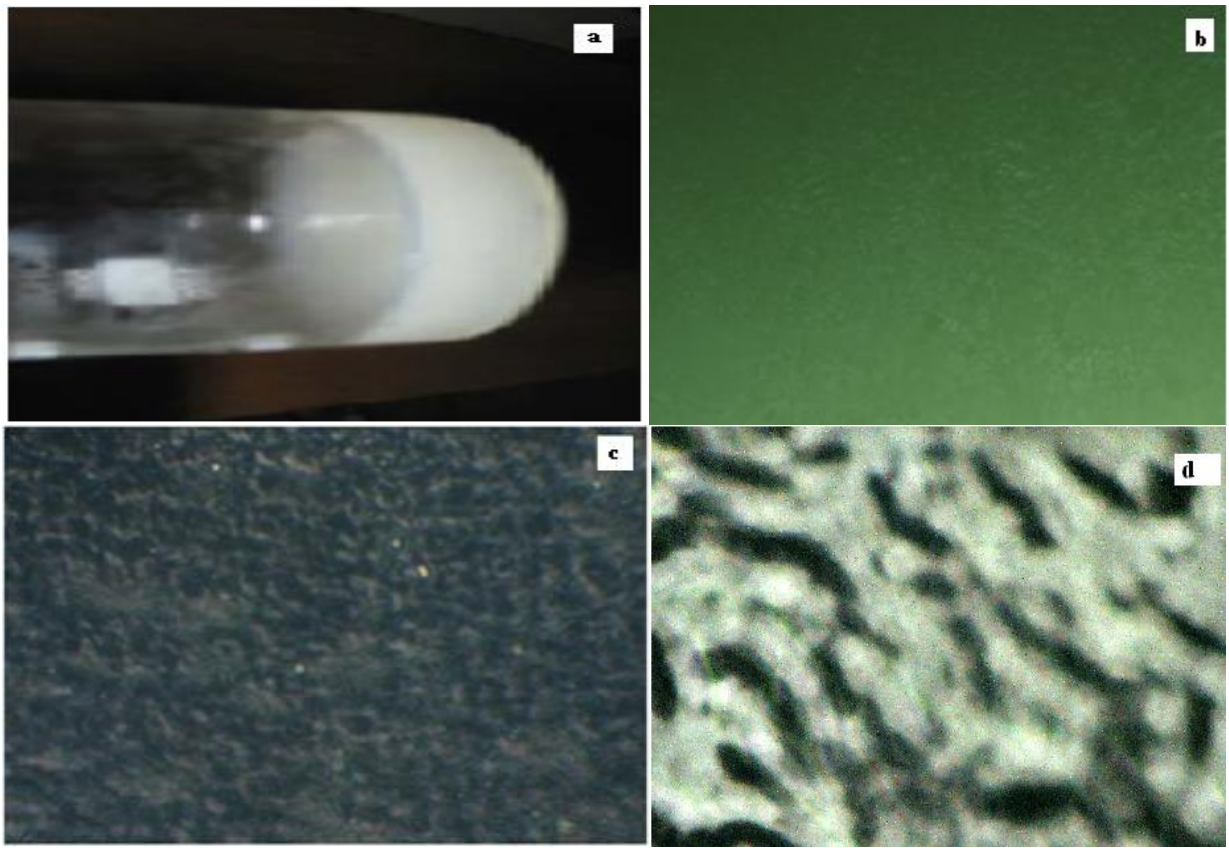

Figure 4.2.1: (a) Simple vertical view and (b,c,d) microscopic images of SF hydrogel obtained from 12% (w/v) aq. SF solution, when kept at 20°C for 3 days observed at magnification (b) 5X, (c) 10X and (d) 20X

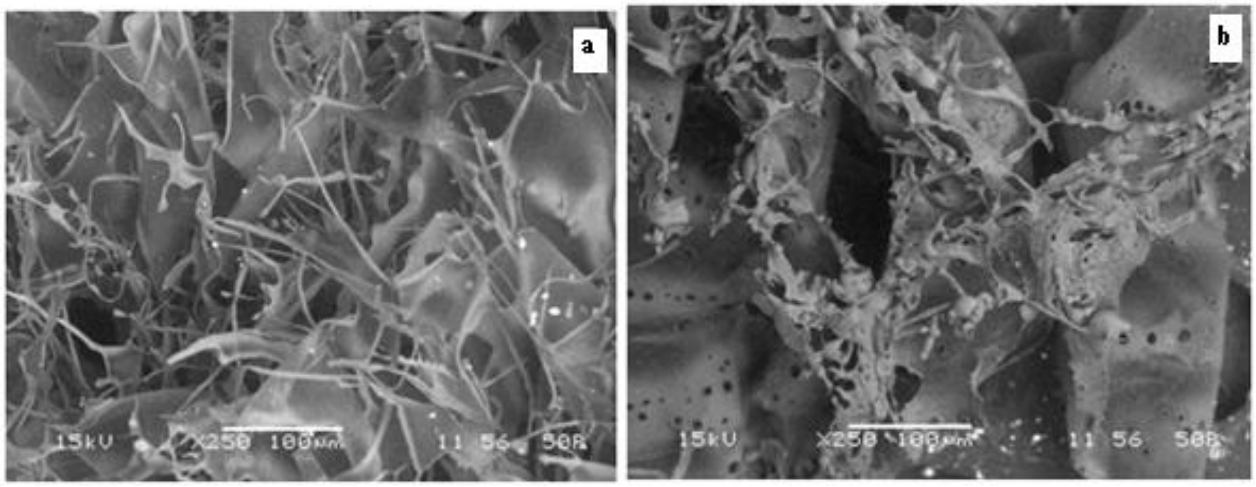

Figure 4.2.2: SEM images of (a) porous lyophilized hydrogel with leaf-like structure prepared from 4 wt % SF and (b) hydrogel sponge prepared from >12 wt % SF solutions.

Regenerated silk fibroin solution when kept at 20ºC in humid environment for more than 72 h, the solution was converted into gel and ultimately hydrogel (thermgel) formed. The process was induced by adding a few drops of methanol as crystallinity inducing solvent. The silk hydrogel intact in shape is formed and stabilized due to inter-networking. The gel doesn't lose its integrity when kept vertically as shown in Fig. 4.2.1(a).Fig. 4.2.1(b, c, d) is a representative optical micrograph of prepared silk fibroin hydrogel sample. Morphological study of silk fibroin porous matrices are observed by SEM (Fig. 4.2.2(a, b)) after lyophilizing the hydrogel samples at −80° C. Lyophilized hydrogels prepared from silk fibroin solutions of 4-12 wt% concentration showed leaf-like morphologies while sponge-like structures were observed with concentration more than 12 wt%. This is in good agreement with the observation reported earlier [Kim et al., 2004]. The sponge-like structure is more liable to be applicable for tissue regeneration as it provides better niche and channel for cellular activities.

4.2.2. Swelling Property

The swelling state of the polymer is reported to be important for its bioadhesive property [Smart et al., 1984; Smart et al., 2005]. It is also reported that the molecular structure of fibroin doesn't change by change in water content of the gel, while the physical properties of the gel changes significantly [Ayub et al., 1993]. Therefore, the swelling behavior of the prepared hydrogel was studied and the experimental data is tabulated in Table 4.2.1. It is observed that water uptake by hydrogels increased with time until equilibrium is reached at 24 h. The swelling was found to occur uniformly in all direction with increase in volume and change in physical appearance from translucent to opaque and semi-fluid was observed (Fig. 4.2.3).

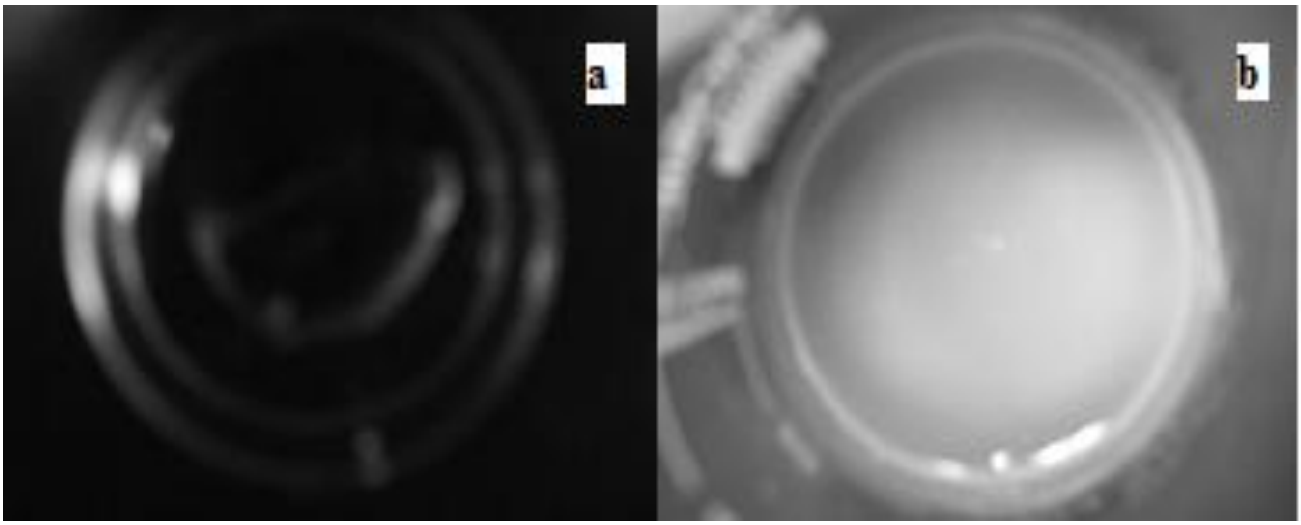

Figure 4.2.3: Pictorial view of (a) dehydrated and (b) swollen SF hydrogel

The dehydrated gel is found to be non-brittle representing the presence of water molecule to maintain equilibrium with respect to physical properties of the gel. The gel became brittle when it was dehydrated in oven. The higher swelling rate at the initial stage indicates the sucking of water molecules into the collapsed gel and adsorption of water over the dried surface of gel. Though the swelling ratio increased with increase in time of soaking, a decline in rate is observed beyond 16 h and the rate becomes constant with further increase in time. Therefore, the maximum swelling index of 286.7 is obtained at 16 h (Table 4.2.1). No further change was observed beyond 24 h of soaking which may be due to the entry of water molecule at a slower rate to the collapsed gel network.

Table 4.2.1: Swelling behaviour of dehydrated SF hydrogel in water at different time period

Time (h)	**Weight of gel (mg)**	**Swelling Index (%)**
0	77.19	0
2	135.12	75.05
4	244.14	216.28
16	298.54	286.76
24	301.12	290.1
28	301.15	290.14
32	301.155	290.15
36	301.155	290.15

4.2.3. Thermo-rheological Behavior

The thermorheological behavior of prepared SF hydrogel was examined by measuring shear stress and viscosity at 5 degrees interval. Fig.4.2.4 shows the changes in viscosity with temperature. Thermal behavior of SF samples recently studied through differential scanning calorimetry (DSC) depicts a broad endotherm with a peak near 45°C indicating gradual structural change with increase in temperature and a new structure is formed above 45°C. This thermal behavior shows consistency with the viscoelastic behaviour of SF hydrogel. Preliminary ATR FT-IR studies have indicated that the fraction of antiparallel β -sheet conformation appreciably increased at 45°C [Ochi et al., 2002]. Irreversible structural change could be considered as a reason to the observed thermoreheological behavior.

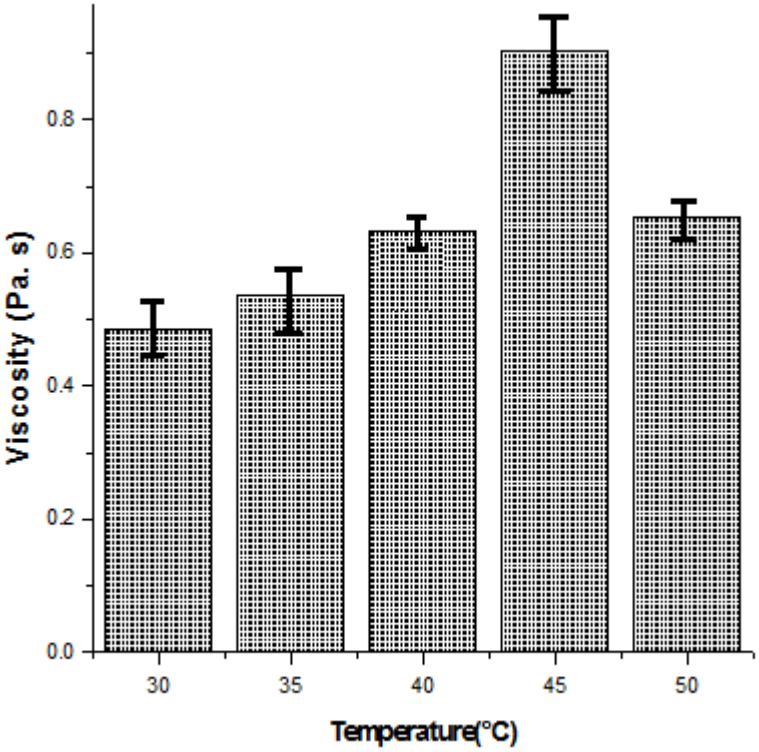

Figure 4.2.4: Thermo-rheological behavior of SF hydrogel

Fig. 4.2.4 shows the linear proportionality between viscosity and temperature at the low shear rate region less than 100 s^{-1}. It has been reported that the rheopectic fluids increase their viscosity over time with application of shear forces, while thixotropic fluids have a reversible time-dependent loss of viscosity accompanying the application of shear force [Miller et al., 1960]. If the time-dependent

loss of viscosity is nonreversible, the fluid is considered to have rheodestructive properties. The present study shows that the prepared gel exhibits rheopectic and either thixotropic or rheodestructive properties. Furthermore, repeated observation reveals that continuous swirling of the mixture leads to an irreversible decrease in the viscosity. Therefore, the time-dependent reduction in viscosity of gel is rheodestructive rather than thixotropic.

4.2.4. Structural Analysis

Structural characterization of silk fibroin fibre and lyophilized hydrogels were performed by X-ray diffraction and FTIR analysis. The XRD patterns and FTIR peaks of degummed silk fiber and lyophilized RSF hydrogel are shown in Fig. 4.2.5 & 4.2.7 respectively.

4.2.4.1. XRD Analysis

X-ray profiles of lyophilized hydrogels prepared from aquous SF solutions are shown in Fig. 4.2.5. It has been reported that when silk fibroin solutions freeze, below the glass transition temperature between −34°C & -20°C, the protein structure doesn't change significantly [Li et al., 2001]. The amorphous structure of lyophilized SF hydrogel samples are indicated by the exhibition of a broad peak at around 20° [Magoshi et al., 1996]. Silk fibroin hydrogels showed a distinct peak at 20.6° and two minor peaks at around 9° and 24°, that is very similar to β-sheet crystalline SF structure (Silk I) [Ayubet al., 1993; Asakuraet al., 1985]. X-ray diffraction result shows that the gelation of silk fibroin solutions induced a transition from random coil to β-sheet conformation (Fig. 4.2.6) which is also reported in published literature [Hanawa et al., 1995; Ayub et al., 1993; Kang et al., 2000].

Furthermore, the regenerated silk fibroin (RSF) hydrogel (line b in Fig. 4.2.5) shows more amorphous state, while the degummed silk fiber (line a in Fig. 4.2.5) shows a typical X-ray diffractogram of β -sheet crystalline structure, depicting four diffraction peaks at 18.9°, 20.6°, 24.3° and 28.1°, corresponding to β-sheet crystalline spacing of 4.69°, 4.31°, 3.66° and 3.17 A°, respectively [Ayub et al., 1993; Asakura et al., 1985]. While the lyophilized fibroin hydrogel shows the characteristic peak at 20.6°. Other peaks corresponding to degummed silk fibre is not visible indicating the more α-helical secondary structure. In conclusion, the processing of silk fibroin results in a loss of β -sheet structure thus making it more biodegradable and lower mechanical strength.

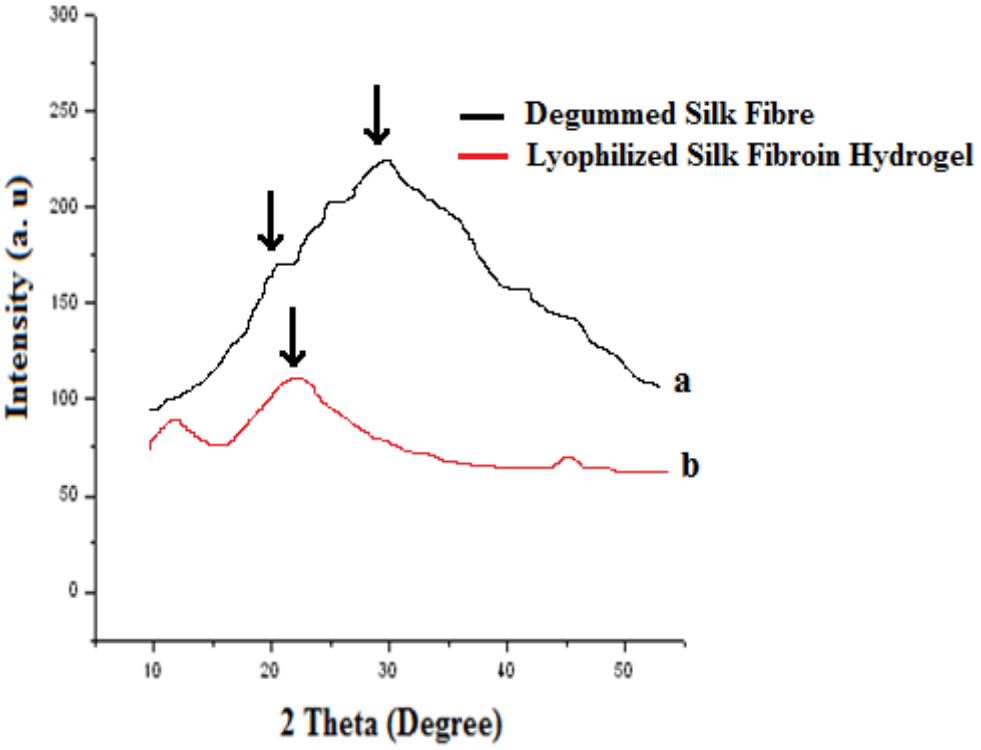

Figure 4.2.5: X-ray diffraction of (a) degummed silk fiber and (b) lyophilized SF hydrogel. RSF hydrogel (line b; 18.9°, 20.6°, 24.3° and 28.1°) shows more amorphous state, while degummed silk fiber (line a; 4.69°, 4.31°, 3.66° and 3.17 A°) shows a typical X-ray diffractogram of β - sheet crystalline structure.

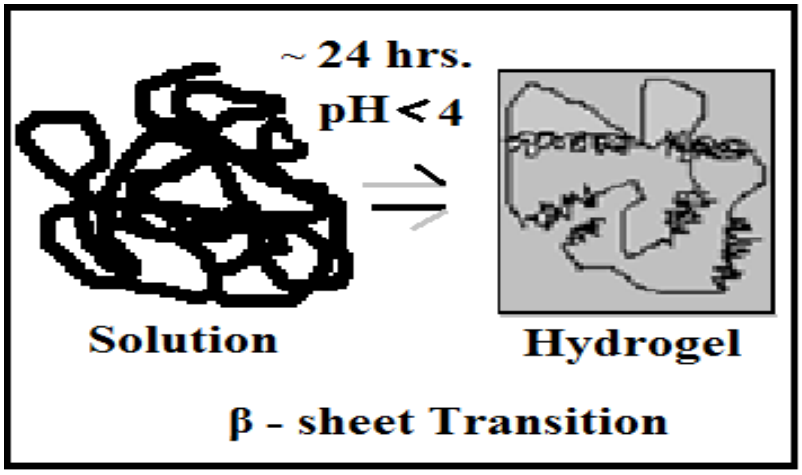

Figure 4.2.6: Sol-gel transition of silk fibroin. Figure depicts the formation of silk fibroin hydrogel with a stable and irreversible intermolecular β-sheet structure.

4.2.4.2. FTIR study

IR spectrum represents typical absorption bands sensitive to the molecular conformation of SF. Therefore, in order to confirm the conformational changes of SF, FTIR spectroscopy of degummed silk fibroin and lyophilized silk fibroin hydrogel was performed and the results are shown in Fig. 4.2.8. Silk protein exists in three conformations, namely, random coil, silk I (R form), and silk II (β-sheet) [Um et al., 2001].The absorption bands at 1657, 1525, 1245 and 651 cm^{-1} which correspond to amide I, amide II, amide III & amide V bands, respectively, confirm that the degummed silk fiber is mainly in β-sheet conformation similar to the native silk fibre [Mandal et al., 2008a; Mandal et al., 2008b]. The corresponding peaks of silk fibroin lyophilized hydrogel are observed at 1625, 1509, 1245, 667 cm^{-1} respectively indicating the β-sheet conformation at the end of processing through regeneration, gelation and lyophilization. Besides, few more peaks were found in lyophilized fibroin powder at frequencies corresponding to 1327-1393 cm^{-1} indicating stretched C-O bonding and thus relatively unstable state. All the peaks observed in three amide band regions varied in their width and intensities.

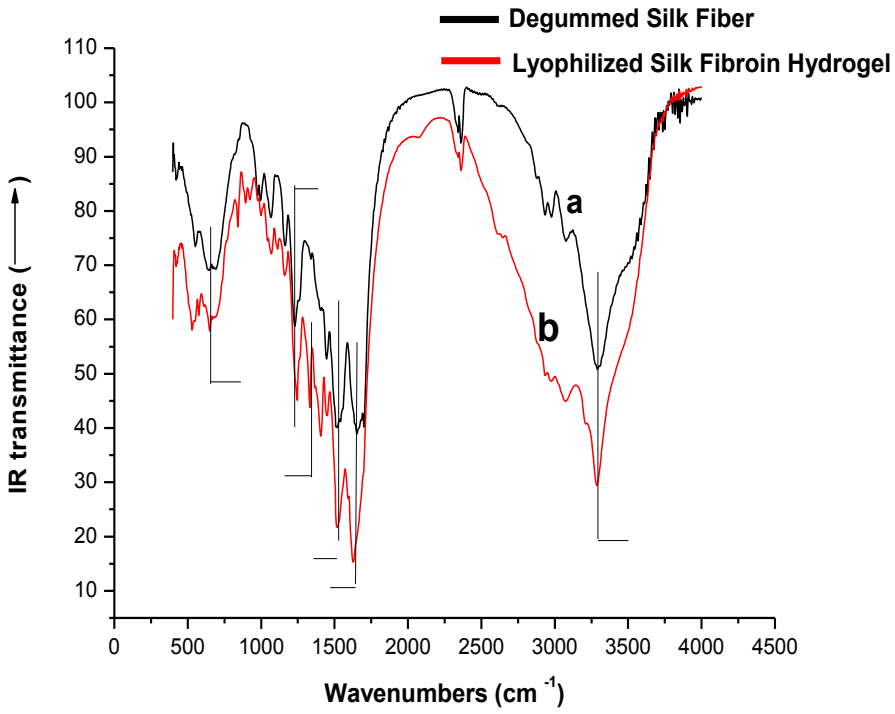

Figure 4.2.7: FT-IR spectra of (a) degummed silk fibers and (b) lyophilized SF hydrogel

4.2.5. Thermal Analysis

The thermal behavior of degummed silk fibre and fibroin hydrogel were assessed by TGA and DSC. Degummed *B. mori* silk fibre and lyophilized fibroin hydrogel showed different thermogravimetric curves. As indicated in Fig. 4.2.8, the initial weight loss below 100 ºC may be due to the water evaporation [Um et al., 2001]. At temperature above 200ºC, the weight loss is observed to occur again. However, silk fiber did not completely decompose even at 700ºC. It is evident from result that silk fibre underwent at least three thermal decomposition stages in the temperature range 200-300ºC, 300-350ºC and 350-400ºC. A similar decomposition pattern is also observed with lyophilized hydrogel. However, the rate of degradation is comparatively faster in case of SF hydrogel.

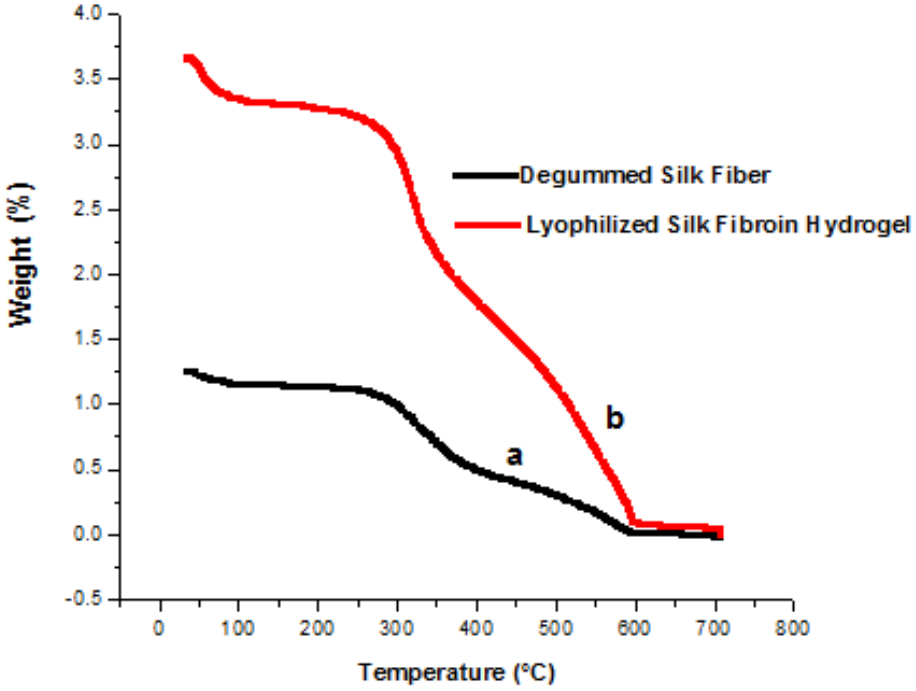

Figure 4.2.8: TGA curves of (a) degummed silk fibers and (b) lyophilized SF hydrogel

The decomposition at approximately 300ºC may be attributed to a disintegration of the intermolecular side chains during the crystalline melting process, while that at around 400 ºC due to a main chain disintegration, coupled with simultaneous carbon atom rearrangements [Hirabayashi et al., 1974]. It has been reported that the decomposition at 300ºC indicates the low crystallinity of the unoriented β-type configuration and, thus it can be concluded that there is less possibility of obtaining a crystalline β-structure, which occurs in the temperature range 325-330 ºC. Furthermore,

the low weight loss at 400ºC observed with gels may be due to its low water content. This suggests that the fibroin molecules come to close contact with each other during lyophilization process and form a dense aggregate which could mechanically resist the carbon atom rearrangements, thus resulting in low weight losses. This phenomenon of the fibroin molecules could be a possible reason for the lyophilized fibroin gel.

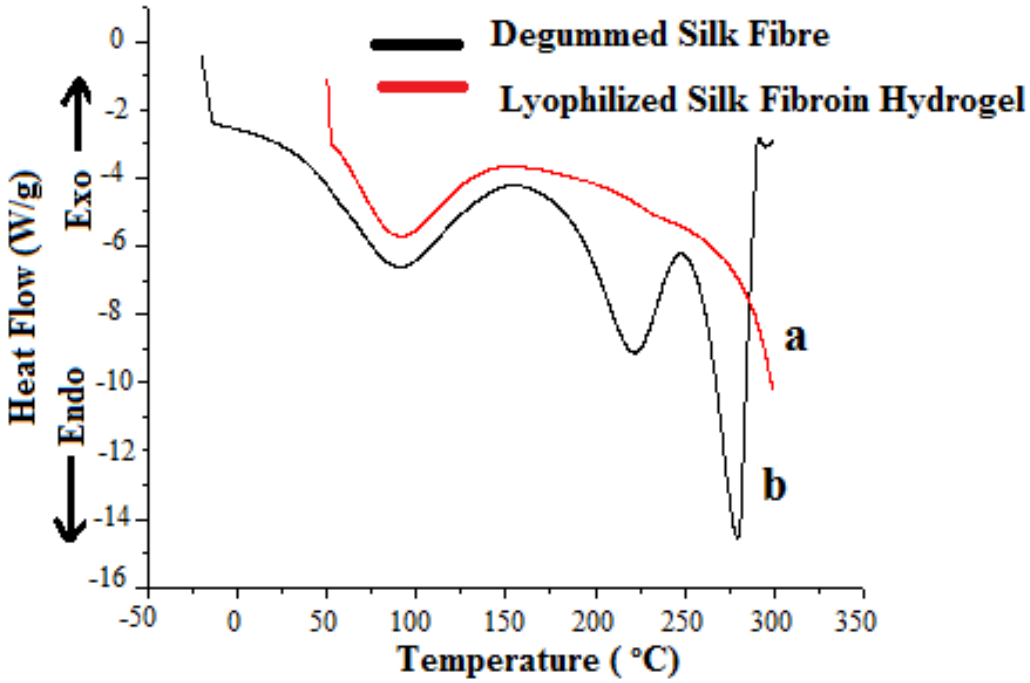

Figure 4.2.9: DSC curves of (a) degummed silk fiber and (b) lyophilized SF hydrogel

Thermal analysis of degummed silk fibroin and lyophilized fibroin hydrogel has shown different thermal calorimetric curves (Fig. 4.2.9). In the DSC curve of degummed silk fiber, an endothermic peak is observed to start at 56.8 ºC and reached maximum at 76.3 ºC without any trace of exothermic transition which may be due to β-sheet structure of the sample. Whereas the DSC curve for lyophilized fibroin hydrogel starts at 35.4 ºC and reached maximum at 67.7 ºC. This difference in results may be attributed to the change in β-sheet conformation. A conformational change through the crystallization of SF from random coil to β-sheet causes an exotherm curve to exist [Chen et al., 2012]. As indicated from DSC curves, two exothermic peaks are observed at around 166 ºC and 255 ºC which can be attributed to the conformational change to β-form, while two endothermic peaks observed around 220 ºC and 286 ºC may be because of the conformational

change of β-form into random coils. The exotherm at 220°C indicates the crystallization of the fibroin random coils to α-form of crystals. The decomposition peaks of all the regenerated fibroins (endotherms around 290 °C) are lower in comparison to the original silk fiber [Warwicker et al., 1954], indicating the lower thermal stability of regenerated samples. The low thermal stability may be due to lower crystallinity as well as decrease in molecular weight during the degumming process of the regenerated SF.

4.2.6. *In vitro* Biocompatibility Study

Human mononuclear cells (hMNCs) have been successfully encapsulated in various hydrogel systems due to the potential regeneration of damaged tissue and prololonged drug release [Liang et al., 2011]. In this work hMNCs were isolated for the study of cytocompatibility of SF hydogels. Due to physical limitation of silk hydrogel prepared from SF with low concentration (< 4% (w/v)), the hMNCs were encapsulated in hydrogel system with higher concentration (prepared from SF aq. solution of concentration >4 % (w/v).

The success of tissue engineering biomaterials not only relies on the non-toxic supportive structure for cell adhesion but also on facilitating cell proliferation. The microscopic images (Fig. 4.2.10) of cells proliferated on hydrogel were taken on consecutive days. Cell size and number were observed to increase with culture period while maintaining the round shape. Fig. 4.2.11 shows the uniform adherence and spreading of mononuclear cells over fibroin hydrogel. The cells are found to be embedded in SF gel matrix. Detachment of cells from the substratum is observed to be minimal after 2 days in vitro cultivation. The morphology of monocytes during *in vitro* cultivation was observed by phase-contrast microscopy. The cells are found to retain round shape and homogenous distribution at day 1 (Fig. 4.2.10a &4.2.10b) and the cells retained their original round shape (Fig. 4.2.10c) at day 3. Initially, the monocytes were found to be small (7-9 pm) [Birmingham et al., 1980] and rounded with cytoplasmic spreading.

A progressive enlargement of monocytes occurs in culture with increasing granulation and vascularization of the cytoplasm. After 1 week of cultivation, the monocytes are observed approximately twice the size of freshly isolated monocytes (Fig. 4.2.10d). With 4% gel, cell numbers are observed to be stopped increasing after 7 days which may be due to limiting spatial and nutrition, indicating that maximal level of cell proliferation is reached (Fig. 4.2.11). The SEM

of hMNCs laden SF hydrogel is depicted in Fig. 4.2.12. Similar observations are found with hydrogel systems such as alginate and PEGas reported earlier [Ramdi et al., 1993; Nuttelman et al., 2006]. However, the morphology of hMNCs encapsulated in > 4% gel is found to change drastically leading to cell death, aggregated and/or dissolved, as evident from the empty cavities in histological images (Fig. 4.2.13). The loss of cellular activity with higher gel concentration is most likely due to mechanical restrictions and mass transport limitations.

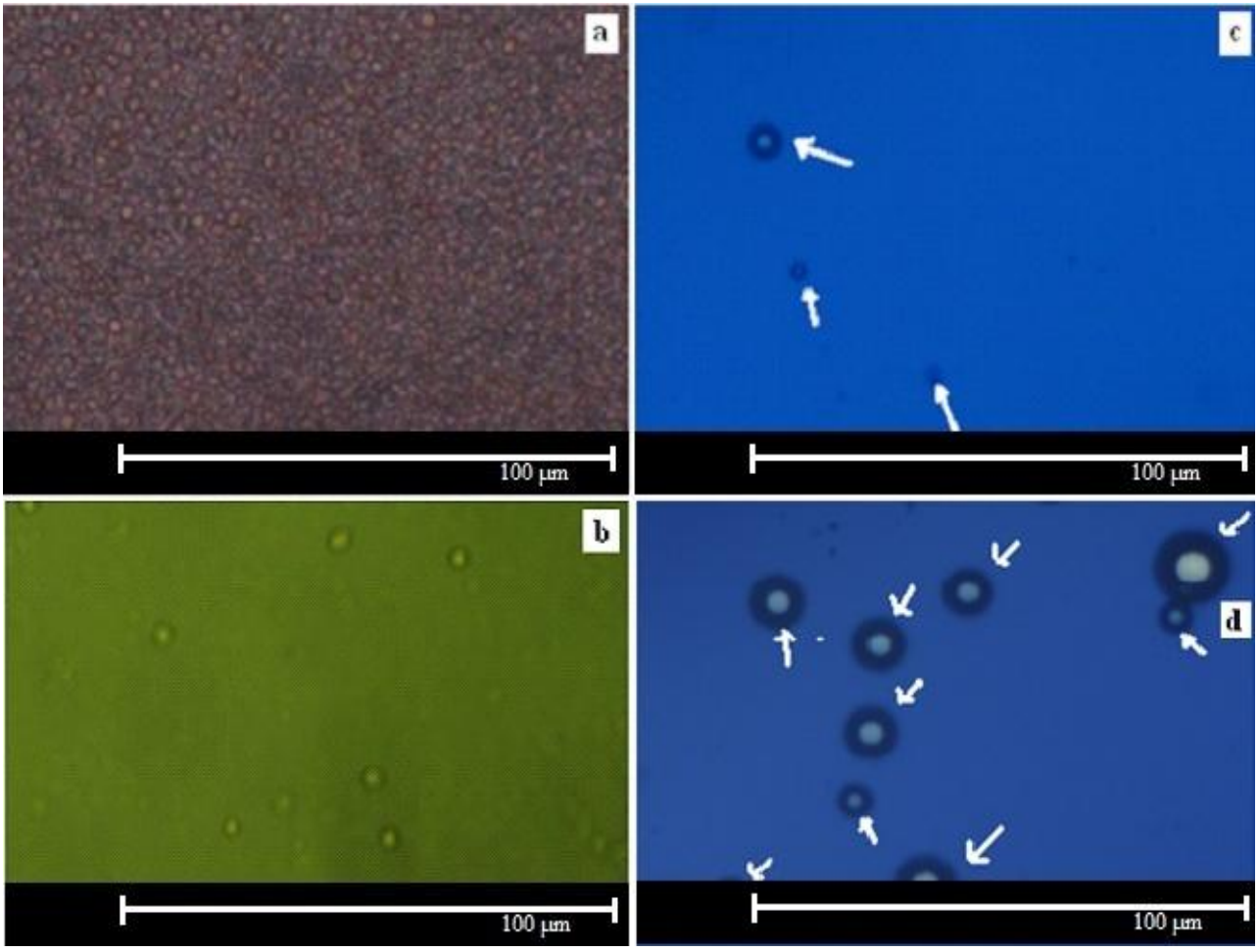

Figure 4.2.10:Microscopic images of hMNCs encapsulated and cultured in SF hydrogels prepared from aquous SF solution at concentration 4%(w/v) after day 1 (a,b), 3 (c), and 7 (d). hMNCs retained round shape morphology and nonaggregated in the gel as compared to floating cell clusters in day 1 (Fig. a). Bar = 100 µm in all images. The viable cells can be seen as bubbles rounded with trypan stain indicated by arrows.

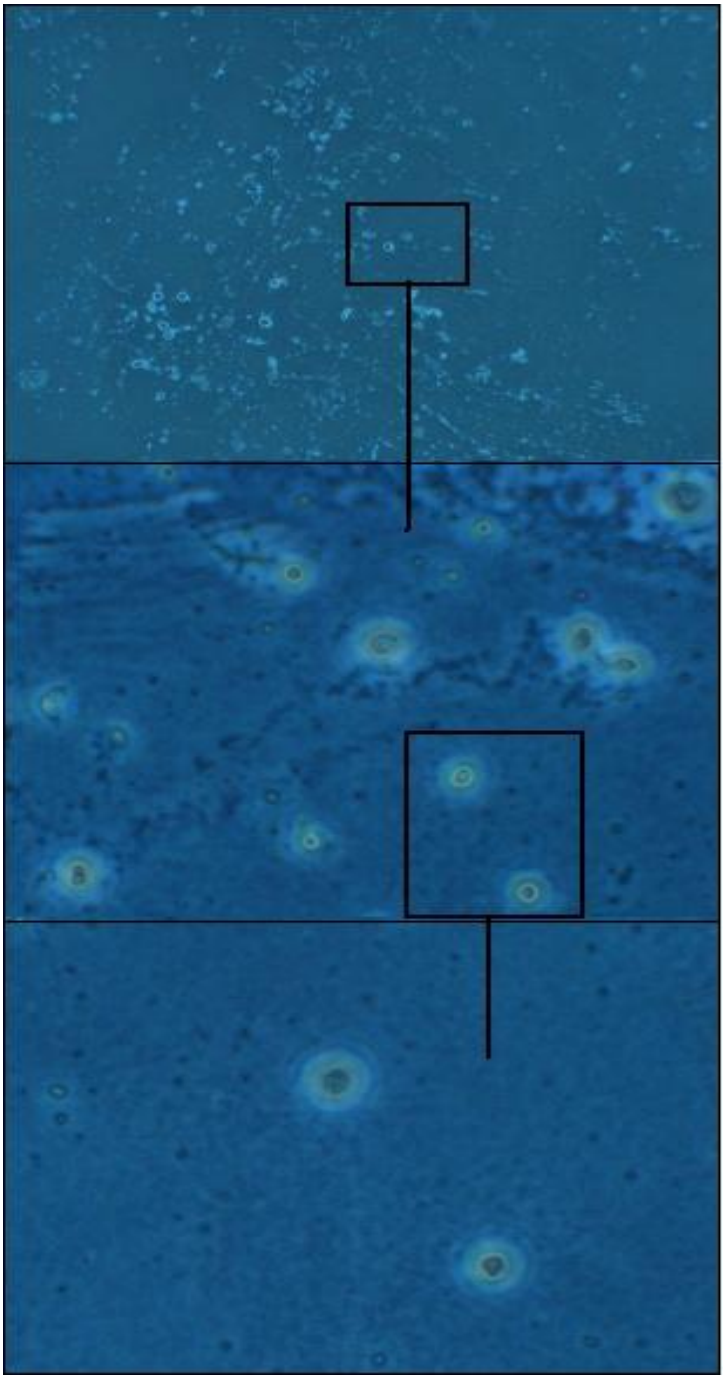

Figure 4.2.11: Micrographs of hMNCs adhered on the hydrogel surface observed by phase contrast microscope at different magnification (5X, 10X, 20X)

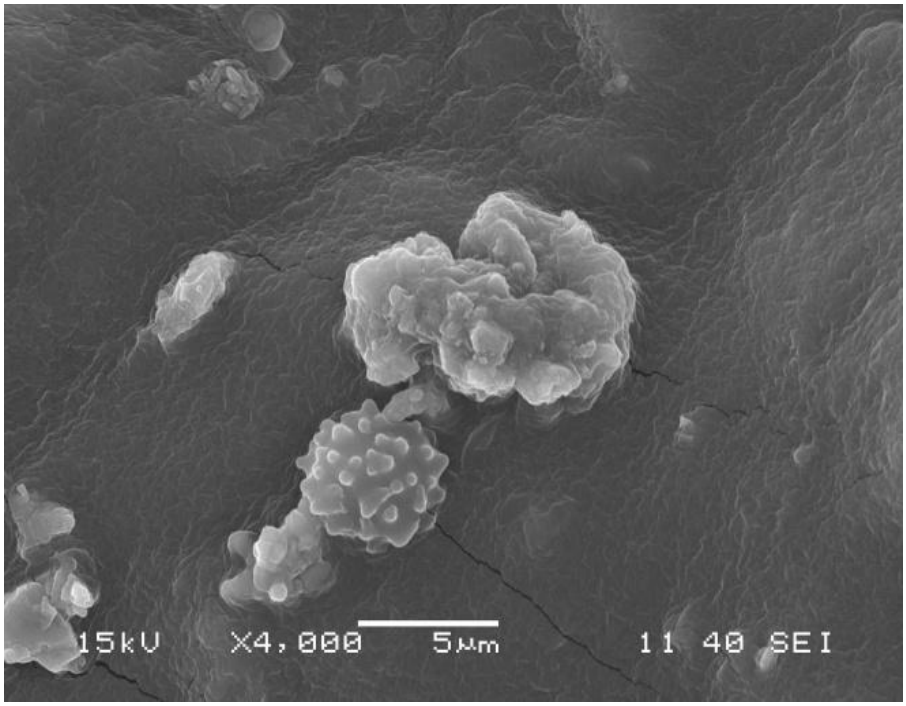

Figure 4.2.12: SEM Morphology of cell encapsulated in SF hydrogel

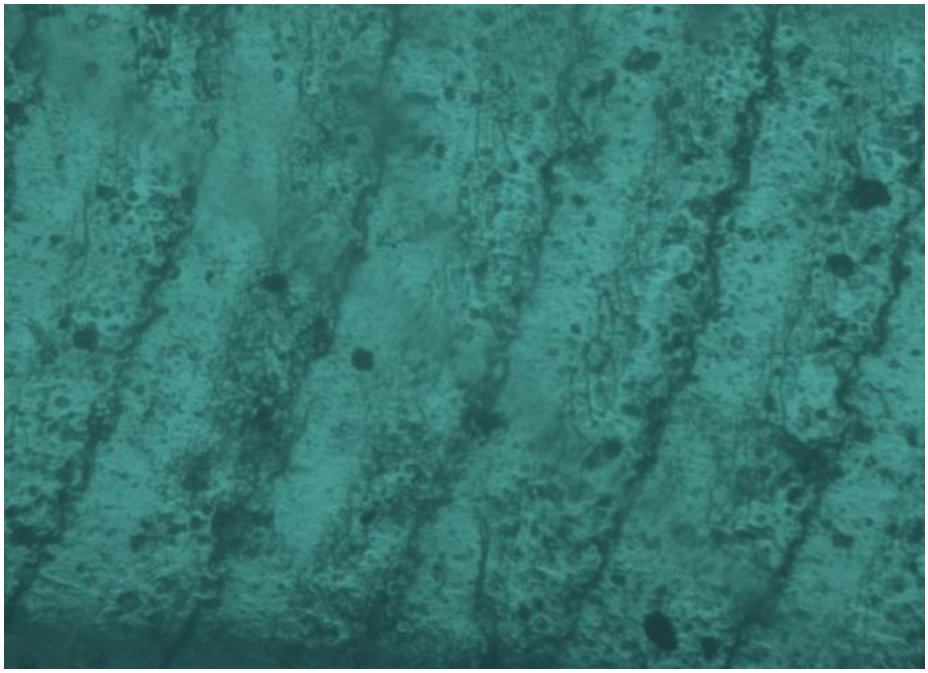

Figure 4.2.13: Micrograph of hMNCs seeded fibroin hydrogel (prepared from >4% (w/v) SF solution) cultured over 2 weeks. Empty cavities are clearly visible indicating non-supportive behavior towards cell proliferation.

PART III

Development of porous SF scaffolds with and without SEP conjugation

A number of surface modification methods that involve the use of radiation [Mathew et al.; 2013] or a variety of bioactive molecules [Son et al., 2008; Mann et al., 2002; Yang et al., 2001; Lee et al., 2000] have been the choice of many researchers to improve scaffold material characteristics. Different biolactive molecules (RGDs and other short repetitive peptide chains) have been immobilized physically or chemically on polymeric scaffolds [Mann et al., 2002; Yang et al., 2001], and amphiphilic block polymers as additives [Lee et al., 2000]. In this study, we used soluble form of egg shell membrane protein (SEP) for surface modification of the developed SF scaffold. To the best of our knowledge, this is the first report of modifying the surface of porous SF scaffold with SEP. The reason behind the selection of eggshell membrane (ESM) biopolymer is the long history of SEP used in Chinese medicine prescribed as, Bencao Gangmu for injuries. Eggshell membrane (ESM) is a double layered insoluble and semipermeable sheet located between the eggshell and egg white [Carrino et al., 1996], and is functionally behave as scaffold for biomineralization to develop egg shell and chick embyo [Nakano et al., 2003; Tsai et al., 2006; Rose and Hincke 2009]. ESM consists of 70% organic, 10% inorganic and 20% water.The major organic components includes insoluble proteins, such as collagens (type I, V, and X), osteopontin, and sialoprotein [Nys et al., 2001], alongwith a small amount of carbohydrates and lipids [Suyama et al., 1977; Baker et al., 1962]. Previous studies have developed SF scaffolds with defined small pore sizes with limited inter connections [Nazarov et al., 2004], or large (>500μm) with well connected pores [Kim et al., 2005c]. Attempt has been made in the present study to fabricate 3-D SF scaffolds with improved surface characteristics using SEP as bioactive molecule. The SEP conjugated SF scaffolds were further evaluated to assess the improvement in their physico-chemical and biochemical characteristics in terms of biodegradability, thermal stability, compressive strength, cell adhesion and proliferation property. Thus it is expected to obtain a novel scaffold with improved bioactivity for its potential use in tissue engineering.

4.3.1. Morphological Study

The light milky white colored fibroin solution (12%w/v), observed under phase contrast microscope shows a porous wet matrix and that of ESM membrane as a bed of granular particles as shown in Fig. 4.3.1a and 4.3.1b. The SEM images of degummed silk fibroin (Fig. 4.3.1c) reveal the fibrous nature of starting material, while ESM (Fig. 4.3.1d) structure as membrane fiber embedded in white collagen-like matrix. ESM fibers come out from the tubular gland cells present in oviduct and wrap

the surface of rotating egg white protein followed by the deposition of mineralized shell as reported earlier [Burley et al. 1989; Kodali et al., 2011]. Thus after peeling off the eggshell from the membrane, it doesn't contain any $CaCO_3$ as observed in Fig. 4.3.1d. This is further confirmed by elemental (Table 4.3.1) and XRD (Fig. 4.3.5) analysis.

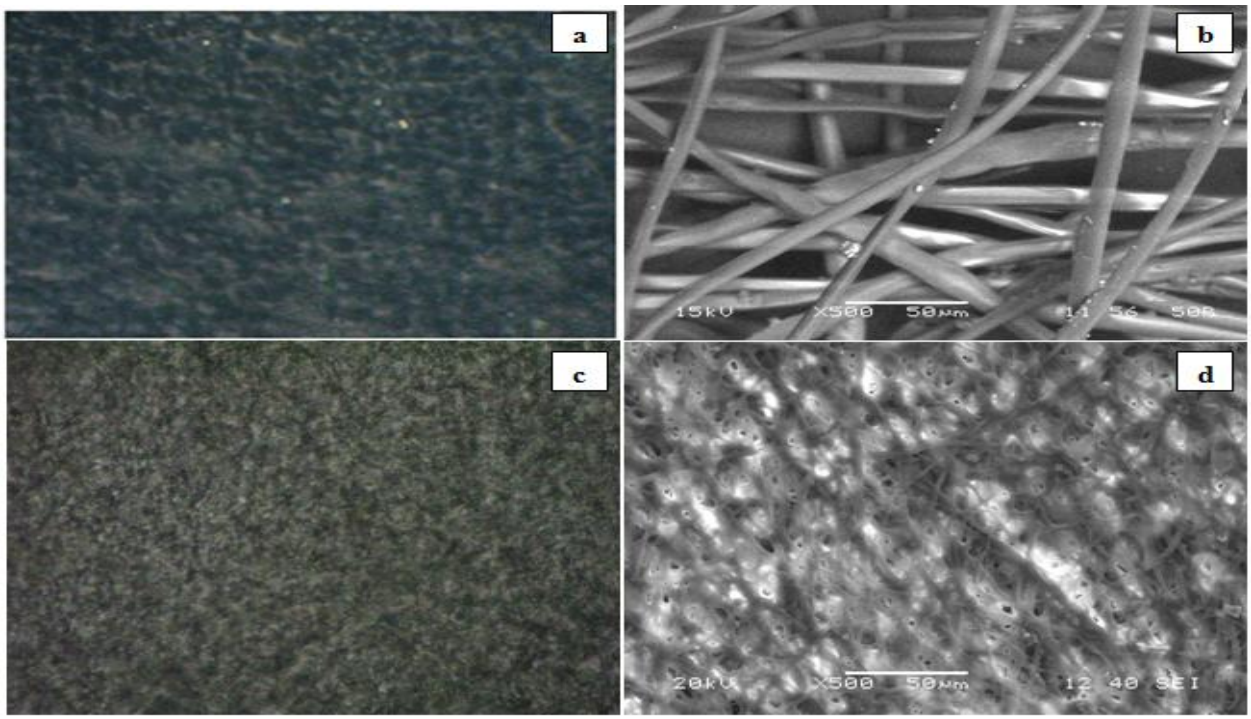

Figure 4.3.1: Microscope images of (a, b) SF hydrogel and (c,d) ESM by (a,c) phase contrast microscope and (b,d) SEM

4.3.2. Pore size and Porosity

SF scaffolds with varying pore size and porosity were prepared using NaCl as porogen from 4-6% SF solution by salt leaching method following the procedure published earlier [Lee et al., 2000]. Table 1 show the pore size and porosity of the scaffolds prepared under study. The pore size was measured from SEM images as shown in Fig. 4.3.2. The particle size of porogen is shown to have a great influence on the pore size and porosity of scaffolds. Scaffolds with pore size in the range of 30 to 350 µm were obtained using porogen of size < 100 µm (Fig. 4.3.2a), 100-200 µm (Fig. 4.3.2b), 200-300 µm (Fig. 4.3.2c) and 300-500 µm (Fig. 4.3.2d). The porosity and pore size of scaffolds were obtained in the range of 81-93% and 30-350 µm respectively using porogen of the size range 100-500 µm. Particle size below 100µm and above 500µm (data not shown) is not found

to be favorable for scaffold due to the limitation in pore interconnectivity [Hulbert et al., 1970]. The pore size of the scaffolds is 10–20% smaller than the particle size of NaCl used which may be due to the partial dissolution of the crystal surface. The recommended pore size for a scaffold system based on cell size and migration is minimum 100 µm as reported earlier [Hulbert et al., 1970]. However, subsequent studies have shown better vascularization and cell migration in implants with pore size >300 µm [Karageorgiou et al., 2005; Murphy et al., 2010; deGrootet al., 1996]. In previous studies, aqueous-derived SF scaffolds prepared with different particle size range of NaCl resulted in similar trend in pore size and supported cell migration and enhanced vascularization during tissue regeneration [Zhau et al., 2009; Kim et al., 2005; Altman et al., 2003].

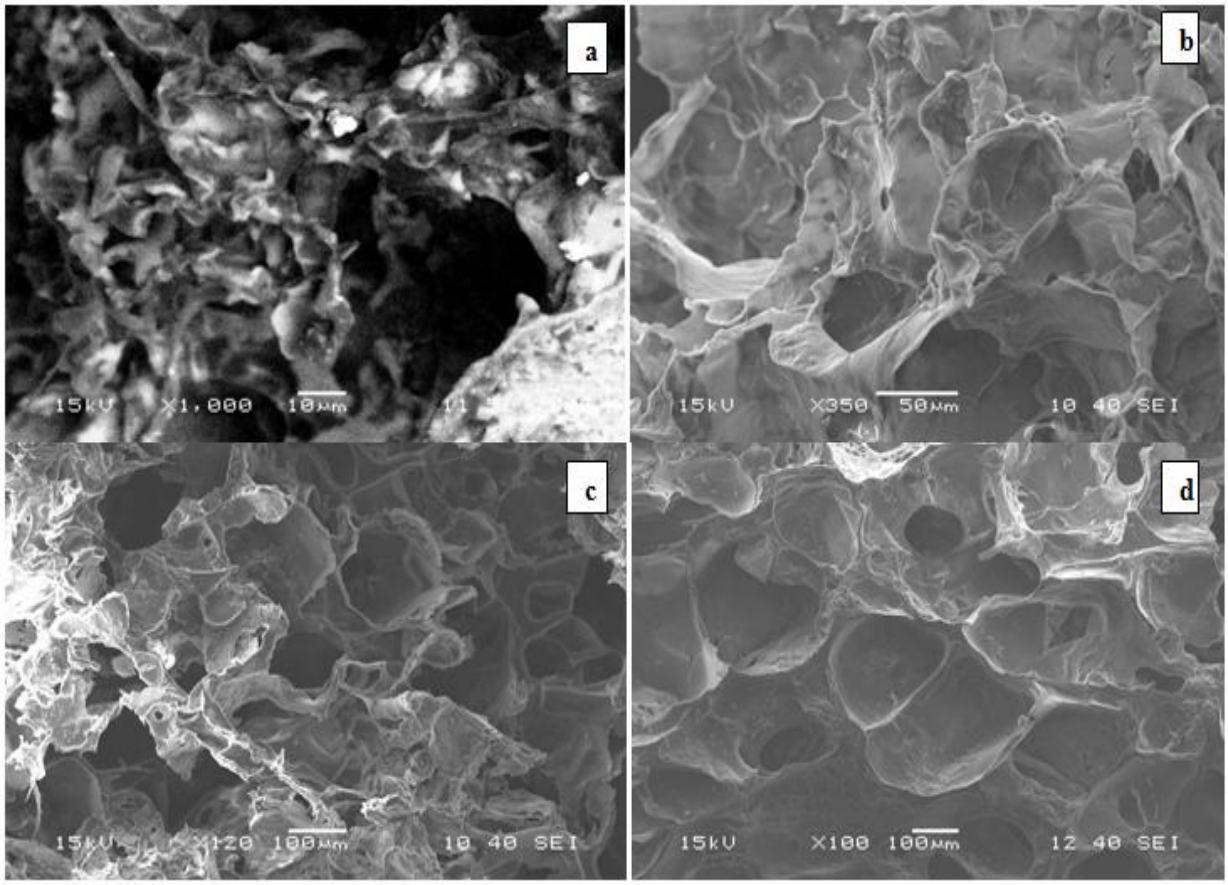

Figure 4.3.2: SEM of SF scaffold prepared by salt leaching method using NaCl as porogen of different particle size range: (a) < 100 µm (b) 100-200 µm (c) 200-300 µm (d) 300-500 µm

Table 4.3.1: Pore size and porosity of SF and SEP-SF scaffolds prepared with RSF 4-6% (w/v) using NaCl as porogen (n=3)

Sample	NaCl particle size	Pore Size	Porosity	Remarks
SF	<100 µm	30-70 µm	85-88 %	Not interconnected
SF	100-200 µm	90-150 µm	81-86 %	Interconnected and suitable for skin TE [Yang et al., 2002]
SF	200-300 µm	140-230µm	87-89%	Interconnected but moderate applicable for osteogenesis [Murphy et al., 2010]
SF	300-500 µm	225-350µm	90-93%	Interconnected and more applicable for osteogenesis and chondrogenesis [Murphy et al., 2010; deGrootet al., 1996]
SEP-SF	300-500 µm	200-300µm	85-90%	Interconnected and more applicable for osteogenesis and chondrogenesis [Murphy et al., 2010; deGroot et al., 1996]

4.3.3. SEP conjugated SF scaffold

The SF scaffold with pore size 225-350 µm were further modified with SEP as bioactive material. As a chemical crosslinker, EDC reacts with the carboxylic acid groups of peptide chain which can then bind to the amino group in the reaction mixture of SEP, loaded in SF scaffold. The detailed mechanism of EDC/NHS crosslinking (Fig. 4.3.3) is reported in the published literature [Burdick et al., 2011]. The SEM image (Fig. 4.3.4) shows the porous structure of SEP-SF scaffold. It is observed that the pore size and porosity of the scaffold are not much affected by the conjugation with 2% (w/v) SEP. The pore size of the modified scaffold was obtained in the range 200-300 µm with porosity approximately 85-90%. The slight reduction in porosity and pore size may be due to blockage of pores after SEP conjugation. However, the scaffold has desired pore size and porosity to be used for tissue engineering applications.

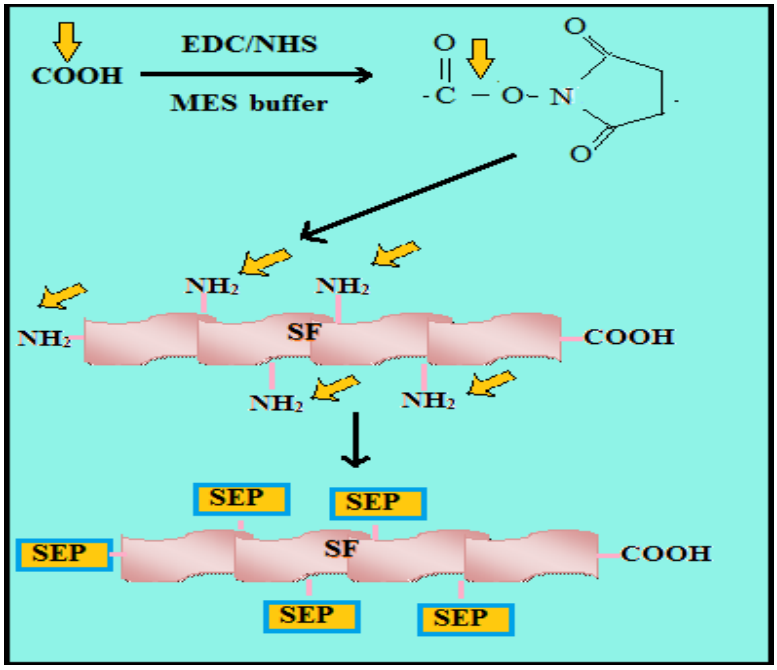

Figure 4.3.3: Mechanism of SEP conjugated with SF scaffold

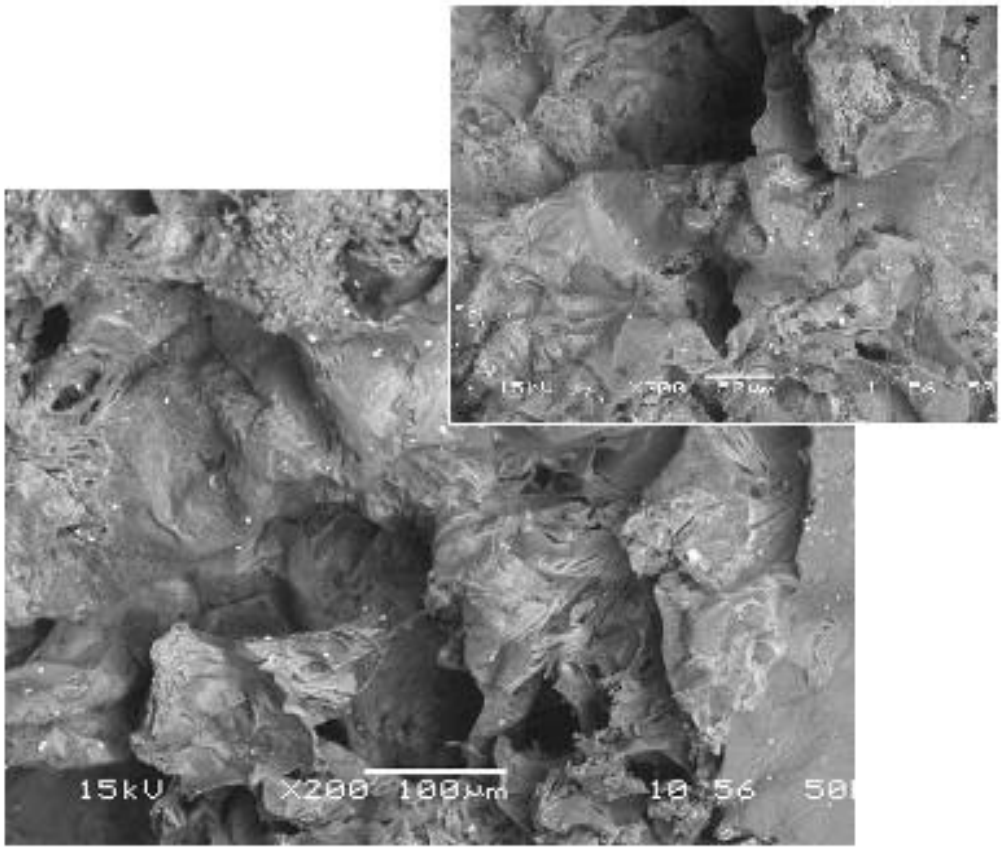

Figure 4.3.4: SEM of SEP conjugated SF scaffold

4.3.4. Elemental Analysis

The elemental analysis was done to measure the elements of SF, SEP and SEP-SF scaffolds. Each analysis was performed in triplicate and average value is shown in Table 2. The elemental composition of SF and SEP are very close to the experimental data published by wang et al. [Wang et al., 2011] and Yi et al. [Yi F. et al., 2004]. The elemental composition of SEP-SF which lies in between SF and SEP indicates the immobilization of soluble eggshell protein throughout the SF scaffold.

Table 4.3.2: Elemental composition of SEP, SF and SEP-SF scaffolds

Sample	wt.(mg.)	C (wt. %)	H (wt. %)	N (wt. %)	O (wt. %)	S (wt. %)
SF	2.001	43.30	6.04	14.78	27.9	0.35
SEP	1.989	46.53	6.7	15.93	11.76	2.89
SEP-SF	2.015	45.33	6.51	15.11	22.7	0.93

4.3.5. Structural Analysis

4.3.5.1. XRD Analysis

The conformational changes during the processing for scaffold fabrication were confirmed by analysing X-ray diffraction patterns of SEP and SF scaffolds as shown in Fig. 4.3.5. According to the research on the molecular conformation of silk fibroin protein [Tao et al., 2007], the XRD patterns (Fig. 4.3.5a) is determined as 12.5° (2θ) for α-helix (Silk I) and 20.4° (2θ) for β-sheet structure (Silk II). The XRD curve of the conjugated SF scaffold (Fig. 4.3.5b) shows two peaks around 12.6° (2θ) and 20.5° (2θ) indicating the co-existence of α-helix and β-sheet with partially induction of α-helix to β-sheet due to SEP conjugation.The XRD pattern of SEP (Fig. 4.3.5c) holds a broad peak at 20.2° (2θ) indicating the amorphous nature of material and the absence of crystalline material (eg. $CaCO_3$).

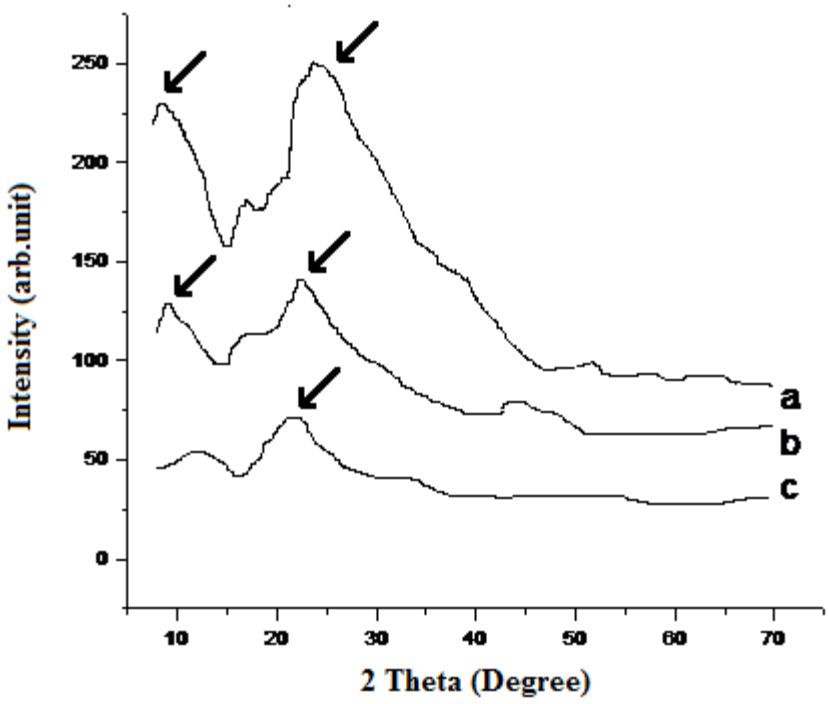

Figure 4.3.5: XRD pattern of (a) SF scaffold; (b) SEP-SF scaffold and (c) SEP

4.3.5.2. FTIR Study

The chemical characteristics of functional groups exposed to the extracellular matrix (ECM) and cells were studied by FTIR spectra. As shown in Fig. 4.3.6, the amide I band (1600-1700 cm^{-1}) is associated with the stretching vibrations of carbonyl groups (C=O bond) along the polypeptide backbone [Payne and Veis, 1988] and has been found most important for infrared spectroscopic analysis of the proteins secondary structure [Surewicz and Mantsch, 1988]. The FTIR spectrum of SF scaffold shows strong absorption bands at amide I (1654 cm^{-1}), amide II (1519 cm^{-1}), amide III (1220 cm^{-1}) and amide V (555 cm^{-1}) which can be attributed to mainly random coil conformation and the helix. It is indicated that the formation of SF scaffolds from regenerated SF solutions induced a conformational transition from random coil to β-sheet. The FTIR spectrum of SEP shows the main absorption bands of amide A (3215 cm^{-1}), amide B (2126 cm^{-1}), amide I (1654 cm^{-1}), amide II (1545 cm^{-1}) and amide III (1253 cm^{-1}). Amide A and amide B bands are related to NH stretching coupled with hydrogen bond and CH_2 asymmetrical stretch respectively. Amide II is associated with NH bending and CN stretching. These results are very close to FTIR analysis curve

of collagen from yellow fin tuna dorsal skin as reported earlier [Wang et al., 2008]. The specific absorption peaks of SF scaffold and SEP are evident in the spectrum of SEP-SF scaffold, indicating conjugation. The amide B group (2126) of SEP is also found to be present in the conjugated silk fibroin. The characteristic amide groups of silk fibroin (amide I, 1654cm^{-1} and amide II, 1519 cm^{-1}) [Gil et al., 2007] are also detected in the SEP-SF scaffold. These results confirm the proper conjugation of SEP to SF by covalent immobilization method. EDC/NHS as a zero-length crosslinking agent is used to link carboxyl groups of SEP and primary amines of SF. The results suggest that the SEP conjugated silk fibroin scaffold contains bioactive functional groups at the interface of surface and ECM/Cells.

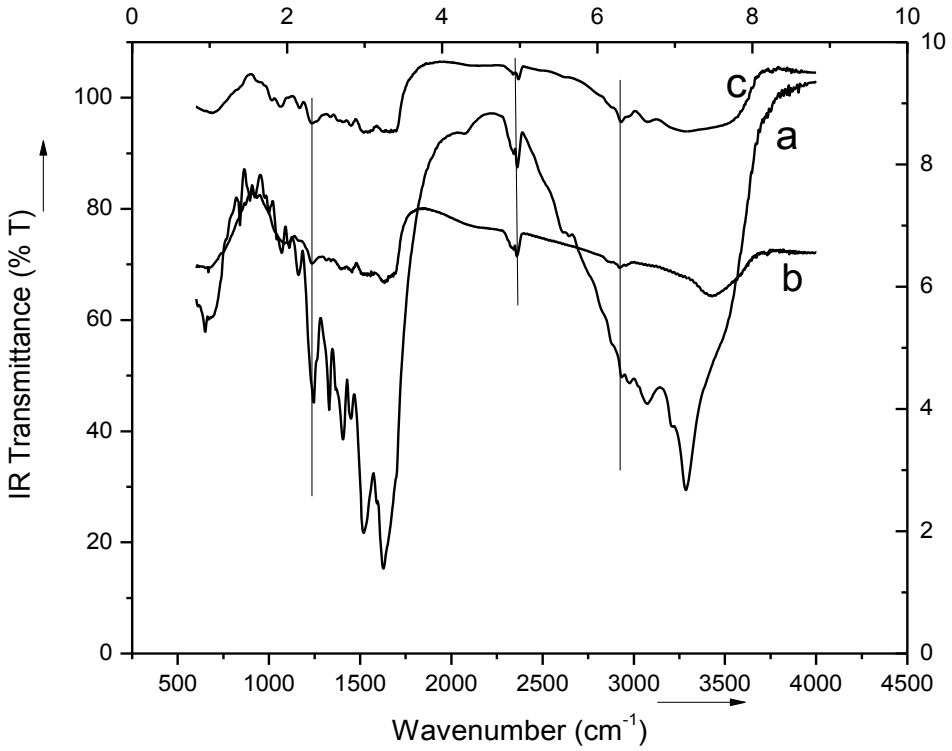

Figure 4.3.6: FT-IR spectra of (a) SF scaffold, (b) SEP-SF scaffold and (c) SEP

4.3.6. Thermal properties

The thermal properties of SEP, SF and SEP conjugated SF scaffolds were investigated by standard DSC and TGA (Figs. 4.3.7-8) methods. The results indicate that the weight loss of SEP (Fig. 4.3.7a) starts at about 180°C whereas the weight loss is observed with SF scaffold at 200°C (Fig. 4.3.7a). A slight weight loss as observed below 100°C may be due to the evaporation of a small

quantity of water which is also reported by Kweon et al. [Kweon et al.,2001b]. The major weight loss with SEP is observed to occur in the temperature range of 230–400°C. However, a sharp and rapid weight loss is observed with SF scaffold at 330°C which may be due to the thermal degradation of SF protein. Thus the result indicates the high crystallinity and molecular configuration of SF proteins which is also supported by the result of structural analysis. The residues of both SEP and SF samples at 500°C is about 25%. Thus SEP is found to be thermally stable.

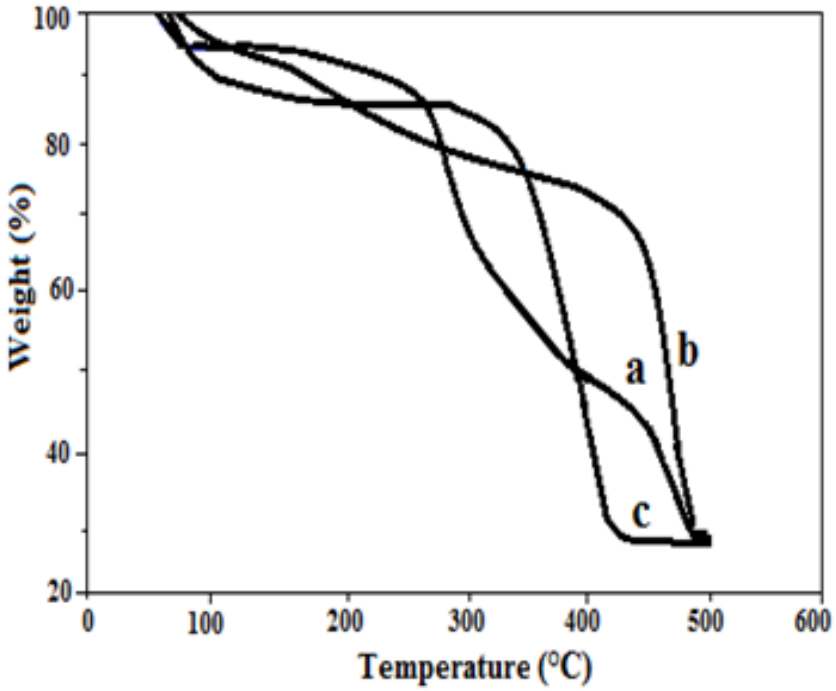

Figure 4.3.7: TGA curves (a) SF scaffold (b) SEP-SF scaffold and (c) SEP

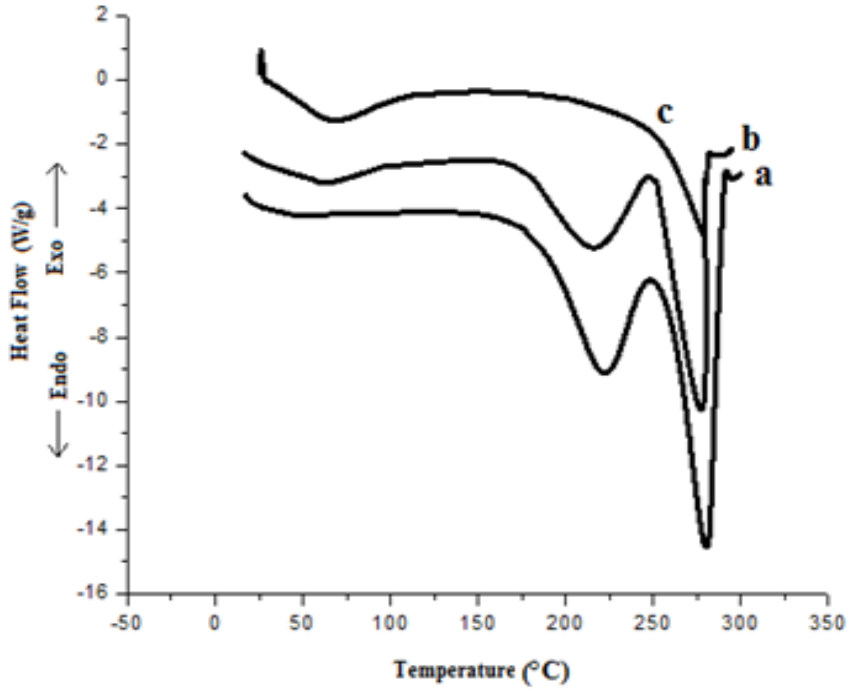

Figure 4.3.8: DSC curves (a) SF scaffold (b) SEP-SF scaffold and (c) SEP

From DSC curve (Fig. 4.3.8), it is indicated that, the denaturation of SEP onset at 46.10°C and reaches maximum at 65.03°C. The thermal stability of ESM is associated with the temperature inside and outside of the body and directly linked with **amino acids** (proline and hydroxyproline) content [Wong et al., 1989]. The thermal analysis of SF scaffold showed a different thermal calorimetric curve as compared to SEP-SF scaffold. SF scaffold exhibited a weak endothermic peak around 100°C which is also indicated in the corresponding TGA curve. This phenomena may be due to the evaporation of low water content of SF scaffold [Kweon et al., 2001b]. The exothermic peaks at 220°C, attributes to the crystallization of thermally induced SF protein and due to β-sheet structure of samples [Chapter 4, Part III; Kweon et al.,2001b]. A slight upward shift of the decomposition peak for SEP conjugated SF sample (endotherms around 260°C) as compared to the SF sample indicate a little higher thermal stability of the conjugated samples. This higher thermal stability of conjugated scaffold may be due to higher crystallinity and higher molecular weight (because of the presence of stabilizing amino acids eg. proline and hydroxyproline) compared to SF scaffold. No denaturation of SF and SF-SEP scaffolds was observed in the temperature range of 30-40°C. Thus it has been demonstrated that the scaffolds are thermally stable at both room and body temperature.

4.3.7. Compressive Strength

Scaffold material must have required mechanical strength to withstand the cellular in situ growth and tissue organization. The mechanical strength was determined from stress–strain graphs of the prepared scaffolds as shown in (Fig. 4.3.9a and4.3.9b). SF and SEP-SF scaffolds are shown to have different line patterns which are the typical characteristics of the elastic/plastic material. For both scaffolds investigated, the steepest portion of the stress-strain curve is occurred in the range of 0-2% strain. The uncoated fibroin scaffold breaks between 200 and 300 KPa with a strain of 1.8 to 2.2%. The mechanical resistance was increased after SEP coating, supporting breaking forces higher than 3 N and strain over 2.8%. However, the average compressive strength was found to be 279.8 ± 36.2 KPa for SF and 321.5 ± 42.2 KPa for SEP-SF scaffolds.

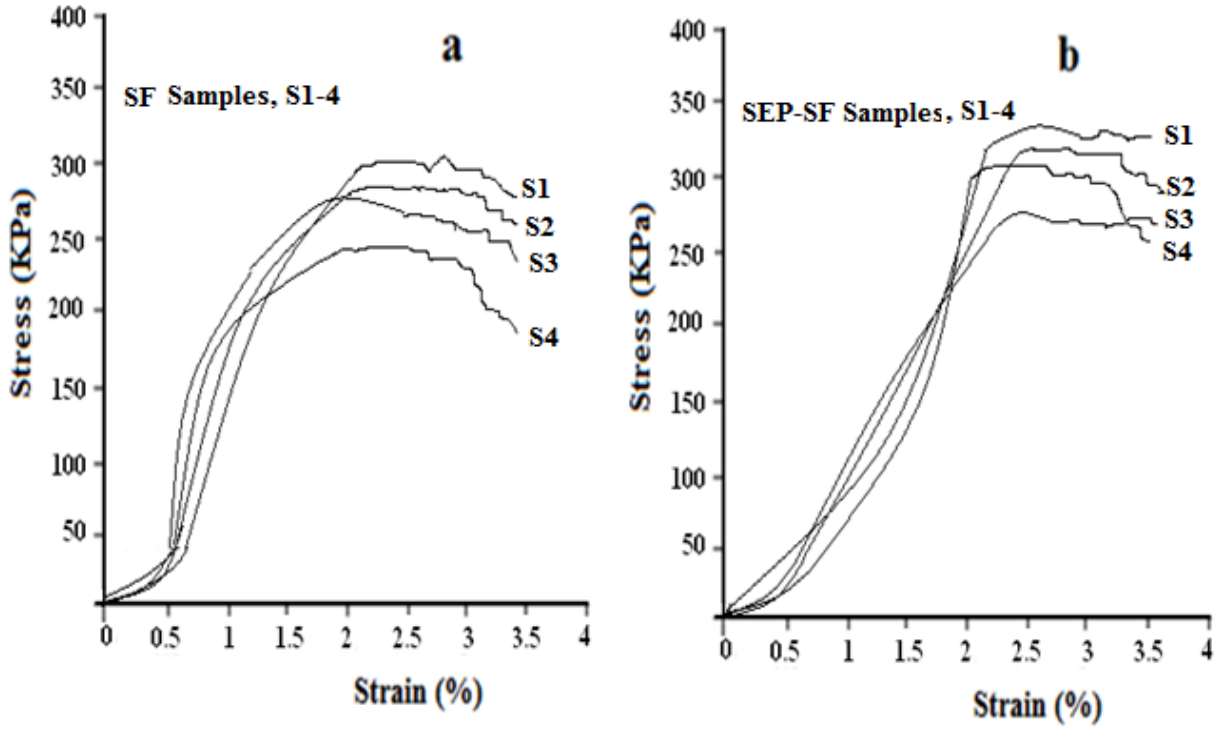

Figure 4.3.9: Stress-Strain Curve of (a) SF and (b) SEP-SF scaffolds

4.3.8. Swelling Behavior

Water molecules, the component of coordination bond act as swelling agent, are undoubtedly needed for the dissolution of silk fibroin. Fig. 4.3.10 shows the swelling behavior of scaffolds. As it is indicated from graph, swelling index of 60.3% is achieved after 30min of soaking and that has

been increased to 133.36% after 48 h. The similar trend was observed with SF scaffold modified with SEP as well with a slight increase in swelling index during the period of study. The increase in swelling index may be due to the enhanced hydrophilicity of scaffold surface after SEP conjugation.

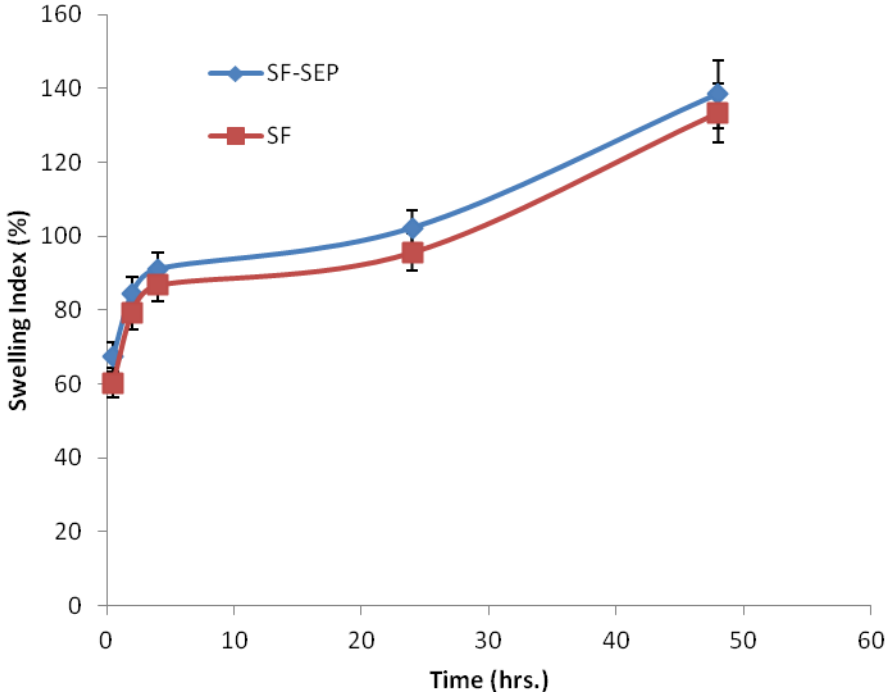

Figure 4.3.10: Swelling behavior of SF & SEP-SF scaffolds

4.3.9. Biodegradability

From Fig. 4.3.11, the initial weight loss of 0.08% and 0.04% were observed with SF and SEP-SF scaffolds respectively. However, the maximum weight loss achieved is 1.89% and 2.38% for SF and SF-SEP respectively after 192 hrs. The increase in biodegradation in conjugated scaffold as compared to control may be due to enhanced hydrophilicity and partial surface erosion from scaffolds in PBS [Jia et al., 2008].

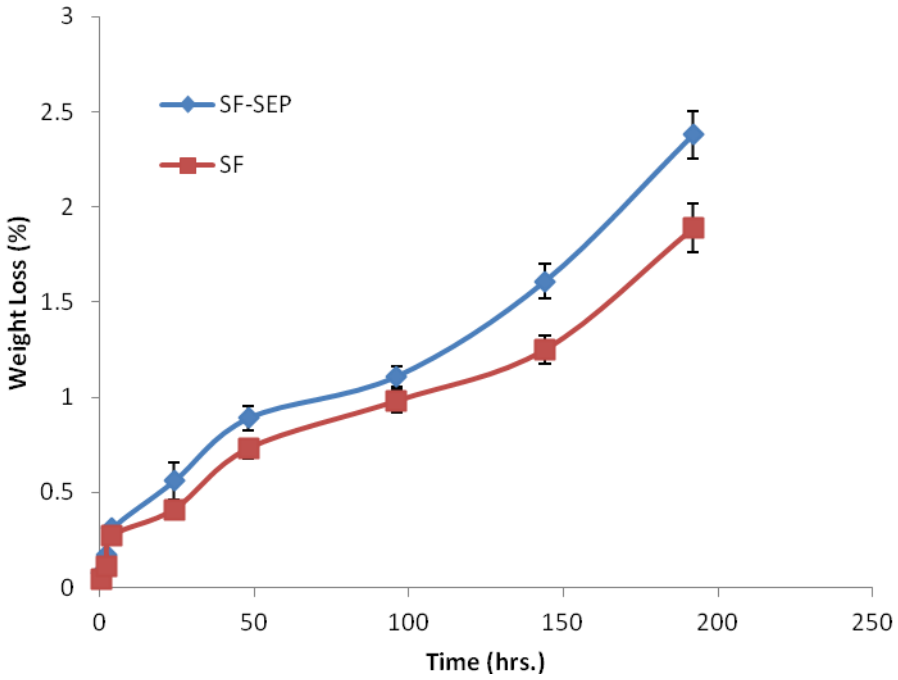

Figure 4.3.11: Biodegradability of SF & SEP-SF scaffolds

4.3.10. Hydrophilicity

The hydrophilicity of the scaffolds was evaluated by contact angle measurement between the scaffold and pure water droplet. It is observed that the initial contact angle of the SF scaffold was 62.4±1.5°, indicating the higher wettability of SF scaffold surface. The contact angle decreases after SEP conjugation to 52.7±1.0° may be due to enhanced hydrophilicity of SEP material. It is evident that conjugation of SEP makes SF scaffold more hydrophilic suitable for cellular reponse in aqueous medium.

4.3.11. Characterization of MSCs

The morphology of UCB derived hMSCs passaged upto 4th cycle is depicted in Fig. 4.3.12. The fibroblast-like cells with protrusions as obtained were further characterized by FACS analysis. The immunophenotypic profiling of cell surface markers CD34, CD45, CD90 and CD105 on isolated hMSCs was done using flowcytometry analysis. Fig. 4.3.13 shows that the isolated and cultured cells from fourth passage were positive for CD90 and CD105 and the expression level were 98.3% and 98.7% respectively but negative expression for CD34 (1.39%) and CD45 (1.30%) confirming the characteristics of mesenchymal stem cells. The cultured MSCs were further used for *in vitro* cytocompatibility evaluation.

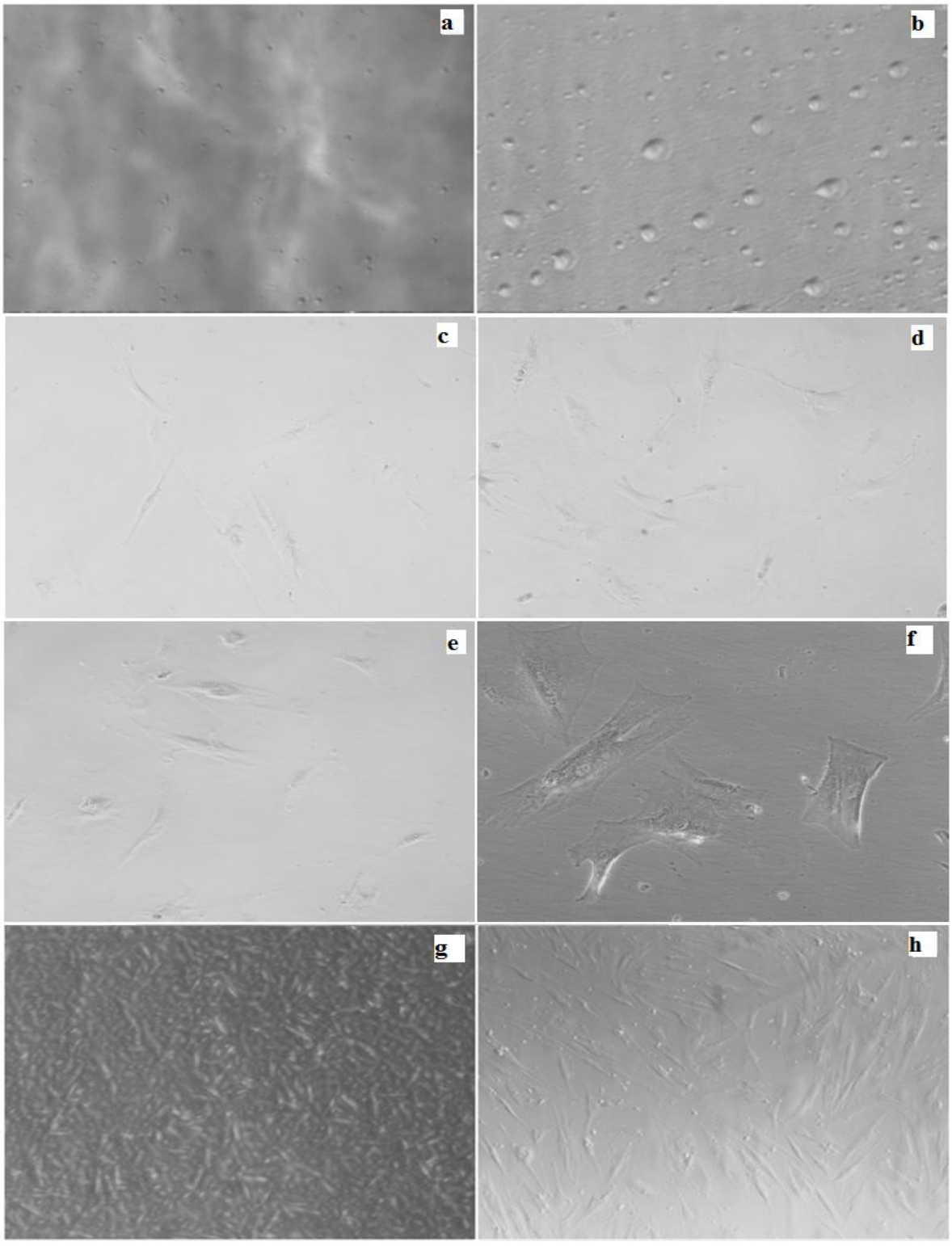

Figure 4.3.12: Morphology of cultured UCB derived hMSCs after passage 1(a, 200X; b, 400X), passage 2 (c, 400X; d, 400X), passage 3 (e, 200X; f, 400X) and passage 4 (g, 200X; h, 400X)

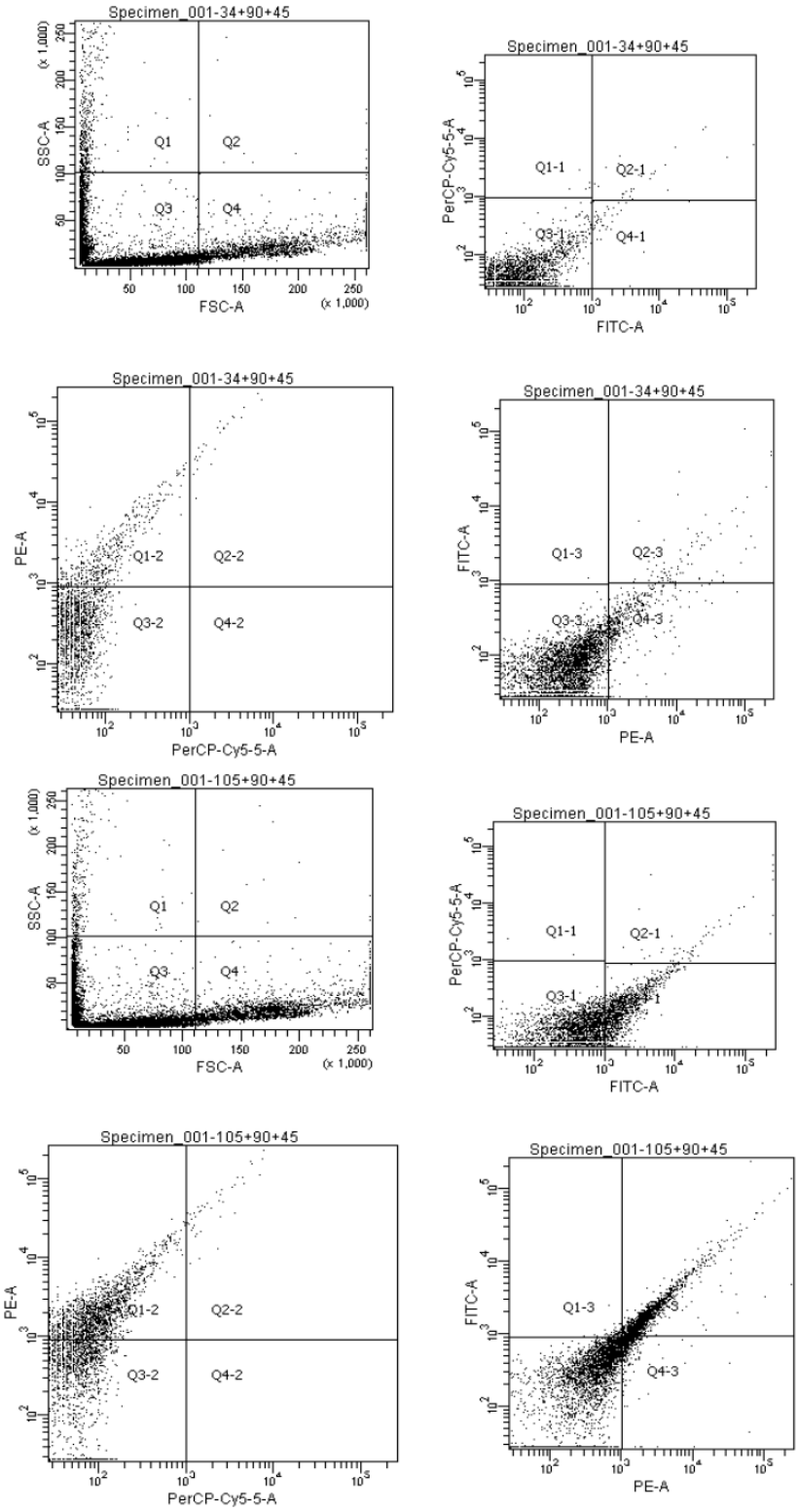

Figure 4.3.13: Surface marker expression of CD34, CD45, CD90 and CD105 for cultured hMSCs analysed via FACS (fluorescence-activated cell sorting) incubated with relevant cell surface antibody.

4.3.12. Cell Morphology in Scaffolds

The SEM images of cell-scaffold constructs are shown in Fig. 4.3.14. After one day of cell seeding, cells were started to adhere and aggregate in the pores of both SF and SEP-SF scaffolds. Though initially cell adherence followed the similar trend for both the scaffolds, however cell adherence and spreading were found to be spread uniformly throughout the SEP-SF scaffolds during 7 to 14 days culture than that in the case of SF scaffold.

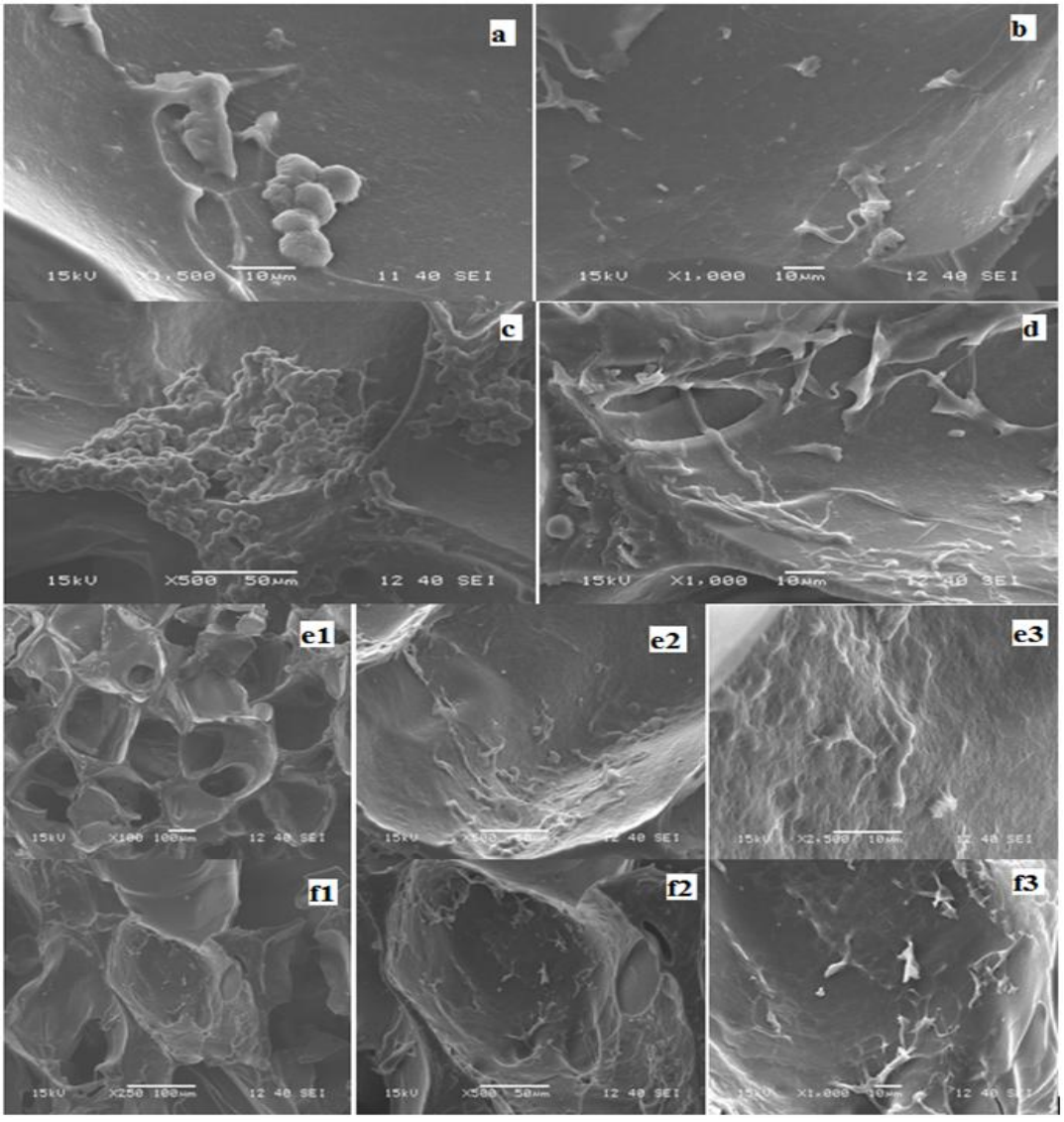

Figure 4.3.14: SEM of cell-scaffold construct on day 3(a, b), 7(c, d) and 14(e, f) days of culture. Figure shows the progressive adherence of MSCs in SEP conjugated scaffolds (b, d, e) and control (a, c). SEP conjugated scaffolds shows early adherence and morphological changes in cell shape than control. After 14 day of MSCs culture in modified scaffold (f1, f2, f3) was compared with SF scaffold (e1, e2, e3). The cells areere found to spread all over the scaffold as depicted from the SEM images. Scale bar= 10 µm (a, b, d, e3, f3); 50µm (c, e1, e2, f1, f2)

4.3.13. Cell Adhesion and Proliferation

Attachment and the proliferation of cells on a given substrate are fundamentals for a functional tissue engineering scaffold. The viability of cells cultured on the scaffold was determined based on the linear correlation between cell count and OD570 value of MTT formazan [Zund et al., 1999]. The number of cells were observed to be increased with increase in culture period as observed with both SF and SEP-SF scaffolds though at varying proliferation rate as shown in Fig. 4.3.15. The viability of the proliferated cells on the SF scaffolds was found to gradually increase from 0.191±0.018 to 0.493±0.015 during 14days culture (Fig. 4.3.15). The proliferation rate was observed to be higher with SF-SEP scaffold achieving 0.675±0.031 OD on day 14 compared to the proliferation rate achieved with SF scaffold used as control. Cells entrapped inside the scaffold without adherence didn't show much spreading and proliferation at all. The cells did not survive during further cell culture as indicated by MTT assay done on 3rd day. Cells adhered over the surface and inside the scaffold were found to be grown, proliferate and differentiate. However, confluence of large number of cells was observed on 7th day of culture covering entirely the conjugated scaffold as compared to the SF scaffold. After 14 days of culture, cells were more prominently and uniformly spread on the pore surface with flat morphology (Fig.4.3.14f). Thus it is demonstrated in this study that the modified SF scaffold is more effective than SF scaffold which is evident from an improved cell proliferation and cell viability observed during cell culture. This enhanced expansion of cell culture could be attributed mainly to the SEP mediated improved surface hydrophilicityrather than the scaffold morphological change, as there is no significant morphological changewas observed using 2% SEP solution for surface modification.

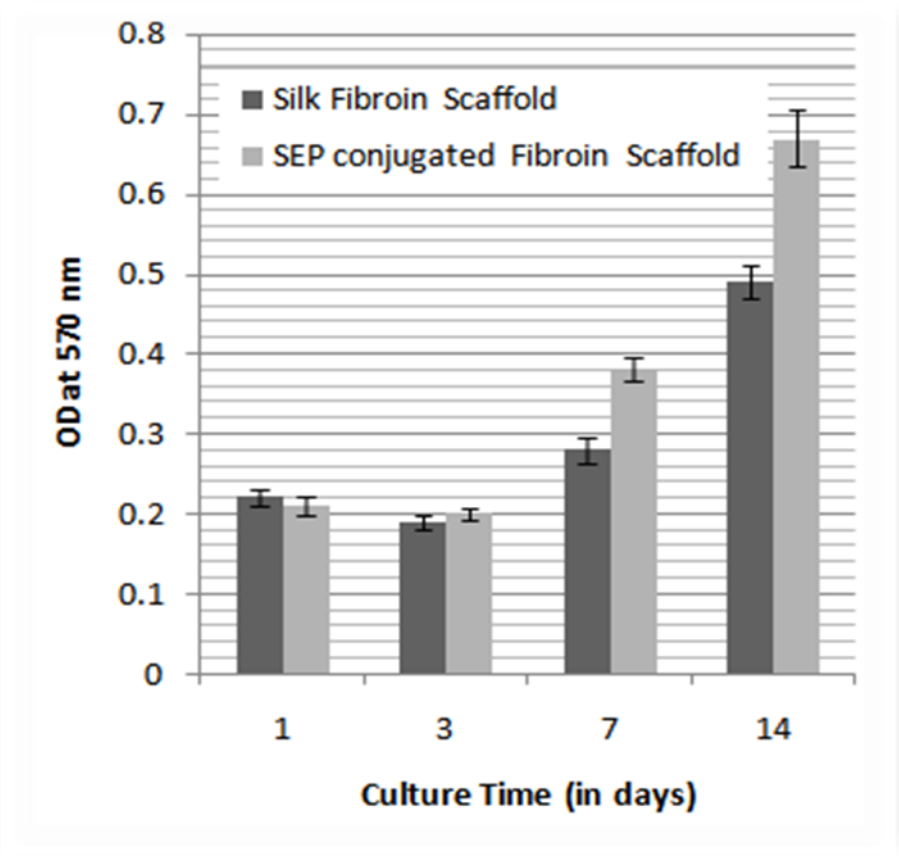

Figure 4.3.15: Comparison of optical density of MTT formazan on SF and SEP-SF Scaffolds during culture period (p<0.05, n=3)

4.3.14. ALP Activity Assay

The osteogenic differentiation of hMSCs on the SF and SEP conjugated SF scaffolds was determined by endogenous alkaline phosphatase (ALP) activity measured on days 1, 7 and 14 of cell culture. Increased ALP production was observed with culture time. However, SEP conjugated SF scaffold showed significantly higher activity than the ALP production achieved with SF scaffold (p < 0.01) as indicated in Fig.4.3.16. This implies that the conjugated scaffolds prepared from SF conjugated with SEP are more favorable for cell differentiation.

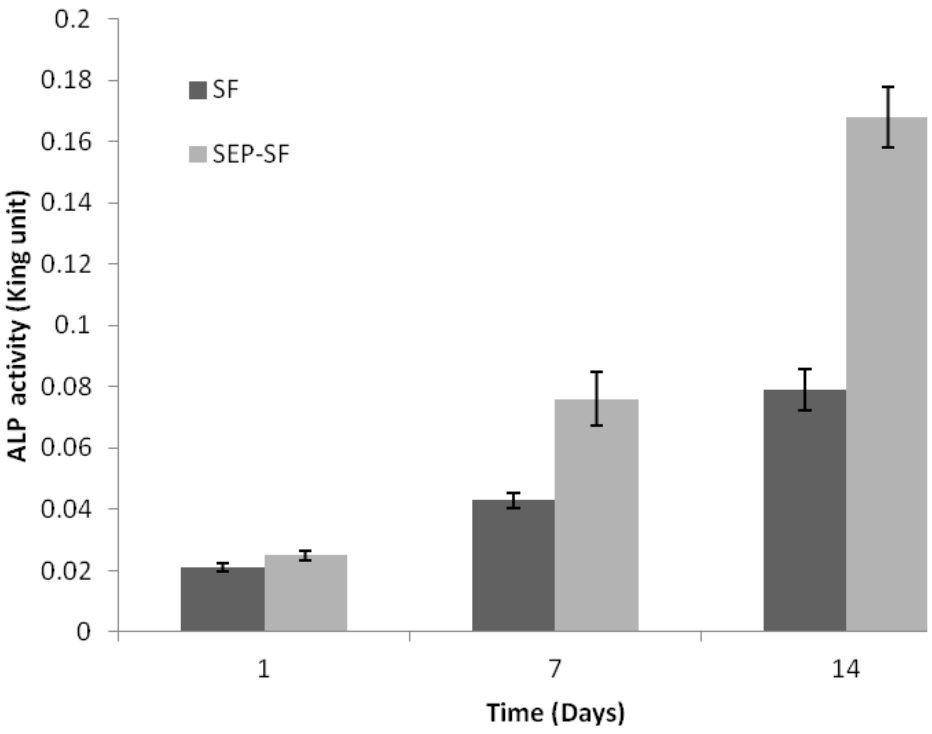

Figure 4.3.16: ALP activity of hMSCs grown on SF and SEP-SF scaffolds for 1, 7 and 14 days. Each value represents the mean value ± SD ($p<0.05$, n=3)

4.3.15. *In vivo* Biocompatibility Study

Transplantation of SEP-SF scaffolds was performed under surgically-created subcutaneous pouch in apparently healthy mice (Fig. 4.3.17a, both male & female for gender effect, if any). During the period of experiment, all mice remained in healthy condition and did not show any wound complications and no inflammatory and/or adverse tissue reactions were observed. Thus, transplanted scaffolds did not have any adverse effect on the physiology of animals (Fig. 4.3.17b). After one and four weeks of transplantation, mice were sacrificed and the host tissue reaction was analyzed by H&E staining. Macroscopically, all the scaffolds were encapsulated in thin fibrovascular tissues of recipient. After implanted for 7 days, more fibroblasts were grown into the scaffold and the inflammatory cells were in existence (Fig. 4.3.18a). However, when the test had processed for 4 weeks, a large number of fibroblasts were infiltrated into the scaffold and the morphology of scaffold was close to the surrounding dermal tissue (Fig. 4.3.18b). Thus, conclusion can be made as SEP-SF scaffold support the attachment, proliferation *in vivo* condition without causing infection, inflammation and/or tissue cell death.

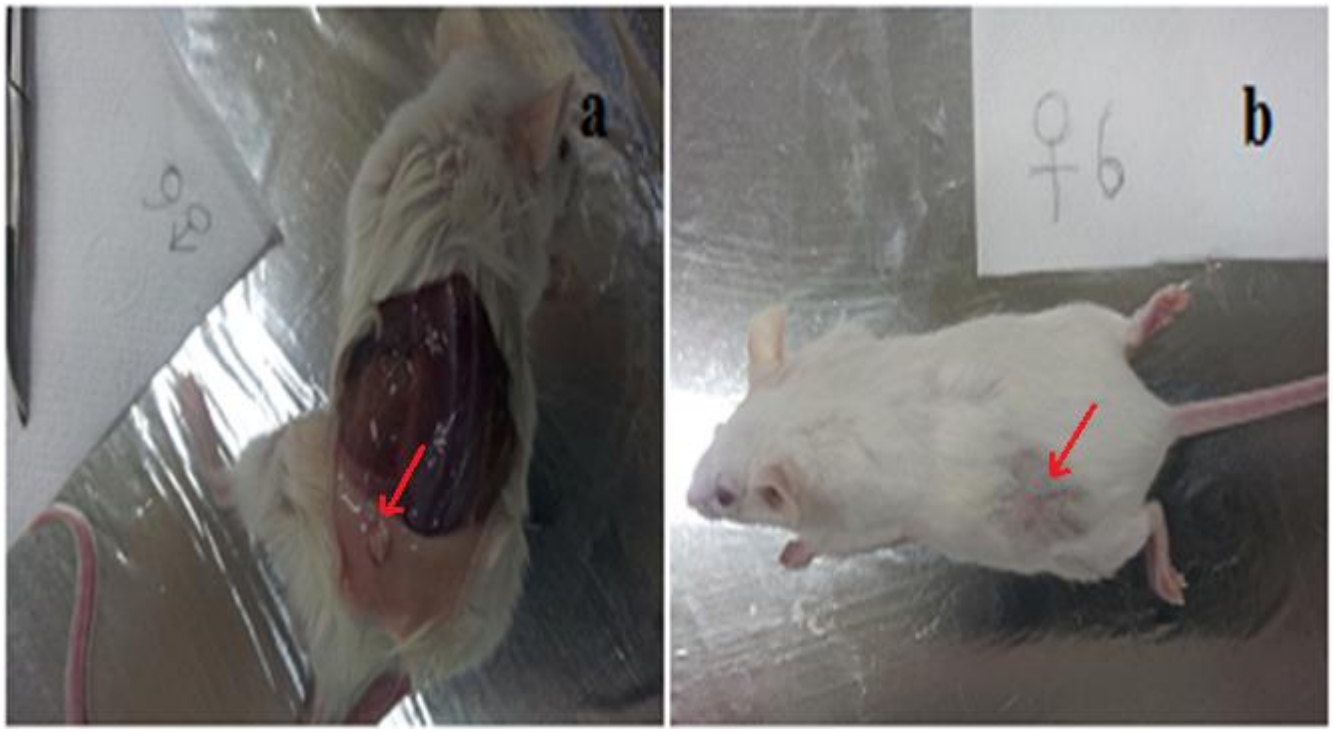

Figure 4.3.17: ***In vivo*** **biocompatibility study of SEP-SF scaffolds using ICR mice strain (a) Implantation of scaffold in male (b) Surgical recovery after one month in female**

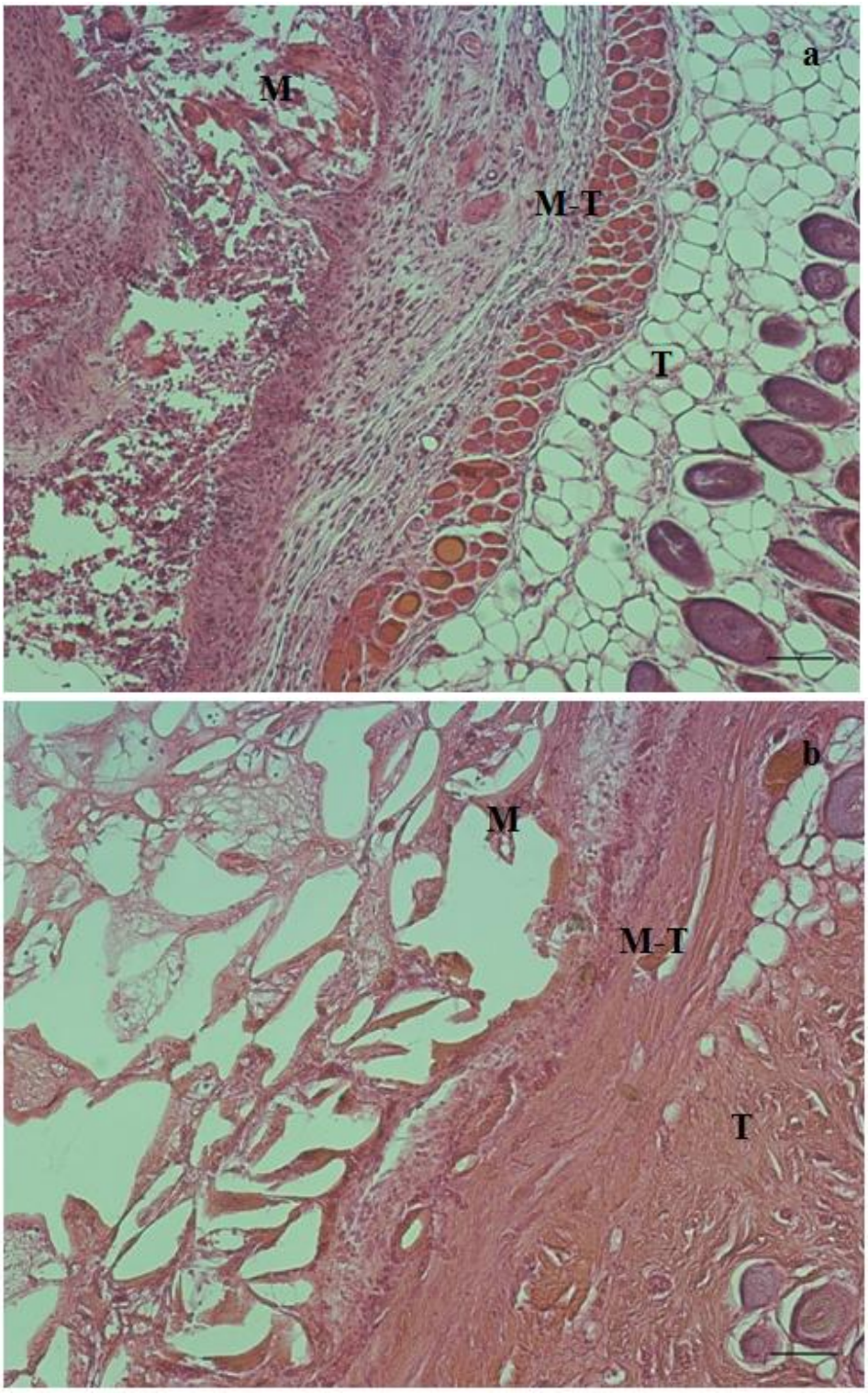

Figure 4.3.18: Histological section of subcutaneous skin at the site of implanted SEP-SF scaffolds in ICR mice model after (a) 7 days and (b) 4 weeks. Bar indicates 200μm. M: the implanted scaffold site. T: the subcutaneous connective tissue. M-T: the meso-dermal site as the interface of scaffold-tissue.

PART IV

Development of porous SF/PVA scaffolds with and without SEP conjugation

It is evident from published literature taht the brittleness of pure SF scaffold limits their application in tissue engineering. The physical properties of SF scaffold can be enhanced by mixing it with other synthetic or natural polymers, such as poly-(vinyl alcohol) (PVA), collagen and chitosane [Gobin et al., 2005; Kweon et al., 2003; Du et al., 2006]. The cytocompatibility behaviour of such polymeric blend scaffolds has not been explored much. It has also been reported that polymer blended crosslinked system may show differential degradation behavior under physiological conditions [Ma et al., 2003]. In addition, a crosslinking process improves permeability and mechanical strength of polymers [Sabato et al., 2001]. Furthermore, the addition of glycerin (a commonly used plasticizer) improves silk film properties [Kawahara et al., 2006] and helps to reduce phase separation between silk and PVA in the blend [Dai et al., 1999]. Glycerin content in blend films is important for the control of silk secondary structural transitions and influencing the mechanical properties of the films [Lu et al., 2010]. PVA, a synthetic polymer has excellent hydrophilicity, biocompatibility, biodegradability and processability with ability to form high strength fibres suitable for medical applications [Mnasur et al., 2008; Mnasur et al., 2004]. In addition, the published literature has indicated that the amount of PVA accumulated in organs is too small to affect the biological fate, which suggested that PVA is excreted to the same extent supporting the cyto-compatibility of PVA [Yamaoka et al., 1995]. Incorporation of PVA solution in chitosan has shown improvement in biocompatibility of the blend system [Huang et al., 2005].Silk fibroin and PVA have been separately investigated as candidate materials for tissue engineered constructs [Meinel et al., 2004a; Hofmann et al., 2007]. Though many research groups have studied the preparation method and properties of SF/PVA blends for improved stiffness of SF [Li et al., 2002; Dai et al., 2002; Li et al., 2001; Tanaka et al., 1998; Tanaka et al., 1997; Tsukada et al., 1994], it has not yet been explored much for its cytocompatibility and potential tissue engineering application. So efforts has been given in this phase of research work to prepare SF/PVA scaffold and its further improvement in surface properties by conjugation with SEP which has been found to enhance cell adhesion and proliferation property of SF scaffold in our previous research work [Chapter 4, Part III]. In the present study, green process has been employed for the fabrication of SF/PVA scaffolds of various pore sizes, modification with SEP and study of their biorelevant properties such as morphology, structure, mechanical properties, *in vitro* cell culture and *in vivo* biocompatibility.

4.4.1. Miscibility of SF/PVA Blend

Due to a noteworthy influence of the miscibility of polymer blend on their properties, the study of phase behavior during blending of polymers has been an important research area [Vucovic et al., 1999]. The effect of glycerin and ultra-sonication on the phase behavior and miscibility of SF and PVA were investigated by SEM. A series of SEM micrographs of SF/PVA (50:50) with different combination of blended system (with and without glycerine) and processing method (with and without ultrasonication) were studied, vizually (-Glycerine/-Ultrasonication), (-Glycerin/+Ultrasonication), (+Glycerine/-Ultrasonication) and (+Glycerine/+Ultrasonication) as shown in Fig. 4.4.1. As reported earlier, SF molecules are unstable and exist as colloidal state in aqueous system due to hydrophobic amino acids of SF and result in to molecular aggregation and gelation [Um et al., 2001]. On the other hand, PVA molecules are readily dissolved in water and are found as stable solution state in aqueous system. Due to the different solution stability in aqueous system between these two components, SF molecules tend to aggregate and form a separated domain in PVA matrix [Wang et al., 2010]. Ultrasonication induces the intra - and interchain crosslinking without any chemical additives [Jakobs, 2013]. In the present study, during sonication some of the silk fibroin chains in the SF/PVA blend were observed to form physical cross-links via β-sheet crystal networks rapidly by absorbing energy from the ultrasound process. The method is controllable and based on the energy input from ultrasonication to the system without involving any additional chemical processes. However, blending under ultrasonication without glycerine couldn't set homogeneity and still the distinct patches of SF and PVA exist (Fig. 4.4.1b).

The SF/PVA blend mixed under magnetic stirring using glycerine as plasticizer shows homogenous phase. SEM reveals patches of SF molecules at many places as shown in Fig. 4.4.1c. The silk fibroin film prepared by adding glycerin to SF solution is highly flexible as reported by Curvelo et al. [Curvelo et al., 2001]. The similar effect may act to reduce the heterogeneity between hydrophobic SF and hydrophilic PVA. The blend film of SF/PVA treated with glycerin, had shown the indistinct homogenous phenomenon, and presumably due to the glycerin induced intermolecular interactions between the polymers, such as hydrogen bonding of -OH groups of PVA, -OH groups of glycerin and -NH groups of SF [Dai et al., 2002]. In glycerin system, since SF molecules exist as a stable form, the possibility of heterogeneity due to solution instability may be excluded. SF molecules have polar groups including CO and NH. Therefore, there is some

possibility of molecular interaction between polar groups of SF and side groups of a second polymer. In addition, as mentioned above, OH group in PVA molecule is partially changed to ester group when PVA interacts with glycerin. It is well known that the miscibility of polymer blend is strongly connected to amorphous phase. Therefore, the increase in amorphous phase of PVA in SF/PVA blend system might enhance the miscibility with SF. Glycerol esterifies with SF and PVA greatly modify the compatibility and processing ability of SF/PVA blends as reported earlier [Dai et al., 2002]. A combination of ultrasonication and glycerine as plasticizer found to make a homogenous phase of SF/PVA blend as shown in Fig. 4.4.1d. This observation can be explained by two separate effects of ultrasonication and glycerine as mentioned above. The uniform blending of SF/PVA polymers influences the physical properties [Vucovic et al., 1999] of processed biomaterials.

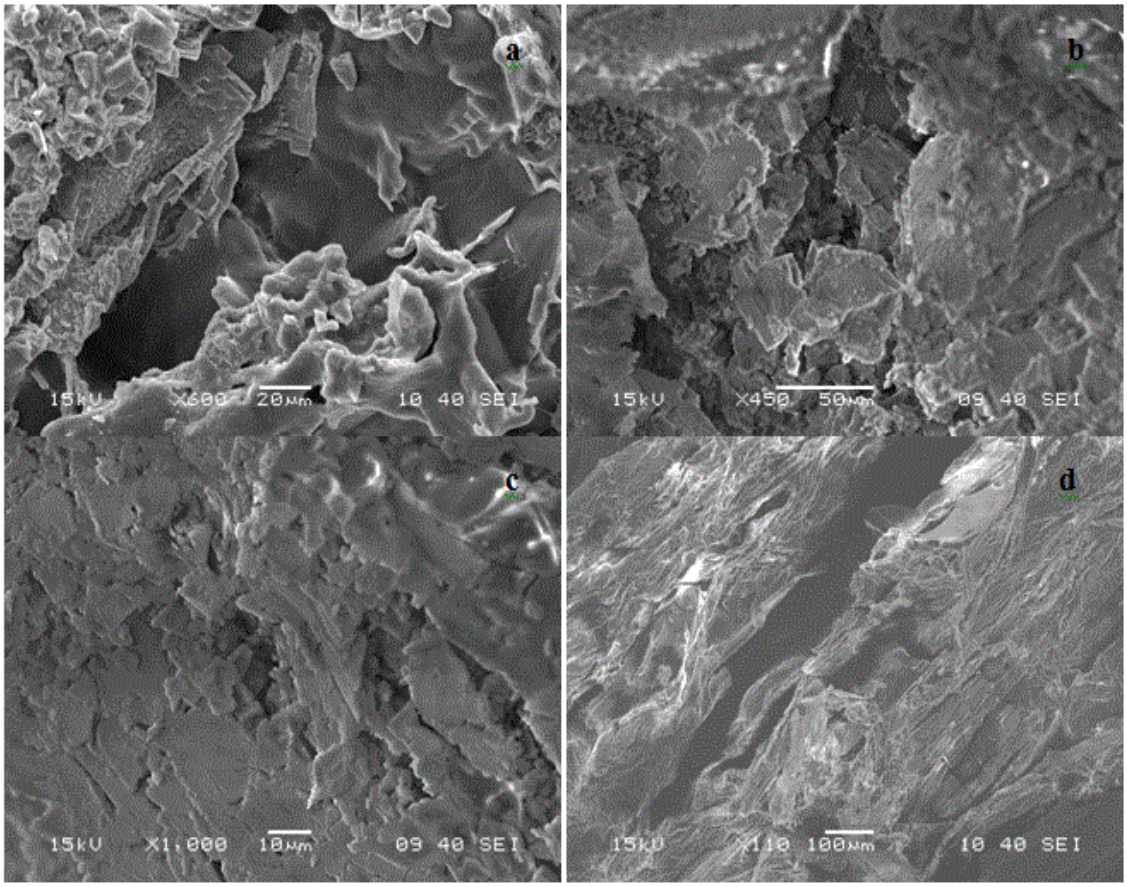

Figure 4.4.1: SEM images of SF/PVA in aq. solution processed (a) without glycerine with magnetic stirring (b) without glycerine under ultrasonication (c) with glycerine with magnetic stirring (d) with glycerine under ultrasonication

4.4.2. Morphological Study

SEM images of salt leached porous SF/PVA (100:0) and SF/PVA (0:100) scaffolds are shown in Fig. 4.3.2 of (Chapter 4, Part III) and Fig. 4.4.2 respectively. Fig. 4.4.3 shows the scaffolds prepared from SF/PVA (75:25; 50:50; 25:75) by salt leaching using NaCl of various particles size as porogen. The pore size and porosity of the scaffolds corresponding to different particle size are presented in Table 4.4.1. The size of porogen is shown to have great influence on the pore size of the scaffold, while the polymer to porogen ratio is directly correlated to the amount of porosity of the final structure. From the SEM morphological study, it is revealed that the pore size is approximately 80% of particle size of NaCl particle. Methanol treatment during the processing for scaffold development is shown to enhance the crystallinity of the scaffold and results into water insoluble PVA component of scaffold. The scaffolds showed rough surface on the pores that are highly interconnected by a number of smaller pores (Fig. 4.4.3). The highly porous scaffolds with 91-94% porosity were developed from SF/PVA (50:50; 25:75) with pore size being in range of 230-360 µm (Table 4.4.1). The SF/PVA scaffolds with pore size range of 225-350 µm as recommended for cell based therapy [Karageorgiou et al., 2005; Murphy et al., 2010] were used for further modification with 2% SEP. The porosity of these modified SEP-(SF/PVA) scaffolds was measured around 84% with pore size range of 200-300 µm. The crystellites of SEP is found embedded with scaffold surface affecting the pore size of scaffold to some extent (Fig. 4.4.4).

Table 4.4.1: Pore size and porosity of SF/PVA scaffolds prepared from different blend ratio of SF (8 wt%) and PVA (10 wt%).*(n=3)

SF/PVA Ratio	NaCl particle size	Pore Size	Porosity*
75:25	100-200 µm	90-150 µm	80 %
	200-300 µm	140-230 µm	85 %
	300-500 µm	225-350 µm	75 %
50:50	100-200 µm	80-150 µm	85 %
	200-300 µm	150-250 µm	87 %
	300-500 µm	230-360 µm	91 %
25:75	100-200 µm	80-140 µm	81 %
	200-300 µm	150-260 µm	89 %
	300-500 µm	250-360 µm	94 %

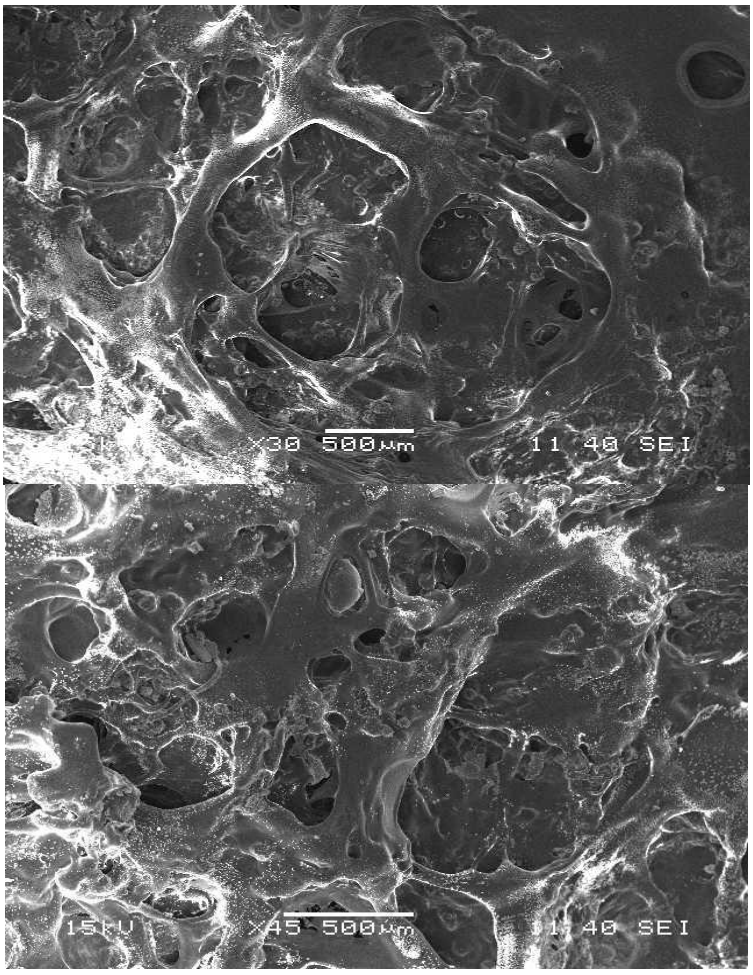

Figure 4.4.2: SEM images of porous SF/PVA (0:100) scaffold prepared using NaCl particle size of range 300-500 μm

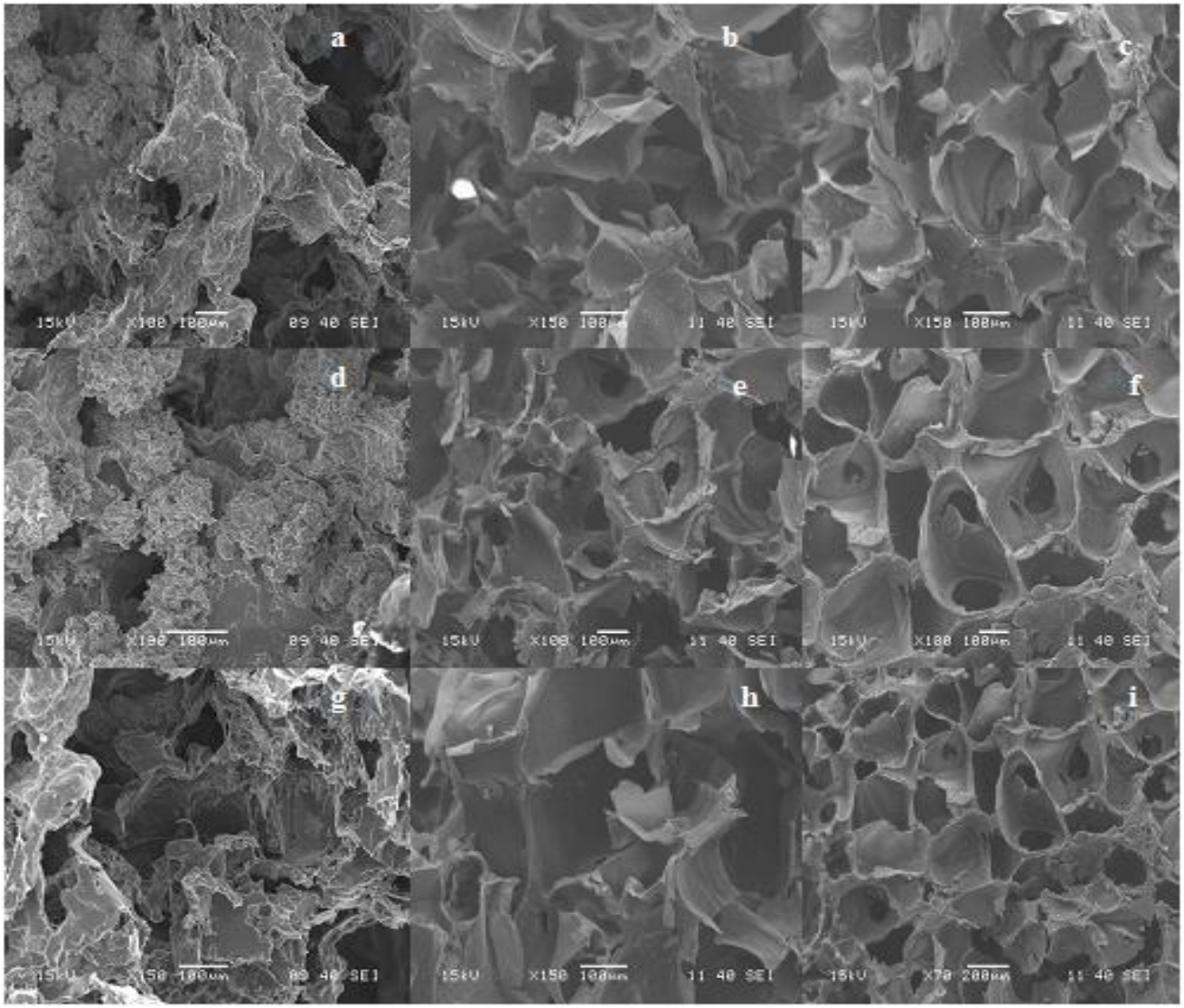

Figure 4.4.3: SEM images of SF/PVA scaffolds with blend ratio: 25/75 (a,d, g), 50/50 (b, e, h), 75/25 (c, f, i) prepared from 10 wt% PVA and 8 wt% SF aqueous solutions with NaCl particle size range of 100-200 (a, b, c), 200-300 (d, e, f) and 300-500 (g, h, i) μm.

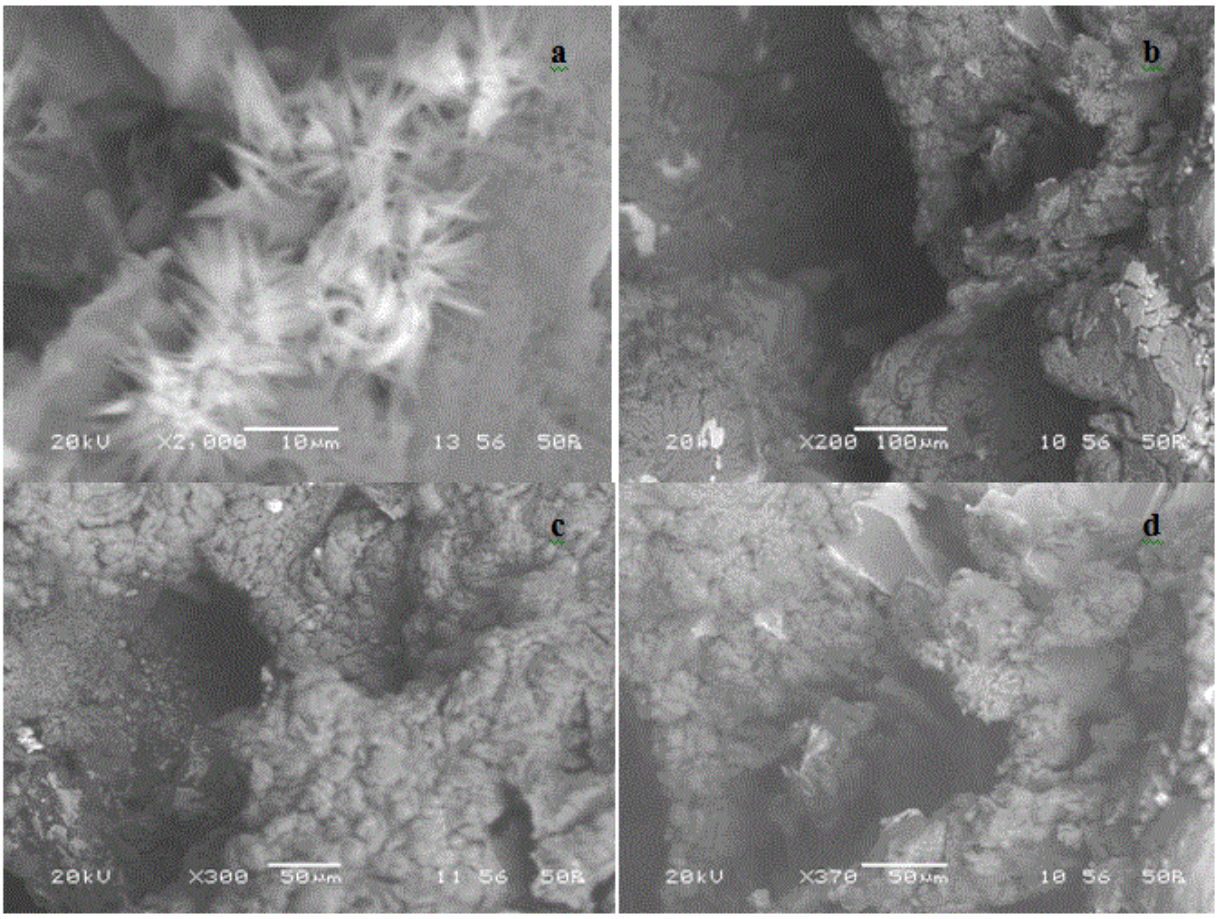

Figure 4.4.4: SEM images of SEP-(SF/PVA) scaffold prepared from SF/PVA (75:25, 50:50 and 25:75, 300-500 µm) scaffolds conjugated with 2 wt% SEP solution. (a) The conjugated SEP macromolecule shows crystalline structure. Porous morphology of SEP-(SF/PVA) scaffolds with SF/PVA blend ratio of 75:25 (b), 50:50 (c) and 25:75 (d) are also accessible.

4.4.3. Structural Characterization

4.4.3.1. X-Ray Diffraction

X-ray diffraction curves of SF, PVA, and SF/PVA scaffolds with and without SEP conjugation are shown in Fig. 4.4.5. Pure SF scaffold showed characteristic major peak at 2θ=19.7° (d=3.5 Å) and minor peaks at 2θ=8.8° (d=8.1 Å) and 2θ=23.2° (d=4.8 Å) which are attributed to the silk II β-sheet crystalline structure [Um et al., 2001, Min et al., 2004]. PVA scaffold (Fig. 4.4.5f) cast from water as solvent is characterized by the presence of a minor broad peak at 2θ=11.9° (d=9.7 Å), in addition to a major broad diffraction peak at 2θ=19° (d=4.4 Å) [Nakane et al., 1999]. It is observed with SF/PVA scaffold that 2θ = 19.7◦ peak broadens and 2θ = 8.8◦ peak disappears with increase in PVA content indicating the increase in total crystallinity. In addition, a new peak not corresponding to SF or PVA lattice spacing appeared at around 2θ=7.4°, which may be originated from crystalline fibroin–PVA complex. The β-sheet crystalline structure of SF in the polymer blend scaffold is partly induced by the addition of glycerine [Dia et al., 2002]. In SEP-(SF/PVA) scaffold, a new characteristic peak for SEP at 2θ=22.6 indicate the conjugation with SF/PVA scaffold [Guo et al., 2011].

4.4.3.2. FT-IR Spectroscopy

FTIR spectroscopy in transmittance mode was used to characterize the presence of specific chemical groups in SF, PVA, SF/PVA and SEP-(SF/PVA) scaffolds (Fig. 4.4.6). To minimize redundancy, the FTIR spectra were normalized and major vibration bands were analyzed for correlation with chemical groups. The FTIR spectrum of SF scaffold as illustrated in Fig. 4.4.6a shows strong absorption bands at amide I (1654 cm^{-1}), amide II (1519 cm^{-1}), amide III (1220 cm^{-1}) and amide V (555 cm^{-1}) which can be attributed to mainly random coil conformation and the α helix [Um et al., 2001]. The FTIR analyses indicatea conformational change from random coil to *β*-sheetwith the formation of SF scaffolds from SF solutions. The PVA scaffold (Fig. 4.4.6f) shows absorption bands at 3425 (OH stretching), 2923 (CH stretching), 2850 (CH stretching), 1735 (C=O stretching), 1429 (CH2 bending), 1250 (C-O stretching of acetate group) and 1091 (OH bending) cm^{-1} resonance which is in good agreement with the published literature [Finch et al., 1973; Finch et al., 1992]. The spectra for PVA also show a peak at 3398 cm^{-1} that indicates the presence of OH and N-H groups with polymeric association. Crystalline fraction of the polymeric chains affects the intensity of this peak for different SF/PVA blend ratio.

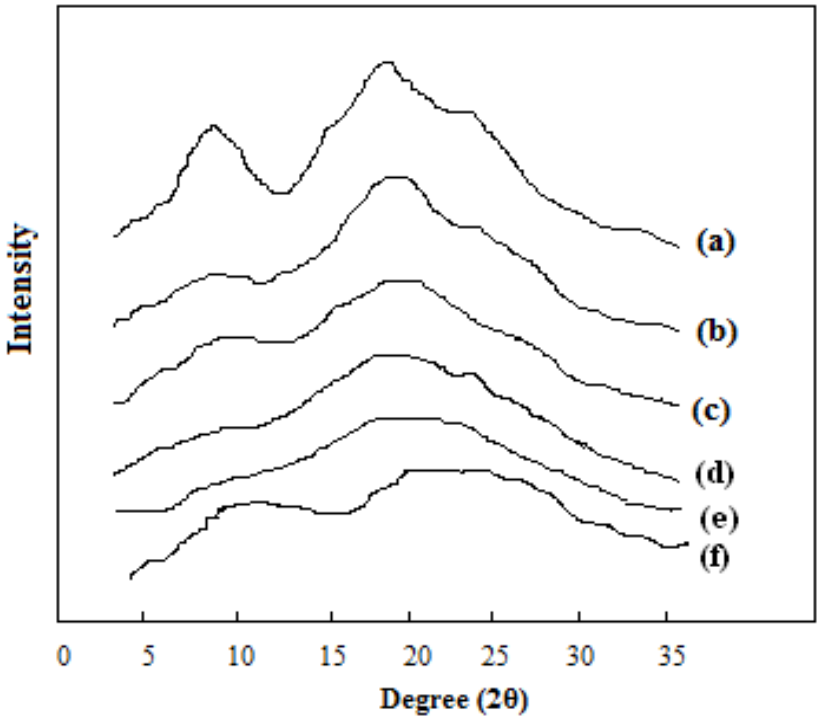

Figure 4.4.5: XRD pattern of SF/PVA scaffolds with different blend ratios (100:0, a; 75:25, b; 50:50, c; 25:75; e 0:100, f) and SEP-(SF/PVA) (50:50, d) scaffolds

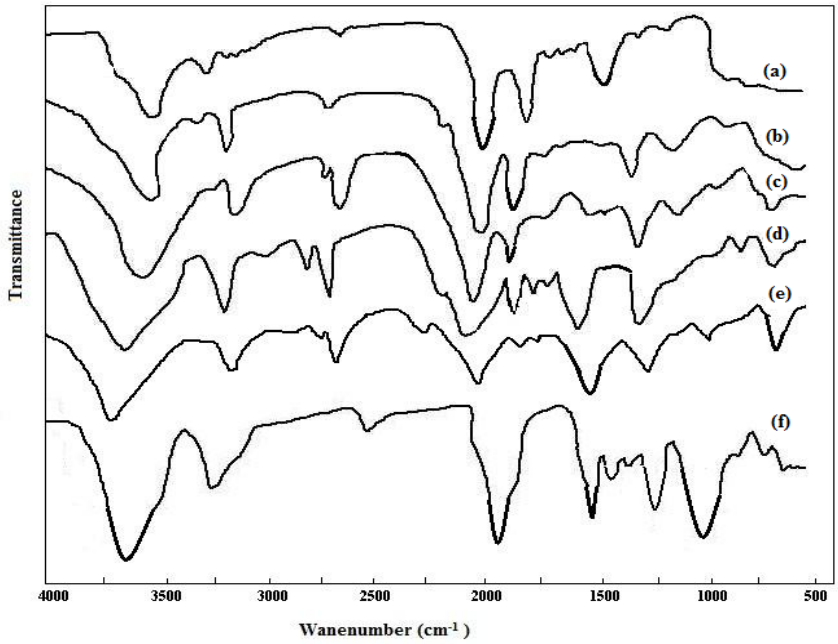

Figure 4.4.6: FTIR spectra of SF/PVA scaffoldS with different blend ratios (100:0, a; 75:25, b; 50:50, c; 25:75; e 0:100, f) and SEP-(SF/PVA) (50:50, d) scaffolds

The FTIR spectra of SF/PVA scaffold (Fig.4.4.6b-e) is characterized by the presence of typical absorption bands of SF and PVA scaffold whose intensity lies in between that of SF and PVA. However, the addition of glycerin causes the stretching of OH group in absorption band (3500-3200 cm^{-1}) [Speakman et al., 1975]. Such alteration in frequencies indicates the induction of intermolecular hydrogen bonding between two polymers namely SF and PVA. The polar OH group of glycerin plays vital role in strengthening OH group of PVA and NH group of SF [Lu et al., 1996]. The shifting of 1735 cm^{-1} of PVA to 1715 cm^{-1} in SF/PVA blend system is attributed to carbonyl groups which may be formed due to the esterification reaction of PVA and glycerol. The conjugation of SEP with SF/PVA (50:50) blend scaffold was confirmed by the presence of characteristics absorption peak of SEP at 2126 cm^{-1} (amide B group) (Fig.4.4.6d) as per reported literature [Wang et al., 2008].

4.4.4. Thermal Analysis

Even though microscopic observations depict no phase separation between SF and PVA, thermal analysis was carried out to make clear the interaction between SF and PVA during scaffold development and the effect of SEP conjugation on their thermal properties. Fig. 4.4.7 shows the DSC thermograms of various scaffolds prepared under study. The DSC curves of SF scaffold showed a weak endothermic peak around 100°C that is attributed to the evaporation of water content [Kweon et al., 2001b]. The typical endothermic peak near 240°C is due to the crystallization of thermally induced SF protein and β-sheet structure of samples while an endothermic peak at 283°C is attributed to thermal decomposition of scaffolds [Chapter 4, Part II; Kweon et al., 2001b]. The main endothermic peak for SF/PVA scaffolds at around 292°C is contributed by the thermal decomposition of both polymers. As the PVA content of SF/PVA scaffold increased, the thermal decomposition temperature increased which is depicted by the shifting of peaks to a higher temperature. The broad endothermic peak of PVA scaffold became sharper in SF/PVA scaffolds and shifted to a lower temperature indicating possible interactions between SF and PVA.

The glycerin content of hybrid scaffolds has been reported to shift melting peak towards the low temperature [Dai et al., 2002]. A weak but somewhat different endothermic peak for SF/PVA (50:50) scaffold is observed with SEP-(SF/PVA) scaffold at around 45°C indicating SEP conjugation. Both group of scaffolds, SF/PVA and SEP-(SF/PVA) scaffolds exhibit similar endothermic peaks at 292°C, that is probably assigned to the breakdown of peptide bonds within

chain and side chain groups of SF and SEP proteins.A slight upward shift in the decomposition peak for SEP conjugated SF/PVA scaffold as compared to SF/PVA (50:50) scaffold indicate higher thermal stability of conjugated samples. This behavior may be due to increasedcrystallinity and molecular weight particularly promoted by the presence of stabilizing amino acids eg. proline and hydroxyproline in SEP.

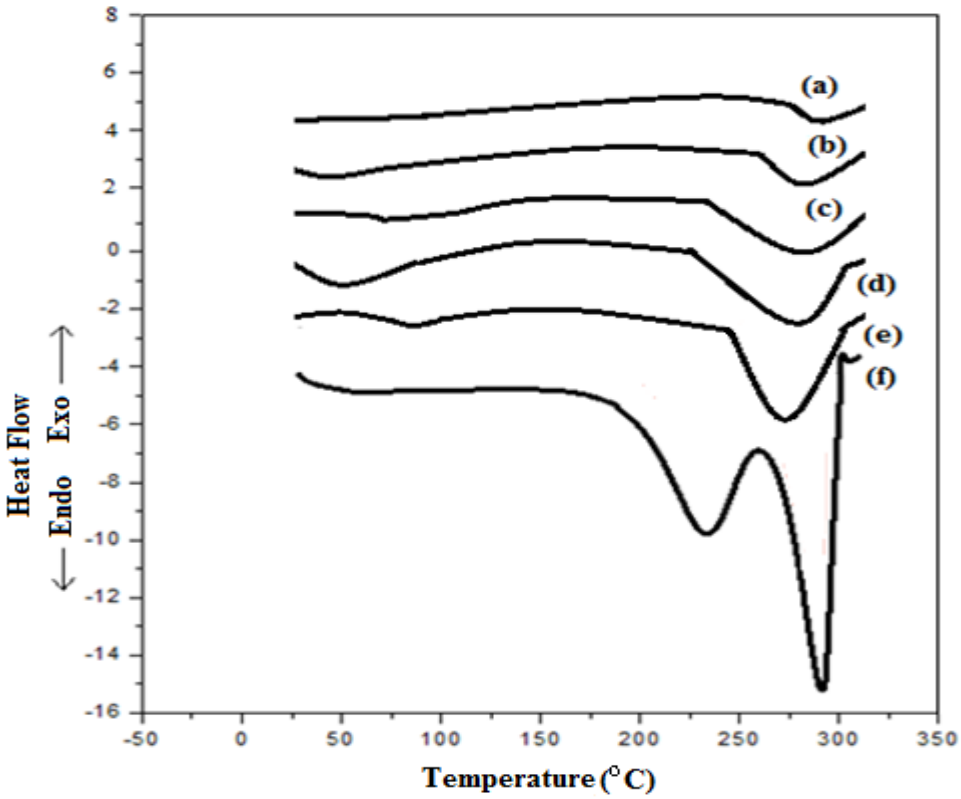

Figure 4.4.7: DSC thermograms of SF/PVA scaffold with different blend ratios (PVA:SF; 100:0, a; 75:25, b; 50:50, c; 25:75, e; 0:100, f) and SEP-(SF/PVA) (50:50, d) scaffolds

4.4.5. Mechanical Property

The optimal mechanical properties of scaffold to withstand the movement of surrounding tissues are required for tissue engineering applications. The mechanical properties of SF, SF/PVA, SEP-(SF/PVA) and PVA scaffolds were assessed based on stress–strain graphs (Fig. 4.4.8). The initial compressive modulus was measured as the maximum slope of the stress-strain curve over a 1.6% strain. It is observed that all scaffolds have the same line shapes which are the typical pattern of the plastic material demonstrating spongy behavior of scaffold materials with different stiffness. The addition of PVA to SF has shown to have a significant change in the mechanical properties. The

compressive strength of SF scaffolds (300 KPa) decreased when it wasblended with PVA (235 ± 67.1 KPa) which maybe due to the closer packing of PVA polymer chains with SF.For most of the scaffolds investigated in this study, the steepest portion of the stress-strain curve is shown to

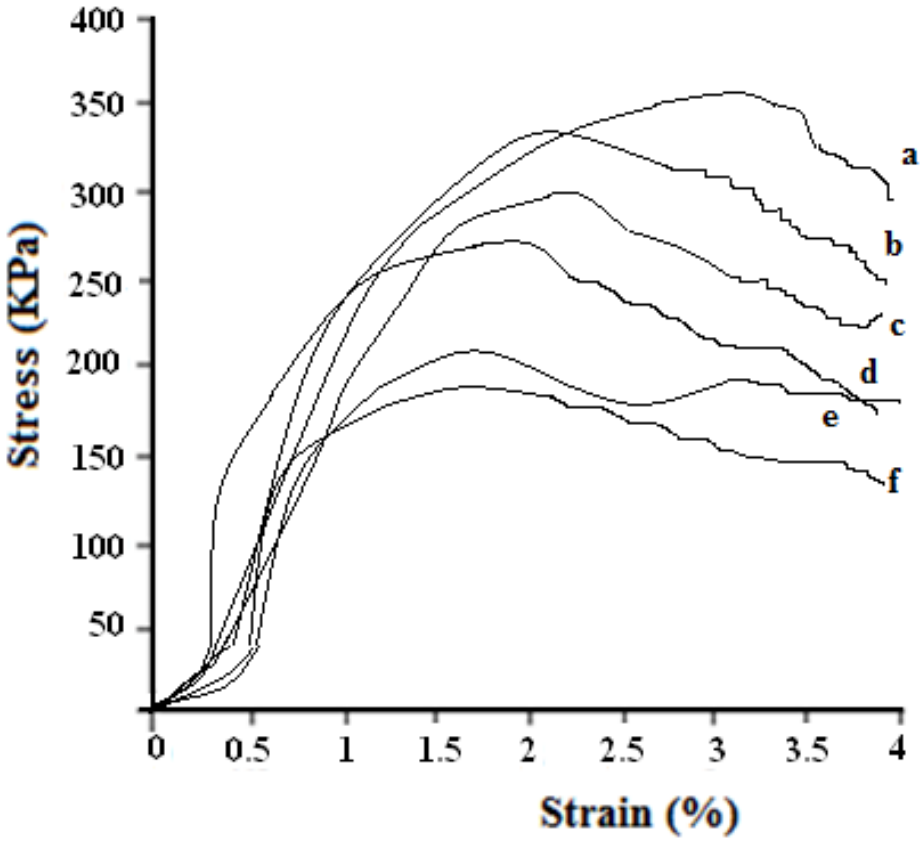

Figure 4.4.8: Stress–strain graph of SF/PVA scaffolds with different blend ratios (100:0, a; 75:25, b; 50:50, c; 25:75, e; 0:100, f) and SEP-(SF/PVA) (50:50, d) scaffolds measured at constant compression rate of 2 mm/min

occur in the range of 0-4% strain. The uncoated SF/PVA scaffolds break by external forces in between 200 and 300 KPa with 1.8 to 2.8% strain. The mechanical resistance is found to be increased with SEP modified scaffold as depicted from Fig. 4.4.8, supporting the breaking forces higher than 2.5 N and strain over 4%. The corresponding average compressive modulus is measures as 235 ± 67.1 KPa for the uncoated scaffolds and 247.5 ± 23.7 KPa for SEP coated scaffolds. The increase in amorphous PVA content has been reported to reduce the crystallinity of SF/PVA blend and act as lubricant for extensibility and flexibility [Lee et al., 2007] resulted into decrease in compressive strength of SF/PVA scaffold in comparison to SF scaffold. Overall, the scaffold

compressive modulus decreased with increased PVA reinforcement with same porosity. The research reports show that the increase in PVA content upto 50% decreases the tenacity while increases the elongation at break [Lee et al., 2007]. Hence, the SF/PVA blend with 40–50% PVA has a optimal mechanical properties (compressive strength and elongation at break) than filaments with lower/higher PVA [Lee et al., 2007]. According to Dai et al., although strength and elongation of the blend films are above that of the pure silk film, the value is relatively low as compare to the blends with the addition of glycerin [Dai et al., 2002]. Therefore SF, SF/PVA (50:50), SEP-(SF/PVA) scaffolds with pore size range of 230-360 μm were used for further study.

4.4.6. Swelling Behavior

From the experimental result shown in Fig. 4.4.9, the swelling pattern indicated an initial rapid water uptake at about 30 min, followed by mass stabilization over a period of 48hrs. Visual examination also showed appreciable increase in volume of the samples. Within a period of 30 min, SF scaffolds showed swelling of 60.3% and about 133.36% up to a period of 48 h. In comparison, the PVA scaffold showed much higher swelling index of 80.94%. As reported earlier, PVA scaffold without physical (cryogelation) or chemical (GA, 5%) crosslinking, doesn't withstand the water penetration and dissolves within a period of 48 hrs. [Dai et al., 2002], however, in our study the chemically crosslinked PVA, showed the swelling of 200% over a period of 48 hrs. Furthermore, SF/PVA (50:50) scaffold showed rapid swelling in comparison to SF scaffold with 227.06% swelling achieved at 48 hrs. The swelling behavior is markedly influenced by the presence of PVA in the blend, crosslinked by ultrasonication and glycerine. The observed swelling pattern is probably related to the crosslinking between –NH group of SF chains and -OH group of PVA chains by ultrasonication and glycerine, causing the formation of a rigid structure amongst the SF/PVA chains and reducing their solution uptake. SEP-(SF/PVA) scaffold shows higher rate of swelling which may be due to the presence of hydrophilic SEP and maximum swelling of 254.9% was observed at 48 h. The initial swelling behavior of SEP-(SF/PVA) scaffold is attributed to the combined effect of a more rigid net-work formed by the inter – intra polymer chain reactions as well incorporation of covalent bonds on scaffold surface, thus reducing the flexibility and number of hydrophilic groups of scaffold surface which is unfavorable to the swelling property. Similar trends in swelling behavior of PVA and SF supported these findings, where PVA has a swelling degree above 300% and SF of about 200%, depending on course of the solution conditions [Wang et al., 2004a; Wang et al., 2004b; Lin et al., 2008; Zhang et al., 2012].

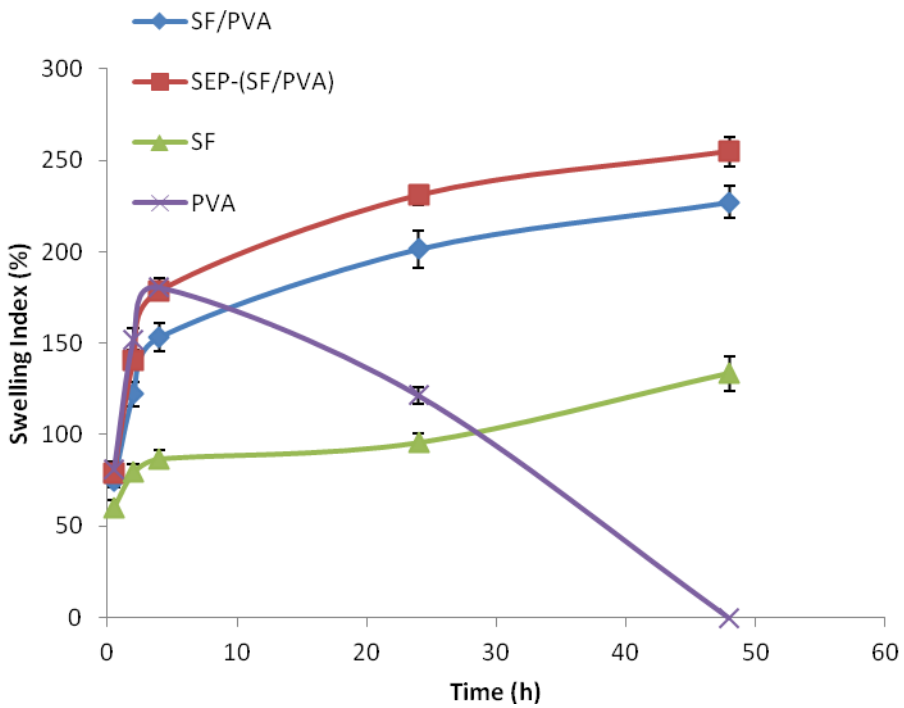

Figure 4.4.9: Swelling Index of SF, PVA, SF/PVA (50:50) and SEP-(SF/PVA) scaffolds in SBF for different time period

4.4.7. *In vitro* Biodegradation

The degradation profile of scaffolds is shown in Fig. 4.4.10. it is observed that the rate of degradation of SF/PVA scaffold is more than SF scaffold. The faster degradation may be due to more hydrophilic PVA that shows strong intra and interchain H-bonding with polar solvent. The rate of degradation is further increased with SEP conjugation which may be due to the surface erosion caused by SEP conjugation. PVA scaffold (without physical or chemical crosslinking) showed low degradation initially and the rate bacame faster after 4 h and complete degradation achieved within 48 h. Polymer solubility in aqueous solution is reported to be controlled by intra and inter-molecular hydrogen bonding in which polymer–polymer hydrogen bonds are replaced by polymer–water hydrogenbonds [Tao et al., 2007]. At the end of 192 h, SF/PVA (50:50) scaffold is shown to have more degradation than SF scaffold which may be attributed to the presence of PVA (-OH group) but was found intact in SBF due to water resistance and penetration into the blend system. The presence of glycerine as plasticizer of thermoplastic blends, influences the degradation behavior of scaffold.

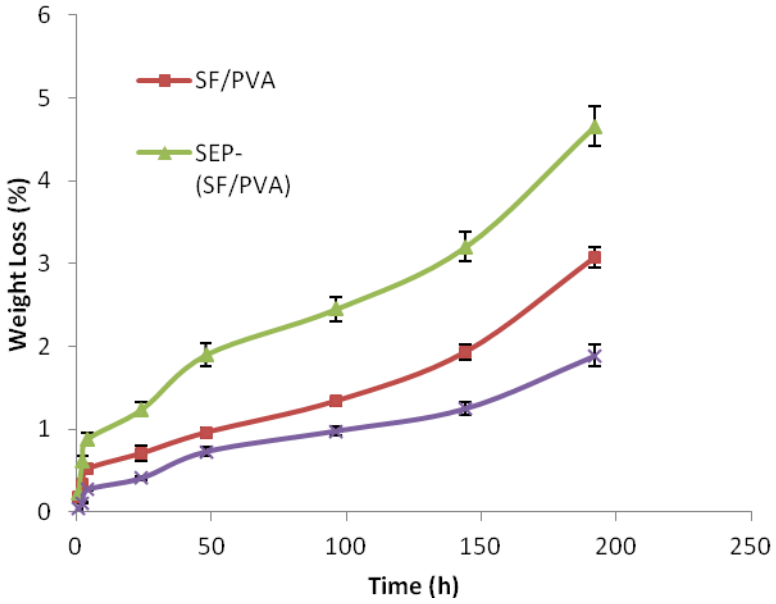

Figure 4.4.10: Weight loss of SF, SF/PVA (50:50) and SEP-(SF/PVA) scaffolds in SBF for different time period. The % weight loss of PVA scaffold (uncrosslinked) is not shown due to rapid dissolution in PBS within a period of 48 h.

4.4.8. Hydrophilicity

The wettability of the developed scaffolds was evaluated by contact angle measurement using sessile drop technique. The results for different scaffolds (SF, SF/PVA (50:50) and SEP-(SF/PVA)) are shown in Table 4.4.2. Results show that scaffold surface of each type is completely wettable. However, considerable decrease in water contact angles from 62.4±1.5° to 41.0±1.3° is observed due to much hydrophilicity of PVA that further decreases to 39.2±1.1° because of the conjugation of SEP over the scaffold surface. It is evident that conjugation of SEP as hydrophilic components make the surface of SF based scaffold more hydrophilic that is suitable for cellular reponse in aqueous medium.

Table 4.4.2: Water contact angles measured on various SF scaffolds

Exp #	Sample	Water contact angle (X^0)*
1.	SF	62.4±1.5
2.	SEP-SF	52.7±1.0
3.	SF/PVA (50:50)	41.0±1.3
4.	SEP-(SF/PVA)	39.2±1.1

*testing at three different sites for each scaffold

4.4.9. *In vitro* CellCulture Study

4.4.9.1. Cell morphology in seeded scaffolds

Human mesenchymal stem cells (hMSCs) isolated from umbilical cord blood by differential density gradient centrifugation and plastic adherence technique are proliferated to achieve required viable cell density. The morphology of hMSCs in different culture time (Fig. 4.3.12), was observed and the cell culture upto 4th passage were seeded into scaffolds by static method for *in vitro* culture study. The morphology of cell-seeded scaffold (construct) as shown in Fig. 4.4.11, depicts the uniform distribution of cells on the scaffolds. hMSCs are observed to be attached and grown well on the SF/PVA and SE-(SF/PVA) scaffolds, as evident from SEM images (Fig. 4.4.11). On day 3, hMSCs are shown to be attached on the scaffold and formed small cell aggregates, which increased in size on day 7.

4.4.9.2. Cell adhesion and proliferation

The hMSCs proliferation on SF, PVA, SF/PVA and SEP-(SF/PVA) scaffolds was evaluated on day 1, 3, 7 and 14 using MTT assay. The results of MTT assay are presented in Fig. 4.4.12. As it is indicated in figure, SF, PVA, SF/PVA and SEP-(SF/PVA) scaffolds show supported cell viability and proliferation. After day 1, the cell count on scaffolds was higher in PVA as compared to SF scaffold. SF/PVA scaffold shows intermediate cell count between SF and PVA scaffold. This may be due to lowering in hydrophilicity and amorphous component of SF. SEP-(SF/PVA) scaffold has lowest value of cell count, may be because of coated SEP over scaffold restricting the cellular movement into the pores. On day 3, cell count is decreased due to washing out of non-adhered cells from the scaffold. While there is no significant difference in cell proliferation observed with PVA and SF/PVA scaffolds, however, the cell viability was found more for SEP-(SF/PVA) scaffold. This indicated the improved surface of composite scaffold due to introduction of SEP and proliferation of viable cells, capable of moving inside and adhered over scaffold. The SEM images (Fig. 4.4.11) show the cell spreading over the SF/PVA and SEP-(SF/PVA) scaffold. hMSCs are observed to be well acclimatized with the blended and conjugated scaffold and showed an increase in cell count with time. On day 7, while the cell count for SF/PVA were found a little more than SF scaffold, the SEP-(SF/PVA) scaffold has shown exponential increase in cell count. The hydrophilicity of PVA sample support the cell adherence but with progress in culture, the viability of cells is not supported much. Introduction of PVA in SF forming SF/PVA scaffold greatly enhances the cell viability and

proliferation. However, SF/PVA scaffold modified with SEP shows the highest cell proliferation, representing biocompatibility and surface property enhancement of SEP. The absorbance value being much higher in hybrid scaffolds as compared to that of control, confirms that hybrid scaffolds (SF/PVA and SEP-(SF/PVA) are having enough pores and desired pore size allowed hMSCs to acclimatize and proliferate inside the scaffolds.

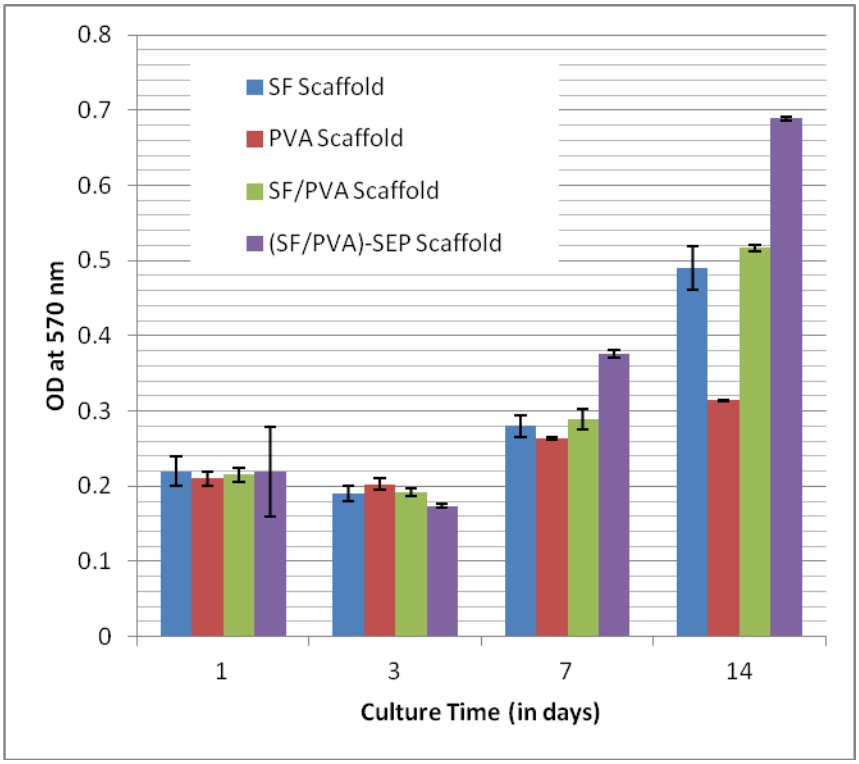

Figure 4.4.11: MTT Assay of hMSCs in SF (control), PVA, SF/PVA (50:50) and SEP-(SF/PVA) scaffolds for different culture period (1, 3, 7 and 14 days)

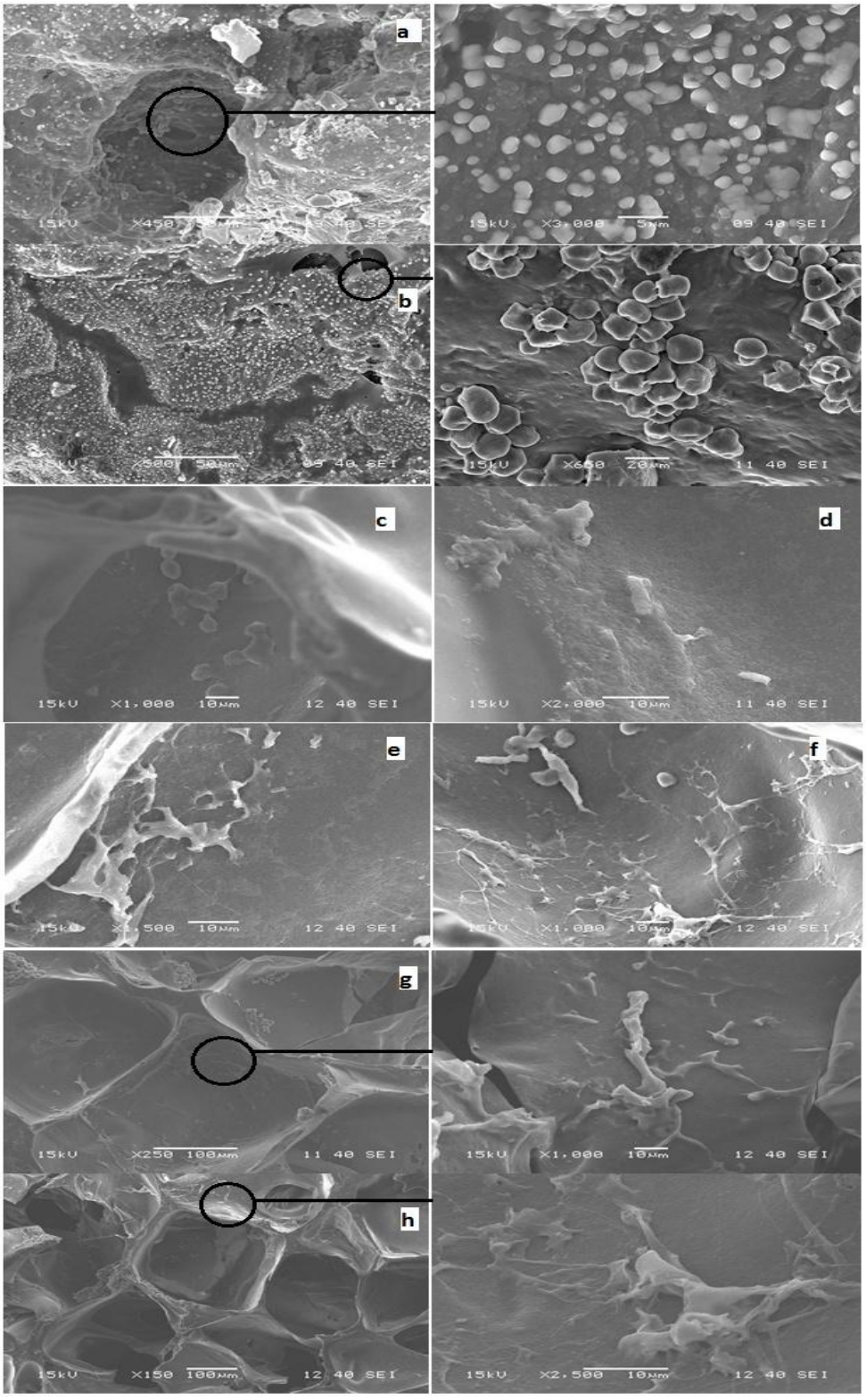

Figure 4.4.12: SEM of cell-scaffold constructs developed from SF/PVA (a, c, e, g) and SEP-(SF/PVA) (b, d, f, h) scaffolds for day 1 (a, b), day 3 (c,d), day 7(e, f) and day 14 (g, h) with umbilical cord blood derived hMSCs

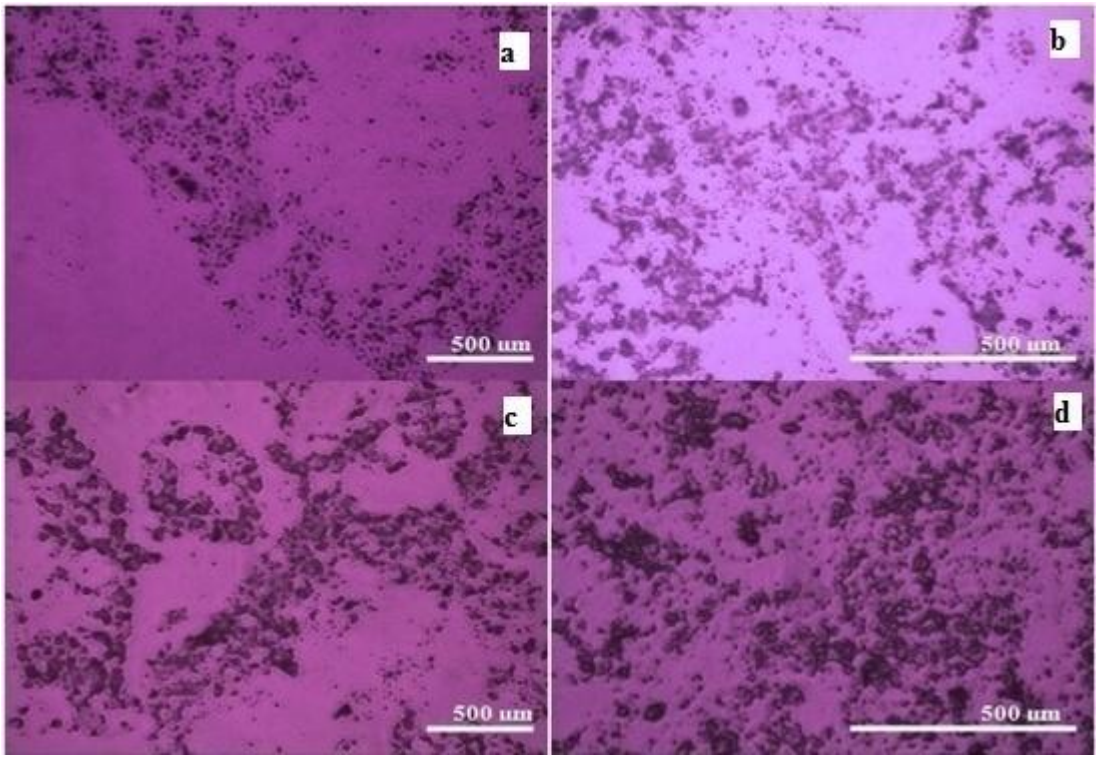

Figure 4.4.13: H&E stained cross-section of the constructs developed from SF/PVA (a&b) and SEP-(SF/PVA) (c&d) cultured for 7(a, c) and 14 (b, d) days (Scale Bar: 500µm)

Thus, UCB derived hMSCs on blended scaffolds showed relatively better cell viability and proliferation compared to the control. The histology of cell seeded scaffolds was examined after 7 and 14 days with H&E staining (Fig. 4.4.13). Stained sections of scaffolds were observed using an inverted light microscope. Both SF/PVA and SEP-(SF/PVA) scaffolds have shown good proliferation of MSCs. These cell viability results based on in vitro MTT assay and H&E staining have offer further investigation on scaffold for *in vivo* testing in biomimic environment involving scaffolds direct contact with cells leading to human tissue regeneration.

4.4.10. ALP Activity of Scaffolds

To determine the early osteogenic differentiation of hMSCs on the scaffolds, the alkaline phosphatase (ALP) activity of the prepared scaffolds was measured. SF, PVA, SF/PVA (50:50) and SEP-(SF/PVA) scaffolds showed an enhanced ALP activity over the culture period of 14 days (Fig. 4.4.14). In comparison, PVA scaffolds showed slightly lower activity than SF and SF/PVA scaffold

($p < 0.01$). SF and SF/PVA scaffolds has shown very close ALP activity ($p < 0.01$), while SEP conjugated SF/PVA scaffolds has the highest level of activity ($p < 0.05$). Elevated level of ALP, a marker for osteoblastic phenotype thus confirm enhanced differentiation of hMSCs on SEP conjugated scaffolds compared to the SF scaffold [Park et al., 2010].

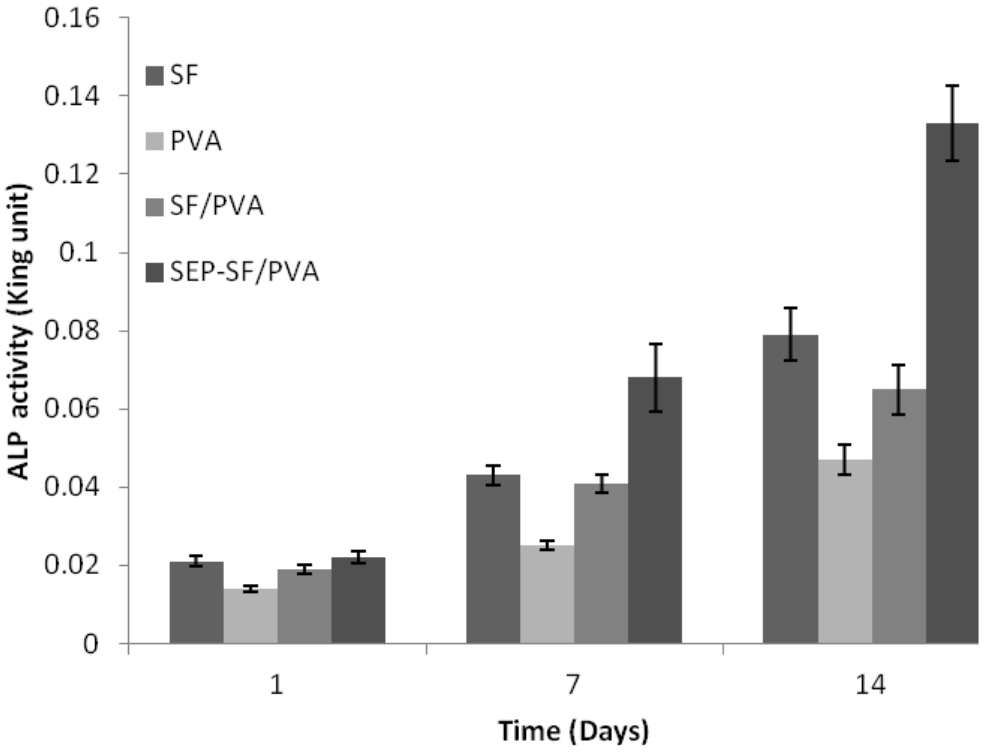

Figure 4.4.14: ALP activity of hMSCs grown on developed scaffolds for 1, 7 and 14 days. Each value represents the mean value ± SD (P<0.05, n=3)

4.4.11. *In vivo* Evaluation of Scaffolds

In vivo biocompatibility evaluation of SF/PVA (50:50) and SEP conjugated SF/PVA scaffolds were performed using ICR mice model (Fig. 4.4.15). Test animals for both groups of scaffolds were recovered after 1 month and showed no inflammatory reactions to host tissue as depicted by H&E stained micrographs (Figs. 4.4.16 & 17). The scaffolds were completely degraded without causing any necrosis. All mice were remained healthy and the scaffolds were found encapsulated in thin fibrovascular tissues of recipient. Observation made after 7 days showed fibroblasts grown into the scaffold with minor inflammation around implantation site (4.4.16a &17a). However, after 4 weeks,

a large number of fibroblasts were infiltrated into the scaffold and the morphology of scaffold was similar to the adjacent dermal tissues (Fig. 4.4.16b &17b). Thus the scaffolds are shown to be 134iocompatible with recipient tissue.

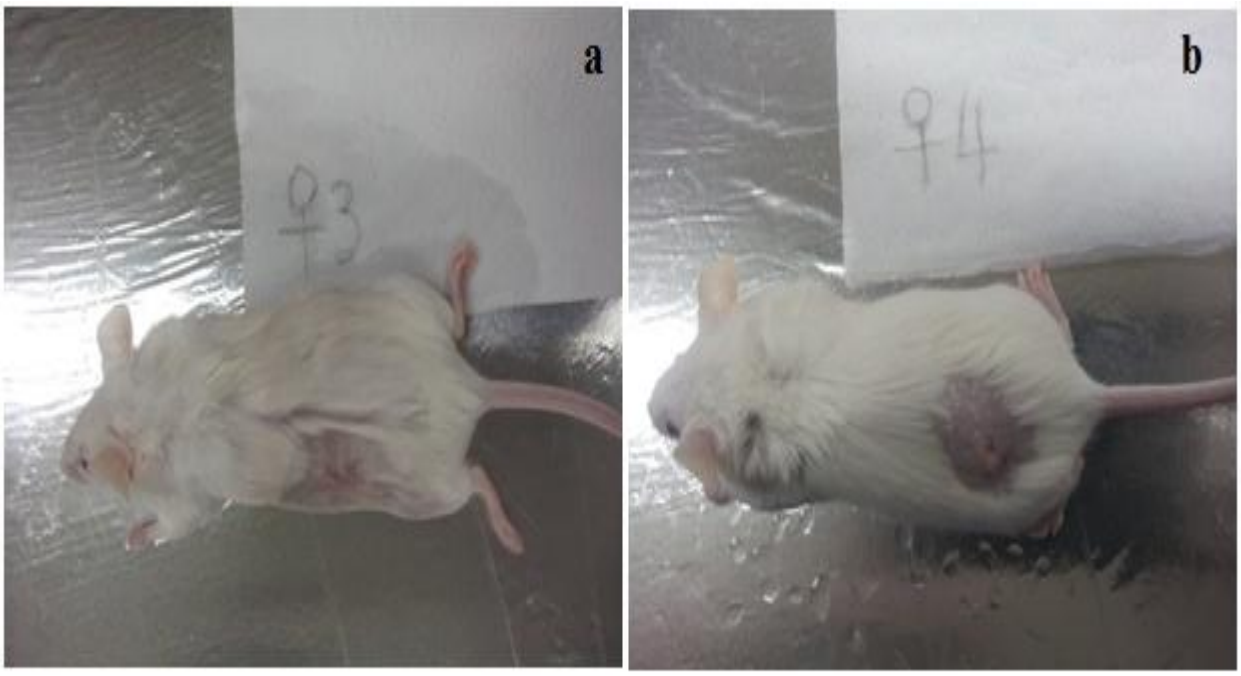

Figure 4.4.15: Implantation of (a) SF/PVA (50:50) and (b) SEP-SF/PVA scaffold into ICR mice strain for *in vivo* biocompatibility study

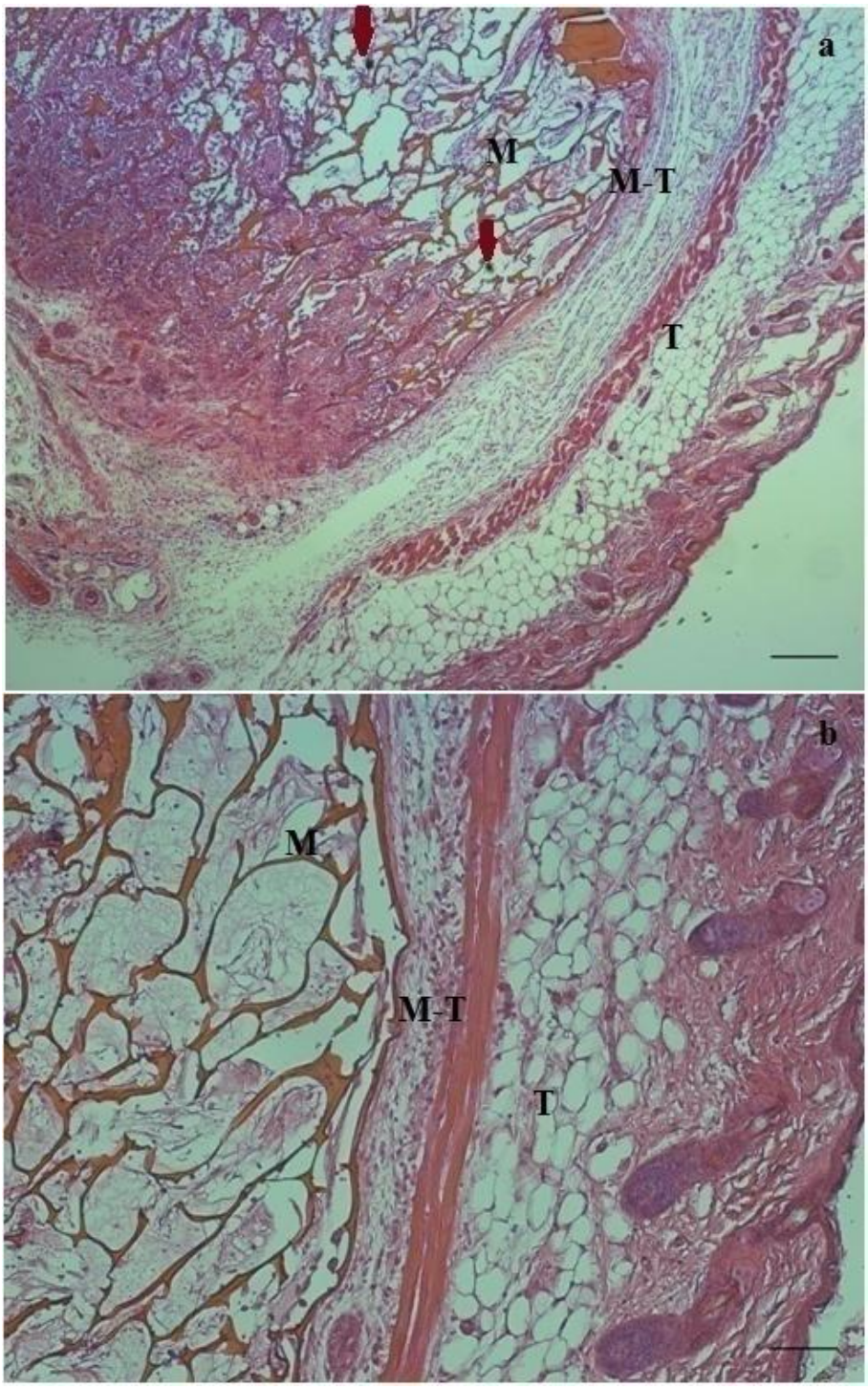

Figure 4.4.16: Histological section of subcutaneous skin of ICR mice at the site of implanted SF/PVA (50:50) scaffolds after (a) 7 days & (b) 4 weeks. Bar indicates 200µm. M: the implanted scaffold site. T: the subcutaneous connective tissue. M-T: the meso-dermal site as the interface of scaffold and tissue

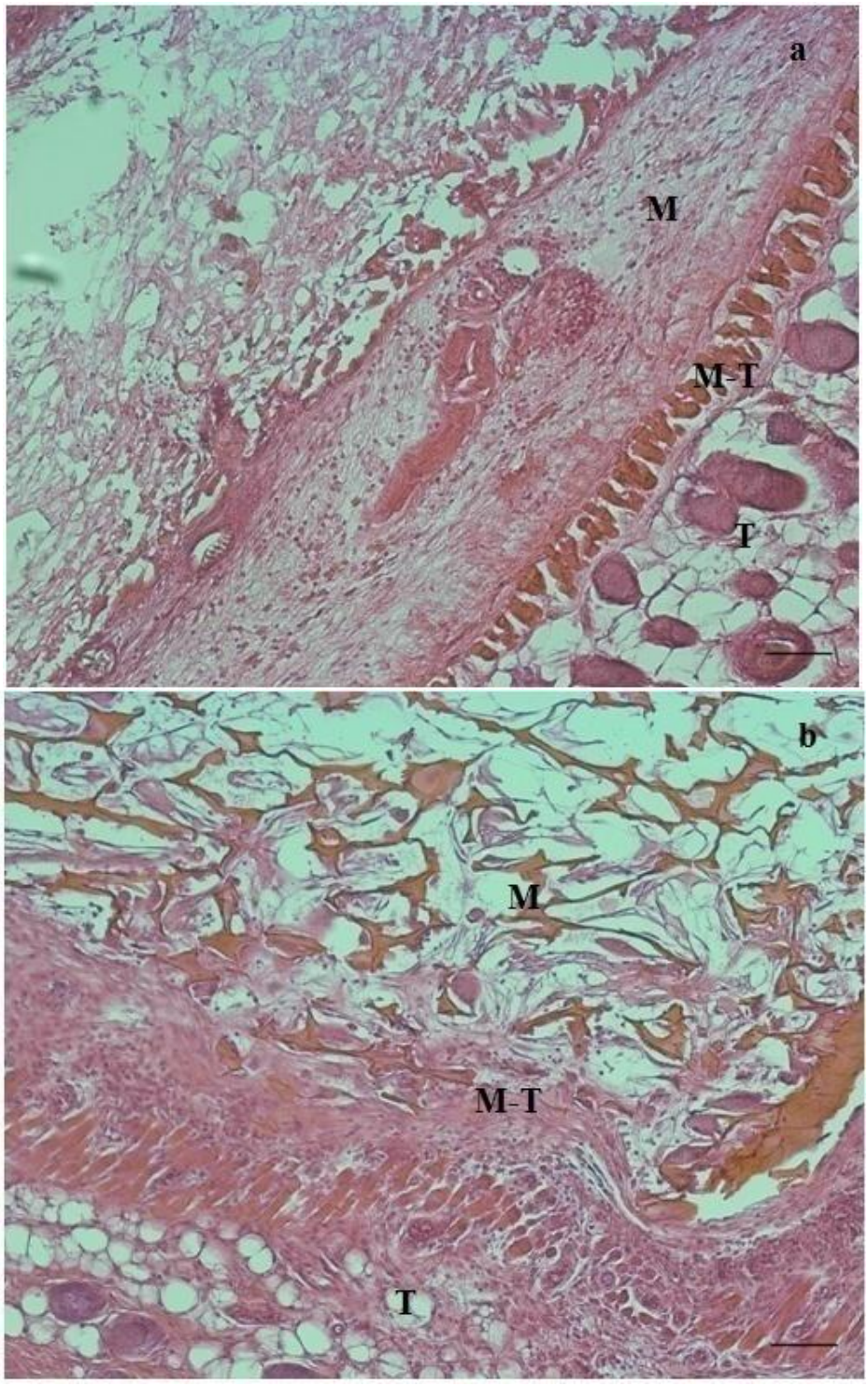

Figure 4.4.17: Histological section of subcutaneous skin of ICR mice at the site of implanted SF/PVA (50:50) scaffolds after (a) 7 days & (b) 4 weeks. Bar indicates 200µm. M: the implanted scaffold site. T: the subcutaneous connective tissue. M-T: the meso-dermal site as the interface of scaffold and tissue

Comparison of the results

A comparison in terms of physico-chemical, thermal and biological properties of the various scaffolds developed under study were made as given in Table 4.4.3. It is observed that all the prepared scaffolds are shown to have integrated structure with interconnected pore network with a slight variation in porosity. The compressive strength of SF scaffold (279.8 ±36.2 KPa) is increased with conjugation with SEP (321.5 ±42.2 KPa), while a decrease in compression strength is observed with SF-PVA blend (235 ± 67.1 KPa). A further increase in compressive strength of SF/PVA (247.5± 23.7 KPa) is achieved with SEP conjugation which is, however, less than SEP-SF scaffold. The wettability of SF scaffolds (62.4±1.5°) are found to be increased with SEP conjugation (SEP-SF;52.7±1.0°) and blending with PVA polymer (SF/PVA;41.0±1.3°). However, the highest wettable surface is obtained with SEP-(SF/PVA) scaffolds (39.2±1.1°) representing better cell support. *In vitro* and *in vivo* study of all matrices showed cell-supportive behaviour with a varying degree. The improved cell adhesion and proliferation were achieved with SF and SF/PVA scaffolds conjugated with SEP. However, SEP-SF/PVA scaffold has shown the superior cell adhesion and proliferation with hMSCs culture. Comparable cell viability is also achieved with SF-SEP scaffold. Though comparatively low compressive stress is shown by SEP-SF/PVA scaffolds, comparing all the properties as shown in table and the added advantage ofovercoming the problem of brittleness of SF scaffold using PVA, it is established that SEP-SF/PVA is the best scaffold among all the prepared SF scaffolds.

Table 4.4.3: Comparison of different SF based matrices based on some of the key properties

Sl. No.	Porous Matrices	Compressive Strength	Swelling Index (%)	Wt. Loss (%)**	Wettability (Degree)$^{\pm}$	Cell Count (OD)$^{\pm\pm}$	Porosity (%)	Morphology
1.	**SF Scaffold**	279.8 ±36.2 KPa	133.36 %	1.89%	62.4±1.5	0.49	90-93%	Porous & interconnected
2.	**SF-SEP**	321.5 ±42.2 KPa	138.42%	2.38%	52.7±1.0	0.67	85-90%	Less porous & interconnected than SF
3.	**SF/PVA (50:50)**	235 ± 67.1 KPa	227.06%	3.07%	41.0±1.3	0.517	90-92%	Porous and interconnected
4.	**(SF/PVA)-SEP**	247.5± 23.7 KPa	254.9%	4.66%	39.2±1.1	0.693	83-87%	Less porous & interconnected than SF/PVA

*Swelling (%) after 48 hrs., **Wt. loss (%) after 192 hrs., $^{\pm}$Contact angle, $^{\pm\pm}$OD of MTT on 14th days of culture

CHAPTER 5

Summary & Conclusion

SUMMARY & CONCLUSION

In recent years tissue engineering has been considered as a promising alternative to the conventional clinical method for the treatment of patients suffering from tissue related diseases. The development of tissue engineered scaffold from a variety of biopolymers with a set of desired properties that can mimic the extracellular matrix is the key aspect of this new technique. In this context, silk fibroin is considered as a promising biopolymer to use as a scaffold material. Keeping this in view, the present work has been undertaken to develop silk fibroin (SF) based scaffolds with improved surface, mechanical and biological properties by blending with other polymers and modified with additive as surface enhancer. The outcome achieved through this research work is summarized as follows:

Part I: In the first phase of the dissertation work, silk fibroin solution was prepared from *B. mori* silk cocoon. Silk fibroin was extracted from raw silk cocoon by degumming method. The effect of key parameters on the extraction process was investigated to find the most favorable degumming condition. The optimum condition thus established as 0.02 M aq.Na_2CO_3, 70°C and 60 min degumming time achieving maximum amount of SF with maximum removal of sericin.

SF solution was prepared by the dissolution of SF in LiBr solution. The maximum solubility of silk fibroin was achieved at 9.3M LiBr concentration, 70°C and 3 hrs of treatment time. The SF solution was characterized by SDS-PAGE and particle size analysis. The extraction process was further optimized by Response Surface Methodology using Box-Behnken Design. The solution thus prepared was used as biopolymer for the development of scaffolds.

Part II: In this phase of study, an effort has been given for the preparation, characterization and *in vitro* biocompatibility study of silk fibroin hydrogel for its possible use in tissue engineering. A structurally and thermally stable fibroin hydrogel with well interconnected and open pores was prepared with β-oriented close network of fibroin molecules. Morphologically, the hydrogels show a sponge-like cross-linked structure formed by physical entanglement as well as chemical bonding envolving hydrogen and covalent bonds. The rheological and swelling behaviors of fibroin hydrogel were appreciable at 37ºC representing to mimic the body tissue. Thermal analysis supported the

prepared hydrogel as biomaterial with degradation characteristics suitable for human *in vivo* application. The cytocompatibility study by hMNCs culture has shown that the three-dimensional network of SF hydrogel facilitated cell adherence, cell proliferstion and distribution throughout the scaffold. Thus it is concluded that the SF hydrogel is suitable as injectable biomaterial for soft tissue engineering.

Part III: In this part of the thesis work, an attempt has been made for the improvement of the surface properties of the SF scaffold. SF scaffolds were fabricated by salt leaching technique using NaCl as porogen. The effect of particle size of porogen was investigated and found to have a great influence on the pore size and porosity of the prepared scaffolds. The pore size and porosity of SF scaffold were measured as 70-350 µm and 85-93%. SF scaffolds were further modified with soluble egg cell protein (SEP) with the intention to improve its surface properties for better cell attachment and proliferation. The elemental analysis, XRD, FTIR, DSC and TGA study confirm successful conjugation of SEP over SF scaffold and structural and thermal stability of the modified scaffold. The pore size of the modified scaffold (SEP/SF) is found to be in the range 200-300 µm with porosity 85-90%. An increased compressive strength of SEP/SF scaffold is achieved (321.5 ±42.2 KPa) in comparison to SF scaffolds (279.8 ±36.2 KPa). The modified scaffold has further shown to have enhanced hydrophilicity (52.7±1.0 contact angle with water droplet) representing more favorable to *in vivo* application as compared to SF scaffold as control.

The *in vitro* cell culture study has shown a significantly higher cell adhesion and proliferation on the conjugated scaffold in comparison to SF scaffold. The *in vivo* animal model evaluation depicted the biocompatibility of SEP-SF scaffolds. Therefore, this study has demonstrated that the porous SF scaffolds modified with SEP offers enhanced cell adhesion and proliferation and hence improved biocompatibility to facilitate its application in practical tissue engineering. Furthermore, the non-inflammatory response towards host ICR mice model indicated *in vivo* biocompatibility of the scaffold.

Part IV: It is evident from literature that the brittleness of SF scaffolds limits their use in tissue engineering. Poly vinyl alcohol (PVA), a synthetic polymer has excellent hydrophilicity, biocompatibility and biodegradability property. It is reported that the blending of SF with PVA can

reduce the crystallinity and improves the surface property as well. Therefore, in this phase of dissertation work, efforts have been given to develop SF/PVA scaffold by blending these two polymers followed by salt leaching. The SF/PVA blend was also modified with SEP to investigate its effect on the further improvement of the properties of SF/PVA scaffold. As in *part III*, three dimensional porous SF/PVA and SEP modified SF/PVA (SEP-SF/PVA) scaffolds were prepared by salt leaching method using NaCl as porogen. These scaffolds exhibited a hierarchical structure with interconnected macropores of different pore size range depending on particle size of porogen. The results have shown that the proportion of PVA to SF has a great impact in controlling porosity and interconnectivity of scaffold. FTIR spectroscopy associated with XRD has proven to very powerful tools for investigating the formation of conjugated and unconjugated SF/PVA blend scaffolds. Among the various SF/PVA scaffolds prepared with different blend ratio, SF/PVA (50:50; 230-360 μm) and SF/PVA (75:25; 250-360 μm)have shown most favorable pore size range, but since the later has more fragile nature causing mechanical stiffness, SF/PVA (50:50; 230-360 μm) is most preferred for tissue engineering application. The SF/PVA and SEP-SF/PVA have the desired compressive strength though the compressive strength is lower than that of SEP/SF scaffold. The corresponding compressive strength of SF/PVA and SEP-SF/PVA are 235 ± 67.1 KPa and 247.5± 23.7 KPa respectively. Further, the swelling and degradation of SEP-SF/PVA scaffolds were higher due to enhanced hydrophilicity (39.2±1.1 contact angle) compared to SF/PVA (50:50) scaffolds (41.0±1.3) and other SF scaffolds developed in this study.

The cytocompatibility of the scaffolds were confirmed by cell viability (MTT) assays. The SF/PVA scaffold was observed to support cell attachment and proliferation during culture of hMSCs in SF/PVA scaffolds. The cell proliferation result was similar to the result observed with SF scaffolds. However, significantly increase in cell proliferation and cell spreading were observed with SF/PVA scaffold conjugated with SEP. Furthermore, the *in vivo* biocompatibility of the scaffolds was confirmed by animal testing using ICR mice model.

Furthermore, though comparatively low compressive stress is shown by SEP-SF/PVA scaffolds, comparing all the other properties and the added advantage of overcoming the problem of brittleness of SF scaffold using PVA, it is established that SEP-SF/PVA is the best scaffold among all the developed SF scaffolds under study.

Overall, the research provides a potential SEP conjugated SF/PVA scaffold (SEP-SF/PVA that has the superior surface property (hydrophilicity), biological property (cell adhesion and proliferation) and compressive strength desired for its use in tissue engineering. It has been further demonstrated that SEP is an excellent additive that can be used as surface modifier for the scaffold biomaterials. Thus it is concluded that the SEP-SF/PVA can be a potential artificial extra cellular matrix particularly for soft and other non-load bearing tissue engineering applications. SEP conjugated SF/PVA scaffolds could be further designed utilizing more advanced fabrication technology according to patient prerequisite. Furthermore, developed scaffold material may be mechanically improved to make it suitable for hard tissue engineering.

Bibliography

BIBLIOGRAPHY

[1] Addis KT, Raina SK (2013). Dissolution Properties of Silk Cocoon Shells and Degummed Fibers from African Wild Silkmoths. *Pak J Biolog Sci;* 16:1199-1203.

[2] Agrawal CM, Ray RB (2001). Biodegradable polymeric scaffolds for musculoskeletal tissue engineering. *J Biomed Mater Res;* 55:41-150.

[3] Ahlborn G, Sheldon BW (2005). Enzymatic and microbiological inhibitory activity in eggshell membranes as influenced by layer strains and age and storage variables. *Poult Sci*; 84:1935–1941.

[4] Altman GH, Diaz F, Jakuba C, Calabro T, Horan RH, Chen J, Lu H, Richmond J, Kaplan DL (2003). Silk-based biomaterials. *Biomaterials;* 24:401–416.

[5] Altman GH, Horan RL, Lu HH, Moreau J, Martin I, Richmond JC, Kaplan DL (2002). Silk matrix for tissue engineered anterior cruciate ligaments, *Biomaterials*; 23: 4131–4141.

[6] Altman, GH, Diaz F, Jakuba C, Calabro T, Horan RL, Chen JS, Lu H, Richmond J, Kaplan DL (2003). Silk-based biomaterials. *Biomaterials;* 24(3):401-416.

[7] Ambrosio AM, Sahota JS, Khan Y, Laurencin CT (2001). A novel amorphous calcium phosphate polymer ceramic for bone repair: I. Synthesis and characterization. *J Biomed Mater Res;* 58(3):295-301.

[8] Aoki H, Tomita N, Morita Y, Hattori K, Harada Y, Sonobe M, Wakitani S, Tamada Y (2003). Culture of chondrocytes in fibroin-hydrogel sponge. *Biomed Mater Eng;* 13(4):309–316.

[9] Araki Y, Akahoshi K, Harada N, Chijiiwa Y, Sasaki I, Nawata H (2001). Two cases of colonic adenomatous polyps accompanied by a migrated surgical suture, *Endoscopy*; 33:85–7.

[10] Asakura T, Kuzuhara A, Tabeta R, Saito H (1985). Conformational characterization of B. mori silk fibroin in the solid state by high-frequency 13 C cross polarization-magic angle spinning NMR, X-ray diffraction and infrared spectroscopy. *Macromolecules*;18:1841-1845.

[11] Asnaghi A, Macchiarini P, Mantero S (2009). Tissue engineering toward organ replacement: a promising approach in airway transplant.*Int J Artif Organs*; 32(11):763 – 768.

[12] Ayub ZH, Arai M, Hirabayashi K (1993). Mechanism of the gelation of fibroin solution. *Biosci Biotech Bioch;*57:1910–1912.

[13] Badylak SF (2007). The extracellular matrix as a biologic scaffold material. Biomaterials; 28(25):3587-3593.

[14] Baker J R, Balch DA (1962). A study of organic material in hen's-egg shell. *Biochem J*; 82: 352–361.

[15] Balakrishnan B, Jayakrishnan A (2005). Self-cross-linking biopolymers as injectable in situ forming biodegradable scaffolds. *Biomaterials*; 26(18):3941-3951.

[16] Beckstead BL, Santosa DM, Giachelli CM (2006). Mimicking Cell-cell Interactions at the Biomaterial-cell Interface for Control of Stem Cell Differentiation, *J Biomed Mater Res*; 79A: 94–103.

[17] Bhat S, Kumar A (2013). Biomaterials and bioengineering tomorrow's healthcare. *Biomatter;*3(2).3:e24717.

[18] Bhattarai SR, Bhattarai N, Viswanathamurthi P, Yi HK, Hwang PH, Kim HY (2006). Hydrophilic nanofibrous structure of polylactide; fabrication and cell affinity. *J Biomed Mater Res Part A*; 78A(2):247-257.

[19] Birmingham JR, Jeska EL (1980). The isolation, long-term cultivation and characterization of bovine peripheral blood monocytes. *Immunology*; 41:807.

[20] Boland ED, Espy PG, Bowlin GL (2004). Tissue engineering scaffolds: In *Encyclopaedia of Biomaterials and biomedical engineering*. Wenk GE, Bowlin GL (edi.), pp 1633-1635, Richmong, Verginia, USA.

[21] Boudriot U, Dersch R, Greiner A, Wendorff JH (2006). Electrospinning Approaches Toward Scaffold Engineering - A Brief Overview. *Artif Organs*; 30(10):785-792.

[22] Bradford M (1976). A Rapid and Sensitive Method for the Quantitation of Microgram Quantities of Protein Utilizing the Principle of Protein-Dye Binding. *Anal. Biochem;* 72: 248.

[23] Burdick JA (2011). *Biomaterials for Tissue Engineering Applications: A Review of Past and Future Trends*. pp. 13-16, Springer, NY, USA.

[24] Burley RW, Vadehra DV (1989). *The avian egg, chemistry and biology*; pp 472, John Wiley &Sons, NY, USA.

[25] Buttafoco L, Engbers-Buijtenhuijs P, Poot AA, Dijkstra PJ, Vermes I, Feijen J (2006). Physical characterization of vascular grafts cultured in a bioreactor. *Biomaterials;* 27(11):2380-2389.

[26] Cai K, Yao K, Lin S, Yang Z, Li X, Xie H, Qing T, Gao L (2002). Poly(D,L-lactic acid) surfaces modified by silk fibroin: effects on the culture of osteoblast in vitro. *Biomaterials;* 23(4):1153–60.

[27] Cai Q, Yang J, Bei J, Wang S (2002). A novel porous cells scaffold made of polylactide-dextran blend by combining phase-separation and particle-leaching techniques. *Biomaterials;* 23:4483-92.

[28] Cao YMDPD, Vacanti JPMD, Paige KTMD, Upton JMD, Vacanti CAMD (1997). Transplantation of Chondrocytes Utilizing a Polymer-Cell Construct to Produce Tissue-Engineered Cartilage in the Shape of a Human Ear. *Plast Reconstr Surg*;100(2):297-302.

[29] Cappello J, Crissman JW, Crissman M, Ferrari FA, Textor G, Wallis O, Whitledge JR, Zhou X, Burman D, Aukerman L, Stedronsky ER (1998). In-situ self-assembling protein polymer gel systems for administration, delivery, and release of drugs. *J Control Rel*; 53:105–117.

[30] Carrino DD, Dennis JE, Wu TM, Arias JL, Fernández MS, Rodríguez JP, Fink DJ, Heuer AH, Caplan AI (1996). The avian eggshell extracellular matrix as a model for biomineralization. *Connect Tissue Res;* 35:325–329.

[31] Cassell OC, Hofer SO, Morrison WA, Knight KR (2002). Vascularisation of tissue-engineered grafts: the regulation of angiogenesis in reconstructive surgery and in disease states. *Br J Plast Surg*; 55:603-10.

[32] Causa F, Netti PA, Ambrosio L, Ciapetti G, Baldini N, Pagani S, Martini D,GiuntiA (2006). Poly-ε- caprolactone/hydroxyapatite composites for bone regeneration: In vitro characterization and human osteoblast response. *J Biomed Mater Res Part A;*76A(1):151-162.

[33] Chen C-S, Soni S, Le C, Biasca M, Farr E, Chen E Y-T, Chin W-C (2012). Human stem cell neuronal differentiation on silk-carbon nanotube composite, *Nanoscale Res Lett;*7(1):126.

[34] Chen G, Sato T, Ushida T, Ochiai N, Tateishi T (2004). Tissue engineering of cartilage using a hybrid scaffold of synthetic polymer and collagen. *Tissue Eng;* 10 (3–4):323–330.

[35] Chen G, Ushida T, Tateishi T (2002). Development of biodegradable porous scaffolds for tissue engineering. *J Mater Sci Eng C;* 17:63–69.

[36] Chen J, Altman GH, Karageorgiou V, Horan R, Collette A, Volloch V, Colabro T, Kaplan DL (2003). Human bone marrow stromal cell and ligament fibroblast responses on RGD-modified silk fibers. *J Biomed Mater ResA;* 67(2):559–70.

[37] Chen J-P, Chen S-H, Lai G-J (2012). Preparation and characterization of biomimetic silk fibroin/chitosan composite nanofibers by electrospinning for osteoblasts culture, *Nanoscale Res Lett;*7(1):170.

[38] Chen Y, Alman BA (2009). Wnt Pathway, an Essential Role in Bone Regeneration. *J Cell Biochem*; 106(3):353-362.

[39] Chen YL, Lee HP, Chan HY, Sung LY, Chen HC, Hu YC (2007). Composite chondroitin-6-sulfate/dermatan sulfate/chitosan scaffolds for cartilage tissue engineering. *Biomaterials*; 28:2294–2305.

[40] Chiarini A, Petrini P, Bozzini S, Pra I, Armato U (2003). Silk fibroin/poly(carbonate)-urethane as a substrate for cell growth: in vitro interactions with human cells. *Biomaterials;* 24(5):789–799.

[41] ChoiSM, SinghD, Kumar A, Oh TH, Cho YW, Han SS (2013) Porous Three-Dimensional PVA/Gelatin Sponge for Skin Tissue Engineering.*Int J Polym Mater*; 62(7): 384-389.

[42] Chrzanowski W, Kondyurin A, Lee JH, Lord MS, Bilek MM, Kim HW (2012). Biointerface: protein enhanced stem cells binding to implant surface. *J Mater Sci Mater Med*; 23(9):2203-15.

[43] Chu CR, Coutts RD, Yoshioka M, Harwood FL, Monosov AZ, Amiel D (1995). Articular cartilage repair using allogeneic perichondrocyteseeded biodegradable porous polylactic acid (PLA): A tissue-engineering study.*J Biomed Mater Res;* 29(9):1147–1154.

[44] Cirillo B, Morra M, Catapano G (2004). Adhesion and function of rat liver cells adherent to silk fibroin/collagen blend films. *Int J Artif Organs;* 27(1):60-68.

[45] Cory AH, Owen TC, Barltrop JA, Cory JG (1991). Use of an aqueous soluble tetrazolium/formazan assay for cell growth assays in culture. *Cancer Commun*; 3:207-212.

[46] Couet F, Rajan N, Vesentini S, Mantovani D (2007). Design of a collagen/silk mechano-compatible composite scaffold for the vascular tissue engineering: Focus on compliance. *Key Eng Mat;* 334-335 II:1169-1172.

[47] Crombie G, Snider R, Faris B, Franxblm C (1981). Lysine-derived cross-links in the egg shell membrane. *Biochem Biophys Acta*; 640:365–357.

[48] Cunniff PM, Fossey SA, Auerbach MA, Song JW, Kaplan DL, Adams WW, Eby RK, Mahoney D, Vezie DL (1994). Mechanical and thermal properties of dragline silk from the spider, Nephila clavipes. *Polym Adv Technol*; 5:401–10.

[49] Curvelo AAS, de Carvalho AJF, Agnell JAM (2001). Thermoplastic starch–cellulosic fibers composites: preliminary results. *Carbohydr Polym*; 45:183-188.

[50] Dai L, Li J, Yamada E (2002). Effect of glycerin on structure transition of PVA/SF blends.*J Appl Polym Sc;*86:2342–2347.

[51] Dai WS, Barbari TA (1999). Hydrogel membranes with mesh size asymmetry based on the gradient crosslinking of poly(vinyl alcohol).*J Membrane Sci;* 156:67–79.

[52] Dal Pra I, Freddi G, Minic J, Chiarini A, Armato U (2005). De novo engineering of reticular connective tissue in vivo by silk fibroin nonwoven materials. *Biomaterials;* 26(14):1987–99.

[53] Dal Pra I, Petrini P, Charini A, Bozzini S, Fare S, Armato U (2003). Silk Fibroin-Coated Three-Dimensional Polyurethane Scaffolds for Tissue Engineering: Interactions with Normal Human Fibroblasts. *Tissue Eng;* 9(6):1113-1121.

[54] Damrongrungruang T (2010).Study of fibroblast adhesion on RGD-modified electrospun Thai silk fibroin nanofiber for scaffold material in Dentistry: A preliminary study,*Khon Kaen Univ Dental J;*13(1):3-14.

[55] Das N, Bera T, Mukherjee A (2012). Biomaterial hydrogels for different biomedical applications.*Int J Pharm Bio Sci*; 3(3): 586 – 597.

[56] Davis ME, Hsieh PC, Grodzinsky AJ, Lee RT (2005). Custom Design of the Cardiac Microenvironment with Biomaterials, *Circ Res.* 97: 8–15.

[57] deGroot JH, de Vrijer R, Pennings AJ, Klompmaker J, Veth RPH, Jansen HWB (1996). Use of porous polyurethanes for meniscal reconstruction and meniscal prostheses.*Biomaterials;*17:163-173.

[58] Deolalikar AB, Jamison DT, Jha P, Laxminarayan R (2008). Financing Health Improvements in India.*Health Aff*; 27(4):978-990.

[59] Dikshit AK, Nandi AK (2001). Gelation Mechanism of Thermoreversible Gels of Poly(vinylidene fluoride) and its Blends with Poly(methyl acrylate) in Diethyl Azelate.*Langmuir*; 17:3607 – 3615.

[60] Dinerman, AA, Cappello J, Ghandehari H, Hoag SW (2002). Solute diffusion in genetically engineered silk-elastin like protein polymer hydrogels. *J Control Rel*; 82: 277–287.

[61] Discher DE, Janmey P, Wang YL (2005). Tissue cells feel and respond to the stiffness of their substrate. *Science*; 310:1139–1143.

[62] Dobkowski J, Kolkos R, Kaminski J, Kowalczynska HM (1999). Cell adhesion to polymeric surfaces: experimental study and simple theoretical approach. *J Biomed Mater Res*; 47(2): 234-242.

[63] Dorfman J, Duong M, Zibaitis A, Pelletier MP, Shum-Tim D, Li C, Chiu RC (1998). Myocardial tissue engineering with autologous myoblast implantation.*J Thorac Cardiovasc Surg;* 116:744-751.

[64] Draghi L, Resta S, Pirozzolo MG, TanziMC (2005). Microspheres leaching for scaffold porosity control. *J Mater Sci: Mater Med*; 16: 1093 –1097.

[65] Drury JL, Mooney DJ (2003). Hydrogels for tissue engineering: scaffold design variables and applications. *Biomater*; 24:4337 – 51.

[66] Du CH, Zhu BK, Chen JY, Xu YY (2006). Metal ion permeation properties of silk fibroin/chitosan blend membranes. *Polym Int;* 55: 377–382.

[67] Duan X, Sheardown H (2006). Dendrimer crosslinked collagen as a corneal tissue engineering scaffold: Mechanical properties and corneal epithelial cell interactions. *Biomaterials*; 27: 4608–4617.

[68] Eberli D, Freitas FL, Atala A, Yoo JJ (2009). Composite scaffolds for the engineering of hollow organs and tissues. *Methods;* 47(2):109-115.

[69] Eiselt P, Kim BS, Chacko B, Isenberg B, Peters MC, Greene KG, RolandWD, LoebsackAB, BurgKJL, CulbersonC, HalberstadtCR, HolderWD, MooneyDJ (1998). Development of technologies aiding large-tissue engineering. *Biotechnol Prog*; 14:134-40.

[70] Evans M (2003). Optimization of Manufacturing Processes: A Response Surface Approach, Carlton House Terrace, London.

[71] Finch CA (1973). *Polyvinyl Alcohol Properties and Applications*. John Wiley & Sons, New York.

[72] Finch CA (1992). *Polyvinyl alcohol*. John Wiley & Sons, New York.

[73] Fini M, Motta A, Torricelli P, Giavaresi G, Nicoli Aldini N, Tschon M, Giardino R, Migliaresi C (2005). The healing of confined critical size cancellous defects in the presence of silk fibroin hydrogel. *Biomaterials;* 26(17):3527–36.

[74] Flemming RG, Murphy CJ, Abrams GA, Goodman SL, Nealey PF (1999). Effects of synthetic microand nano-structured surfaces on cell behavior. *Biomaterials*; 20(6):573-588.

[75] Folkman J, Haudenschild C (1980) Angiogenesis in vitro. Nature; 288:551-6.

[76] Fong P, Shin'oka T, Lopez-Soler RI, Breuer C (2006). The use of polymer based scaffolds in tissueengineered heart valves. *Prog Pediatr Cardiol*; 21(2):193-199.

[77] Freddi G, Allara G, Candiani G (1996). Degumming of silk with tartaric acid. *JSDC;* 112:191–195.

[78] Freed LE, Vunjaknovakovic G. Biron RJ, Eagles DB, Lesnoy DC, Barlow SK, Langer R (1994). Biodegradable polymer scaffolds for tissue engineering. *Biotechnology*; 12: 689–693.

[79] Fuchs JR, Nasseri BA, Vacanti JP (2001). Tissue engineering: A 21st century solution to surgical reconstruction. *Annual Thorac Surgery*; 72:577-591.

[80] Fuchs S, Motta A, Migliaresi C, Kirkpatrick CJ (2006). Outgrowth endothelial cells isolated and expanded from human peripheral blood progenitor cells as a potential source of autologous cells for endothelialization of silk fibroin biomaterials. *Biomaterials;* 27(31):5399–408.

[81] Fujita EO, Konno T, Shimizu M, Ishihara K, Sugitate T, Miyake J, Yoshimura K, Taniwaki K, Sakurai T, Hasebe Y, Atom Y (2011). Hydrolyzed eggshell membrane immobilized on phosphorylcholine polymer supplies extracellular matrix environment for human dermal fibroblasts. *Cell Tissue Res*; 345(1):177-190.

[82] Fukada E (1983). Piezoelectric Properties of Biological Polymers, *Q Rev Biophys*; 16(1):59-87.

[83] Furuzono T, Ishihara K, Nakabayashi N, Tamada Y (2000). Chemical modification of silk fibroin with 2-methacryloyloxyethyl phosphorylcholine. II. Graft-polymerization onto fabric through 2-methacryloyloxyethyl isocyanate and interaction between fabric and platelets. *Biomaterials;* 21(4):327-333.

[84] Gandhi MR (2007). Silk Protein as a Biomaterial for Tissue Engineering Application: Theoretical and Experimental Study. *PhD Thesis*; pp 8.

[85] Garg T, Singh O, Arora S, Murthy R (2012). Scaffold: a novel carrier for cell and drug delivery.*Crit Rev Ther Drug Carrier Syst*;29(1):1-63.

[86] Gil ES, Frankowski DJ, Hudson SM, Spontak RJ (2007). Silk Fibroin Membranes from solvent crystallized silk fibroin/gelatin blend: Effects of blend and solvent composition. *Mater Sci Eng C: Mater Biol Appl*; 27:426-431.

[87] Giridhar K, Mahanya JC, Kantharaju BM, Nagesh S (2010). Raw Silk production. *Indian Silk*; 8(1): 27-29.

[88] Gobin AS, Froude VE, Mathur AB (2005). Structural and mechanical characteristics of silk fibroin and chitosan blend scaffolds for tissue regeneration. *J Biomed Mater Res A;* 74:465–473.

[89] Gomathi K, Gopinath D, Ahmed MR, Jayakumar R (2003). Quercetin incorporated collagen matrices for dermal wound healing processes in rat, *Biomaterials*; 24:2767–72.

[90] Gosline JM, Guerette PA, Ortlepp CS, Savage KN (1999). The mechanical design of spider silks: from fibroin sequence to mechanical function. *J Exp Biol*; 202:3295–303.

[91] Gotoh K, Izumi H, Kanamoto T, Tamada Y, Nakashima H (2000).Sulfated fibroin, a novel sulfated peptide derived from silk, inhibits human immunodeficiency virus replication in vitro, *Biosci Biotechnol Biochem*; 64:1664–1670.

[92] Gotoh Y, Minoura N, Miyashita T (2002). Preparation and characterization of conjugates of silk fibroin and chitooligosaccharides. *Colloid Polym Sci*; 280:562–568.

[93] Gotoh Y, Tsukada M, Baba T, Minoura N (1997). Physical properties and structure of poly(ethylene glycol)-silk fibroin conjugate films. *Polymer;* 38(2):487–90.

[94] Gotoh Y, Tsukada M, Minoura N (1998). Effect of the chemical modification of the arginyl residue in Bombyx mori silk fibroin on the attachment and growth of fibroblast cells. *J Biomed Mater Res;* 39(3):351–357.

[95] Griffith LG, Naughton G (2002). Tissue engineering—Current challenges and expanding opportunities. *Science*; 295:1009-14.

[96] Guan J, Fujimoto KL, Sacks MS, Wagner WR (2005). Preparation and characterization of highly porous, biodegradable polyurethane scaffolds for soft tissue applications. *Biomaterials;* 26(18):3961-3971.

[97] Guaracho VV, Kaminari NMS, Ponte MJJS, Ponte HA (2009). Central Composite experimental design applied to removal of lead and nickel from sand. *J Hazard Mater*;172(2-3):1087-92.

[98] Guo X, Zhang F, Peng Q, Xu S, Lei X, Evans DG, Duan X (2011). Layered double hydroxide/eggshellmembrane: An inorganic biocomposite membrane as an efficient adsorbent for Cr(VI) removal. *Chem Eng J*; 166:81–87.

[99] Gupta S, Webster TJ, Sinha A (2011). Evolution of PVA gels prepared without crosslinking agents as a cell adhesive surface. *J Mater Sci Mater Med*; 22(7):1763-72.

[100] Gupta VN, Shivakumar HG (2010). Preparation and characterization of superporous hydrogels as gastroretentive drug delivery system for rosiglitazone maleate, *DARU J. Pharm. Sc.;* 18(3):200-210

[101] Guvenc A, Kapucu N, Kapucu H, Aydogan O, Mehmetoglu U (2007). Enzymatic esterification of isoamyl alcohol obtained from fusel oil: Optimization by response surface methodology. *Enzyme Microb Tech*; 40:778–785.

[102] Hafemann B, Ghofrani K, Gattner HG, Stieve H, Pallua N (2001). Cross-linking by 1-ethyl-3- (3-dimethylaminopropyl)-carbodiimide (EDC) of a collagen/elastin membrane meant to be used as a dermal substitute: effects on physical, biochemical and biological features in vitro. *J Mater Sci Mater Med;* 12:437-446.

[103] Hanawa T, Watanabe A, Tsuchiya T, Ikoma R, Hidaka M, Sugihara M (1995). New Oral dosage form for elderly patients: Preparation and characterization of silk fibroin gel. *Chem. Pharm. Bull*; 43:284-288.

[104] Harris LD, Kim B-S, Mooney DJ (1998). Open pore biodegradable matrices formed with gas foaming. *J Biomed Mater Res*; 42(3):396-402.

[105] Hartgerink, J. D.; Beniash, E. & Stupp, S. I. (2002). Peptide-amphiphile nanofibers: a versatile scaffold for the preparation of self assembling materials. *Proc Natl Acad Sci;* 99, 5133–8.

[106] Hayashi T (1994). Biodegradable polymers for biomedical uses. *Prog Polym Sci;* 19:663–702.

[107] Hench LL (1998).Bioceramics.*J Am Ceram Soc;*81**:**1705-1728.

[108] Hermanson GT (1996). *Bioconjugate Techniques*. (1st Ed.), pp. 785, Academic Publisher, New York.

[109] Hersel U, Dahmen C, Kessler H (2003). RGD modified polymers: biomaterials for stimulated cell adhesion and beyond, *Biomaterials*; 24: 4385–4415.

[110] Hirabayashi K, Sujuki T, Nagyra M, Ishikawa H (1974). *Bunseki kiki*;12:437.

[111] Ho MH, Kuo PY, Hsieh HJ, Hsien TY, Hou LT, Lai JY, Wang DM (2004). Preparation of porous scaffolds by using freeze-extraction and freeze-gelation methods. *Biomaterials;* 25(1):129-138.

[112] Hofmann S, Hagenmuller H, Koch AM, Muller R, Vunjak-Novakovic G, Kaplan DL, Merkle HP, Meinel L (2007). Control of in vitro tissue-engineered bone-like structures using human mesenchymal stem cells and porous silk scaffolds. *Biomaterials*; 28:1152-1162.

[113] Hollister, SJ (2005). Porous scaffold design for tissue engineering. Nat mater; 4:518-524.

[114] Horan RL, Antle K, Collette AL, Wang Y, Huang J, Moreau JE, Volloch V, Kaplan DL, Altman GH (2005). *In vitro*degradation of silk fibroin. *Biomaterials*; 26(17):3385-3393.

[115] Horiba Scientific Inc, USA (2012). A guidebook to particle size analysis. http://www.horiba.com/us/particle

[116] Hou QP, Grijpma DW, Feijen J (2003). Porous polymeric structures for tissue engineering prepared by a coagulation, compression moulding and salt leaching technique. *Biomaterials;* 24:1937–1947.

[117] Hu K, Lv Q, Cui FZ, Feng QL, Kong XD, Wang HL, Huang LY, Li T (2006). Biocompatible fibroin blended films with recombinant human-like collagen for hepatic tissue engineering. *J Bioactive Compatible Polym* ; 21(1):23–37.

[118] Hua FJ, Kim GE, Lee JD, Son YK, Lee DS (2002). Macroporous poly(L-lactide) scaffold 1. Preparation of a macroporous scaffold by liquid-liquid phase separation of a PLLA-dioxane-water system. J Biomed Mater Res;63(2):161-167.

[119] Huang Y, Onyeri S, Siewe M, Moshfeghian A, Madihally SV (2005). In vitro characterization of chitosan-gelatin scaffolds for tissue engineering. *Biomaterials;* 26:7616-7627.

[120] Huang YC, Mooney DJ (2005). Gas foaming to fabricate polymer scaffolds in tissue engineering. In*: Scaffoldings in tissue engineering*, Ma XP, Elisseeff J, (Ed.), pp. 159, CRC press.

[121] Huang YX, Ren J, Chen C, Ren TB, Zhou XY (2008). Preparation and properties of poly(lactide-co- glycolide) (PLGA)/nano-hydroxyapatite (NHA) scaffolds by thermally induced phase separation and rabbit MSCs culture on scaffolds. *J Biomater Appl*; 22:409–432.

[122] Hulbert SF, Young FA, Mathews RS, Klawitter JJ, Talbert CD, Stelling FH (1970). Potential of ceramic materials as permanently implantable skeletal prostheses. *J Biomed Mater Res*; 4: 433-456.

[123] Hutmacher DW (2000). Scaffold in tissue engineering bone and cartilage. *Biomaterials;* 21:2529-2543.

[124] Hutmacher DW (2001). Scaffold design and fabrication technologies for engineering tissues-state of the art and future perspectives. *J Biomat Sci. Polym. Ed.;* 12:107-124.

[125] Hutmacher DW, Cool S (2007). Concepts of Scaffold-Based Tissue Engineering: The Rationale to use Solid Free-Form Fabrication Techniques, *J Cell Mol Med*; 11: 654–669.

[126] Ikada Y (2006). Scope of tissue engineering In: *Tissue engineering: fundamental and applications*, Ikada Y. (Ed.). pp. 29, Academic press, USA.

[127] Jakobs RTM (2013). Catalysis and Luminescence in Mechanically Activated Polymers. *PhD Thesis.*

[128] Jawad H, Ali NN, Lyon AR, Chen QZ, Harding SE, Boccaccini AR (2007). Myocardial tissue engineering: a review. *J Tissue Eng Regen Med*; 1(5):327-342.

[129] Jayasinghe SN (2010).Engineering towards functional tissues and organs. *Organogen*; 6(3):139-40.

[130] Jia J, Duan Y-Y, Yu J, Lu J-W (2008). Preparation and immobilization of soluble eggshell membrane protein on the electrospun nanofibers to enhance cell adhesion and growth.*J Biomed Materi Res A;* 86(2):364–373.

[131] Jin HJ, Chen J, Karageorgiou V, Altman GH, Kaplan DL (2004). Human bone marrow stromal cell responses on electrospun silk fibroin mats. *Biomaterials*; 25(6):1039–1047.

[132] Joshi KB, Singh P, Verma S (2009). Fabrication of platinum nanopillers on peptidebased soft structure using a focused ion beam. *Biofabrication;* 1(2):025002.

[133] Jung H, Kwak B, Yang HS, Tae G, Kim J-S,Shin K (2008). Attachment of cells topoly(styrene-co-acrylic acid) thin films with various charge densities. Colloids and Surfaces A: *Physiochem Engg Aspect*; 313:562-566.

[134] Kadhar KMA, Hariraj G, Roy S, Somashekar TH (2008). Studies on degumming of indian bivoltine silk. *J Silk Sci Tech Jpn;* 17:43-49.

[135] Kai H, Wang X, Madhukar KS, Qin L, Yan Y, Zhang R, Wang X (2009). Fabrication of two-level tumor bone repair biomaterial based on rapid prototyping technique. *Biofabrication;*1(2):025003.

[136] Kamihira M, Kumar A (2007). Development of separation technique for stem cells. *Adv Biochem Engg/Biotechnol;* 106:173-193.

[137] Kang GD, Nahm JH, Park JS, Moon JY, Cho CS, Yeo JH (2000). Effects of poloxamer on the gelation of silk fibroin. Macromol. *Rapid Commun;*21: 788–791.

[138] Karageorgiou V, Kaplan D (2005). Porosity of 3D biomaterial scaffolds and osteogenesis. *Biomaterials;*26:5474–5491.

[139] Karageorgiou V, Meinel L, Hofmann S, Malhotra A, Volloch V, Kaplan D (2004). Bone morphogenetic protein-2 decorated silk fibroin films induce osteogenic differentiation of human bone marrow stromal cells. *J Biomed Mater Res A*; 71:528–537.

[140] Karageorgiou V, Tomkins M, Fajardo R, Meinel L, Snyder B, Wade K, Chen J, Vunjak-Novakovic G, Kaplan DL (2006). Porous silk fibroin 3-D scaffolds for delivery of bone morphogenetic protein-2 in vitro and in vivo,*J Biomed Mater Res A*; 78:324–334.

[141] Karande ST, Agrawal MC (2008). Functions and requirement of synthetic scaffolds in tissue engineering. In: *Nanotechnology and Tissue Engineering: The scaffolds*. Laurencin CT & Nair LS (Ed.), pp 53, CRC Press, Taylor and Francis group.

[142] Kardestuncer T, McCarthy MB, Karageorgiou V, Kaplan DL, Gronowicz G (2006). RGD-tethered silk substrate stimulates the differentiation of human tendon cells. *Clin Orthop Rel Res*; (448):234-239.

[143] Kasoju N, Bora U (2012). Silk fibroin in tissue engineering. *Adv Healthc Mater*;1(4):393-412.

[144] Katoh K, Tanabe T, Yamauchi K (2004). Novel approach to fabricate keratin sponge scaffolds with controlled pore size and porosity. *Biomaterials*; 25(18):4255-4262.

[145] Kawahara Y, Furukawa K, Yamamoto T (2006). Self-Expansion Behavior of Silk Fibroin Film. Macromol Mater Eng; 291:458–462.

[146] Khademhosseini A, Langer R, Borenstein J, Vacanti JP (2006). Microscale technologies for tissue engineering and biology. *Proc Natl Acad Sci USA*; 103:2480–2487.

[147] Kim HJ, Kim U-J, Vunjak-Novakovic G, Min B-H, Kaplan DL (2005a). Influence of macroporous protein scaffolds on bone tissue engineering from bone marrow stem cells. *Biomaterials*; 26(21):4442-4452.

[148] Kim HM, Kishimoto K, Miyaji F, Kokubo T, Yao T, Suetsugu Y, Tanaka J, Nakamura T (1999). Composition and structure of the apatite formed on PET substrate in SBF modified with various ionic activity products. *J Biomed Mater Res*; 46:228–235.

[149] Kim KH, Jeong L, Park HN, Shin SY, Park WH, Lee SC, Kim TI, Park YJ, Seol YJ, Lee YM, Ku Y, Rhyu IC, Han SB, Chung CP (2005b). Biological efficacy of silk fibroin nanofiber membranes for guided bone regeneration. *J Biotechnol*; 120(3):327–339.

[150] Kim KJ, Lee S-B, Han N-W (1993). Effect of the Degree of Crosslinking on Properties of Poly(vinyl alcohol) Membranes). *Polym J*; 25:1295–302.

[151] Kim K, Yu M, Zong X, Chiu J, Fang D, Seo Y-S, Hsiao BS., Chu B (2003). Hadjiargyrou M, Control of degradation rate and hydrophilicity in electrospun non-woven poly(d,l-lactide) nanofiber scaffolds for biomedical applications. *Biomaterials*; 24(27):4977–4985.

[152] Kim SS, Park MS, Jeon O, Choi CY, Kim BS (2006). Poly(lactide-*co*-glycolide)/hydroxyapatite composite scaffolds for bone tissue engineering. *Biomaterials*; 27(8):1399–1409.

[153] Kim SY, Kanamori T, Noumi Y, Wang O-C, Shinbo T (2004). Preparation of porous poly(d,l-lactide) and poly(d,l-lactide-co-glycolide) membranes by a phase inversion process and investigation of their morphological changes as cell culture scaffolds. *J Appl Polym Sci;* 92:2082-2092.

[154] Kim UJ, Park J, Kim HJ, Wada M, Kaplan DL (2005c). Three-dimensional aqueous-derived biomaterial scaffolds from silk fibroin. *Biomaterials*; 26(15):2775–2785.

[155] Kino R, Ikoma T, Monkawa A, Yunoki S, Munekata M, Tanaka J, Asakura T (2006). Deposition of bone-like apatite on modified silk fibroin films from simulated body fluid. *J Appl Polym Sci*; 99(5):2822–30.

[156] Kirker-Head C, Karageorgiou V, Hofmann S, Fajardo R, Betz O, Merkle HP, Hilbe M, von Rechenberg B, McCool J, Abrahamsen L, Nazarian A, Cory E, Curtis M, Kaplan D, Meinel L (2007). BMP-silk composite matrices heal critically sized femoral defects, *Bone*; 41:247–255.

[157] Ko H, Milthorpe B, McFarland C (2007). Engineering thick tissues—the vascularisation problem. *Eur Cells Mat*; 14:1-19.

[158] Kodali VK, Gannon SA, Paramasivam S, Raje S, Polenova T, Thorpe C (2011). A Novel Disulfide-Rich Protein Motif from Avian Eggshell Membranes. *PLoS ONE*; 6(3): e18187.

[159] Kretlow JD, Klouda L, Mikos AG (2007). Injectable matrices and scaffolds for drug delivery in tissue engineering. *Adv Drug Deliv Rev*; 59(4-5):236-273.

[160] Kumar A,Prasad B, Mishra IM (2008). Adsorptive removal of acrylonitrile using powdered activated carbon.*J Environ protection Sci;*2:54 – 62.

[161] Kweon H, Park YH (2001a). Dissolution and Characterization of Regenerated Antheraea pernyi Silk Fibroin.*J Appl Polym Sci;* 82:750–758.

[162] Kweon H, YooMK, ParkIK, KimTH, LeeHC, Lee HS, Oh J-S, Akaike T, Cho C-S (2003). A novel degradable polycaprolactone networks for tissue engineering. *Biomaterials*; 24**:**801–808.

[163] Kweon HY, Um IC, Park YH (2001b). Structural and thermal characteristics of *Antheraea pernyi* silk fibroin/chitosan blend film. Polym; 42(15): 6651-6656.

[164] Kwon IK, Kidoaki S, Matsuda T (2005). Electrospun nano- to microfiber fabrics made of biodegradable copolyesters: structural characteristics, mechanical properties and cell adhesion potential. *Biomaterials*; 26:3929–3939.

[165] Laemmli UK (1970). Cleavage of structural proteins during the assembly of the head of bacteriophage T4. *Nature;*227(259): 680-5.

[166] Langer R, Vacanti JP (1993). Tissue engineering. *Science*; 260: 920–926.

[167] Lanza RP, Langer RS, Vacanti J (2000). *Principles of tissue engineering*. (2nd ed.) Academic Press, San Diego, CA.

[168] Leach RM, Rucker RB, Duke GP (1981). Egg shell membrane protein— A nonelastin desmosine/isodesmosine-containing protein. *Arch Biochem Biophys*; 207:353–359.

[169] Lee CH, Singla A, Lee Y (2001). Biomedical applications of collagen. *Int J Pharm;* 221:1 –22.

[170] Lee JH, Ju YM and Kim DM (2000). Platelet adhesion onto segmented polyurethane film surfaces modified by addition and crosslinking of PEO-containing block copolymers. *Biomaterials*; 21: 683-691.

[171] Lee K, Kong S, Park W, Ha W, Kwon I (1998). Effect of surface properties on the antithrombogenicity of silk fibroin/S-carboxymethyl kerateine blend films. *J Biomater Sci- Polym Ed*; 9(9):905–914.

[172] Lee KH, Baek DH, Ki CS, Park YH (2007). Preparation and characterization of wet spun silk fibroin/ poly(vinyl alcohol) blend filaments. *Int J Biol Macromol;* 41:168–172.

[173] Lee KY, Mooney DJ (2001). Hydrogel for tissue engineering. *Chem Rev*; 101:1869–79.

[174] Leong MF, Rasheed MZ, Lim TC, Chian KS (2008). *In vitro* cell infiltration and invivo cell in filtration and vascularization in fibrous highly porous poly (D,L-Lactic acid) scaffold fabrication by electrospining technique. *J Biomed ResA;* 91:231-240.

[175] Lewin M, (2006). *Handbook of Fiber Chemistry.* (3rd ed.) CRC press, Taylor and Francis group.

[176] Li C, Vepari C, Jin HJ, Kim HJ, Kaplan DL (2006). Electrospun silk-BMP-2 scaffolds for bone tissue engineering, *Biomaterials*; 27:3115–3124.

[177] Li J, Shi R (2007). Fabrication of patterned multi-walled poly-l-lactic acid conduits for nerve regeneration. J. *Neuroscience Methods;* 165, 257-264.

[178] Li M, LuS, WuZ, YanH, MoJ, Wang LJ (2001). Study on porous silk fibroin materials. I. Fine structure of freeze dried silk fibroin. *Appl Polym Sci*; 79: 2185-2191.

[179] Li M, Lu S, Wu Z, Tan K, Minoura N, Kuga S (2002).Structure and properties of silk fibroin–poly(vinyl alcohol) gel.*Int J Biol Macromol;*30:89–94.

[180] Li M, Minoura N, Dai L, Zhang L (2001). Preparation of Porous Poly(vinyl alcohol)-Silk Fibroin (PVA/SF) Blend Membranes. *Macromol Mater Eng*;286:529–534.

[181] Li S, Carrubba VL, Piccarolo S, Sannino D, Brucato V (2004). Preparation and properties of poly(Llactic acid) scaffolds by thermally induced phase separation from a ternary polymer-solvent system. *Polym Int*; 53(12):2079-2085.

[182] Li WJ, Laurencin CT, Caterson EJ, Tuan RS, Ko FK (2002). Electrospun nanofibrous structure:a novel scaffold for tissue engineering. *J Biomed Mater Res;* 60(4): 613-21.

[183] Li WJ, Tuan RS (2009). Fabrication and application of nanofibrous scaffolds in tissue engineering. *Curr Protoc Cell Biol;* 25:Unit 25.2.

[184] Liang D, Hsiao BS, Chu B (2007). Functional electrospun nanofibrous scaffolds for biomedical applications. *Adv. Drug Deliv. Rev;* 59:1392–1412.

[185] Liang Y, Jensen TW, Roy EJ, Cha C,DeVolder RJ, Kohman RE, Zhang BZ, Textor KB, Rund LA, Schook LB, Tong YW, Kong H (2011). Tuning the non-equilibrium state of a drug-encapsulated poly(ethylene glycol) hydrogel for stem and progenitor cell mobilization. *Biomaterials;* 32(7): 2004–2012.

[186] Lin F, Li Y, Jin J, Cai Y, Wei K, Yao J (2008). Deposition behavior and properties of silk fibroin scaffolds soaked in simulated body fluid.*Mater Chem Phys*; 111:92–97.

[187] Lin L, Ju S, Cen L, Zhang H, Hu Q (2008). *Fabrication of porous, TCP scaffolds by combination of rapid prototyping and freeze drying technology*. Yi Peng, Xiaohong Weng (Eds.), pp. 88–91, IFMBE Proceedings 19, Springer-Verlag, Berlin Heidelberg.

[188] Liu C, McKenna FM, Liang H, Johnstone A, Abel EW (2010). Enhanced cell colonization of collagen scaffold by ultraviolet/ozone surface processing.*Tissue Eng Part C Methods*;16(6):1305-14.

[189] Liu H, Ge Z, Wang Y, Toh SL, Sutthikhum V, Goh JCH (2007). Modification of sericin-free silk fibers for ligament tissue engineering application. *J Biomed Mater Res B: Appl Biomater*; 82(1):129-138.

[190] Liu H, Slamovich EB, Webster TJ(2006). Less harmful acidic degradation of poly(lacticco-glycolic acid) bone tissue engineering scaffolds through titania nanoparticle addition. Int J Nanomedicine; 1(4):541-5.

[191] Liu H, Slamovich EB, Webster TJ (2006). Less harmful acidic degradation of poly(lactic-co-glycolic acid) bone tissue engineering scaffolds through titania nanoparticle addition.*Int J Nanomedicine;* 1(4): 541–545.

[192] Liu H-C, Lee IC, Wang J-H, Yang S-H, Young T-H (2004). Preparation of PLLA membranes with different morphologies for culture of MG-63 Cells. *Biomaterials*; 25(18):4047-4056.

[193] Liu L, Liu J, Wang M, Min S, Cai Y, Zhu L, Yao J (2008). Preparation and characterization of nano hydroxyapatite/silk fibroin porous scaffolds.*J Biomater Sci Polym Ed*; 19:325–338.

[194] Liu X, Ma PX (2004). Polymeric scaffolds for bone tissue engineering. *Ann Biomed Eng*; 32: 477–486.

[195] Loveland BE, Johns TG, Mackay IR, Vaillant F, Wang ZX, Hertzog PJ (1992). Validation of the MTT dye assay for enumeration of cells in proliferative and antiproliferative assays. *Biochem Int*; 27:501-510.

[196] Lu S, Wang X, Lu Q, Zhang X, Kluge JA, Uppal N, Omenetto F, Kaplan DL (2010).Insoluble and flexible silk films containing glycerol.*Biomacromol*; 11:43–150.

[197] Lu L, Peter SJ, Lyman MD, Lai H-L, Leite SM, Tamada JA, Uyama S, Vacanti JP, Langer R, Mikos AG (2000).*In vitro* and *in vivo* degradation of porous poly(DL-lactic-*co*-glycolic acid) foams. *Biomaterials;* 21:1837-45.

[198] Lu Q, Zhang S, Hu K, Feng Q, Cao C, Cui F (2007). Cytocompatibility and blood compatibility of multifunctional fibroin/collagen/ heparin scaffolds. *Biomaterials*; 28:2306–2313.

[199] Lu X, Okazaki M, Hirabayashi K (1996). Softness of laminated silk sheet.*J Sericul Sci Jpn*; 65:81-85.

[200] Ma L, Gao C, Mao Z, Zhou J, Shen J, Hu X, Han C (2003). Collagen/chitosan porous scaffolds with improved biostability for skin tissue engineering.*Biomaterials*; 24:4833-4841.

[201] Ma P X (2008). Biomimetic materials for tissue engineering. *Adv Drug Deliv Rev;* 60:184– 98.

[202] Ma PX (2004). Scaffolds for tissue fabrication. *Mater Today*; 7:30–40.

[203] Ma PX (2005). *Tissue Engineering Encyclopedia of Polymer Science and Technology.* (3rd Ed.), 12: pp.261-291, John Wiley &Sons, Inc.: Hoboken, NJ, USA.

[204] Ma PX, Langer R (1999). Fabrication of biodegradable polymer foams for cell transplantation and tissue engineering. In *Tissue Engineering Methods and Protocols*, Morgan J, Yarmush M (Eds.), pp. 47, Humana Press, NJ.

[205] Ma X, Cao C, Li J, Zhu H (2005). Novel prosthesis using silk fibroin for small caliber vascular. *Key Eng Mater*; 288-289:461-464.

[206] Ma X, Cao C, Zhu H (2006). The biocompatibility of silk fibroin films containing sulfonated silk fibroin, *J Biomed Mater Res B Appl Biomater*; 78:89–96.

[207] Ma Z, Kotaki M, Inai R, Ramakrishna S (2005). Potential of nanofiber matrix as tissue engineering scaffolds. *Tissue Engineering*; 11:101–109.

[208] Maeda K, Sasaki Y (1982). An experience of hen-egg membrane as a biological dressing. *Burns Incl Therm Inj*; 8:313–316.

[209] Magoshi J, Magoshi Y, Becker MA, Nakamura S (1996). *Biospinning (Silk fibre formation, multiple spinning mechanism).* In Polymeric Materials Encyclopedia (Ed. 1st Salamone JC), pp. 667-679, CRC Press, Boca Raton (FL, USA).

[210] Malda J, Martens DE, Tramper J, van Blitterswijk CA, Riesle J (2003). Cartilage tissue engineering: controversy in the effect of oxygen. *Crit Rev Biotechnol*; 23:175-94.

[211] Mandal BB, Kundu SC (2008). Non-bioengineered silk fibroin protein 3D scaffolds for potential biotechnological and tissue engineering applications. *Macromol Biosci;* 8:807–18.

[212] Mandal BB, Kundu SC (2008). Non-bioengineered silk gland fibroin protein: characterization and evaluation of matrices for potential tissue engineering applications. *Biotechnol Bioeng;* 100:1237–50.

[213] Mandal BB, Kundu SC (2009a). Cell proliferation and migration in silk fibroin 3D scaffolds. *Biomaterials;* 30:2956-2965.

[214] Mandal BB, Kundu SC (2009b). Osteogenic and adipogenic differentiation of rat bone marrow cells on non-mulberry and mulberry silk gland fibroin 3D scaffolds. *Biomaterials;* 30:5019–5030.

[215] Mann BK, West JL (2002). Cell adhesioin peptides alter smooth muscle cell adhesion, proliferation, migration, and matrix protein synthesis on modified surfaces and in polymer scaffolds. *J Biomed Mater Res*; 60:86.

[216] Mano JF, Silva GA, Azevedo HS, Malafaya PB, Sousa RA, Silva SS, Boesel LF, Oliviera JM, Santos TC, Marques AP, Neves NM, Reis RL (2007). Natural origin biodegradable systems in tissue engineering and regenerative medicine: present status and some moving trends. *J R Soc Interface;* 4:999–1030.

[217] Mansur HS, Costa HS (2008). Nanostructured poly(vinyl alcohol)/bioactive glass and poly (vinyl alcohol)/chitosan/bioactive glass hybrid scaffolds for biomedical applications. *Chem Eng J*; 137:72-83.

[218] Mansur HS, Oréfice RL, Mansur AAP (2004). Characterization of poly(vinyl alcohol)/poly(ethylene glycol) hydrogels and PVA-derived hybrids by small-angle X-ray scattering and FTIR spectroscopy. *Polymer*; 45:7193-7202.

[219] Mao JS, Liu HF, Yin YJ, Yao KD (2003). The properties of chitosan-gelatin membranes and scaffolds modified with hyaluronic acid by different methods. *Biomaterials*; 24(9):1621-9.

[220] Maquet V, Jerome R (1997). Design of macroporous biodegradable polymer scaffolds for cell transplantations. *Mater Sci Forum;* 250:15-24.

[221] Marelli B, Alessandrino A, Farè S, Freddi G, Mantovani D, Tanzi MC (2010). Compliant electrospun silk fibroin tubes for small vessel bypass grafting.*Acta Biomater*; 6(10):4019-26.

[222] Marolt D, Augst A, Freed LE, Vepari C, Fajardo R, Patel N, Gray M, Farley M, Kaplan D, Vunjak-Novakovic G (2006). Bone and cartilage tissue constructs grown using human bone marrow stromal cells, silk scaffolds and rotating bioreactors. *Biomaterials*; 27(36):6138-6149.

[223] Martin A, Zhou A, Gordon RE, Henderson SC, Schwartz AE, Friedman EW, Davies TF (2000). Thyroid Organoid Formation in Simulated Microgravity: Influence of Keratinocyte Growth Factor.*Thyroid*; 10(6):481-487.

[224] Martins AM, Pham Q, Malafaya PB, Sousa RA, Gomes ME, Raphael RM, Kasper FK, Reis RL, Mikos, AG (2009). The Role of Lipase and alpha- Amylase in the Degradation of Starch/Poly(varepsilon-Caprolactone) Fiber Meshes and the Osteogenic Differentiation of Cultured Marrow Stromal Cells. *Tissue Eng Part A;* 15(2):295-305.

[225] Masaeli E, Morshed M, Nasr-Esfahani MH, Sadri S, Hilderink J, Apeldoorn A, Blitterswijk CA, Moroni L (2013). Fabrication, Characterization and Cellular Compatibility of Poly(Hydroxy Alkanoate) Composite Nanofibrous Scaffolds for Nerve Tissue Engineering. *PLoS ONE;* 8(2): e57157.

[226] Matas AJ, Sutherland DER, Steffes MW, Mauer SM, Sowe A, Simmons RL, Najarian JS (1976). Hepatocellular transplantation for metabolic deficiencies: Decrease of plasma bilirubin in Gunn rats. *Science*; 192:892-4.

[227] Mathew AP, Oksman K, Pierron D, Harmand MF (2013). Biocompatible fibrous networks of cellulose nanofibres and collagen crosslinked using genipin: potential as artificial ligament/tendons. *Macromol Biosci*; 13(3):289-98.

[228] Mathew AP, Oksman K, Pierron D, Harmand MF (2013). Biocompatible fibrous networks of cellulose nanofibres and collagen crosslinked using genipin: potential as artificial ligament/tendons. *Macromol Biosci*;13(3):289-98.

[229] Matthews JA, Wnek GE, Simpson DG, Bowlin GL (2002). Electrospinning of collagen nanofibers. *Biomacromolecules;* 3:232-238.

[230] Mauney JR, Jaquiéry C, Volloch V, Heberer M, Martin I, Kaplan DL(2005).*In vitro* and *in vivo* evaluation of differentially demineralized cancellous bone scaffolds combined with human bone marrow stromal cells for tissue engineering.*Biomaterials*; 26:3173-85.

[231] Mayer J, Karamuk E, Akaike T, Wintermantel E (2000). Matrices for tissue engineering-scaffold structure for a bio-artificial liver support system. *J Control Rel*; 64: 81–90.

[232] Megeed Z, Cappello J, Ghandehari H (2002). Genetically engineered silk-elastinlike protein polymers for controlled drug delivery. *Adv Drug Delivery Rev*; 54:1075–1091.

[233] Mei Y, Goldberg M, Anderson D (2007). The development of high-throughput screening approaches for stem cell engineering. *Curr Opin Chem Biol*; 11: 388–393.

[234] Meinel L, Fajardo R, Hofmann S, Langer R, Chen J, Snyder B, Vunjak-Novakovic G, Kaplan D (2005). Silk implants for the healing of critical size bone defects. *Bone*; 37(5):688–698.

[235] Meinel L, Hofmann S, Betz O, Fajardo R, Merkle HP, Langer R, Evans CH, Vunjak-Novakovic G, Kaplan DL (2006a). Osteogenesis by human mesenchymal stem cells cultured on silk biomaterials: comparison of adenovirus mediated gene transfer and protein delivery of BMP- 2. *Biomaterials;* 27(28):4993–5002.

[236] Meinel L, Hofmann S, Karageorgiou V, Zichner L, Langer R, Kaplan D, Vunjak-Novakovic G (2004a). Engineering cartilage-like tissue using human mesenchymal stem cells and silk protein scaffolds. *Biotechnol Bioeng;* 88(3):379–391.

[237] Meinel L, Karageorgiou V, Hofmann S, Fajardo R, Snyder B, Li C, Zichner L, Langer R, Vunjak-Novakovic G, Kaplan DL (2004b). Engineering bone-like tissue in vitro using human bone marrow stem cells and silk scaffolds. *J Biomed Mater Res A*; 71:25–34.

[238] Meinel L, Betz O, Fajardo R, Hofmann S, Nazarian A, Cory E, Hilbe M, McCool J, Langer R, Vunjak-Novakovic G, Merkle HP, Rechenberg B, Kaplan DL, Kirker-Head C (2006b). Silk based biomaterials to heal critical sized femur defects. *Bone*;39(4):922-931.

[239] Mikos AG, Bao Y, Cima LG, Ingber DE, Vacanti JP, Langer R (1993b). Preparation of Poly (glycolic acid) bonded fiber structures for cell attachment and transplantation. *J Biomed Mater Res;* 27:183-189.

[240] Mikos AG, Lu L, Temenoff JS, Temmser JK (2004). Synthetic Bioresorbable polymer scaffolds. In *An introduction to material in medicine*, Ratner BD, Hoffman AS, Schoen FJ, Lemons JE, (Ed.), pp. 743, Elsevier Academic Press, USA.

[241] Mikos AG, Sarakinos G, Leite SM, Vacanti JP, Langer R (1993a). Laminated threedimensional biodegradable foams for use in tissue engineering. *Biomaterials;* 14:323-330.

[242] Mikos AG, Sarakinos G, Vacanti JP, Langar RS, Cima LG (1996). Biocompatible polymer membranes and methods of preparation of three dimensional membrane structures. *U.S. patent* 5, 514:378.

[243] Miller JT (1960). *The Instrument Manual*, 3rd Ed. United Trade Press Ltd.. London.

[244] Min BM, Jeong L, Nam YS, Kim JM, Kim JY, Park WH (2004). Formation of silk fibroin matrices with different texture and its cellular response to normal human keratinocytes. *Int J Biol Macromol*; 34(5):281–8.

[245] Min BM, Lee G, Kim SH, Nam YS, Lee TS, Park WH (2004). Electrospinning of silk fibroin nanofibers and its effect on the adhesion and spreading of normal human keratinocytes and fibroblasts in vitro. *Biomaterials*; 25(7–8):1289–1297.

[246] Minas T, Peterson L (1999). Advanced techniques in autologous chondrocyte transplantation.*Clin Sports Med;* 18:13-44.

[247] Minoura N, Aiba SI, Gotoh Y, Tsukada M, Imai Y (1995). Attachment and growth of cultured fibroblast cells on silk protein matrices. *J Biomed Mater Res*; 29(10):1215-1221.

[248] Minoura N, Tsukada M, Nagura M (1990a). Physico-chemical properties of silk fibroin membrane as a biomaterial. *Biomaterials*; 11(6): 430-434.

[249] Minoura N, Tsukada M, Nagura M (1990b). Fine structure and oxygen permeability of silk fibroin membrane treated with methanol. *Polym;* 31: 265-269.

[250] Mooney DJ, Baldwin DF, Suh NP, Vacanti JP, Langer R (1996). Novel approach to fabricate porous sponges of poly(D,L-lactic-coglycolic acid) without the use of organic solvents. *Biomaterials*; 17:1417-22.

[251] Mooney DJ, Mikos AG (1999). Growing new organs. *Scientific Am*; 280:60-5.

[252] Moore MJ, Jabbari E, Ritman EL, Lu LC, Currier BL, Windebank AJ, Yaszemski MJ (2004). Quantitative analysis of interconnectivity of porous biodegradable scaffolds with micro computed tomography. *J Biomed Mater Res Part A;* 71:258–267.

[253] Moreau JE, Chen J, Horan RL, Kaplan DL, Altman GH (2005). Sequential Growth Factor Application in Bone Marrow Stromal Cell Ligament Engineering. *Tissue Eng*; 11(11-12):1887-1897.

[254] Morita Y, Tomita N, Aoki H, Wakitani S, Tamada Y, Suguro T, Ikeuchi K (2002). Visco-elastic properties of cartilage tissue regenerated with fibroin sponge. *Biomed Mater Eng;* 12(3):291-298.

[255] Moroni L, Hamann D, Paoluzzi L, Pieper J, de Wijn JR, van Blitterswijk CA (2008). Regenerating articular tissue by converging technologies. *PLoS One* 3(8) e3032.

[256] Mosmann, T (1983). Rapid colorimetric assay for cellular growth and survival: Application to proliferation and cytotoxicity assays. *J Immunol Methods;* 65: 55-63.

[257] Murphy CM, Haugh MG, O'Brien FJ (2010). The effect of mean pore size on cell attachment, proliferation and migration in collagenglycosaminoglycan scaffolds for tissue engineering. *Biomaterials*; 31(3):461-466.

[258] Murphy WL, Dennis RG, Kileny JL, Mooney DJ (2002). Salt fusion: an approach to improve pore interconnectivity within tissue engineering scaffolds. *Tissue Eng;* 8:43–52.

[259] Nakane K, Yamashita T, Iwakura K, SuzukiF (1999). Properties and structure of poly(vinyl alcohol)/silica composites. *J Appl Polym Sci*; 74:133–138.

[260] Nakano T, Ikawa NI, Ozimek L (2003). Chemical composition of chicken eggshell and shell membranes. *Poult Sci*; 82:510–514.

[261] Naksupan N, Saelim N, Taepavarapruk P, Aepavarapruk N (2012). Toxicity Testing And Wound Healing Efficacy Of Fibroin Gel In Animal Model, 1st Mae FahLuang University International Conference.

[262] Nam YS, Park TG (1999). Porous biodegradable polymeric scaffolds prepared by thermally induced phase separation. *J Biomed Mater Res;* 47(1):8-17.

[263] Nazarov R, Jin HJ, Kaplan DL (2004). Porous 3-D scaffolds from regenerated silk fibroin. *Biomacromol*; 5:718-26.

[264] Neagu M, Suciu E, Ordodi V, Paunescu V (2005). Human mesenchymal stem cells as basic tools for tissue engineering: Isolation and Culture. *Romanian J. Biophys*; 15(1–4): 29–34.

[265] Nerem R, (1992). Tissue engineering in the USA, *Med Bio Eng Comp*; 30 (4):CE8-12.

[266] Nerem RM, Alexander RW, Chappell DC, Medford RM, Varner SE, Taylor WR (1998). The study of the influence of flow on vascular endothelial biology. *Am J Med Sci*; 316:169-75.

[267] Nesic D, Whiteside R, Brittberg M, Wendt D, Martin I, Mainil-Varlet P (2006). Cartilage tissue engineering for degenerative joint disease. *Adv Drug Deliver Rev*; 58(2):300-322.

[268] Nguyen LL, D'Amore PA (2001). Cellular interactions in vascular growth and differentiation. *Int Rev Cytol*; 204:1-48.

[269] Nguyen M, Arkell J, Jackson CJ (2001). Human endothelial gelatinases and angiogenesis. *Int J Biochem Cell Biol*; 33:960-70.

[270] Ning L, Xue L, Huang HN (1999). Explorations on correlation of biological tests of skin reproductive membrane. *China J Mod Med;* 9(5).

[271] Nuttelman CR, Benoit DS, Tripodi MC, Anseth KS (2006). The effect of ethylene glycol methacrylate phosphate in PEG hydrogels on mineralization and viability of encapsulated hMSCs. *Biomaterials*; 27:1377–86.

[272] Nys Y, Gautron J, Mckee MD, Gautron JM, Hincke MT (2001). Biochemical and functional characterization of eggshell matrix proteins in hens. *Worlds Poultry SciJ*; 57:401–413.

[273] Ochi A, Hossain KS, Magoshi J, NemotoN (2002). Rheology and Dynamic Light Scattering of Silk Fibroin Solution Extracted from the Middle Division of *Bombyx mori* Silkworm. *Biomacromolecules;3*(6):1187–1196.

[274] Oh SH, Kang SG, Kim ES, Cho SH, Lee JH (2003). Fabrication and characterization of hydrophilic poly(lactic-co-glycolic acid)/poly(vinyl alcohol) blend cell scaffolds by melt-molding particulate-leaching method. *Biomaterials;* 24(21):4011-4021.

[275] Ohgo K, Zhao C, Kobayashi M, Asakura T (2003). Preparation of non-woven nanofibers of Bombyx mori silk, Samia cynthia ricini silk and recombinant hybrid silk with electrospinning method. *Polymer*; 44:841–846.

[276] Ohkawa K, Cha D, Kim H, Nishida A, Yamamoto H (2004). Electrospinning of Chitosan. *Macromol Rapid Comm;* 25:1600-1605.

[277] Oki A, Qiu X, Alawode O, Foley B (2006). Synthesis of organic-inorganic hybrid composite and its thermal conversion to porous bioactive glass monolith. *Mater Lett*; 60:2751–2755.

[278] Omstead DR, Baird LG, Christenson L, Moulin GD, Tubo R, Maxted DD, Davis J, Gentile FT (1998).Voluntary Guidance for the Development of Tissue-Engineered Products. *Tissue Eng;* 4 (3), 239–266.

[279] Panilaitis B, Altman GH, Chen JS, Jin HJ, Karageorgiou V, Kaplan DL (2003). Macrophage responses to silk, *Biomaterials*; 24:3079–3085.

[280] Park JB, Lakes RS (1992). *Biomaterials: an introduction.* Vol. 2. Plenum Press. New York.

[281] Park SH, Gil ES, Kim HJ, Lee K, Kaplan DL (2010). Relationship between degradability of silk scaffolds and osteogenesis. *Biomaterials;* 31:6162–6172.

[282] Pati F, Kalita H, Adhikari B, Dhara S (2013). Osteoblastic cellular responses on ionically crosslinked chitosan-tripolyphosphate fibrous 3-D mesh scaffolds. *J Biomed Mater Res Part A*:00A:000–000.

[283] Payne KJ, Veis A (1998). Fourier transform ir spectroscopy of collagen and gelatin solutions: Deconvolution of the amide I band for conformational studies. *Biopolymers*; 27:1749-1760.

[284] Percival E, McDowell RH (1990). Algal polysaccharides. In Methods in plant biochemistry. In *Carbohydrate*; (ed. P. M. Dey), vol 2:pp. 523–547, Academic Press, London, UK.

[285] Peretti GM, Randolph MA, Villa MT, Buragas MS, YaremchukMJ (2000).Cell-based tissue-engineered allogeneic implant for cartilage repair. *Tissue Eng;* 6(5):567-576.

[286] Perez-Rigueiro J, Viney C, Llorca J, Elices M (1998). Mechanical properties of single- brin silkworm silk. *J Appl Polym Sci*; 70:2439– 2447.

[287] Perez-Rigueiro J, Elices M, Llorca J (2002). Effect of degumming on the tensile properties of silkworm (Bombyx mori) silk fibre. *J Appl Polym Sci;* 84:1431–7.

[288] Peters A, Brey DM, Burdick JA (2009). High-throughput and combinatorial technologies for tissue engineering applications. *Tissue Eng;* 15B: 225–239.

[289] Petrini M, Ferrante M, Su B (2013) Fabrication and characterization of biomimetic ceramic/polymer composite materials for dental restoration. *Dent Mater*;29(4):375-81.

[290] Petrini P, Parolari C, Tanzi MC (2001). Silk fibroin-polyurethane scaffolds for tissue engineering. *J Mater Sci Mater Med*; 12: 849–853.

[291] Phillips DM, Drummy LF, Conrady DG, Fox DM, Naik RR, Stone MO, Trulove PC, De-Long HC, Mantz RA (2004). Dissolution and regeneration of Bombyx mori silk fibroin using ionic liquids. *J Am Chem Soc*; 126(44):14350-1.

[292] Plikk P, Målberg S, Albertsson AC (2009). Design of resorbable porous tubular copolyester scaffolds for use in nerve regeneration. *Biomacromol;* 10(5):1259-64.

[293] Ramdi H, Legay C, Lievremont M (1993). Influence of matricial molecules on growth and differentiation of entrapped chondrocytes. *Exp Cell Res*; 207:449–54.

[294] Ramirez F, Rifkin DB (2003). Cell signaling events: a view from the matrix. *Matrix Biol*; 22:101–107.

[295] Riboldi SA, Sampaolesi M, Neuenschwander P, Cossu G, Mantero S (2005). Electrospun degradable polyesterurethane membranes: potential scaffolds for skeletal muscle tissue engineering. Biomaterials; 26(22):4606-4615.

[296] Rice MA, Dodson BT, Arthur JA, Anseth KS (2005). Cell-based therapies and tissue engineering. *Otolaryngol Clin North Am*; 38:199–214.

[297] Rigby BJ (1968). Amino-Acid Composition and Thermal Stability of the Skin Collagen of the Antarctic Ice-fish. *Nature*; 219:166-167.

[298] Roh DH, Kang SY, Kim JY, Kwon YB, Hae YK, Lee KG, Park YH, Baek RM, Heo CY, Choe J, Lee JH (2006). Wound healing effect of silk fibroin/alginateblended sponge in full thickness skin defect of rat. *J Mater Sci: Mater Med*; 17(6):547-552.

[299] Rose ML, Hincke MT (2009). Protein constituents of the eggshell: eggshell-specific matrix proteins. *Cell Mol Life Sci*; 66:2707–2719.

[300] Rosso F, Marino G, Giordano A, Barbarisi M, Parmeggiani D, Barbarisi A (2005). Smart Materials as Scaffolds for Tissue Engineering. *J Cell Physiol;* 203:465–470.

[301] Rowlands AS, Lim SA, Martin D, Cooper-White JJ (2007). Polyurethane/poly(lactic-co-glycolic) acid composite scaffolds fabricated by thermally induced phase separation.*Biomaterials;* 28:2109-2121.

[302] Rui HG (1998). *Silk Reeling,* Oxford & IBH Publishing Co Pvt Ltd, New Delhi.

[303] Rujiravanit R, Kruaykitanon S, Jamieson AM, Tokura S (2003). Preparation of crosslinked chitosan/silk fibroin blend films for drug delivery system. *Macromol Biosci*; 3:604–611.

[304] Ruoslahti E, Pierschbacher MD (1987). New perspectives in cell adhesion: RGD and integrins. *Science;*238:491–7.

[305] Sabato SF, Ouattara B, Yu H, D'Aprano G, Tien CL, Mateescu MA, Lacroix M (2001).Mechanical and barrier properties of cross-linked soy and whey protein based films. J Agri Food Chem; 49:1397-1403.

[306] Sachlos E, Czernuszka JT (2003). Making tissue engineering scaffolds work. Review on the application of solid free from fabrication technology to the production of tissue engineering scaffolds. *European cells and materials;* 5:29-40.

[307] Sakabe H, Itoh H, Miyamoto T, Noishiki Y, Hu W (1989). *In vivo* blood compatibility of regenerated silk fibroin. *Sen-i Gakkaishi*; 45:487–90.

[308] Salgado AJ, Gomes ME, Chou A, Countinho OP, Reis RL, Hutchmacher DW (2002). Preliminary study on the adhesion and proliferation of human osteoblasts on stach-based scaffolds. *Mater Sci Eng C*; 20(1-2):27-33.

[309] Saltzman WM (2004). Tissue Engineering: principles for the design of replacement organs and tissues. (1st ed.) Oxford: Oxford University Press.

[310] Santin M, Motta A, Freddi G, Cannas M (1999). In vitro evaluation of the inflammatory potential of the silk fibroin. *J Biomed Mater Res;* 46:382–389.

[311] Sashina ES, Bochek AM, Novoselov NP, Kirichenko DA (2006). Structure and solubility of natural silk fibroin.*Russ J Appl Chem;* 79(6): 869-876.

[312] Schoof H, Apel J, Heschel I, Rau G (2001). Control of pore structure and size in freeze dried collagen sponges. *J Biomed Mater Res;* 58:352–7.

[313] Schwartz Z, BD Boyan (1994). Underlying mechanisms at the bone-biomaterial interface. *J Cell Biochem*; 56**:**340–347.

[314] Seo YK, Choi GM, Kwon SY, Lee HS, Park YS, Song KY, Kim YJ, Park JK (2007). The biocompatibility of silk scaffold for tissue engineered ligaments. *Key Eng Mater*; 342-343:73-76.

[315] Shi R, Zhang Z, Liu Q,Han Y, ZhangL, Chen D, Tian W (2007). Characterization of citric acid/glycerol co-plasticized thermoplastic starch prepared by melt blending.*Carbohyd Polym;* 69: 748–755.

[316] Singh L, Kumar V, Ratner BD (2004). Generation of porous microcellular 85/15 poly (dl-lactide-co-glycolide) foams for biomedical applications. *Biomaterials*; 25(13):2611-2617.

[317] Smart JD (2005). The basics and underlying mechanisms of mucoadhesion. *Adv Drug Deliv Rev*; 57:1556-1568.

[318] Smart JD, Kellaway IW, Worthington HEC (1984). An *in vitro* investigation of mucosa – adhesive materials for use in controlled drug delivery. *J Pharm Pharmacol*;36:295-299.

[319] Smidsrod O, Skjaok–Br k G (1990). Alginate as immobilization matrix for cells. *Trends Biotech*; 8:71–78.

[320] Smith LA, Beck JA, Ma PX (2006). Nano fibrous scaffolds and their biological effects. In *Tissue Cell and Organ Engineering*, Kumar C (Ed.), pp. 195, Wiley-VCH.

[321] Soffer L, Wang X, Zhang X, Kluge J, Dorfmann L, Kaplan DL, Leisk G (2008). *Silk-based electrospun tubular scaffolds fortissue-engineered vascular grafts. J Biomater Sci Polym Ed*; 19(5):653-664.

[322] Sofia S, McCarthy MB, Gronowicz G, Kaplan DL (2001). Functionalized silk-based biomaterials for bone formation. *J Biomed Mater Res*; 54(1):139–148.

[323] Son JS, Park K, Oh S, Kim J-J, Han DK (2008). Preparation and Characterization of Porous Heparin-immobilized PLGA Scaffolds Using Novel Solid Hydrogen Peroxide for Cartilage Regeneration. *Tissue Eng Regen Med;* 5(3):528-534.

[324] Spain TL, Agrawal CM, Athanasiou KA(1998). New technique to extend the useful life of a biodegradable cartilage implant. *Tissue Eng*; 4:343–352.

[325] Speakman JC (1975). *The Hydrogen Bond and Other Intermolecular Forces*. The Chemical Society, London.

[326] Sugihara A, Sugiura K, Morita H, Ninagawa T, Tubouchi K, Tobe R, Izumiya M, Horio T, Abraham NG, Ikehara S (2000). Promotive effects of a silk film on epidermal recovery from full-thickness skin wounds. *Proc Soc Exp Biol Med*; 225(1):58–64.

[327] Sukigara S, Gandhi M, Ayutsede J, Micklus M, Ko F (2003). Regeneration of Bombyx mori silk by electrospinning—part 1: processing parameters and geometric properties. *Polymer;* 44:5721–5727.

[328] Sun W, Darling A, Starly B, Nam J (2005). Bio-CAD modeling and its applications in computer-aided tissue engineering. *J Compu Aid Des*; 37:1097–1114.

[329] Sun XJ, Zhang ZY, Wang SY, Gittens SA, Jiang XQ, Chou LL (2008). Maxillary sinus floor elevation using a tissue-engineered bone complex with osteobone and bMSCs in rabbits. *Clin Oral Implants Res*; 19(8):804–13.

[330] Sundaram NS, Ravichandran P, Reddy PN, Ramamurty N, Pal S, Rao KP (2001). Collagen/chitosan polymeric scaffolds for the in vitro culture of human epidermoid carcinoma cells. *Biomaterials*; 22:1943-1951.

[331] Sundelacruz S, Kaplan DL (2009). Stem Cell- and Scaffold-Based Tissue Engineering Approaches to Osteochondral Regenerative Medicine. *Semin Cell Dev Biol;* 20:646–655.

[332] Surewicz WK, Mantsch HH (1988). New insight into protein secondary structure from resolution enhanced infrared spectra. *Biochimica Biophysica Acta*; 952:115-130.

[333] Suyama K, Nakamura H, Ishida M, Adachi S (1997). Lipids in the exterior structures of the hen egg. *J Agric Food Chem*; 25:799–803.

[334] Takahashi K, Shirai K, Kitamura M, Hattori M (1996). Soluble egg shell membrane protein as a regulating material for collagen matrix reconstruction. *Biosci Biotech Biochem*; 60:1299–1302.

[335] Takezawa T, Ozaki K, Takabayashi C (2007). Reconstruction of a Hard Connective Tissue Utilizing a Pressed Silk Sheet and Type-I Collagen as the Scaffold for Fibroblasts. *Tissue Eng*; 13(6):1357-1366.

[336] Tamada Y (2004). Sulfation of silk fibroin by chlorosulfonic acid and the anticoagulant activity, *Biomaterials*; 25:377–383.

[337] Tanaka T, Suzuki M, Kuranuki N, Tanigami T, Yamaura K (1997).Properties of Silk Fibroin/Poly(vinyl alcohol) Blend Solutions and Peculiar Structure Found in Heterogeneous Blend Films.*Polym Int*;42:107–111.

[338] Tanaka T, Tanigami T, Yamaura K (1998).Phase separation structure in poly(vinyl alcohol)/silk fibroin blend films.*Polym Int*;45:175–184.

[339] Tancred DC, Carr AJ, McCormack BAO (1998). Development of a new synthetic bone graft. *J Mater Sci Mater Med;* 9, (12):819-823.

[340] Tao W, Li MZ, Zhao CX (2007). Structure and properties of regenerated Antheraea pernyi silk fibroin in aqueous solution. *Int J Bio Macromol*;40: 472–478.

[341] Tarangini K, Kumar A, Satpathy GR, Sangal VK (2009). Statistical Optimization of Process Parameters for Cr (VI) Biosorption onto Mixed Cultures of Pseudomonas aeruginosa and Bacillus subtilis. *Clean*; 37(4 – 5):319 – 327.

[342] Teixeira J, Urist M (1998). Bone morphogenetic protein induced repair of compartmentalized segmental diaphyseal defects. *Arch Orthop Trauma Surg*; 117(1–2):27–34.

[343] Thompson RC, Wake MC, Yaszemski, Mikos AG (1995a). Biodegradable polymer scaffolds to regenerate organs. *Adv Polymer Sci;*122: 245-274.

[344] Thompson RC, Yaszembksi MJ, Powers JM, Harrigan TP, Mikos AG (1995b). Poly (a-hydroxy ester)/short fiber hydroxyapatite composite foams for orthopaedic applications. In *Polymers in Medicine and Pharmacy*. Mikos AG, Leong KW, Yaszemski MJ, (Ed.), Vol. 394, pp. 25-30, Materials Research Society Symposium.

[345] Torres FG, Nazhat SN, Sheikh MF, Maquet V, Boccaccini AR (2007). Mechanical properties and bioactivity of porous PLGA/TiO2 nanoparticle-filled composites for tissue engineering scaffolds. *Compos Sci Technol*; 67:1139–1147.

[346] Tsai WT, Yang JM, Lai CW, Cheng YH, Lin CC, Yeh CW (2006). Characterization and adsorption properties of eggshells and eggshell membrane. *Bioresource Technol*; 97:488–493.

[347] Tsukada M, Freddi G, Crighton JS (1994).Structure and compatibility of poly(vinyl alcohol)-silk fibroin (PVA/SA) blend films.*J Polym Sci Part B: Polym Phys*;32:243–248.

[348] Um IC, Kweon HY, Park YH, Hudson S (2001). Structural characteristics and properties of the regenerated silk fibroin prepared from formic acid.*Int J Biol Macromol*; 29:91-97.

[349] Unger RE, Peters K, Wolf M, Motta A, Migliaresi C, Kirkpatrick CJ (2004). Endothelialization of a nonwoven silk fibroin net for use in tissue engineering: growth and gene regulation of human endothelial cells. *Biomaterials*; 25(21):5137–5146.

[350] Vacanti CA (2006). History of Tissue Engineering and A Glimpse Into Its Future. *Tissue Eng*; 12(5):1137-1142.

[351] Vazquez B, Roman JS, Peniche C, Cohen ME (1997). Polymeric hydrophilic hydrogels with flexible hydrophobic chains control of the hydration and interaction with water molecules. *Macromolecules*; 30:8440–8446.

[352] Venkatesan J, Kim S-K (2010). Chitosan Composites for Bone Tissue Engineering-An Overview. *Mar Drugs;8:* 2252-2266.

[353] Vepari C, Kaplan DL (2007). Silk as a biomaterials. *Prog Polym Sci*; 32:991–1007.

[354] Vepari C, Matheson D, Drummy L, Naik R, Kaplan DL (2010). Surface modification of silk fibroin with poly(ethylene glycol) for antiadhesion and antithrombotic applications. *J Biomed Mater Res A*; 93(2):595-606.

[355] von der Mark K, Park J, Bauer S and Schmuki P (2010). Nanoscale engineering of biomimetic surfaces: cues from the extracellular matrix. *Cell Tissue Res*; 339:131–153.

[356] Vuković R, Bogdanić G, Karasz FE, MacKnight WJ (1999). Phase Behavior and Miscibility in Binary Blends Containing Polymers and Copolymers of Styrene, of 2,6-Dimethyl-1,4-Phenylene Oxide, and of Their Derivatives. *J Phys Chem Ref Data;* 28:851-69.

[357] Vunjak-Novakovic G, Altman G, Horan R, Kaplan DL (2004). Tissue engineering of ligaments.*Ann Rev Biomed Eng;* 6:131-156.

[358] Wallace DG, Rosenblatt J (2003). Collagen in drug delivery and tissue engineering. *Adv Drug Deliv Rev;* 55(12):1631-1649.

[359] Wan YZ, Hong L, Jia SR, Huang Y, Zhu Y, Wang YL, Jiang HJ (2006). Synthesis and characterization of hydroxyapatite-bacterial cellulose nanocomposites. *Comp Sci Tech;* 66(11-12):1825-32.

[360] Wang BL, Kodama M, Mukataka S, Kokufuta E (1998). On the intermolecular crosslinking of PVA chains in an aqueous solution by g-ray irradiation. *Polym Gels Netw;* 6:71-81.

[361] Wang D, Williams CG, Yang F, Elisseeff JH (2004). Enhancing the tissue-biomaterial interface: Tissue-initiated integration of biomaterials. *Adv Func Mater;* 14:1152–1159.

[362] Wang J, Hu W, Liu Q, Zhang S (2011). Dual-functional composite with anticoagulant and antibacterial properties based on heparinized silk fibroin and chitosan. *Colloids Surf, B*; 85(2): 241-247.

[363] Wang L, An XX, Yang FM, Xin ZH, Zhao LY, Hu QH (2008). Isolation and characterization of collagens from the skin, scale and bone of deep-sea redfish (*Sebastes mentella*). *Food Chem*; 108:616-623.

[364] Wang M (2003). Developing bioactive composite materials for tissue replacement.*Biomaterials*, 24:2133–2151.

[365] Wang T, Turhan M, Gunasekaran S (2004). Selected properties of pH-sensitive, biodegradable chitosan-poly(vinyl alcohol) hydrogel. *Polym Int*; 53:911–918.

[366] Wang X, Kim HJ, Xu P, Matsumoto A, Kaplan DL (2005). Biomaterial coatings by stepwise deposition of silk fibroin. *Langmuir*; 21(24):11335–41.

[367] Wang X, Li W, Kumar V (2006). A method for solvent-free fabrication of porous polymer using solid state foaming and ultrasound for tissue engineering applications. *Biomaterials*; 27(9):1924-1929.

[368] Wang X, Yucel T, Lu Q, HuX, Kaplan DL (2010). Silk Nanospheres and Microspheres from Silk/PVA Blend Films for Drug Delivery. *Biomaterials*; 31(6): 1025–1035.

[369] Wang Y, Kim HJ, Vunjak-Novakovic G, Kaplan DL (2006). Stem cell-based tissue engineering with silk biomaterials. *Biomaterials*; 27(36):6064-82.

[370] Wang Y, Kim UJ, Blasioli DJ, Kim HJ, Kaplan DL (2005). *In vitro* cartilage tissue engineering with 3D porous aqueous-derived silk scaffolds and mesenchymal stem cells. *Biomaterials*; 26(34): 7082–94.

[371] Wang Y, Rudym DD, Walsh A, Abrahamsen L, Kim HJ, Kim HS, Kirker-Head C, Kaplan DL (2008). In vivo degradation of three dimensionalsilk fibroin scaffolds.*Biomaterials*; 29:3415–3428.

[372] Wang YZ, Blasioli DJ, Kim HJ, Kim HS, Kaplan DL (2006). Cartilage tissue engineering with silk scaffolds and human articular chondrocytes. *Biomaterials*; 27(25):4434-4442.

[373] Warwicker JO (1954). The crystal structure of silk fibroin. *Acta Cryst;* 7: 565–573.

[374] Wei GB, Ma PX (2006). Macroporous and nanofibrous polymer scaffolds and polymer/bone-like apatite composite scaffolds generated by sugar spheres. *J Biomed Mater Res Part A*; 78:306–315.

[375] Whang K, Thomas CH, Healy KE, Nuber G (1995). A novel method to fabricate bioabsorbable scaffolds. *Polymer*; 36(4):837-842.

[376] Williams DF (1999). *The Williams Dictionary of Biomaterials*, Liverpool University Press, Liverpool.

[377] Wilson AP (2000). Cytotoxicity and viability assays. In JRW Masters, *Animal Cell Culture*. (3rd ed.), pp. 175-219, Oxford University, Oxford.

[378] Wong DWS (1989). *Mechanism and Theory in Food Chemistry*. (1st ed.), Springer, New York.

[379] Wong PFC, Kaplan DL (2002). Genetic engineering of fibrous proteins: Spider dragline silk and collagen. *Adv Drug Delivery Rev*;54(8):1131–1143.

[380] Woodfield TB, Guggenheim M, von Rechenberg B, Riesle J, van Blitterswijk CA, Wedler V (2009). Rapid prototyping of anatomically shaped, tissue engineered implants for restoring congruent articulating surfaces in small joints. *Cell Prolif;* (4):485-97.

[381] Wu W, Feng X, Mao T, Feng X, Ouyang HW, Zhao G, Chen F (2007). Engineering of human tracheal tissue with collagen-enforced poly-lactic-glycolic acid non-woven mesh: A preliminary study in nude mice. *Br J Oral Maxillofac Surg*; 45(4):272-8.

[382] Xu WP, Zhang W, Asrican R, Kim HJ, Kaplan DL, Yelick PC (2008). Accurately shaped tooth bud cell-derived mineralized tissue formation on silk scaffolds,*Tissue Eng Part A*; 14:549–557.

[383] Yamaoka T, Tabata Y, Ikada Y (1995). Comparison of Body Distribution of Poly(vinyl alcohol) with Other Water-soluble Polymers after Intravenous Administration.*J Pharm Pharmacol*; 47:479-486.

[384] Yang XB, Roach HI, Clarke NMP, Howdle S M, Quirk R, Shakesheff KM, Oreffo ROC (2001). Human osteoprogenitor growth and differentiation on synthetic biodegradable structures after surface modification. *Bone*; 29:523-531.

[385] Yang J, Shi G, Bei J, Wang S, Cao Y, Shang Q, Yang G, Wang W (2002). Fabrication and surface modification of macroporous poly(L-lactic acid) and poly(L-lactic co-glycolic acid) (70/30) cell scaffolds for human skin fibroblasts cell culture. *J Biomed Mater Res;* 62:438-446.

[386] Yang S, Leong K-F, Du Z, Chua C-K (2001). The Design of Scaffolds for Use in Tissue Engineering. Part I. Traditional Factors. *Tissue Eng*; 7(6):679-689.

[387] Yang Y, Chen X, Ding F, Zhang P, Liu J, Gu X (2007). Biocompatibility evaluation of silk fibroin with peripheral nerve tissues and cells in vitro. *Biomaterials*; 28(9):1643-1652.

[388] Yaylaoglu MB, Yildiz C, Korkusuz F, Hasirci V (1999). Novel osteochondral implant. *Biomaterials*; 20:1513-1520.

[389] Yeo JH, Lee KG, Kim HC, Oh HYL, Kim AJ, Kim SY (2000). The effects of Pva/chitosan/fibroin (PCF)- blended spongy sheets on wound healing in rats. *Biol Pharm Bull*; 23(10):1220–1223.

[390] Yeong W-Y, Chua C-K, Leong K-F, Chandrasekaran M (2004). Rapid prototyping in tissue engineering: challenges and potential. Trends in Biotechnology; 22(12):643-652.

[391] Yi F, Guo ZX, Zhang LX, Yu J, Li Q (2004). Soluble eggshell membrane protein: preparation, characterization and biocompatibility. *Biomaterials*;25(19):4591-4599.

[392] Yi F, Yu J, Guo ZX, Zhang LX, Li Q (2003). Natural bioactive material: A Preparation of soluble eggshell membrane protein. *Macromol Biosci*; 3:234–237.

[393] Zarkoob S, Eby RK, Reneker DH, Hudson SD, Ertley D, Adams WW (2004). Structure and morphology of electrospun silk nanofibers. *Polymer;* 45:3973–3977.

[394] Zhang S (2003). Fabrication of novel biomaterial through molecular self assembly. *J Nat Biotechnol;* 21:1171-1178.

[395] Zhang S, Zhao X, Spirio L (2006). Pura matrix: self assembling peptide nanofiber scaffolds. In *Scaffolding in Tissue Engineering,* Ma PX, Elisseeff J (Eds.), pp. 217-236, CRC press, Boca Raton, FL.

[396] Zhang X, Baughman CB, Kaplan DL (2008). *In vitro* evaluation of electrospun silk fibroin scaffolds for vascular cell growth. *Biomaterials;* 29:2217-2227.

[397] Zhang X, Cao C, Ma X, Li Y (2012). Optimization of macroporous 3-D silk fibroin scaffolds by salt-leaching procedure in organic solvent-free conditions. *J Mater Sci Mater Med*; 23(2):315-24.

[398] Zhang YQ, Zhou WL, Shen WD, Chen YH, Zha XM, Shirai K, Kiguchi K (2005). Synthesis, characterization and immunogenicity of silk fibroin-L-asparaginase bioconjugates. *J Biotechnol*; 21; 120(3):315-26.

[399] Zhao H, Wang J, Lu Z (2009). Optimization of process parameters of the Pholiota squarrosa extracellular polysaccharide by Box–Behnken statistical design. *Carbohyd Polym*; 77:677–680.

[400] Zhou CZ, Confalonieri F, Jacquet M, Perasso R, Li ZG, Janin J (2001). Silk fibroin: structural implications of a remarkable amino acid sequence. *Proteins*; 44:119–122.

[401] Zhou J, Cao C, Ma X (2009). A novel three-dimensional tubular scaffold prepared from silk fibroin by electrospinning.*Int JBiolog Macromol*; 45:504-510.

[402] Zoppi RA, Contant S, Duek EAR, Marques FR, Wada MLF, Nunes SP (1999). Porous poly(L-lactide) films obtained by immersion precipitation process: morphology, phase separation and culture of VERO cells. *Polymer*; 40(12):3275-3289.

[403] Zund G, Ye Q, Hoerstrup SP, Schoeberlein A, Schmid AC, Grunenfelder J, Vogt P, Turina M (1999). Tissue engineering in cardiovascular surgery: MTT, a rapid and reliable quantitative method to assess the optimal cell seeding on polymeric meshes. *Eur J Cardio-thoracic Surg*; 15:519-524.

Appendix A

Amino acid	one letter code	Three letters code
Alanine	A	Ala
Cysteine	C	Cys
Aspartic acid	D	Asp
Glutamic acid	E	Glu
Phenylanine	F	Phe
Glycine	G	Gly
Histine	H	His
Isoleucine	I	Ile
Lysine	K	Lys
Leucine	L	Leu
Methionine	M	Met
Asparginine	N	Asn
Proline	P	Pro
Glutamine	Q	Gln
Arginine	R	Arg
Serine	S	Ser
Threonine	T	Thr
Valine	V	Val
Tryptophan	W	Trp
Tyrosine	Y	Tyr

PUBLICATIONS

Journal Publications:

- **M. K. Sah**, K. Pramanik*, "**SEP modified Porous Silk Fibroin Scaffolds with enhanced cell adhesion and proliferation property**". *Journal of Applied Polymer Science, 2014* DOI: 10.1002/APP.40138.
- **M. K. Sah**, K. Pramanik*, "**Surface Modification and Analysis of Natural Polymers for Orthopaedic Tissue Engineering: A Review**", *International Journal of Biomedical Engineering and Technology*, 2012 Vol.9(2), pp.101 – 121.
- **M. K. Sah**, K. Pramanik*, "**Preparation and Characterization and *in vitro* study of biocompatible Fibroin hydrogels for tissue engineering**", *African Journal of Biotechnology*, 2011, Vol. 10(40), pp. 7878-7892.
- **M. K. Sah*,** A. Kumar & K. Pramanik, "**The extraction of fibroin protein from *Bombyx mori* silk cocoon: Optimization of process parameters"**, *International Journal of Bioinformatics Research*, 2010, Vol. 2 (2), pp. 33-41.
- **M. K. Sah**, K. Pramanik*, "**Regenerated Silk Fibroin from B. mori Silk Cocoon for Tissue Engineering Applications**", *International Journal of Environmental Science and Development*, 2010, Vol. 1(5), pp. 404-408.
- **M. K. Sah**, K. Pramanik*, "**Preparation, Characterization and Cyto-compatibility of modified Silk Fibroin/PVA scaffolds for bone tissue engineering**". Communicated

Conference Publications:

- **M. K. Sah**, J Sadanand & A Kumar, Development and Biorelevant study of Salt Leached Polyvinyl Alcohol (PVA) Scaffolds, Proceeding of International conference on Biomedical Engineering and Assistive Technologies (**BEATS- 2010**) to be organized by NIT Jalandhar during December 17-19, 2010. (Full Paper)
- **M. K. Sah**, K. Pramanik, Regenerated Silk Fibroin from *B. mori Silk Cocoon for Tissue Engineering Applications,* Proceeding of International conference of Biotechnology and food science (**ICBFS- 2010**) held at Bangalore during February 9-10, 2010. ISBN 978-1-84626-036-0, pp-206-212. (Full Paper)
- K. Pramanik, **M. K. Sah**, Preparation and Characterization of Porous Silk Fibroin Scaffolds using Salt Leaching Method for Tissue Engineering Applications, Proceeding of World Conference on Regenerative Medicine (**WRM-2009**) held at Leipzig, Germany during October 2009. (Abstract)
- **M. K. Sah**, K. Pramanik, Surface Modification and Analysis of Natural Polymers for Orthopaedic Tissue Engineering, Proceeding of International Conference on Medical Materials, devices & Regenerative Medicine (**MMDRM-2008**) organized by SBAOI & STERMI at College of Biomedical Engg. & Applied Sciences, Kathmandu, Nepal during November 23 -25, 2008. (Abstract)

BIOGRAPHY

Mahesh K. Sah is a PhD candidate in the Department of Biotechnology and Medical Engineering at National Institute of Technology Rourkela, India. He received his B.Tech. (Biotechnology) in 2007 from IET, Bundelkhand University, Jhansi (India) and joined NIT Rourkela. His interests include biomaterials processing and application for bone and cartilage tissue engineering, nanotechnology and stem cell research for efficient and improved tissue regeneration. He has won a number of prizes/ awards and more than twenty publications (journals and conferences) goes to his credit. He is member of Society for Biomaterials and Artificial Organs (India).

Personal Details:

Father's Name	Mr. Janardan Pd. Sah
Mother's Name	Mrs. Sushila Devi
Date of Birth	28th February, 1982
Gender	Male
Nationality	Indian
Language Known	Hindi, English, Bengali, Oriya
Permanent Address	c/o Shri Janardan Pd. Sah (Vikas Dresses) At+PO-Palojori Dist.: Deoghar, Jharkhand India-814146